Advanced Optimisation of Batch Plant Design and Operation

by

Michael Charalambous Georgiadis

A thesis submitted for the degree of Doctor of Philosophy of the University of London

Department of Chemical Engineering and Chemical Technology
Imperial College of Science, Technology and Medicine
London SW7 2BY, U.K.

BIBL
LONDON
UNIV.

To my parents Charalambo & Anastasia
who taught me how to appreciate hard work

Abstract

The use of accurate and efficient design and operation methodologies for batch plants is becoming increasingly important mainly due to the business environment which becomes more competitive, complex and uncertain. This gives rise to the need for substantially improved predictive accuracy. However, most of the existing methods are based on simplified models employing many assumptions and approximations to make their solution tractable. This essentially has limited the scope of applying these design and operating decisions.

This thesis considers the applicability of advanced design and operation techniques to batch plants, including individual unit operations and entire processes in order to derive more accurate and efficient designs and operating policies.

In the first part, the plant layout problem is considered. This is a key problem where interactions between design and operation arise. More specifically, techniques for the 2-D and 3-D plant layout problem are developed based on mathematical programming approaches. Particular emphasis is placed on constructing formulations suitable for large scale problems and compatible with existing tools for grassroot and retrofit design without sacrificing their generality for other applications. A key feature of these formulations is that they rely on a detailed representation of the layout problem thus capturing major trade-offs between capital and operating costs, and taking into account limitations arising due to equipment sizes and geometries.

In the second part, we consider the interactions arising between design and operation at the detailed unit operations level. As an example, the case of heat exchangers under fouling, typical time varying units, is considered. First, a detailed mathematical model of tubular and plate heat exchangers under milk fouling is developed to describe the underlying energy, mass and momentum processes. The model comprises a mixed set of integral, partial and

ordinary differential and algebraic equations. State-of-the-art numerical methods are used for the efficient solution of this problem. The model is validated against experimental data. The effect of key parameters on the simulation results is investigated and evaluated.

Then, a technique for determining optimal design and operating strategies for tubular heat exchangers under milk fouling is developed. It is based on the above detailed model, as well as a rigorous mathematical formulation and the use of an advanced optimisation algorithm. The problem is formulated as an optimal control one which employs an economic objective function and takes directly account of all key constraints.

Finally, this thesis also considers the problem of optimal short-term cleaning scheduling of heat exchanger networks (HENs) under fouling as an example of the general class of problems where the optimal operation of processing units interacts with overall production scheduling aspects. The simulation results provided by the above detailed dynamic models are used to quantify the decaying equipment behaviour with time. Then a mixed integer non-linear programming (MINLP) problem is developed minimising the cleaning and energy cost and taking account of various trade-offs. We show that this model can then be linearized exactly to a tight mixed integer linear programming (MILP) formulation. The latter has been applied to large HENs to determine the optimal timing of cleaning operations as well as the corresponding energy utilization profile.

Acknowledgments

First and foremost, I would like to thank my supervisor, Professor Sandro Macchietto for his invaluable support and guidance through the course of this work. I greatly appreciate the independence and the various opportunities he gave me. Furthermore, I am grateful to Dr. Stratos Pistikopoulos for his vital contribution and moral support throughout and beyond my Ph.D. work. Financial support from the Centre for Process Systems Engineering at Imperial College and the EPSRC is greatly acknowledged.

I would also like to express my deep appreciation to Professor Costas Pantelides for the valuable discussions and help on mathematical modelling problems, and for sharing with me a small fraction of his knowledge and experience in process modelling and optimisation in general.

I am also grateful to Dr. Willy Rotstein who inspired part of this work.

Special thanks go to Dr. Lazaros Papageorgiou for his significant contribution on the work presented in chapter 7 and for being a good friend over the last year. Credit is also due to my friend Gordian Schilling for working together on chapter 3.

I shall always remember the presence in the Centre of my friends Stavros and Jezri for their advice and sincere friendship. Stavros stood close to me for more than ten years, even during my military service, and Jezri's assistance was invaluable during my early years in the Centre.

Many thanks to all friends I made in the Centre, especially to Vassilis, Costas, Andreas, Akis, Katerina, Thanasis, Nikos, to friends like Anestis from the restless years back in Thessaloniki and my childhood friend Nikos for always being there for me.

Last but not least, I wish to express my gratitude to my parents Charalambo and Anastasia, my sister Fotini and my grandmother Anna for their love, invaluable support and encouragement through all these years.

Contents

List of Figures 10

List of Tables 14

1 Introduction 16

1.1 The Batch Plant Design Problem 16

1.2 Modelling and Simulation of Batch Processes 18

1.3 Project Objectives and Thesis Outline 20

I Part I-Optimisation Approaches for Optimal Layout Design of Process Plants 22

2 Optimal Layout Design of Multipurpose Batch Plants 23

2.1 **Introduction** 23

2.2 **Problem Statement** 27

2.3 **Motivating Example** 28

2.4 **Mathematical Model** 28

2.4.1 The Objective Function 31

2.4.2 Problem Constraints 33

2.4.3 Overall Formulation 34

2.5 Handling Degeneracies 35

2.6 A Heuristic Method for the Reduction of the Computational Cost 37

2.7 Motivating Example Revisited 38
2.8 Trade-offs Between Capital and Operating Cost in the 3-D Layout Problem . . 41
2.9 Layout Considerations in the Retrofit Design of Multipurpose plants 49
2.10 Streaming and Layout Optimization in an Industrial Multipurpose Batch Plant 54
2.11 Concluding Remarks 58
2.12 Nomenclature 59

3 A Mathematical Programming Approach to Plant Layout with Equipment size Constraints 61

3.1 **Introduction** 61
3.2 Problem Statement 62
3.3 Mathematical Formulation 64
3.3.1 Basic Variables 65
3.3.2 Objective Function 65
3.3.3 Assignment Constraints 67
3.3.4 Distance constraints 67
3.3.5 Equipment shape constraints: single level 68
3.3.6 Equipment Constraints: Multi-Level 72
3.3.7 Calculation of the Land Area 74
3.3.8 Degeneracy Reduction Constraints 76
3.3.9 Comments 76
3.4 Examples 77
3.4.1 Example 1 78
3.4.2 Example 2 85
3.4.3 Example 3 89
3.5 Conclusions 93

II Part II-Modelling, Simulation and Optimisation of Heat Treatment Processes in Batch Plants 94

4 Modelling and Simulation of Tubular Heat Exchangers under Milk Fouling 95

4.1 **Introduction** 95

4.2 Mathematical Model 98
4.2.1 Description of the Fouling Model 98
4.2.2 Shell and Tube Heat exchanger Model under Fouling 99
4.2.3 Fundamental Equations 101
4.2.4 Boundary Conditions 104
4.2.5 Initial Conditions 106
4.2.6 Calculation of the Transport Phenomena Variables 108
4.2.7 Quantifying Fouling 111
4.3 Numerical Simulation and Results 113
4.3.1 Parameter Estimation and Verification of the Simulation Results with Experimental Data 114
4.3.2 Simulation Results and Discussion 115
4.3.3 Sensitivity Analysis 119
4.4 Concluding Remarks 124
4.5 Nomenclature 124

5 Modelling and Simulation of Complex Plate Heat Exchanger Arrangements under Milk Fouling 126
5.1 **Introduction** 126
5.2 A General PHE Dynamic Model 128
5.3 Material Balances 130
5.4 Numerical Simulation and Results 132
5.4.1 Arrangement 1 133
5.4.2 Arrangement 2 137
5.4.3 Arrangement 3 141
5.5 Concluding Remarks 149
5.6 Nomenclature 149

6 Optimal Design and Operation of Heat Exchangers under Milk Fouling 151
6.1 **Introduction** 151
6.2 Mathematical Model 154
6.3 A Comprehensive Objective Function 155

6.3.1 Cost of Cleaning 155
6.3.2 Cost of Heating Medium 156
6.3.3 Heating Medium Pumping Cost 157
6.3.4 Cost of Heat Exchanger 158
6.3.5 Cost due to interruption of production 158
6.3.6 Summary of Objective Function 159
6.4 The Optimisation Problem 160
6.4.1 Optimisation Decision Variables 160
6.4.2 Spatial Domain Normalization 161
6.4.3 Constraints 161
6.5 Solution Approach 163
6.6 Results and Discussion 166
6.6.1 Constant Wall Temperature Case 167
6.6.2 Co-Current Operation 167
6.6.3 Counter-Current Operation 170
6.6.4 Sensitivity Analysis of the Optimization Results 175
6.6.5 Discussion 175
6.7 Concluding Remarks 177
6.8 Nomenclature 178

7 Optimal Cleaning policies in Heat Exchanger Networks under Fouling 180
7.1 **Introduction** 180
7.2 Description of the Problem 183
7.3 Motivating Example 184
7.4 Problem Statement 186
7.5 Serial Heat Exchanger Network Case 190
7.5.1 Mathematical Formulation 190
Energy Balance Constraints 193
Fouling Constraints 195
Timing Constraints 197
Cleaning Constraints 198

Objective Function 199
7.5.2 Summary of Formulation 200
7.5.3 MILP Reformulation 201
7.6 Parallel Heat Exchanger Network Case 202
7.7 Block Heat Exchanger Network Case 205
7.7.1 Fluid as Heating Medium 207
7.7.2 Summary of the Mathematical Model 208
7.8 Case Studies 209
7.8.1 Serial Heat Exchangers 209
7.8.2 A Complex Arrangement of Serial Blocks 212
7.9 Concluding Remarks 216

8 Conclusions & Future Directions **218**
8.1 **Conclusions** 218
8.1.1 Plant Layout Design 218
8.1.2 Modelling, Simulation, Optimal Design and Operation of Heat Treatment Processes with application to Dairy Processes 219
8.2 Main Contributions of this Work 220
8.3 Recommendations for Future Directions 221

References **224**

A The Parameter Estimation Problem **236**

B Simulation of the Cleaning Operation **239**

List of Figures

2.1 Discrete locations and their coordinates in a 2-D layout area 28

2.2 Flowsheet of Instant Coffee Process 29

2.3 Degeneracies in the optimal plant layout problem 36

2.4 Optimal layout on two levels-case 1 and 2 40

2.5 Optimal layout on three levels-case 1 and 2 42

2.6 Optimal layout on four levels-case 1 42

2.7 Optimal layout on four levels-case 2 43

2.8 Optimal layout on five levels-case 2 43

2.9 Flowsheet of the second example 44

2.10 Optimal plant layout in two floors for the second example-case 1 46

2.11 Optimal plant layout in three floors for the second example-case 1 46

2.12 Optimal plant layout in four floors for the second example-case 1 47

2.13 Optimal plant layout in five floors for the second example-case 1 48

2.14 Optimal plant layout in two floors for the second example-case 2 51

2.15 Plant Superstructure for the retrofit example 51

2.16 Maximal State-Task Network for the retrofit example 52

2.17 Optimal plant structure for the retrofit example without layout limitations . . 53

2.18 Final process schedule for the retrofit example 55

2.19 Optimal plant layout for the retrofit example-case 2 55

2.20 Optimal plant structure for the retrofit example with layout limitations 57

2.21 Optimal streaming at the dispersion and mixing stage 57
2.22 Optimal plant layout for the streaming optimization problem 60

3.1 Grid representation in the layout area 63
3.2 Equipment shape discretization 64
3.3 Equipment orientation in the $x-y$ level 75
3.4 Determination of the required land in the 2-D problems 75
3.5 Process units shapes for example 1 79
3.6 Optimal 2-D layout for example 1-case A1 80
3.7 Optimal 2-D layout for example 1-case A2 81
3.8 Optimal 2-D layout for example 1-case A3 81
3.9 Optimal layout in two levels for example 1 82
3.10 Optimal layout in three levels for example 1 83
3.11 Optimal layout in four levels for example 1 84
3.12 Optimal layout in three levels with multilevel units for example 1 86
3.13 Process flowsheet for example 2 86
3.14 Process units shapes for example 2 87
3.15 Process layout for example 2 89
3.16 Process units shapes for example 3 90
3.17 Process layout for example 3 92

4.1 The protein reaction scheme 98
4.2 Shell and tube heat exchangers for milk heat treatment 101
4.3 A differential element in a shell and tube heat exchanger 102
4.4 Solution strategy of the model 113
4.5 Comparison between simulation and experimental results 115
4.6 Effect of Reynolds number and comparison with experimental results 116
4.7 3-D representation of milk temperature for constant wall temperature, T_w=374 K 117
4.8 Layer proteins concentrations at $t = 20,000$ sec (case i) 117
4.9 Bulk aggregated protein concentration profiles at different times (case i) 118
4.10 Biot number profile for constant wall temperature, T_w=374 K at different times 118
4.11 Deposit thickness profile for heating time 100,000 sec (case i) 120

4.12 Overall heat transfer coefficient (case i) 120
4.13 Effect of all cases of operation on milk outlet temperature 122
4.14 Effect of native protein concentration on fouling (case i) 122
4.15 Effect of Reynolds number on fouling 123
4.16 Effect of initial denaturated protein on fouling 123

5.1 PHE arrangement-1 127
5.2 A differential element in a Plate Heat Exchanger 129
5.3 Model decomposition for PHE–arrangement 1 132
5.4 Steady state temperature profile of the process fluid for PHE–arrangement 1 . 135
5.5 Comparison of predicted and experimental values of overall heat transfer coefficient-arrangement 1 138
5.6 Deposit profiles for plates 1-4-arrangement 1 138
5.7 Deposit profiles for plates 5-8-arrangement 1 142
5.8 Milk outlet temperature profile for two values of inlet native protein concentration-arrangement 1 143
5.9 Heating medium outlet temperature profile-arrangement 1 144
5.10 Milk outlet temperature for different Reynolds numbers-arrangement 1 144
5.11 Effect of initial protein concentration and comparison with experimental data . 145
5.12 PHE-arrangement 2 145
5.13 Steady state temperature profile for PHE-arrangement 2 146
5.14 Comparison between experimental and predicted values-arrangement 2 146
5.15 Effect of changing the initial protein concentration and comparison between experimental and predicted values-arrangement 2 147
5.16 PHE-arrangement 3 147
5.17 Steady state temperature profile for PHE–arrangement 3 148
5.18 Deposit mass profiles for plates 9 to 12-arrangement 3 148

6.1 Algorithm of Dynamic optimization 166
6.2 Profile of the objective function vs heating time 169
6.3 Milk outlet temperature under optimal control-constant wall temperature case 169
6.4 Optimal Control action (piecewise constant profile, 12 intervals) 171
6.5 Milk outlet temperature profile under control for optimal co-current operation 171

6.6 Heating medium inlet temperature profile for the co-current operation 172
6.7 Heating medium flowrate profile for the co-current operation 172
6.8 Milk outlet temperature profile under control for the counter-current operation 173
6.9 Optimal heating medium inlet temperature profile for the counter-current operation 174
6.10 Optimal heating medium flowrate profile for the counter-current operation . . 174

7.1 Serial Heat Exchanger Network with two processing units 184
7.2 Schedule with frequent cleaning policy for two serial exchangers 185
7.3 Schedule with infrequent cleaning policy for two serial exchangers 187
7.4 Optimal cleaning schedule for two serial exchangers 187
7.5 Operating cost as a function of the number of cleaning tasks 189
7.6 A unit representation with its bypasses for a serial HEN 189
7.7 Serial heat exchanger network 191
7.8 Piecewise constant approximation of the heat transfer coefficient 191
7.9 Non linear decaying profile 195
7.10 Graphical illustration of the cleaning constraints 198
7.11 Parallel heat exchanger network arrangement 203
7.12 Complex HEN of serial blocks of parallel heat exchangers 206
7.13 Optimal cleaning schedule for the serial heat exchanger network case 212
7.14 Optimal hot utility temperature profile for the serial heat exchanger network case 214
7.15 Optimal cleaning schedule for the complex heat exchanger network case 214
7.16 Optimal hot utility temperature profile for the complex heat exchanger network case 215
7.17 Optimal cleaning schedule for the complex heat exchanger network case with utility temperature bound 215
7.18 Hot oil inlet temperature profile 216

List of Tables

2.1 Connection cost for the illustrative example 39

2.2 Cost data for the motivating example 39

2.3 Cost data for the second example 45

2.4 Floor construction cost data for the second example 45

2.5 Coordinates of the allocation areas for the second example 47

2.6 Optimization Results for the second example-case 1 48

2.7 Optimization Results for the second example-case 2 48

2.8 Unit characteristic for the retrofit example 50

2.9 Connection characteristic for the retrofit example 50

2.10 Product values and raw material prices for the retrofit example 52

2.11 Optimal unit capacities for the retrofit example 53

3.1 Equipment sizes (rectangular footprint) for example 1 79

3.2 Cost data for example 1 79

3.3 Results for example 1-2D Layout 84

3.4 Results for example 1-3D Layout 85

3.5 Equipment sizes for example 2 87

3.6 Connectivity matrix and costs for example 2 88

3.7 Equipment sizes (floor space) for example 3 91

3.8 Cost data for example 3 91

4.1 Kinetic data for the reactions of β-lactoglobulin 99

4.2 Details of heat exchangers used in simulation (steady state) 107
4.3 Heat exchanger data used in simulation 107
4.4 Parameter values used in simulation 107
4.5 Physical property data used in simulation 108
4.6 Values of particle diameters for the three proteins from optimal fit of experimental data 110
4.7 Effect of fouling on milk outlet temperature for four cases of operation 119

5.1 Technical details of the PHE-arrangement 1 133
5.2 Parameter Estimation Results-arrangement 1 135
5.3 Comparison of experimental with predicted mass deposit values-arrangement 1 136
5.4 Parameter Estimation Results-arrangement 2 140
5.5 Parameter Estimation Results-arrangement 3 142
5.6 Comparison of experimental with predicted deposit mass values-arrangement 3 142

6.1 Bounds and Initial Points for the Optimization Variables 168
6.2 Summary of optimization results for constant wall temperature case 168
6.3 Summary of optimization results for co-current operation 168
6.4 Optimisation results for co-current operation with one control variable 170
6.5 Summary of optimisation results for the counter current operation 173
6.6 Optimisation results for the counter current operation with one control variable 173
6.7 Sensitivity analysis of the objective function for the constant wall temperature operation 175

7.1 Fouling data for the serial heat exchanger network case 210
7.2 Cost data 210
7.3 Computational results for the serial HEN case 211
7.4 Fouling data for the complex HEN case 213

Chapter 1

Introduction

An increasing interest in batch processing in the process industries has been evident in recent years (Shah, 1998). Changing market conditions which favour high value-added, low volume products appears to be the main cause of this interest. Product lifetimes on average are diminishing and the number of products produced per plant is increasing. Furthermore, growing uncertainties in the economic environment upset product demands increasing the need for operational flexibility. Multipurpose batch plants can easily be reconfigured or adapted to allow for production modifications thus covering a wide range of operating conditions within the same plant configuration.

This thesis is concerned with some principal aspects in the design and operation of batch processes. This introductory chapter examines first some modelling and simulation issues. It then discusses the motivation and basis of the work described in this thesis. An outline of the latter is also given.

1.1 The Batch Plant Design Problem

The design of batch plant can be posed as the problem of selecting the number and type of processing units and their sizes, so as to minimise a selected design objective while satisfying production requirements over a given planning time horizon (Shah, 1992; Barbosa-Povoa, 1994).

One problem of particular interest is the retrofit design which can be defined as the design of appropriate modifications to an existing plant in order to accommodate changes in the product slate, demand requirements and/or plant operability, so as to improve the overall

plant performance by increasing process flexibility, reduction of energy, operating costs etc. Retrofit design decisions include potential purchase of new units, elimination of old ones and modifications of the existing connectivity network. In fact, retrofit projects play a particularly important role in the fine chemicals industry due to the constant need to upgrade the large base of existing facilities. In many cases the retrofit design may involve only reconfiguration of the connection network, without addition/removal of any units. Space constraints often impose the need for relocation and repiping of equipment items in existing plants and should also be considered when addressing a more general problem (Reklaitis, 1992). When redesigning existing facilities different problems may be encountered due to space limitations. For example, the addition of two small reactors might provide a more flexible operation but due to space limitations a single bigger reactor must be added. Also, it may happen that although both small reactors can be added to the existing plant, an extensive repiping is necessary and an increased cost configuration is obtained. The introduction of layout considerations is thus required to identify least cost configurations of the new equipment within the constraints imposed by the existing facilities. In this context, a generic layout technique which can be integrated with generic methods for grassroots and retrofit design/scheduling will be particularly useful (Barbosa-Povoa, 1994).

The optimal layout in batch plants is important not only for the reduction of piping cost but also from the operation point of view. In batch plants it is often advantageous to transfer materials by using gravity flow to avoid troubles of contamination, unstable intermediate problems etc. Therefore, the equipment items in batch plants are often allocated in multifloor structures and their exact location should be decided to enable the most use of the gravity flow. However, such a decision is difficult to be made intuitively since the processing paths in the plant are determined by the processing requirements of different batches and affected by the type of products and equipment. Moreover, layout decisions in batch plants affect production losses taking place due to cleaning operations of the piping route. For example, in the food industry the pipework which depends on the plant layout represents a major cost component (Ball, 1990). This is due to the need of providing a maximum flexibility of operation while still guaranteeing the final product quality.

Although some progress has been made on the 2-D plant layout problem, systematic approaches for the 3-D plant layout problem, taking into account broad operating considerations, are only in their infancy. The main difficulty is due to the need to consider the high interactions between design and operating decisions (Macchietto, 1993).

1.2 Modelling and Simulation of Batch Processes

Mathematical process models are currently employed, directly or indirectly, for almost all aspects of plant design and operation. Model usage covers the entire process lifestyle, from designing the plant and its control system, training the personnel who are responsible for operating it and detecting and diagnosing faults in its operation (Pantelides and Britt, 1995). The number of experiments during scale-up or even during commissioning of the plant can be reduced if increasingly detailed models of all kind of unit operations are available. On the other hand, more accurate models with increasing detail and fidelity can advantageously be used during the screening of process alternatives as the conceptual design progresses towards the final flowsheet (Marquardt, 1991, 1996).

Two major types of models are used in process development and engineering: empirical and fundamental. Empirical models need a lot less knowledge and creativity. The constants used in empirical models normally have no physical basis. They are simply statistical values that describe the data. As a result, the data obtained show little or nothing about the underlying physics. On the other hand, fundamental models are theoretically based. In batch plants (*e.g.* food industries), this usually means defining the underlying transport (momentum, heat and mass transfer) phenomena. Physically based models can be extrapolated to unexplored, or unexplorable regions, in other words can help to solving the scale-up problem, which implies extrapolation. For commodity processes, or those which have been operated for a long time a high degree of predictive accuracy using fundamental models is essential. One reason for this is that such processes in many cases, have been undergoing incremental improvements based on practical experience and simple theoretical analysis over several decades. Consequently, it is unlikely that any further improvement that remains to be achieved will exceed a few percentage points of the total operating cost. This may still be a very substantial amount in absolute terms given the very large throughput of some of these processes. However, in order to realise this benefit, models that characterize all important aspects of the behaviour and the economics of the process with an accuracy of about 1% are needed (Pantelides, 1996). In this context, Charalambides (1996) considered the optimal design of integrated batch processes, using detailed dynamic models, where plant design and scheduling are considered simultaneously. The importance of using accurate dynamic models was clearly illustrated in the optimisation of an existing batch plant by Ishikawa *et al.* (1997).

On the other hand, many of the batch processes are only vaguely understood at the fundamental level. For example, the food industry constitutes a major part of the batch processes.

It is claimed that food processes exhibit different characteristics to those of chemical processes, and empirical models are far more commonly used (Levine, 1997). Most of the problems in the modelling and simulation of food operations are posed by the intrinsic complexity of the material and transformation involved and the difficulty in describing them in terms of fundamental models. Specific aspects with respect to the optimal operation of batch food processes arise from: (i) the need to meet hygienic requirements which requires the equipment to be periodically shut down for cleaning and sterilization, hence turning even otherwise continuous processes into batch, and (ii) the need to account for product perishability, and thus limits on residence and wait times, which dictates segregation into batches and makes production scheduling much more difficult (Macchietto, 1997). Product quality assurance is often critical in batch plants (*e.g.* pharmaceutical, food, biochemical, beverage) and poses significant constraints on cleaning and general precondition on the operation of both the processing units and the piping network. Again the main difficulty arises from the need to take into account, on the one hand, the detailed (dynamic) performance of process units (which determines the product quality, yields and time/resource requirements of individual units operations), and on the other hand, the interactions between the various operations (how batches are scheduled to flow through a plant, accounting for conflicting resources requirements and other constraints) which determine the overall performance of the manufacturing plant.

So far, in most studies, the design of batch plants relies on simple models depicting the time requirements of batch operations (*e.g.* cycle times) and possibly the capacity requirements (*e.g.* size factors). These models have typically been used for two tasks: design and retrofit of manufacturing facilities (*e.g.* selecting and sizing the vessels to install) and production planning and scheduling (Rippin, 1993). On the other hand, these models do not take into account special and/or detailed characteristics of crucial items of equipment. This "upper" level of optimal design may not exploit all the flexibility actually available, in particular by manipulation of controls. More recently, design techniques are being developed which use more complex models, including detailed dynamic models accounting for the transient behaviour of batch plants. One additional way to increase plant flexibility is by extending the range of operating conditions of individual equipment. In this context, ways to increase plant flexibility by better design/control of crucial equipment (often plant bottlenecks) can be explored. The idea is to develop "smarter" equipment capable of large degree of autonomous operation, control, self monitoring and diagnosis (Macchietto, 1998). A specific example is used here to investigate the issues involved and to assess the validity of the thesis. In particular, the design and operation of heat exchangers subject to fouling in the food industries is used. This example is of interest

since the economic impact of fouling in food plants is significant (Walker, 1997).

A second area which gives rise to the strong interactions between design and operation decisions in batch plants is changeovers. For example, significant productions losses during changeovers take place in the connectivity network which is imposed by the plant layout. On the other hand, the timing and synchronisation of changeover tasks (where cleaning operations takes place) are determined by the state of each equipment and the trade-offs between scheduling decisions.

1.3 Project Objectives and Thesis Outline

In order to address some of the issues posed above this work is concerned with:

- *mathematical programming approaches for the optimal layout in batch processes.* Such approaches can be used at the early design stage and can also be embedded in the retrofit design problem to account for potential layout limitations on the optimal plant design.

- *detailed mathematical models for sterilization/pasteurization processes under fouling.* These processes play a particularly important role in a wide class of batch plants and their detailed modelling, so far, has been neglected. Such models can then be used to define the optimal process design and operating policies.

- *optimal cleaning policies in heat exchanger networks under fouling conditions.* The simulation results using the above detailed dynamic models are first used to quantify the behaviour of each heat exchanger over time. Then, suitable mathematical programming techniques are developed to solve the short-term cleaning scheduling even for networks with large number of exchangers.

The rest of the thesis is structured as follows:

- Chapter 2 presents a mathematical programming approach addressing the 2-D and 3-D layout problem in batch plants. The implications of layout limitations on retrofit decisions are investigated through a number of illustrative examples.

- Chapter 3 extends the mathematical formulation of chapter 2 by modelling explicitly the equipment sizes and geometries.

- Chapter 4 presents a detailed dynamic model of tubular heat exchangers under milk fouling. The simulation results are verified against experimental data and typical industrial techniques for fouling mitigation are verified.

- Chapter 5 presents detailed mathematical models of typical industrial plate heat exchangers under milk fouling. The simulation results agree well with experimental data.

- Chapter 6 uses the mathematical model of chapter 4 to define optimal control strategies for heat exchangers under milk fouling. The approach identifies the main operability bottlenecks and the best control schemes.

- Chapter 7 is concerned with optimal cleaning policies in heat exchanger networks under fouling. An efficient mathematical programming approach is developed accounting for various trade-offs.

- Finally, chapter 8 presents the main conclusions derived from this work and indicates some areas of future research.

Part I-Optimisation Approaches for Optimal Layout Design of Process Plants

Chapter 2

Optimal Layout Design of Multipurpose Batch Plants

A mathematical formulation is proposed for addressing the problem of allocating items of equipment in a given two or three dimensional geometric space. The problem is formulated as a mixed integer linear programming model where specific attention is paid to constructing a formulation which is suitable for the solution of large scale problems. Case studies are presented to illustrate the applicability of the proposed approach to retrofit problems in multipurpose plants. Trade-offs between capital and operating costs are captured so that the optimal number of required floors may be determined.

2.1 Introduction

Plant layout is concerned with the spatial arrangement of processing equipment, storage vessels and their interconnecting pipework. Deciding a good layout is an important activity in the design of chemical and process plants. A good layout will facilitate a correct operation of the plant. It will also provide an economic balance between the often conflicting constraints deriving from safety, environment, construction, maintenance, operation, space for future expansion and process relationships such as those determined by gravity flow (Kern, 1977; Mecklenburgh, 1985; Madden and Walters, 1988). The traditional method of locating equipment in chemical plants has been to allocate it over a large area, with only a secondary concern for land usage. However, this may often contradict new trends in designing plants with a greater concern for compact plots, enclosed structures and modular plants.

Chemical plant layout by itself has only recently been the subject of study. However, the problem of layout and location has been extensively studied by industrial engineers under the title of *facility layout and location*, with application to job shops and manufacturing units (Francis and White, 1974). The most relevant approach to the facility layout problem have been studied under the title of "Quadratic Assignment Problem". This problem addresses the allocation of a number of production facilities to an equal number of locations. The cost function depends on the flow between the facilities and their respective allocations. Several formulations and algorithms based on heuristics have been proposed for the solution of these problems (Fortenberry and Cox, 1985; Bozer *et al.*, 1994). Combined exact and heuristic methods were also presented by Bazaraa and Sherali (1980), Bazaraa and Kirca (1983) Adams and Sherali (1986) and Rosenblatt (1979). A comprehensive review is presented by Kusiak and Heragu (1987). Recently, Bazargan-Lari (1997) presented a mathematical model for layout design in cellular manufacturing problems. In this type of problems a poor shop floor layout considerably affects the material movements and therefore the lead time of products to customers.

The general layout problem for chemical plants has been considered by other researchers. Gunn (1970) and Gunn and Al-Asadi (1987) proposed the decomposition of the plant into plant modules. The module arrangement in a building or in a site area was related to an objective function by introducing piping cost. The problem was formulated as a non-linear programming (NLP) problem and a method of direct search was applied to minimise the objective function. Following a different approach (Suzuki *et al.*, 1991*a*) considered the layout problem in a multi-objective framework in which not only piping costs but also preferences about the equipment arrangement were taken into account. To reduce the computational cost they grouped the equipment into modules which were further grouped into sections. The whole formulation results in a mixed integer non-linear programming (MINLP) problem which was solved using a heuristic approach. Amorese *et al.* (1991) presented a method for the minimisation of the connection cost imposing constraints for the non-interference of the areas of influence for each unit. They proposed some heuristic rules to solve the resulting model. The drawback of their approach is the large number of the heuristic rules proposed which can lead to non optimal solutions. A small example was presented where the optimal layout improves the connection cost by only 2% compared with the initial allocation.

Bradley and Nolan (1985) and Nolan and Bradley (1987) considered the chemical plant layout under safety considerations. They presented a layout policy which considers the effect of potential hazards to the processing units. A minimum distance was imposed between any

two equipment items which are considered as a source of hazard. This distance is determined explicitly as a function of the intensity and sensitivity of items to hazards. The whole problem is formulated as a NLP. Fuchino *et al.* (1997) proposed a method for arrangement of equipment modules under safety considerations. The whole approach relies on a large number of heuristic rules and input information.

The application of operation research methods to the layout design of chemical or process plants is relatively new. Penteado and Ciric (1996) presented an optimization formulation that can aid in the development of safe and economical layouts. The problem was solved as a relaxed MINLP and illustrated with a small case study for the two dimensional layout. Jayakumar and Reklaitis (1994) proposed a graph theoretical approach to single floor layout establishing the analogy between distributing units on a single floor and the traditional graph partitioning problem. The same authors also considered the multilevel or multifloor layout for batch plants (Jayakumar and Reklaitis, 1996). Here, the objective of their work was not to find the optimal plant layout but the optimal allocation of units to floors, a particular subset of the general layout problem. A graphical heuristic approach was presented which provides an upper bound to the true optimal value. Problems with up to 50 equipment units were solved using this approach. A mathematical programming approach was also presented providing a lower bound which together with the upper bound "brackets" the optimal value. This approach relies on a tight linearization scheme of the initial MINLP (compared with the well known Glover transformations). The continuous relaxation of the resulting MILP was solved using the *Lagrangean relaxation technique* together with the subgradient optimisation for the calculation of the required Lagrange multipliers. However the solution of the relaxed LP may often result in non integer solutions (Fisher, 1981). In fact, even for the small illustrative example presented, the solution in one of the cases examined was fractional. In general, for large problems, non integer solutions cannot be converted easily to integer solutions even if the continuous optimal point is very close to the integer one. Suzuki *et al.* (1991*c*) proposed a method for assigning each piece of equipment to any of the floors available in multipurpose plants. Since the distances between units were not calculated, approximate expressions were used for the transportation and floor construction cost. The same authors presented a method for multi-floor equipment arrangements in batch plants. Their approach assumes that the floor assigned to each equipment unit is known a-priori. The objective function is based only on weighted preferences for the allocation of equipment without economic considerations (Suzuki *et al.*, 1991*b*).

The layout problem was also considered in the case of pipeless batch plants by Realff *et al.* (1996). A mathematical programming formulation was presented addressing the combined design, layout and scheduling problem. For this type of batch plants, the plant layout strongly influences the scheduling since it determines the relative position of the processing stations and as a consequence the transfer times for the vessels. The robust scheduling of pipeless batch Plants under layout considerations is discussed in the work of Gonzalez and Realff (1995). The problem was formulated as an MILP and a discrete event simulator has been coupled to the output of the MILP to simulate plant operation while allowing for variations in its operation.

Most of the previous work in process plant layout has been mainly focused on the use of heuristic approaches while optimisation based techniques were usually applied in small example problems. In the area of multipurpose batch plants, very little work has been done on the effect of layout considerations in the retrofit design problem, following the initial work of Barbosa-Povoa (1994). Here, layout issues are particularly relevant, since typically there is little opportunity for changing the plant boundaries which may pose significant limitation on type, size and location of new equipment. Furthermore, management considerations are often affected by the process layout. For example, in the industrial case study presented later there is a strong interaction between the desired organisation of labour and the desired plant layout.

In this chapter we present a novel formulation and a mathematical programming solution addressing the problem of allocating items of equipment in a given two or three dimensional space. The objective function to be minimized is the total transport (operating), connection and floor construction (capital) cost. Detailed cost factors are used to account for the flow direction between two connected units. It should be noted here, that the transportation cost can represent pumping, conveying or even manual transfer cost. The problem is formulated as a mixed integer *linear* programming (MILP) problem, with specific attention given to a formulation suitable for the solution of large scale problems (up to 25-30 processing units). Trade-offs between the capital and operating cost are illustrated, with an industrial case study resulting in the optimal number of floors required. Furthermore, the simultaneous retrofit design/scheduling and layout problem is considered with an example, where the effect of layout limitations on the plant structure is investigated. Finally, the applicability of the proposed approach to an industrial case study, the "streaming" problem in a manufacturing plant is also illustrated.

2.2 Problem Statement

The problem addressed in this chapter can be stated formally as follows:

Given:

- a set of process equipment units, indexed i, or $j = 1..n$
- a set of available locations, distributed over a 2-D area or a number of floors, and their coordinates, indexed $k = 1..K$
- the material flowrates between connected units in kg/s.
- the maximum number of available floors for the multilevel layout
- the purchase and installation cost of piping in $\$/m$, the floor construction cost in $\$/\mathrm{m}^2$
- the retrofit plant superstructure for the retrofit design problem
- space limitations for the retrofit problem
- minimum safety distance between units i and j which are considered as a source of hazards

Determine:

- the allocation of each unit to floors and location on the floors
- the optimal number of floors
- the optimal plant structure (processing units and connectivity network) for the retrofit case

Such that:

the cost of the layout is minimized.

In this work it is assumed that the layout area is discretized into a number of available locations (2-D or 3-D grids) which are represented by unique x, y and z coordinates. The size of each location is determined in order to allow access for inspection, maintenance and repair. The feasible allocation of each unit to each of the available locations may also given (Figure 2.1). This is determined by the unit size or other operating constraints. The same formulation is applicable to the design case. It should be emphasized that in other approaches

(Penteado and Ciric, 1996) the layout problem is treated as a continuous nonlinear non-convex optimization problem, because the equations needed to prevent two units from occupying the same physical space are non-convex. This results in a very difficult mathematical problem. The discretization proposed here avoids the problems of the nonlinearities and nonconvexities by transforming the problem into a mixed integer linear programming problem.

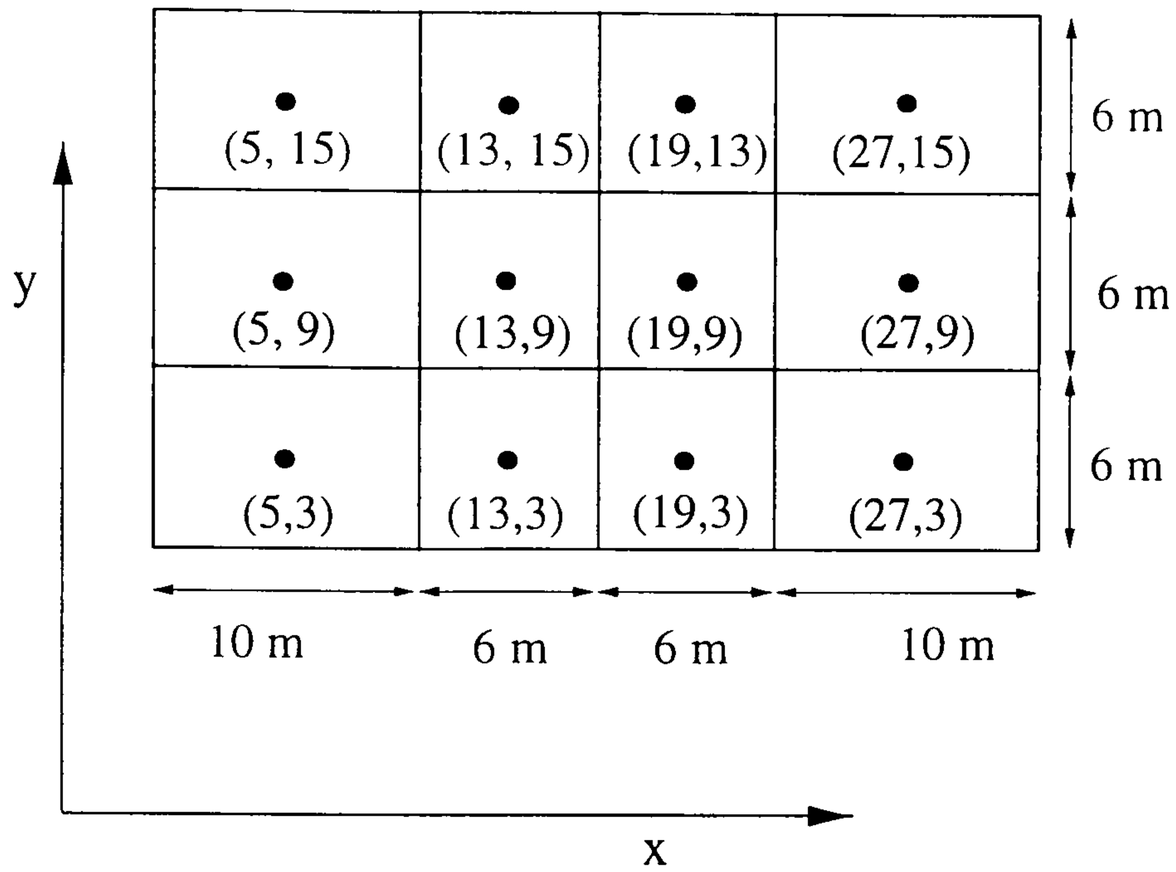


Figure 2.1: Discrete locations and their coordinates in a 2-D layout area

2.3 Motivating Example

Consider the Instant Coffee process shown in Figure 2.2 and first proposed by Jayakumar and Reklaitis (1996). Suppose that the connection cost between units and the floor construction cost is given. Is it possible to find the optimal allocation of units in a multifloor layout such that the total annual connection, pumping and floor construction cost is minimized? Are there any trade-offs between the capital and operating cost? Is there an optimal number of floors for which the above cost is minimized? These are some of the issues addressed in this chapter.

2.4 Mathematical Model

For the purpose of our analysis the following parameters and variables are introduced:

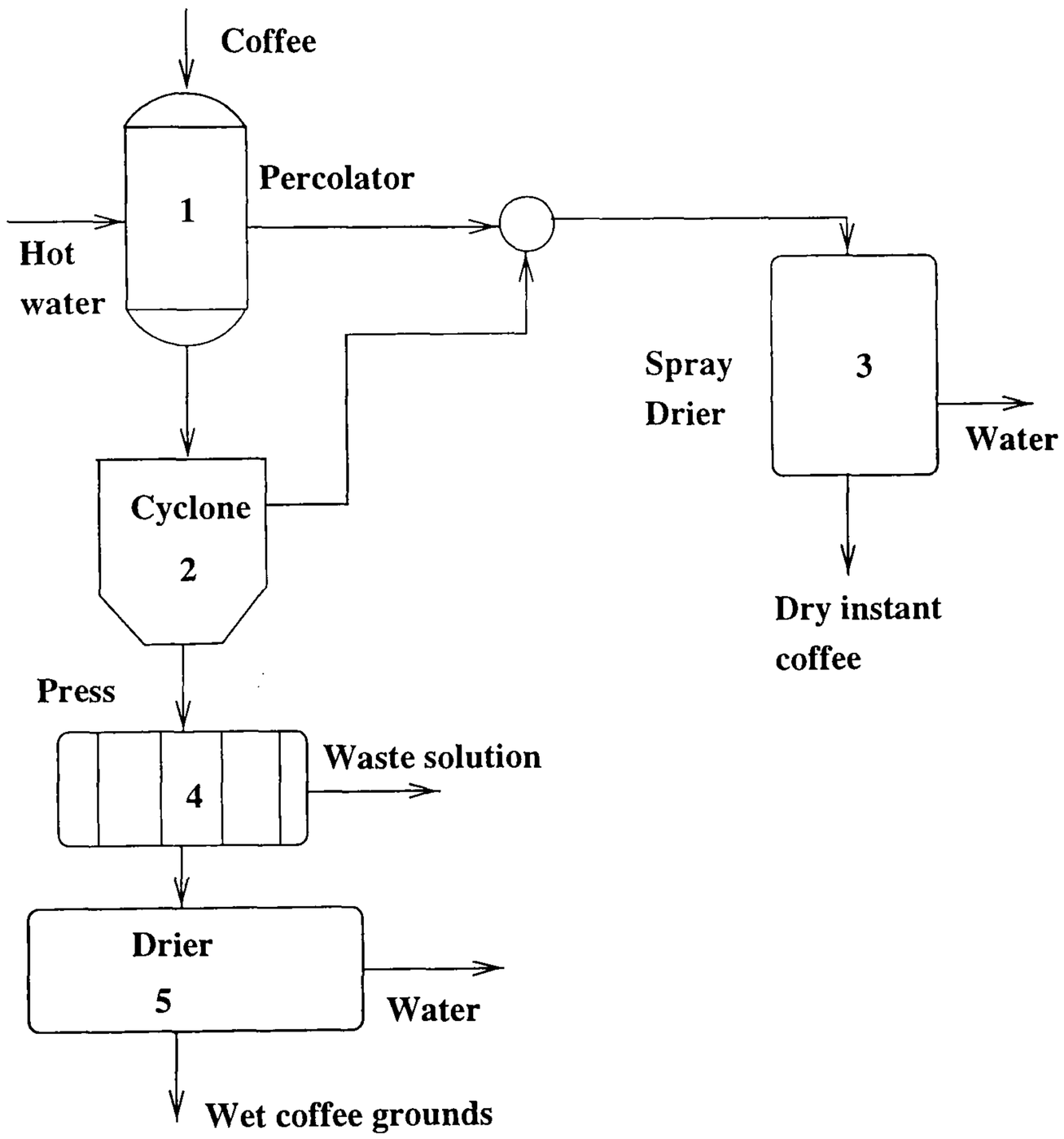


Figure 2.2: Flowsheet of Instant Coffee Process

Parameters:

n : total number of units

K : total number of grid points (locations)

CC_{ij}: connection cost between unit i and unit j in $\$/m$

CCF: Capital charge factor, set equal to 1/3 (Douglas, 1988), $(1/yr)$

CF_{ij}^{hor}: horizontal transportation cost of unit i to unit j in $\$/(m \cdot yr)$

CF_{ij}^{up}: upward transportation cost of unit i to unit j in $\$/(m \cdot yr)$

CF_{ij}^{down}: downward transportation cost of unit i to unit j in $\$/(m \cdot yr)$

FA: area per floor in m^2

FCC: floor construction cost in $\$/m^2$

x_k, y_k, z_k: coordinates of area k

Continuous Variables:

A_{ij}: vertical distance between unit i and unit j in the y direction if unit i is above unit j

AB_{ij}: vertical distance between unit i and unit j if unit i is on a higher floor than unit j

B_{ij}: vertical distance between unit i and unit j in the y direction if unit i is below unit j

BEL_{ij}: vertical distance between unit i and unit j if unit i is on a lower floor than unit j

L_{ij}: horizontal distance between unit i and unit j if unit i is to the left of unit j

NF: number of floors in the 3-D layout problem

R_{ij}: horizontal distance between unit i and unit j if unit i is to the right of unit j

x_i, y_i, z_i: coordinates of unit i

Binary Variables:

$$y_{ik} = \begin{cases} 1, & \text{if unit i is allocated to site area k} \\ 0, & \text{otherwise} \end{cases}$$

$$E_i = \begin{cases} 1, & \text{if unit i exist in the retrofit design problem} \\ 0, & \text{otherwise} \end{cases}$$

2.4.1 The Objective Function

The plant layout is formulated as an optimization problem where the cost of layout is minimized. This cost is comprised by two major terms: (i) the operating cost (upward and horizontal transportation cost) and (ii) the cost of investment (connection and floor construction). The possible allocation of units to different floors requires the use of different cost factors than those for the 2-D case. The additional piping cost for the elevation of materials to higher floors cannot typically be neglected and must be included in the objective function. In the case of a downward flow there is often no pumping cost due to gravity, but the connection cost ($/m) still exists. Finally, where two connected units are allocated to the same floor a (low) pumping and a connection cost are taken into account. So unlike other works (*e.g.* Jayakumar and Reklaitis (1996)) where arbitrarily cost values are assigned (especially where the distances can not be calculated explicitly) a more accurate objective function is presented in this work.

The transportation cost comprises three cost parameters, depending on the flow direction between the connected units:

- Upward cost, CF_{ij}^{up}. In this case there is typically a high transportation cost due to the height difference. For pumping of liquids this cost is a function of the flowrate between the connected units and of the height and given approximately by Coulson and Richardson (1985):

$$CF_{ij}^{up} = \text{Energy_unit_Cost} \cdot \text{Flow} \cdot \text{g} \qquad \$/m \cdot yr$$

The above cost must be multiplied by suitable variables representing the height difference. The gravity constant g is equal to 9.81 m/s^2, the flow must be given in kg/s and the energy unit cost in $\$/kwh$. The above expression is multiplied by 1.2-3 to account for

other factors such as the bend of the pipes, roughness of the pipe surface, corrosion etc. The final expression for CF_{ij}^{up} is:

$$CF_{ij}^{up} = \beta^{up} \cdot \text{Flow} \qquad \$/m \cdot yr$$

where β^{up} is a case depended constant which for the purpose of our analysis is taken equal to 1515 $\$ \cdot s/(kg \cdot m \cdot yr)$.

- Downward flow, CF_{ij}^{down}. In this case there is often no transportation cost since the flow is gravity driven.

- Horizontal cost, CF_{ij}^{hor}. This cost concerns two connected units located in the same floor. The transportation cost is a function of the flowrate and the distance. It can be taken approximately as 10% of the upward pumping cost and is given as follows (Coulson and Richardson, 1985):

$$CF_{ij}^{hor} = \beta^{hor} \cdot Flow \qquad \$/m \cdot yr$$

where β^{hor} is a case depended constant equal to 151.5 $\$s/(kg \cdot m \cdot yr)$ for the problems considered here.

The above cost parameter must be multiplied by the horizontal distance.

The direction matrix d_{ij} between two units is specified as in Jayakumar and Reklaitis (1996):

$$d_{ij} = \begin{cases} 1, & \text{if flow is from unit i to unit j} \\ 0, & \text{otherwise} \end{cases}$$

The annualized cost of connections between units, in $\$/m$, is included in the objective function together with the floor annualized construction cost. A connection cost is a function of the distance between two connected units in the x, y and z directions. Capital costs are transformed into annualised costs through the capital charge factor, CCF (Douglas, 1988).

The overall objective function of the plant layout optimization model is given by:

$$\begin{aligned} \min OF = & \sum_{((i,j),i<j)} [(d_{ij} \cdot BEL_{ij} + d_{ji} \cdot AB_{ij}) \cdot CF_{ij}^{up}] + \\ & \sum_{((i,j),i<j)} [CF_{ij}^{hor} \cdot (R_{ij} + L_{ij} + A_{ij} + B_{ij})] + \\ & \sum_{((i,j),i<j)} [CC_{ij} \cdot CCF \cdot (R_{ij} + L_{ij} + A_{ij} + B_{ij} + AB_{ij} + BEL_{ij})] + \\ & CCF \cdot FCC \cdot FA \cdot NF) \quad [\$/yr] \end{aligned}$$

2.4.2 Problem Constraints

Specific constraints are imposed in order to identify the relative positions of units and the distances between them. Here, the distance between two connected units is taken to be rectangular which is more appropriate in industrial problems than straight-line distances. This is defined by the following set of constraints:

$$R_{ij} - L_{ij} = \sum_{k=1}^{K} x_k \cdot (y_{ik} - y_{jk}), \quad i = 1..n-1, \quad j = i+1..n \tag{2.1}$$

$$A_{ij} - B_{ij} = \sum_{k=1}^{K} y_k \cdot (y_{ik} - y_{jk}), \quad i = 1..n-1, \quad j = i+1..n \tag{2.2}$$

$$AB_{ij} - BEL_{ij} = \sum_{k=1}^{K} z_k \cdot (y_{ik} - y_{jk}), \quad i = 1..n-1, \quad j = i+1..n \tag{2.3}$$

Constraint (2.4) specifies that unit i must be allocated to one of the given n locations, while constraint (2.5) specifies that each location may be occupied at most by one unit. The last constraint provides the flexibility to have more grids than units in case there is enough space.

$$\sum_{k=1}^{K} y_{ik} = 1, \qquad \forall i \tag{2.4}$$

$$\sum_{i=1}^{n} y_{ik} \leq 1, \qquad \forall k \tag{2.5}$$

Constraints (2.6) serve to find the optimal number of floors. Here, $NU(k)$ is the floor allocation of grid point k. For example if grids 1, 2, 3 and 4 belong to the first floor, the corresponding $NU(k)$ will be 1. If they belong to the second floor then $NU(k)$ will be 2. Depending on the trade-offs between capital and operating costs, equation (2.6) will force the creation of the minimum number of floors required. This also will eliminate degeneracies.

$$NF \geq y_{ik} \cdot NU(k) \qquad \forall i, k \tag{2.6}$$

Finally, non-negativity constraints are imposed for all the continuous variables. It must be emphasized that the variables $R_{ij}, L_{ij}, A_{ij}, B_{ij}, AB_{ij}, BEL_{ij}$ are not integer but continuous

variables. For example when unit 2 is allocated to the right of unit 3, then R_{23} takes a positive value while L_{23} is zero. This is due to the optimisation problem being solved involving minimisation of a distance related objective function. Consequently, only one variable *at most* of each pair - *i.e.* (R_{ij}, L_{ij}), (A_{ij}, B_{ij}) and (AB_{ij}, BEL_{ij})- is guaranteed to be non-zero at the optimal solution of each Linear Programming (LP) problem during the branch-and-bound procedure used for the MILP solution. The summation $(R_{ij} + L_{ij} + A_{ij} + B_{ij} + AB_{ij} + BEL_{ij})$ represents the total distance between units i and j. It is worthwhile to note that the variables AB_{ij} and BEL_{ij} determine automatically the floor sequence.

$$R_{ij} \geq 0, \quad L_{ij} \geq 0, \quad A_{ij} \geq 0, \tag{2.7}$$

$$B_{ij} \geq 0, \quad AB_{ij} \geq 0, \quad BEL_{ij} \geq 0, \tag{2.8}$$

$$y_{ik} = 0 \ \ or \ \ 1 \quad k = 1..K \quad i = 1..n \tag{2.9}$$

The coordinates for each unit (x_i, y_i, z_i) can be easily calculated, if required, by adding the following set of constraints:

$$x_i + y_i + z_i = \sum_{k=1}^{K} (x_k + y_k + z_k) y_{ik} \tag{2.10}$$

$$x_i + y_i - z_i = \sum_{k=1}^{K} (x_k + y_k - z_k) y_{ik} \tag{2.11}$$

$$x_i - y_i + z_i = \sum_{k=1}^{K} (x_k - y_k + z_k) y_{ik} \tag{2.12}$$

2.4.3 Overall Formulation

The overall formulation for the plant layout optimisation model is given by the following problem **[P1]**:

$$\begin{aligned} \min OF = & \sum_{((i,j),i<j)} [(d_{ij} \cdot BEL_{ij} + d_{ji} \cdot AB_{ij}) \cdot CF_{ij}^{up}] + \\ & \sum_{((i,j),i<j)} [CF_{ij}^{hor} \cdot (R_{ij} + L_{ij} + A_{ij} + B_{ij})] + \\ & \sum_{((i,j),i<j)} [CC_{ij} \cdot CCF \cdot (R_{ij} + L_{ij} + A_{ij} + B_{ij} + AB_{ij} + BEL_{ij})] + \\ & (\mathrm{CCF} \cdot \mathrm{FCC} \cdot \mathrm{FA} \cdot NF) \quad [\$/yr] \end{aligned} \tag{P1}$$

subject *to*

$$R_{ij} - L_{ij} = \sum_{k=1}^{K} x_k \cdot (y_{ik} - y_{jk}), \qquad i = 1..n-1, \quad j = i+..n$$

$$A_{ij} - B_{ij} = \sum_{k=1}^{K} y_k \cdot (y_{ik} - y_{jk}), \qquad i = 1..n-1, \quad j = i+1..n$$

$$AB_{ij} - BEL_{ij} = \sum_{k=1}^{K} z_k \cdot (y_{ik} - y_{jk}), \qquad i = 1..n-1, \quad j = i+1..n$$

$$\sum_{k=1}^{K} y_{ik} = 1, \qquad \forall i$$

$$\sum_{i=1}^{n} y_{ik} \leq 1, \qquad \forall k$$

$$NF \leq y_{ik} \cdot NU(k) \qquad \forall i, k$$

$$R_{ij} \geq 0 \quad L_{ij} \geq 0 \quad A_{ij} \geq 0$$

$$B_{ij} \geq 0 \quad AB_{ij} \geq 0 \quad BEL_{ij} \geq 0$$

The main advantage of the above formulation is the fact that it involves n^2 binary variables as opposed to other formulations where the number of variables is much greater (*e.g.* some of the formulations of the *quadratic assignment problem* where the number of integer variables is n^4). Thus, even large scale problems with number of units greater than 20-25 can be solved efficiently using a commercial mixed integer linear code (*e.g.* CPLEX). In some cases, it is desirable to place some equipment close together in configurations forming "sub-plants". These "sub-plants" may be spread rather far apart. The proposed formulation can handle such cases by imposing maximum distances between subsets of the equipment involved or by using simple integer cuts for the binary variables. Finally, it can easily accommodate locational constraints (*e.g.* due to safety considerations). For example, if it is required to fix the allocation of unit i to area k we can force the corresponding integer variable y_{ik} to take the value of 1. Similar constraints for a minimum distance (*e.g.* for safety) between two units can be easily included. Clearly the proposed formulation can also consider the two dimensional layout problem as a subproblem, using the same number of integer variables.

2.5 Handling Degeneracies

A major problem encountered during the solution of the MILP formulation **[P1]**, is the existence of degenerate solutions, i.e. there may exist many permutations of a feasible layout with exactly the same value of the objective function. Each permutation may often be obtained from the

previous one by shifting its allocation by one site area. In fact, degeneracies may exist due to any symmetric layout geometry. These are due to the fact that in [**P1**] all contributions to the objective function depend on the *relative* position of the units. However, some of the degeneracies will be eliminated if the locations of feed, products and utility ports pre-assigned to specific locations. It is difficult to develop general methods to avoid degeneracies since they depend not only on the layout geometry but also on the number of units.

One general way to eliminate some degeneracies is to introduce additional preferences in the allocation of processing units. For example, prefer units closer to the origin of the axis ($x = y = 0$). This can be done by introducing some penalty in the objective function so as to give different values to the absolute position of the units.

Here we propose another way to handle degeneracies for the most symmetric case (equal segments in x and y direction). For example, the two solutions (denoted by circles and crosses) shown in figure 2.3 are equivalent, but one (denoted by circles) results in a layout more compact (around the $x = y = 0$ coordinate). In this case degenerate solutions can be obtained by:

1. Desplacing each unit by an equal number of grids (left or right/up or down).
2. Rotating a given configuration of units and applying shifts to maintain layout feasibility when encountering a boundary grid (left/right top/bottom)

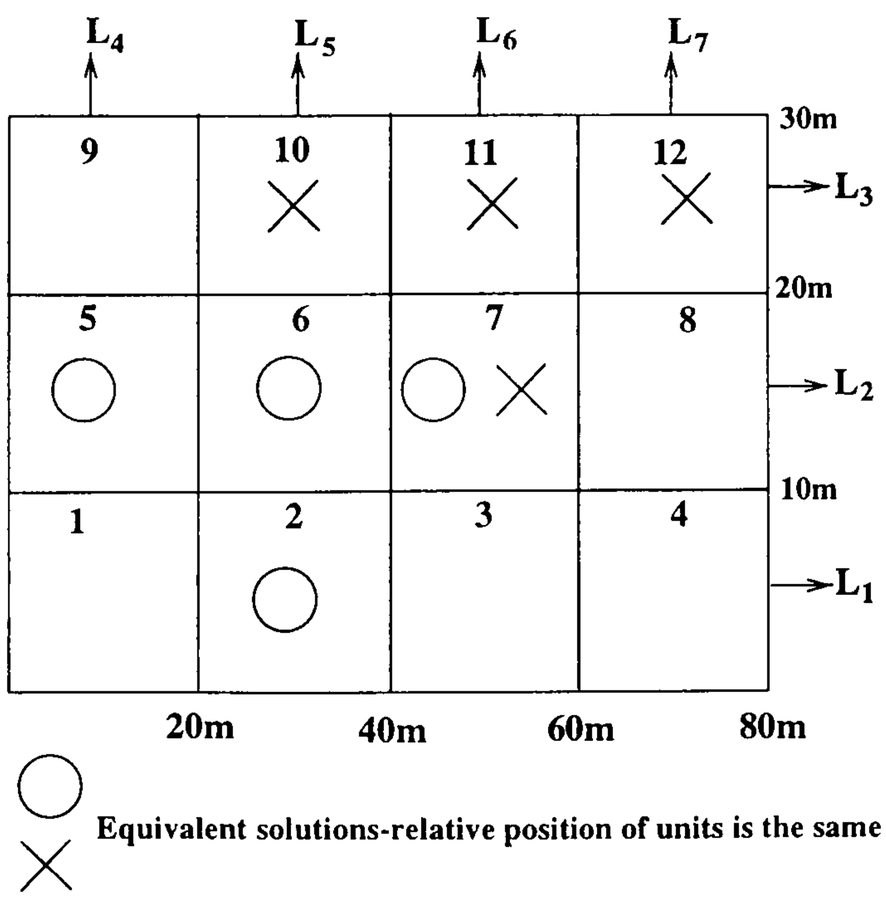


Figure 2.3: Degeneracies in the optimal plant layout problem

If no constraints imposing minimal distance between units exist (e.g. due to safety considerations), then forcing at least one unit to be in row 1 and at least one unit to be in column

1 (for the 2-D geometry) will eliminate many of the degeneracies generated by the above case 1 with no loss of optimality. Another way to handle degenerate solutions is by adding the following constraints in order to obtain the solution closest to the left hand and bottom corner of the site area:

$$\sum_i \sum_{k \in L_m(k)} y_{ik} \leq \sum_i \sum_{k \in L_{m-1}(k)} y_{ik} \cdot \text{MNU} \tag{2.13}$$

where $L_m(k)$ and $L_{m-1}(k)$ are two neighbour subsets of areas (rows or columns in the 2-D layout area) for which the side difference (x and y directions) is zero. MNU is the maximum number of units which can be allocated in each subset of areas considered. For example according to Figure 2.3 the above constraints must be applied for L_2 (grids 5, 6, 7, 8) and L_1 (grids 1, 2, 3, 4) since they have the same side (y directions). Here MNU is 4. Similarly, the same constraints will be also applied for L_5 (grids 2, 6, 10) and L_4 (grids 1, 5, 9) (same size in the x direction). In that case MNU is 3. It is clear that for the simple example considered in Figure 2.3 the above constraints will enforce the creation of the solution denoted by circles instead of its equivalent denoted by crosses, thus resulting in a more compact layout. Similar constraints can be also imposed for the 3-D optimal layout problem taking into account the z direction as well.

However, it should be emphasized that the above methods only apply to the case of equal segments in the x and y direction and the proposed constraints (2.13) can generate suboptimal solutions in other cases.

2.6 A Heuristic Method for the Reduction of the Computational Cost

The above rigorous mathematical approach for the plant layout can lead to good solutions in a reasonable computational time for medium to large size problems (up to 20-25 process units). However, for some problems of industrial nature with a number of equipment units greater than 25 the computational cost can increase considerably. Two solutions are proposed for this case only.

First, a *heuristic* method is proposed for the 2-D layout based on the pre-allocation of specific units. Although in such a way suboptimal solutions may be obtained, several tests have

shown that these solutions are very close to the optimal. The steps of the proposed method are described as follows:

1. Find the two units with the largest sum of flowrates between them (highest degree of connectivity) and locate them at two central site areas.

2. Find a third unit which has the highest degree of connectivity to the two already fixed units.

3. Allocate this unit at an area so that the connection cost between itself and the two fixed units is smallest.

4. The fourth unit is chosen and located in a similar way by treating the first three units fixed.

5. Continue in the same way until the number of the unallocated units can be handled by the optimizer. This number is about 25-30 units.

Having fixed the allocation of specific units by setting the corresponding integer variables to one, the optimization procedure will then decide about the optimal allocation of the remaining units. In this case the integer variables for the unallocated units will be zero for the areas occupied by the units which were determined by the proposed heuristic approach. An extension of the above method to the 3-D problem is also possible.

In practice, the allocation of units to some of the site areas may be prohibited due to safety or operational considerations. Thus, imposing such constraints the computational cost can be reduced without the need to use the above algorithm. An alternative way is to use *aggregate equipment modules.* A module would include a group of units which have similar operating characteristics or high degree of interconnection. Once the choice of modules has been made and equipment in each module has been specified (including relative position), the plant layout problem takes the form of deciding the relative position of the plant modules.

2.7 Motivating Example Revisited

Consider again the instant coffee process shown in Figure 2.2 . Since the real connection cost is now taken into account, the solution where units are stacked one on top of the other has

now a cost and thus is not optimal. Following our approach there is no need for the inclusion of hypothetical units to avoid zero cost as in Jayakumar and Reklaitis (1996).

Four cases are considered: the optimal allocation of equipment on two, three, four and five floors. For the sake of clarity in our presentation only the x and z directions are considered. In principle, the optimal number of floors could have been directly obtained. However, here we are interested in depicting the trade-offs between capital (connection) and operating (pumping) cost. For this example floor construction cost is not taken into account. Each case is studied for two different sets of connection costs. The first set includes typical values for connection costs (Table 2.1) while the second assumes zero connection cost. Other cost data given in Table 2.2. The commercial MILP solver CPLEX V4.0 was used for the solution of all the problems. The initial layout geometry is assumed to include 4 grids in the x direction with grid sizes as in Figures 2.4 to 2.8. Each processing unit is allowed to be allocated to any available grid. The results for each case are summarised below:

Stream	Connection cost, $\$/(m \cdot yr)$
(1,2)	60
(2,4)	40
(4,5)	50
(2,3)	60
(1,3)	70

Table 2.1: Connection cost for the illustrative example

Stream	CF_{ij}^{up} $\$/m \cdot yr$	CF_{ij}^{hor} $\$/m \cdot yr$
(1,2)	166.7	16.7
(1,3)	249.9	24.99
(2,3)	41.6	4.16
(2,4)	124.2	12.42
(4,5)	93.7	9.37

Table 2.2: Cost data for the motivating example

Two Floor Levels

- Case 1. An optimal layout with an annual cost of 2172 $\$/yr$ is obtained (Figure 2.4). Units 1, 2 and 4 are allocated on the first floor with all the other units on the ground floor. Unit

3 is allocated below unit 1 (largest flow in the plant) in order to minimize the transport cost. Comparing to Jayakumar and Reklaitis (1996) a different partition is obtained. Their approach results in an "optimal" partition 1,2,3,4(first floor)/5,6,7(ground floor). Units 5 and 6 are hypothetical units which serve to avoid zero operating cost. Note also that the geometry for our approach is given assuming that each floor has a maximum capacity of 4 units.

- Case 2. If zero capital connection costs are assumed the optimal layout is the same. The objective takes the non realistic value of 417 $\$/yr$. Thus, this layout minimizes the pumping cost according to the allocation of units.

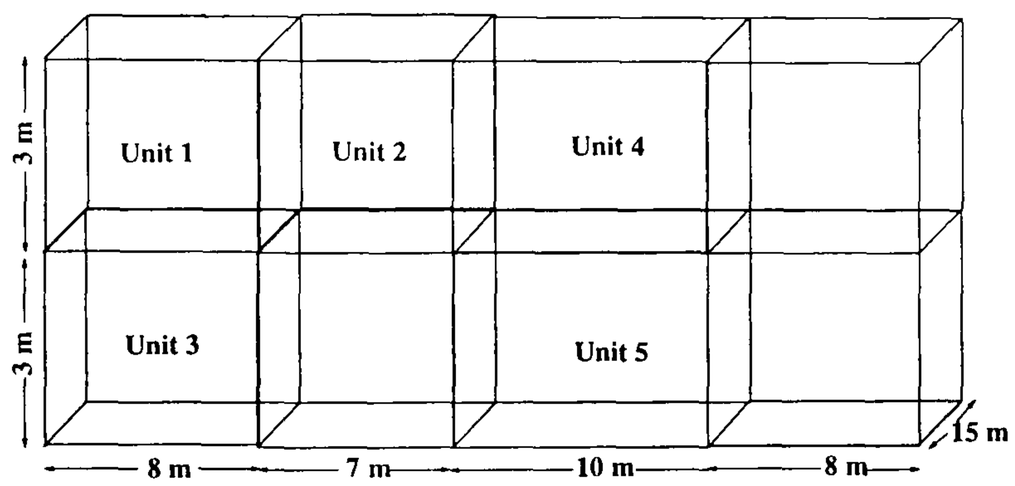


Figure 2.4: Optimal layout on two levels-case 1 and 2

Three Floor Levels

- Case 1. A less expensive layout with a total annual cost of \$1308 is obtained (Figure 2.5) compared with the two level approach. Unit 1 is allocated on the second floor, units 2 and 4 on the first and units 3 and 5 on the ground floor. Again the results are different from the optimal partition of Jayakumar and Reklaitis (1996) which was 1,2/3,4,5/6,7. The reduction in cost is due to the smaller pumping cost. Therefore, having one more floor the units are allocated in such way (the one below the other) that the pumping cost (due to the height difference) is less than in the one level problem.

- Case 2. With zero connection cost the same layout is obtained as in case 1.

Four Floor Levels

- Case 1. The same layout is obtained as with three floors (Figure 2.6). Here the extra floor does not improve the objective function and it is not utilized. This is because,

although it would further reduce the pumping cost, the connection cost would increase. This highlights the trade-offs between the two cost factors.

- Case 2. A different layout is obtained compared with case 1 (Figure 2.7). Unit 1 is allocated on the third floor, unit 2 on the second, unit 3 on the first and unit 4 and 5 on the ground. The extra floor is now used to minimize the pumping cost allocating the connected units one below the other. This confirms the trade off between the connection and pumping cost. Since the connection cost is zero, the problem is trying to minimize only the pumping cost. The optimal partition of Jayakumar and Reklaitis (1996) is again different (1/2/3,4/5,6,7).

Five Floor Levels

- Case 1. As expected, the optimal layout is exactly the same as in the three level approach. The two extra floors are not required.

- Case 2. Here in the optimal layout (Figure 2.8) units are stacked one below the other, a situation leading to gravity flows only, to give a zero operating cost.

Concluding, the proposed layout approach provides not only the optimal partition of units between floors (see for example Jayakumar and Reklaitis (1996)) but also their exact position. More realistic cost values can then be considered taking into account the connection cost. The above illustrative example shows some trade offs between the pumping cost (due to the height difference) and the connection cost. Therefore, useful information can be obtained about the optimal number of floors required.

2.8 Trade-offs Between Capital and Operating Cost in the 3-D Layout Problem

The proposed formulation for the 3-D optimal layout includes the floor construction cost in the objective function. This gives the opportunity to explore possible trade-offs between pumping and capital cost including the floor construction cost.

Consider the case study from Barbosa-Povoa (1994)(Figure 2.9). It is an industrial multipurpose batch plant, with a high degree of connectivity and the total number of units is 18.

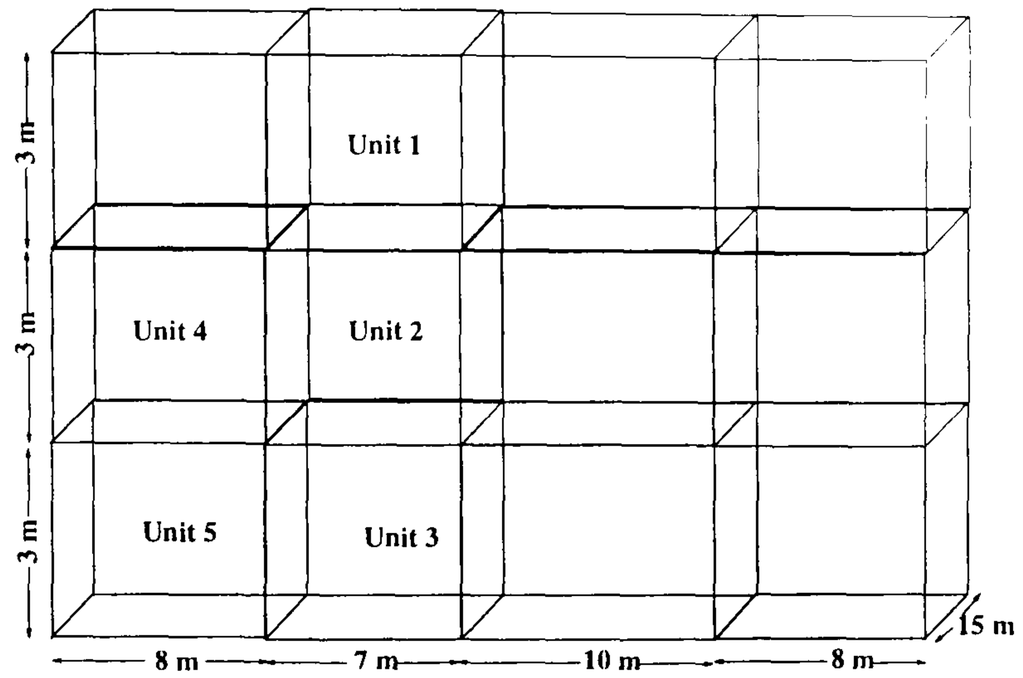


Figure 2.5: Optimal layout on three levels-case 1 and 2

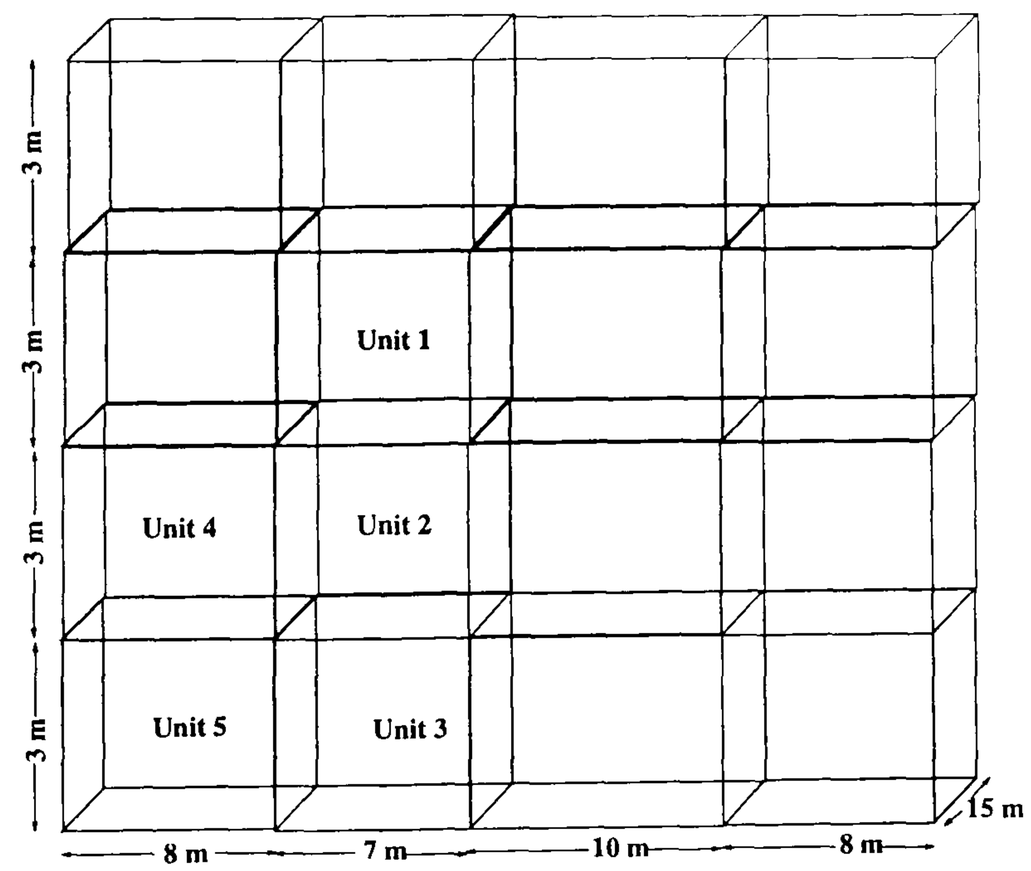


Figure 2.6: Optimal layout on four levels-case 1

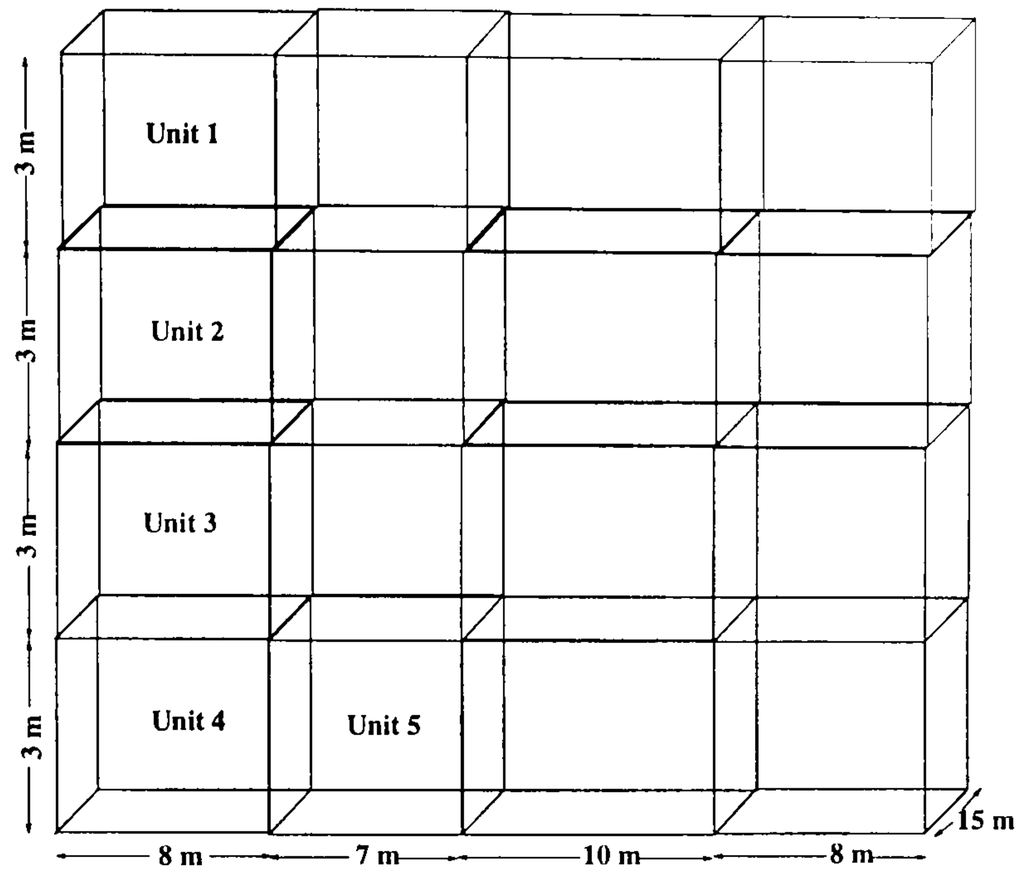


Figure 2.7: Optimal layout on four levels-case 2

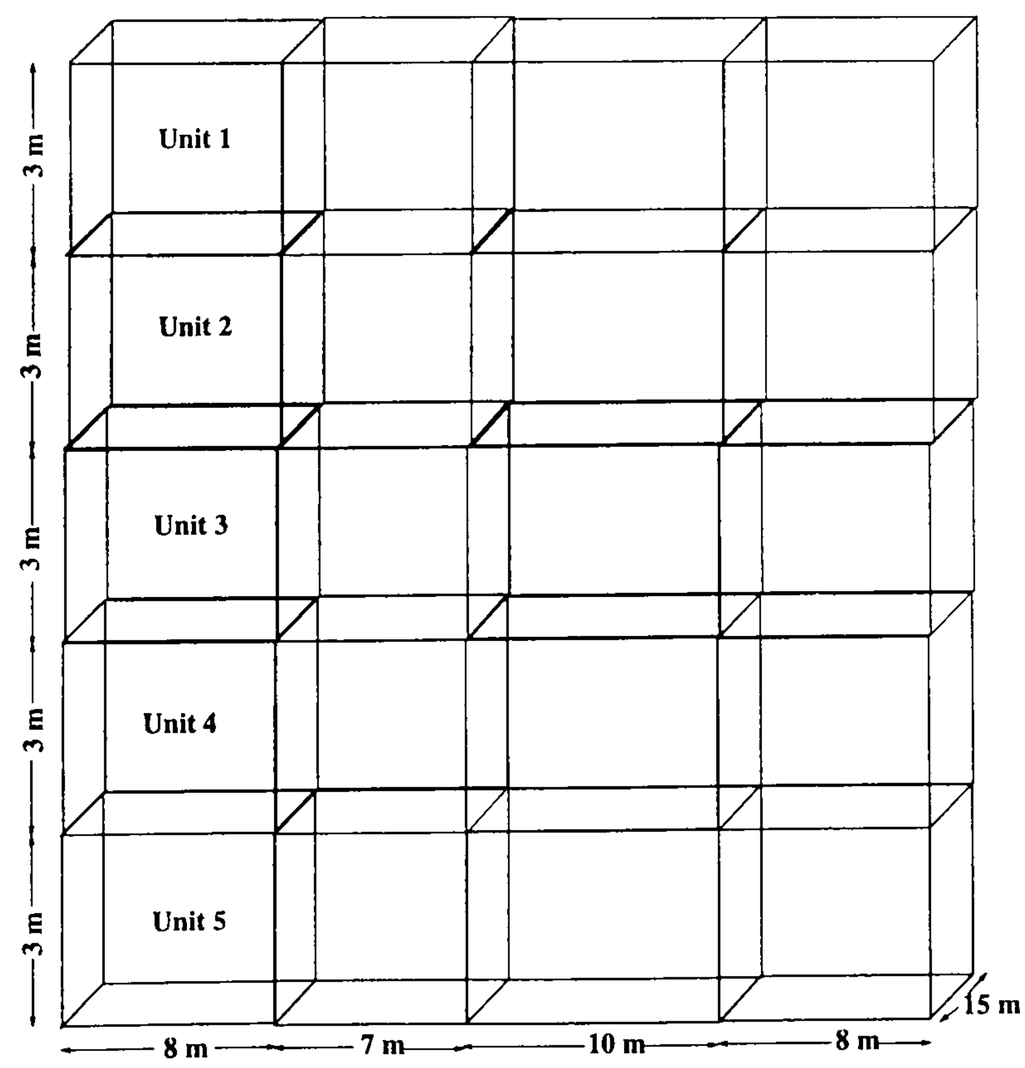


Figure 2.8: Optimal layout on five levels-case 2

It is assumed that the connections have different nominal diameters. The purchase cost in $\$/m$ is given in Table 2.3. The floor construction cost, for a typical floor heigh of 4 m, in approximately current values is given in Table 2.4 (taken from the Institute of Chemical Engineers, 1988). Although the formulation can determine the optimal number of floors directly, in order to illustrate the trade-offs between capital and operating cost we solve the problem parametrically for different number of floors.

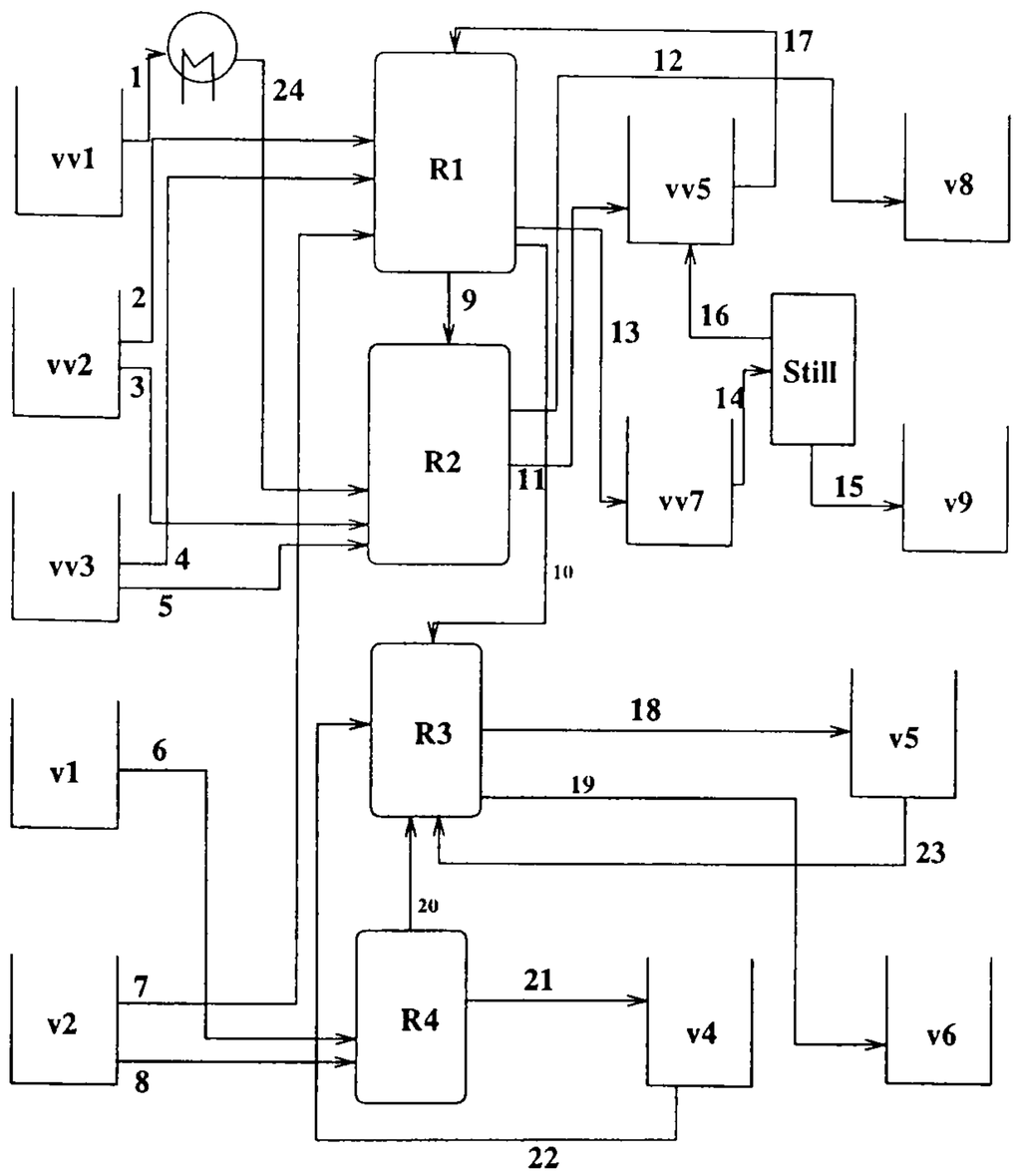


Figure 2.9: Flowsheet of the second example

The optimal multifloor layout problem is thus considered for the cases of having two, three, four and five floors. The layout geometry for each problem is discretized into a number of 3-D grids. For example, for the two floor case, the grid coordinates are given in Table 2.5. Here, each floor is discretised into 9 grids of size 56 m^2 each. Full flexibility is allowed for the allocation of units to grid areas. The total area available per floor is 504 m^2 and the corresponding floor construction cost is 500 $\$/m^2$ (Table 2.4).

The optimal plant layout in two, tree, four and five floors is depicted in Figures 2.10 to 2.13 respectively. In all cases units are allocated in such a way that the high upward cost is minimised. Substantial reduction of the pumping cost is achieved as the number of floors increases (see Table 2.6). Units are stacked one below the other in order let as many flows as possible be aided by gravity. There is a trend which is worth noticing. The floor construction cost increases as the number of floor increases but the pumping cost decreases. These trade-

Connection number	CC_{ij} $\$/m$	CF_{ij}^{up} $\$/yr$	CF_{ij}^{hor} $\$/yr$
1	200	1085	108.5
2	240	1227	122.7
3	230	1181	118.1
4	240	1227	122.7
5	230	1181	118.1
6	160	898	89.8
7	240	1227	122.7
8	160	890	89
9	230	1262	126.2
10	170	934	93.4
11	270	1767	176.7
12	270	1767	176.7
13	280	1838	183.8
14	170	1838	183.8
15	170	919	91.9
16	300	919	91.9
17	250	2686	268.6
18	250	1398	139.8
19	250	1398	139.8
20	175	934	93.4
21	170	890	89
22	175	934	93.4
23	140	404	40.4
24	230	1181	118.1

Table 2.3: Cost data for the second example

Cost, $\$/m^2$	Area, m^2
480	500-700
500	400-500
520	300-400
560	250-300
610	200-250

Table 2.4: Floor construction cost data for the second example

offs result in an optimal number of floors together with an optimal equipment layout. For the example considered here the optimal number of floors is three (Table 2.6) and the corresponding total annual cost is 240,000 $\$/yr$. However, the total cost is rather insensitive to the number of floors.

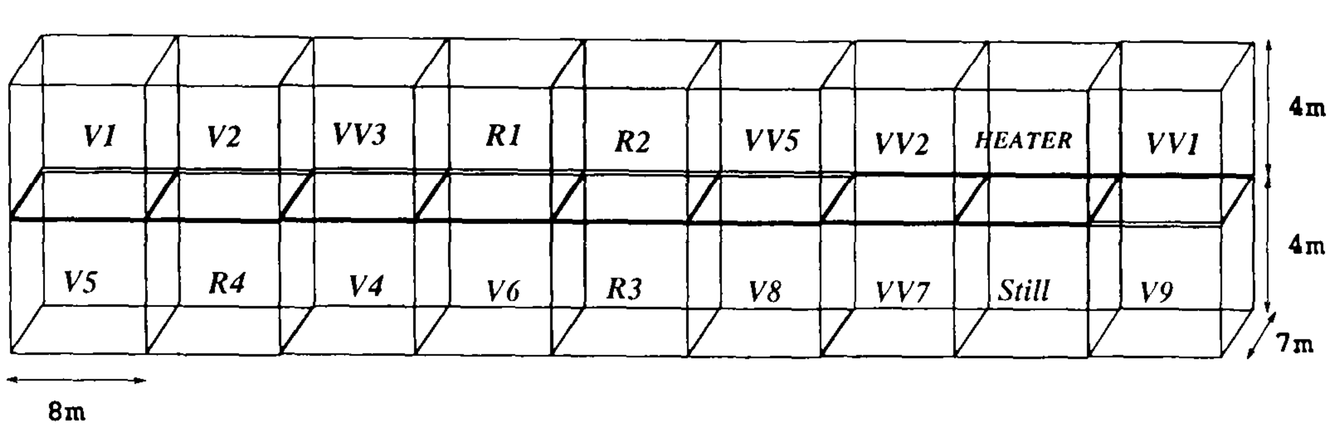


Figure 2.10: Optimal plant layout in two floors for the second example-case 1

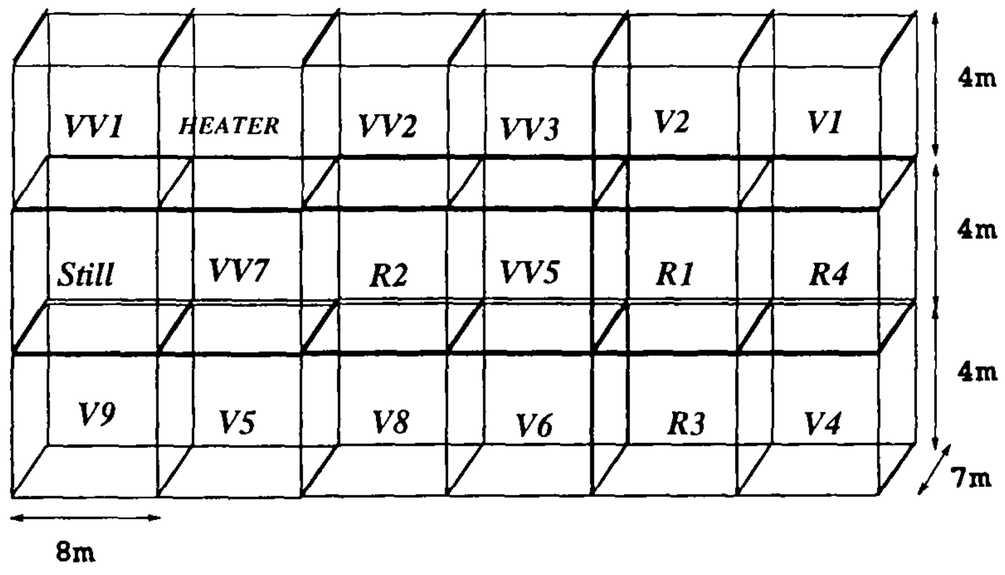


Figure 2.11: Optimal plant layout in three floors for the second example-case 1

The same case study is considered for another geometry where the allowable number of units is greater than one in all directions. For this purpose 5 grids are assumed for the x direction and 2 for the y direction. The optimal layout in two floors is shown in Figure 2.14. The same trend holds as in the previous case. The units become stacked one above another in order that as many flows as possible are aided by gravity, and the floor construction cost increases as the number of floors increases. The optimal number of floors is again three in that case but the annualised cost is marginally lower (238,700 \$/yr) compared with the previous geometry (Table 2.7). It should be noted that the annualized layout cost for this case and for 4 floors (269,100 \$/yr) differs from that of the previous case (254,00 \$/yr) since the layout geometry is different.

grid number	x-coordinates m	y-coordinates, m	z-coordinates, m
1	4	3.5	6
2	12	3.5	6
3	20	3.5	6
4	28	3.5	6
5	36	3.5	6
6	44	3.5	6
7	52	3.5	6
8	60	3.5	6
9	68	3.5	6
10	4	3.5	2
11	12	3.5	2
12	20	3.5	2
13	28	3.5	2
14	36	3.5	2
15	44	3.5	2
16	52	3.5	2
17	60	3.5	2
18	68	3.5	2

Table 2.5: Coordinates of the allocation areas for the second example

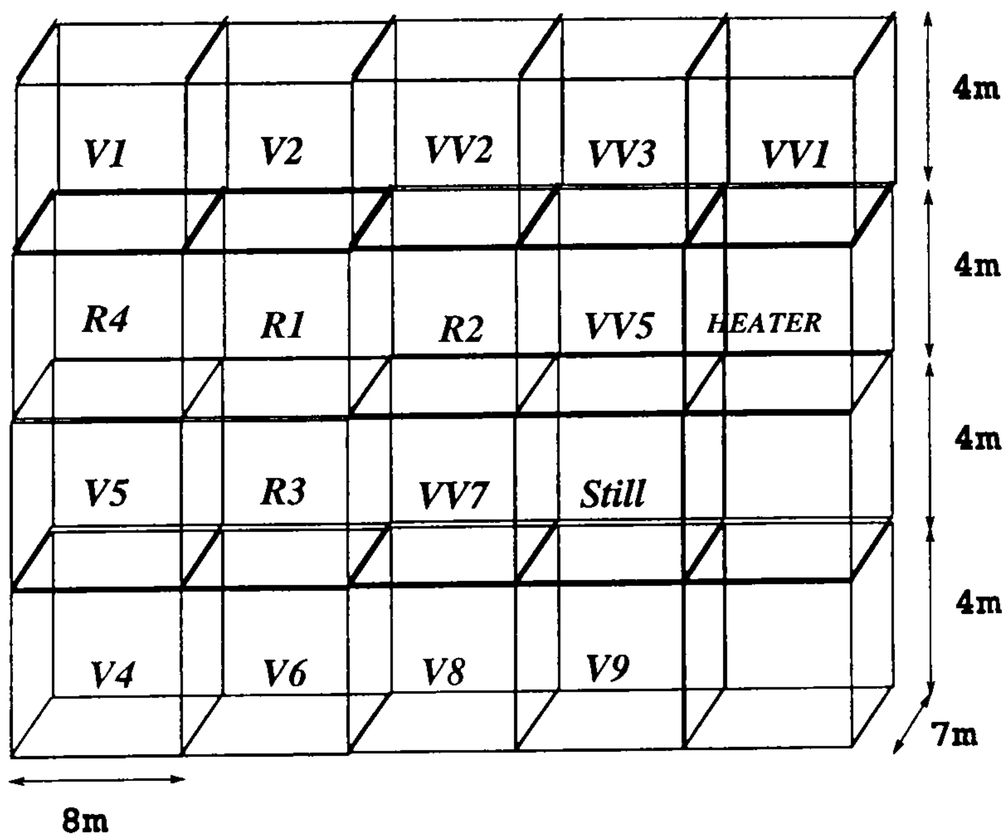


Figure 2.12: Optimal plant layout in four floors for the second example-case 1

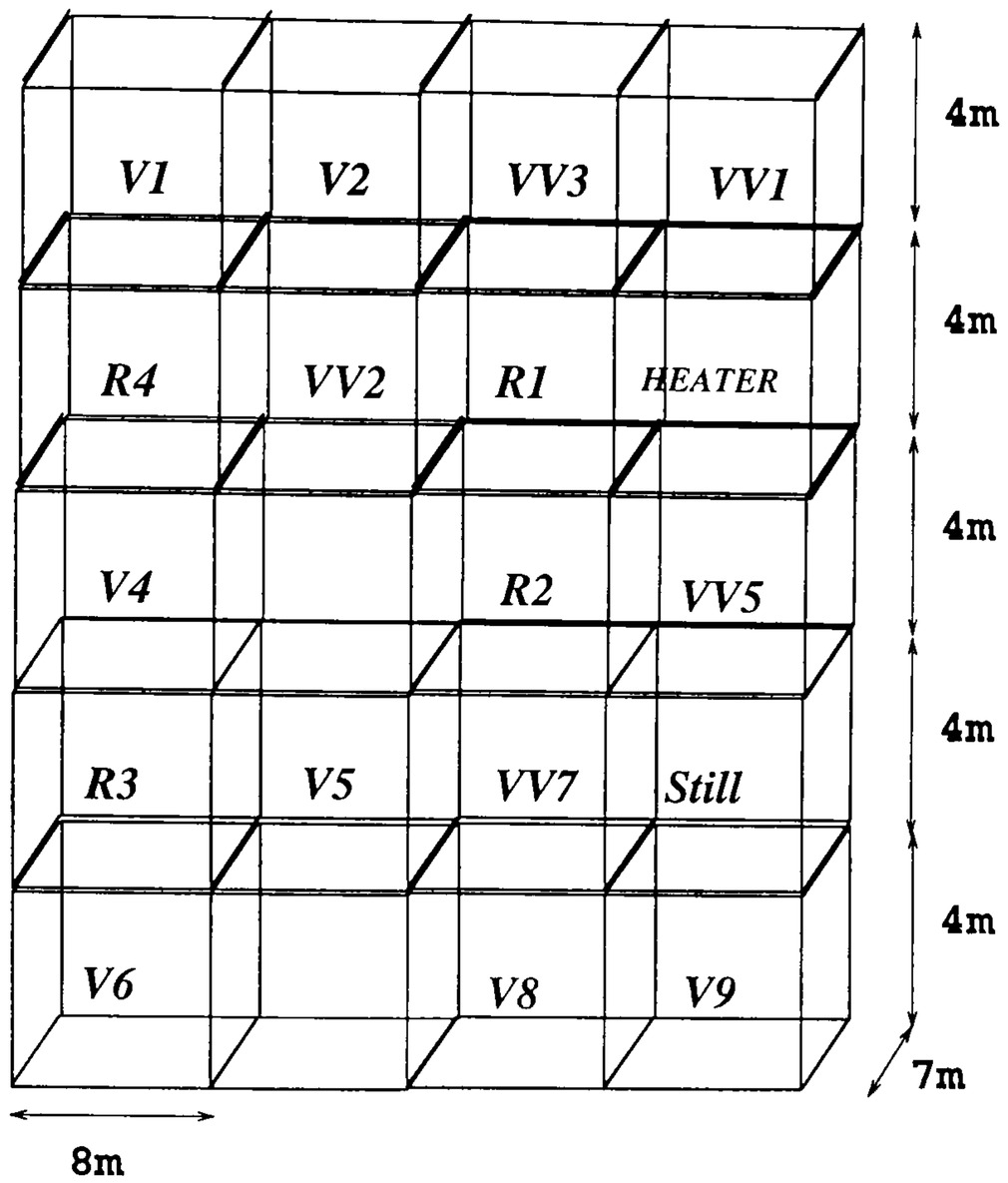


Figure 2.13: Optimal plant layout in five floors for the second example-case 1

Number of Floors	Transportation cost, $/yr	Connection cost, $/yr	Floor construction cost $/yr	Total cost $/yr
2	57,000	45,000	168,000	270,000
3	35,000	31,000	174,000	240,000
4	22,000	23,000	209,000	254,000
5	17,000	19,000	224,000	267,000

Table 2.6: Optimization Results for the second example-case 1

Number of Floors	Transportation cost, $/yr	Connection cost, $/yr	Floor construction cost $/yr	Total cost $/yr
2	43,800	36,900	179,100	259,800
3	27,800	36,400	174,500	238,700
4	16,700	19,700	232,700	269,100

Table 2.7: Optimization Results for the second example-case 2

2.9 Layout Considerations in the Retrofit Design of Multipurpose plants

The proposed approach for optimal layout can be coupled with the retrofit design/scheduling problem in order to take into account possible layout limitations early in the retrofit decisions. Layout considerations have been taken into account in the retrofit design of multipurpose plants, in a simplified way by Barbosa-Povoa (1994). For each equipment a footprint was assumed (given by a fixed term and an equipment size dependent term). Space availability constraints influence the choice of whether or not to use some of the units. The retrofit design model developed by Barbosa-Povoa (1994) is used here together with the proposed layout model discussed in section 4, for the optimal retrofit design case. In the model of Barbosa-Povoa, (1994) (not described here) binary variables describing the existence of equipment units and continuous variables describing the capacity of units or connections are created for any new units potentially added as part of the retrofit. For the existing units these values are fixed and already known.

The layout constraint concerning the allocation of units is written as follows:

$$\sum_{k=1}^{K} y_{ik} = E_i \quad \forall i$$

where E_i is a binary (0-1) variable. If an item of equipment i is included in the design ($E_i = 1$), then the above constraint ensures that it is placed at exactly one position in the layout. On the other hand, if the item is not selected ($E_i = 0$), then this constraint will force all position variables y_{ik} for this item to zero.

The connection cost is again taken into account in the objective function and includes two terms: one is a fixed capital cost which as before is taken to be a function of the length of the connection, and the other represents a size dependent capital cost. The length of each connection is calculated explicitly by the layout model equations. The bilinear term arising due to the product of existence and length variables (e.g. $E_c \cdot l_c$) is reformulated to a linear form using standard techniques (Grossmann *et al.*, 1993).

A case study taken from Barbosa-Povoa (1994) is used as an illustrative example. The objective is to redesign a plant in order to accommodate new demands for product states S5 and S6, modified from 100 tonnes to 150 tonnes. The operation is non periodic over a time horizon

BIBL LONDON UNIV.

of 8 hours as in the original process. The characteristics of the new equipment potentially to be used in the new plant are shown in Tables 2.8 and 2.9 and the superstructure describing the new possible expanded plant is shown in Figure 2.15. Combining the plant/process information, the maximal State-Task Network (describing all potentially feasible operations) is derived as shown in Figure 2.16 (Crooks, 1992; Barbosa-Povoa, 1994). In the retrofit design problems the objective is the maximisation of the annualised profit. An annual working basis of 8150 hours was assumed and the product values and the prices of the raw materials are given in Table 2.10. A cost of 0.01 \$/kg is also taken for operating cost depending on the batch size. None of the existing units were considered eligible for removal.

Unit	Suitability	Minimum capacity [te]	Maximum capacity [te]	Cost: Fixed [10^3 \$] Variable [\$/kg]
Unit R2 (R2)	T1-T2	10	200	20 - 0.1
Unit R4 (R4)	T3-T4	10	200	35 - 0.3
Unit R5 (R5)	T4	10	200	25 -0
Vessel V4a (V4a)	State S4	5	100	5-0.01
Vessel V5a (V5a)	State S5	10	100	3
Vessel V6a (V6a)	State S6	10	100	3

Table 2.8: Unit characteristic for the retrofit example

Connection Number	Capacity [te]	Fixed Cost [\$ /m]	Variable Cost [\$ /kg]
7	Unl.	230	0.001
8	Unl.	180	0.001
9	Unl.	270	0.001
10	Unl.	200	0.001
11	Unl.	350	0.0015
12	Unl.	260	0.001
13	Unl.	440	0.0015
14	Unl.	180	0.001
15	Unl.	220	0.001
16	Unl.	180	0.001
17	Unl.	160	0.001
18	Unl.	200	0.001
19	Unl.	300	0.1
20	Unl.	200	0.001
21	Unl.	300	0.001
22	Unl.	200	0.001

Table 2.9: Connection characteristic for the retrofit example

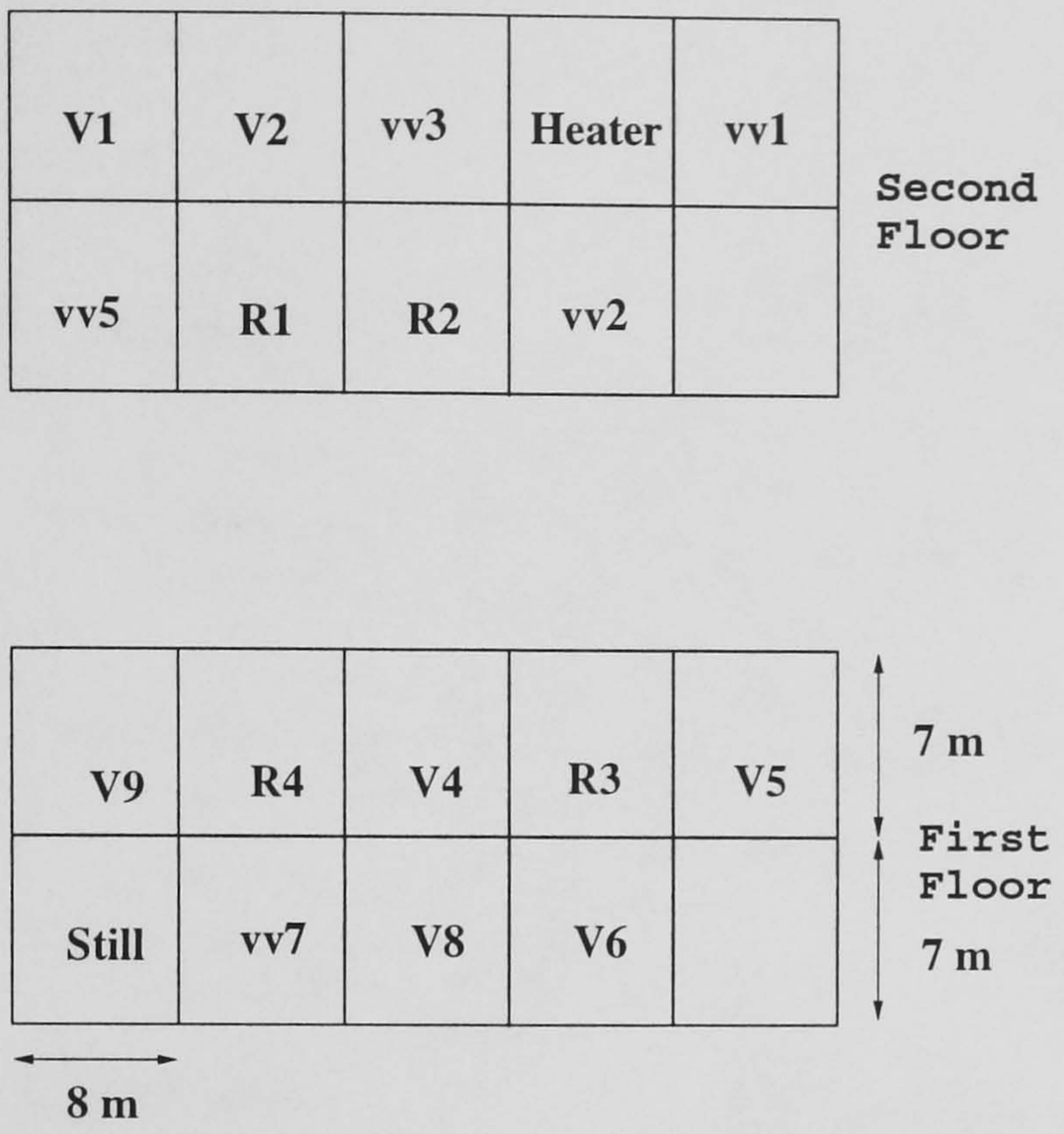


Figure 2.14: Optimal plant layout in two floors for the second example-case 2

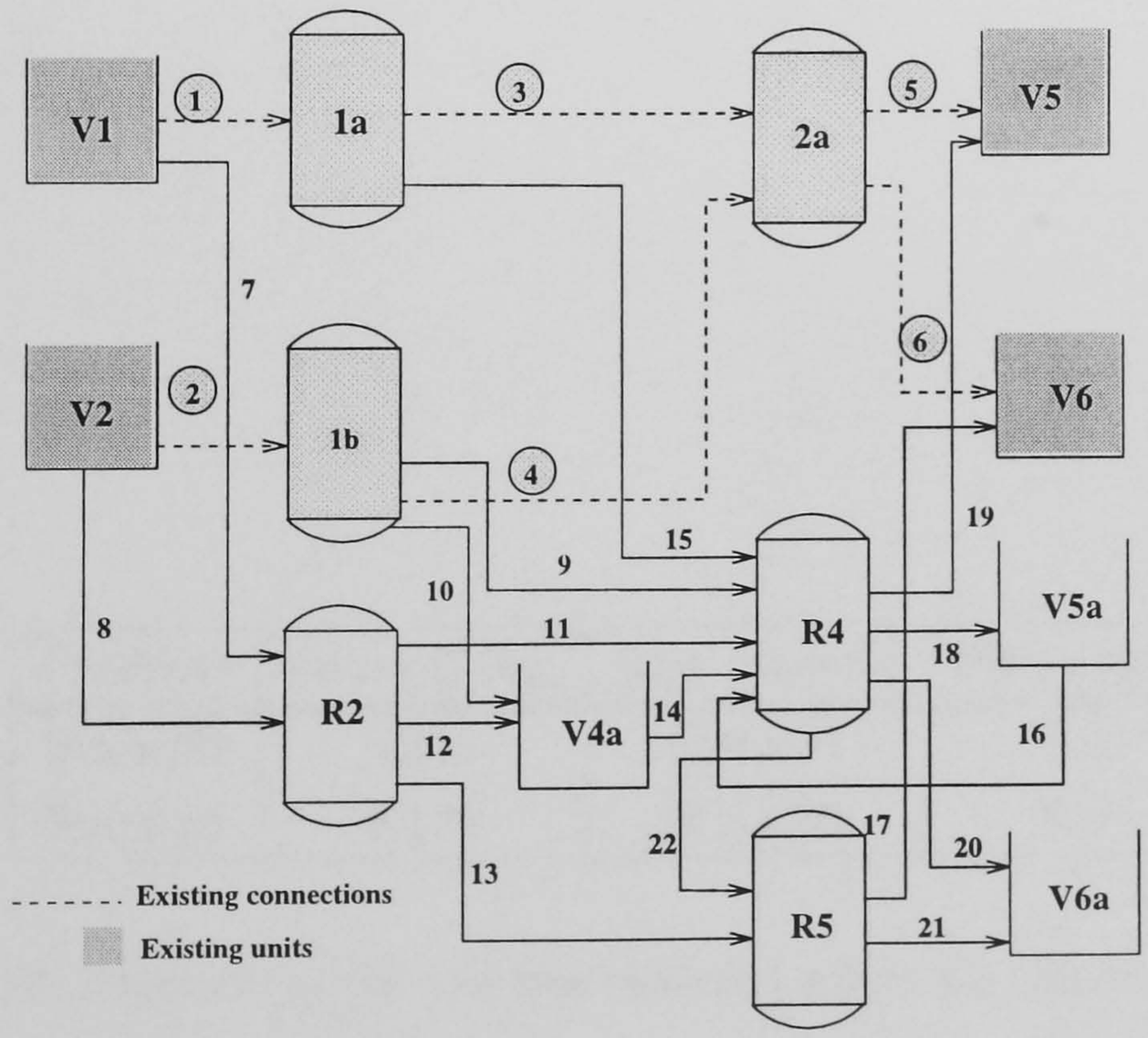


Figure 2.15: Plant Superstructure for the retrofit example

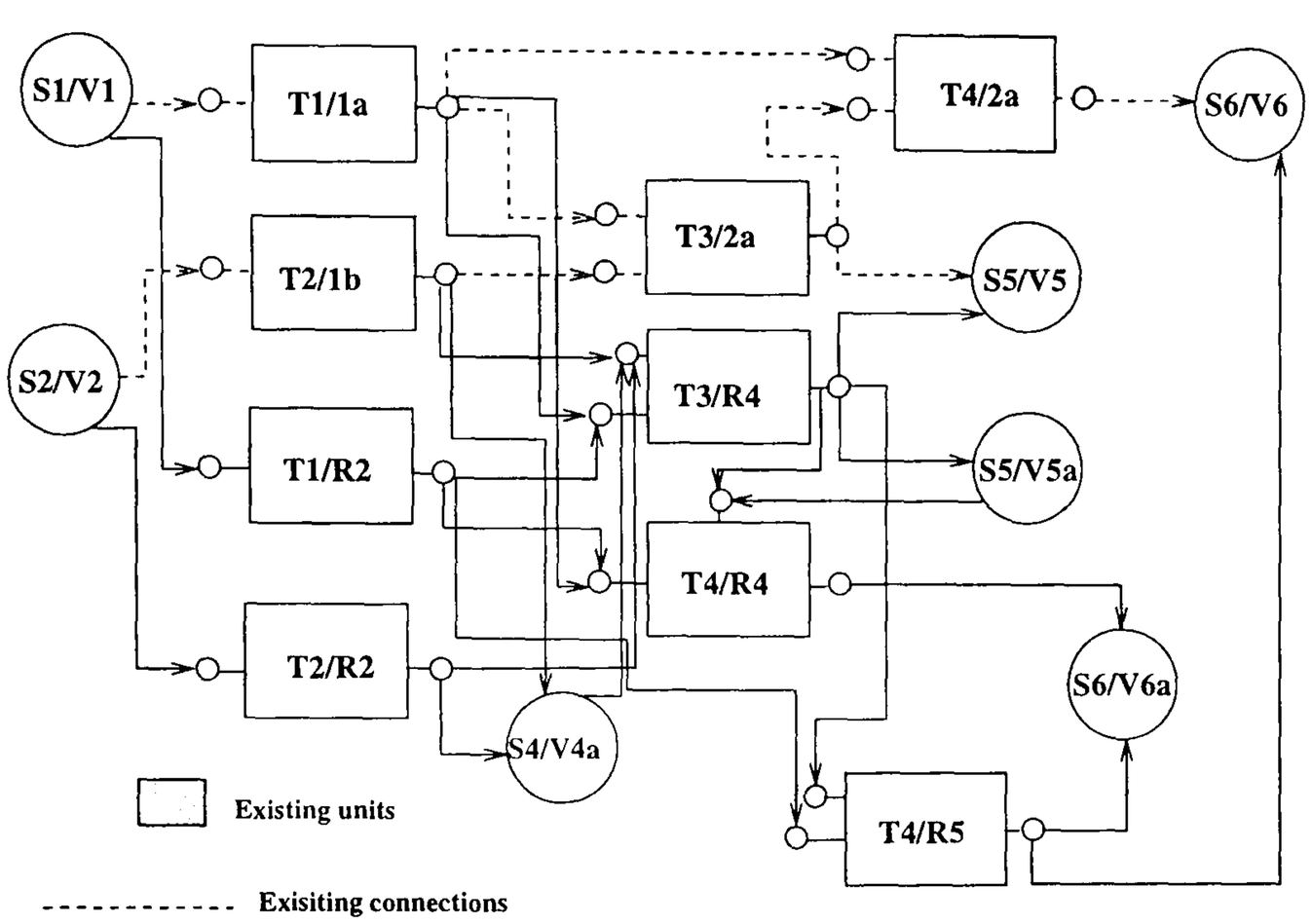


Figure 2.16: Maximal State-Task Network for the retrofit example

Products	values [$/kg]	Raw material	Prices [$/kg]
State S5	0.115	State S1	0.01
State S6	0.125	State S2	0.01

Table 2.10: Product values and raw material prices for the retrofit example

Two cases were considered:

- Case 1- the retrofit design of the plant without layout limitations.
- Case 2- the retrofit design under layout limitations. Here it is assumed that the new units must be allocated in a 2-D space for which there are 3 available sites (site 9, 10 and 11). No units are allowed to be allocated to the old site area 5 (see Figure 2.19).

The results for the two cases are summarised as follows:

- Case 1- the optimal retrofit design without layout limitations is shown in Figure 2.17 with an annual profit of \$17,687,802. The sizes of the new equipment are shown in Table 2.11. We observe that two new process equipments are selected (R2 and R4). R2 performs only task 2 while R4 performs Tasks 3 and 4. No intermediate storage is selected. The extra amounts of products S5 and S6 are stored in vessels V5a and V6a respectively. The process schedule is depicted in Figure 2.18.

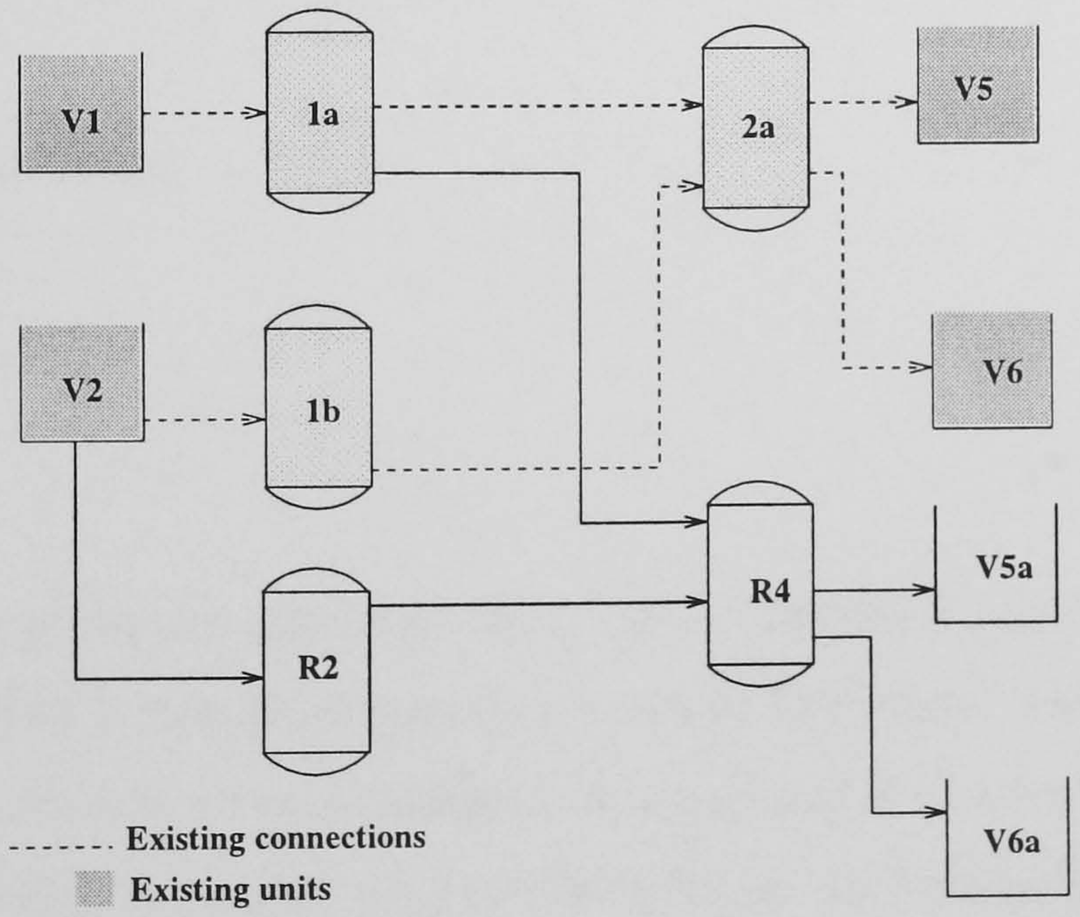


Figure 2.17: Optimal plant structure for the retrofit example without layout limitations

Unit	R2	R4	R5	V5a	V6a
Capacity, [te]	44	150	-	50	50

Table 2.11: Optimal unit capacities for the retrofit example

- Case 2- the old units are allocated to fixed positions according to the initial layout. The simultaneous design/scheduling and layout problem results in the plant layout structure shown in Figure 2.19 and 2.20. We observe that due to layout limitations vessel V5a is now not chosen and product S5 from equipment R4 is stored in the old vessel V5. Note that without layout limitations vessel V5a was chosen because connection 19 (R4 - V5) was more expensive than connection 18 (R4 - V5a). The annual plant profit after the layout constraints is only marginally lower ($17,636,208) with no change in the plant optimal schedule for the main equipment.

2.10 Streaming and Layout Optimization in an Industrial Multipurpose Batch Plant

This section considers the problem of equipment relocation for an industrial multipurpose batch plant (paint production) (Rotstein *et al.*, 1997). The process involves the manufacturing of 73 products. The process recipe consists of three main stages:

1. Milling and Dispersion.
2. Mixing.
3. Filling.

Products in this plant are classified into "colour families", such as whites, reds, etc. Each family is forced to follow a specific dispersion route in the plant. This enables operators to gain experience in the production of each product in a particular dispersion route. Also, production is implemented following a master cyclic schedule, so as to simplify the plant logistics (i.e. supply of raw materials and products). Similar managerial considerations make desirable the extension of the production routes concept to the mixing stage. A mathematical model was developed by Rotstein *et al.* (1997) in order to optimize:

- The allocation of colour families ("streams") to dispersion routes.
- The production cycle.
- The conversion cost.

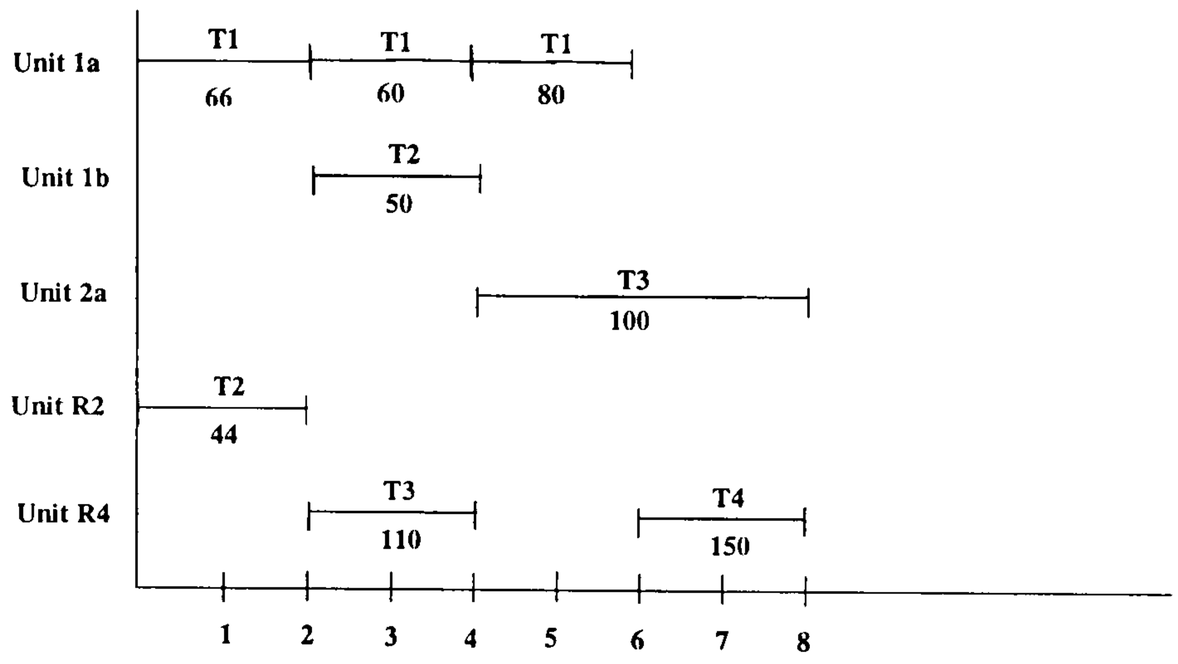


Figure 2.18: Final process schedule for the retrofit example

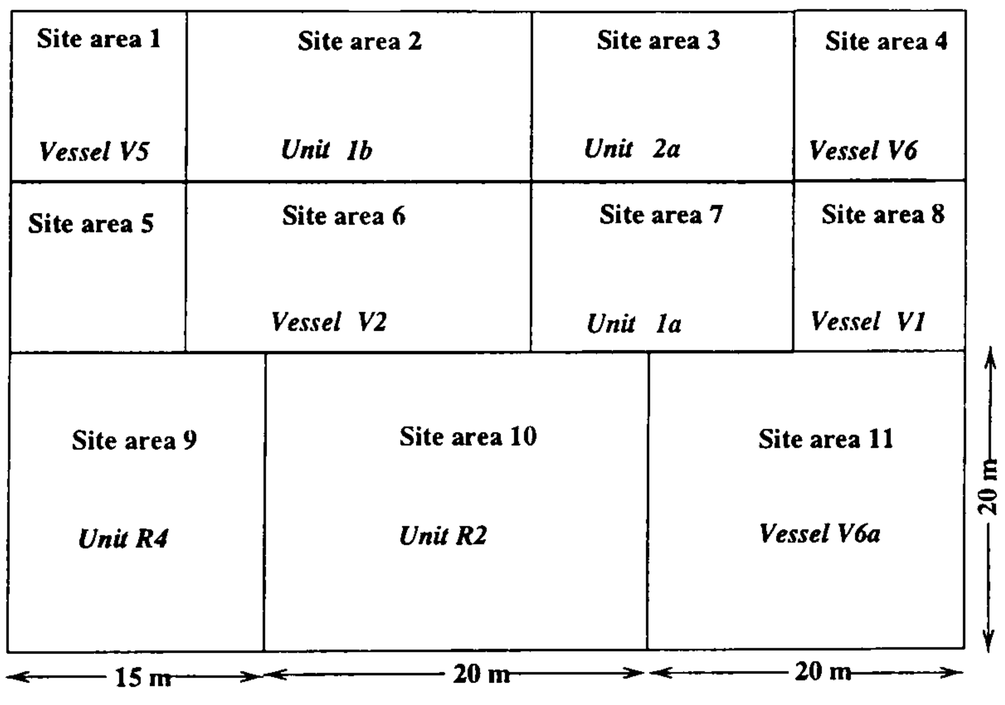


Figure 2.19: Optimal plant layout for the retrofit example-case 2

A similar model was developed for the optimal definition of "streams" at the mixing stage. The optimal streaming at the dispersion and mixing stage is shown in Figure 2.21 for a production cycle of 480 hours. The initial plant layout is as indicated in Figure 2.21. All the models are mixed integer linear programming problems and are easily combined with the proposed layout formulation.

The plant management is considering the organisation of labour into production teams. Each team would service a subset of the product families (e.g. a "whites" team, a "reds and blues" team) and of the corresponding dispersers and mixers required. This aims at enabling a better understanding of the process, helping operators to concentrate on the production of a particular set of products and making the team responsible for the Right First Time performance achieved for that family. The effective implementation of this idea requires also the reallocation of existing equipment in the plant. The objective is to create "clusters" of dispersers and mixers, associating each subset of families with a specific plant section where the corresponding team operates. Also, the present allocation of units resulted in very large distances between the dispersers and mixers processing a colour family. Since the material is transferred manually in pans the labour requirements increase with distance.

The formulation presented in this chapter was used to decide on the optimal reallocation of dispersers and mixers in the plant for the proposed dispersion and mixing routes. Here, there is no physical connection between dispersers and mixers because the intermediates are transported using movable containers (pans). Thus, the fixed cost coefficient ($\$/m$) has no economic meaning. However, in order to enforce the creation of clusters of dispersers and mixers sharing product families, we assume that the cost factors expressing connection and transport costs are proportional to the amount of material transfered between the connected units.

The plant area is divided into a number of sections for the two main process stages. Each item of equipment can only take up at most one section (grid). Mixers are not allowed to be allocated in the dispersion area and dispersers in the mixing area. The intermediate section used for transfer of the pans is not modelled and is treated as an empty space. The number of sections is not equal to the number of equipment.

The optimal layout obtained is depicted in Figure 2.22. The computational time required for this problem was 15 min., using a Sun10 machine. A very compact layout is obtained with the connected units allocated close to each other in three distinct product trains. The time and manpower required for the transfer of materials from the dispersion to mixing stage is

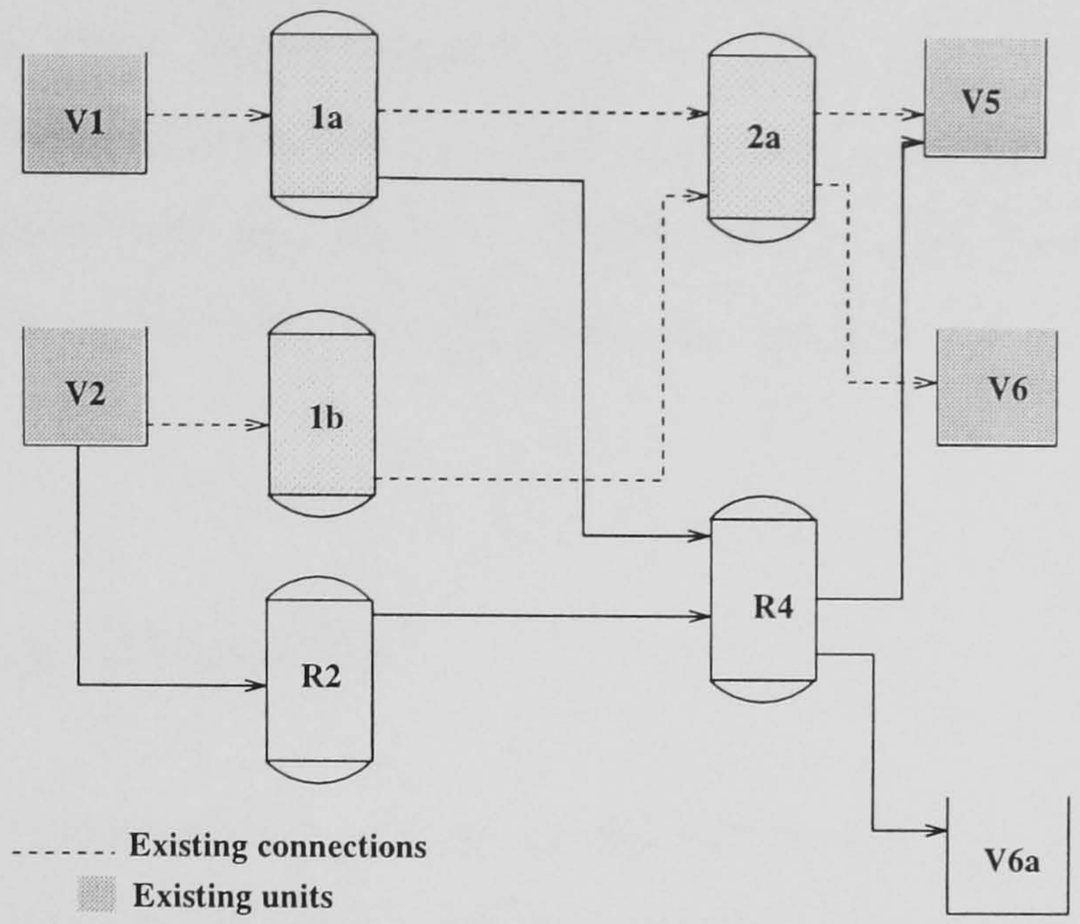


Figure 2.20: Optimal plant structure for the retrofit example with layout limitations

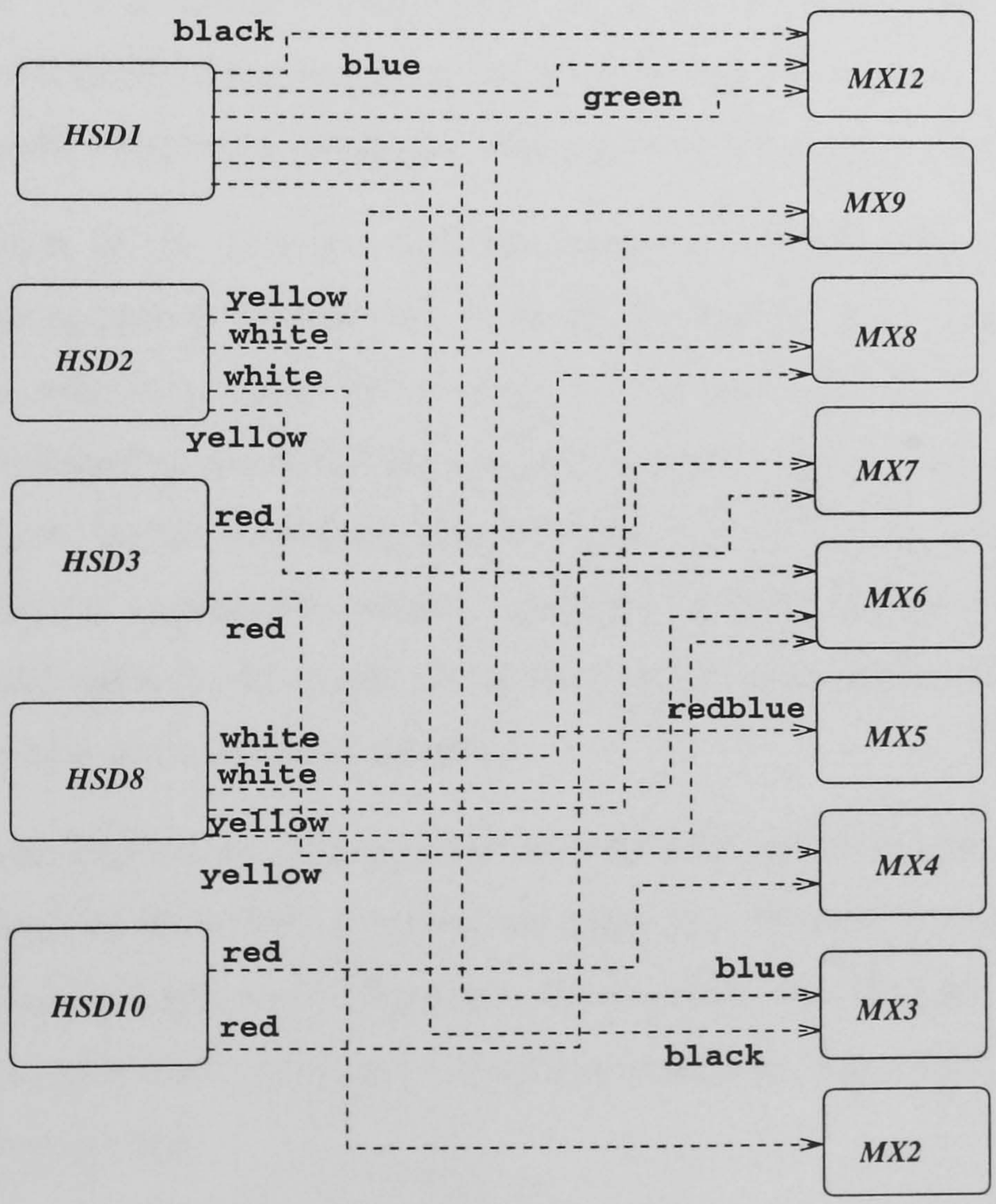


Figure 2.21: Optimal streaming at the dispersion and mixing stage

minimized. The equipment items to which the same product families are assigned are also allocated close to each other. For example dispersers HSD3 and HSD10 and the corresponding mixers MX4 and MX7 for the red family are allocated in neighbouring grids. The same holds for all the other families and equipment. Therefore, the requirements discussed above are satisfied. This layout would permit the allocation of a dedicated service crew to each group of colour families.

2.11 Concluding Remarks

A novel optimization formulation has been presented for the 2-D and 3-D Batch plant layout. The low number of integer variables and constraints make the approach suitable for large scale problems and applicable to a number of different problems. The objective function is the minimisation of the transportation, piping, and floor construction cost using detailed cost models. Constraints due to safety considerations (e.g. minimum distance between units) can be easily imposed. The problem is formulated as an MILP which may be used on its own for problems with up to 20-25 units and together with a heuristic approach for problems of larger size. A way to handle degenerate solutions was presented for a specific layout geometry.

The linear form of the problem and the realistic objective function used facilitate the application of this approach to different type of problems. Trade-offs between capital and operating cost are reflected in the 3-D layout, thus resulting in the optimal number of floors required. The simultaneous retrofit design/scheduling and layout problem in batch plants was also considered. Here, layout consideration are taken into account in terms of space limitations. It is shown that layout constraints result in changes of the optimal plant structure. For the specific example addressed in this paper there are only changes in the selection of storage units, but changes in process units are also possible.

The layout formulation was also applied to a retrofit industrial problem, where the layout of an existing industrial plant was modified to allow the effective re-organisation of the plant into separate production lines with dedicated labour crews. In this case, the allocation of units affects management and other economic considerations and was an important decision in the overall optimal plant design.

The formulation presented in this chapter can be used to obtain a good initial layout at the early design stage. Is can also be used for the optimal partitioning of units in multilevel plants. Moreover, it can easily be integrated with other tools for retrofit design decisions in

batch plants. The most important feature in the proposed approach is the discretization of the layout area into a number of location characterized by unique coordinates. This may result in an overestimation of the required area if the grid discretization is improperly selected (for example if a small unit is allocated to a large area). In the next chapter we present a new formulation taking into account explicitly the equipment shapes.

2.12 Nomenclature

FA = area per floor in m^2

FCC = floor construction cost in $\$/m^2$

$L_m(k)$ = set of areas to handle degeneracies

l_c = length of connection c for the retrofit design problem, m

NF = number of floors in the 3-D layout problem

$NU(k)$ = set of numbers according to the assignment of locations to floors

y_{ik} = integer variable defining the allocation of unit i at area k

x_i, y_i, z_i = coordinates of unit i

x_k, y_k, z_k = coordinates of area k

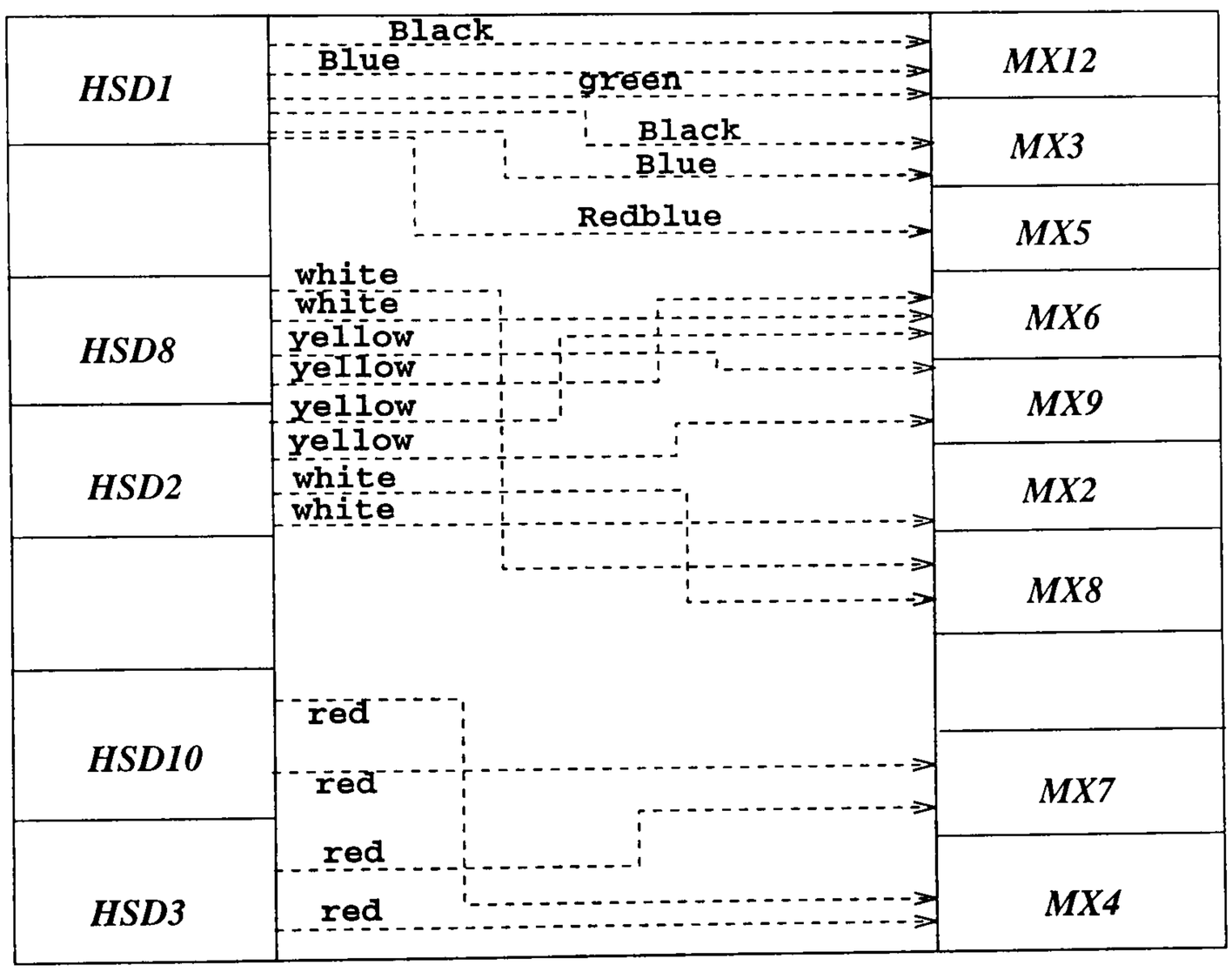


Figure 2.22: Optimal plant layout for the streaming optimization problem

Chapter 3

A Mathematical Programming Approach to Plant Layout with Equipment size Constraints

The formulation presented in chapter 2 is extended by taking into account explicitly constraints due to equipment sizes and geometries. Examples are presented to illustrate the applicability of the proposed approach.

3.1 Introduction

Most of the previous work on the chemical plant layout using mathematical programming techniques has been mainly focused on the use of special formulations and addresses a part of the layout problem. A major deficiency is that equipment sizes and orientation are often neglected since units are allowed to be allocated to predetermined discrete locations (Jayakumar and Reklaitis, 1996; Suzuki *et al.*, 1991c) . This may result in an overestimation or underestimation of the actual area and pipework required (for example if a small unit is allocated to a large area) and may also impose significant limitations during the latter design stage. Also cost of land and floor construction cost are typically not taken into account. Furthermore, most of the approaches are only restricted to 2-D layout problems.

This chapter extends the work presented in the previous one and propose an even more general formulation and a mathematical programming solution for addressing the problem of

allocating items of equipment in a given two or three dimensional space. Detailed cost factors are used to account for the cost of land, piping, transportation and floor construction cost. The extensions considered here address the following aspects: (i) first we take into account the sizes and different rectangular geometric shapes of process equipment and their proper orientation and (ii) multilevel units (*i.e.* those which require space on more than one floor) are also considered. The proposed approach can be applied at the conceptual phase of the plant design, when a plant flowsheet (giving number and type of each piece of equipment, and their connectivity) and the dimensions of the equipment are available. Three case studies are presented to illustrate the applicability of this approach to different type of problems.

3.2 Problem Statement

The problem addressed in this paper can be stated formally as follows:

Given:

- a set of process equipment units and their geometric shapes and sizes, indexed here as either i or $j = 1..n$
- the geometric shape of each piece of equipment defined in terms of rectangles of various sizes
- a set of available locations and their coordinates and sizes, indexed $k = 1..K$
- the material flowrates between connected units in kg/s.
- the purchase and installation cost of piping in $\$/m$; floor construction cost and land cost in $\$/m^2$
- minimum safety distance between units i and j when their proximity is considered as source of hazards

Determine:

- the allocation of each unit to a location in the 3-D grid area and the orientation of the unit
- the area required on each floor for the 3-D problems

- the land required for the 2-D problems

Such that:

the cost of layout including connection, transportation, land and floor construction cost is minimized.

In this work the idea of uniform area discretization (UAD) is employed. The layout area is discretized into a number of K equal grids (sequentially indexed) which are represented by unique x_k, y_k and z_k relative coordinates. For the sake of simplicity and with no loss of generality unit grids are assumed. In order to illustrate the representation used, consider the layout area shown in Figure 3.1. For the first grid $x_1 = 1, y_1 = 1, z_1 = 1$. Similarly for grid 7 $x_7 = 2, y_1 = 2, z_1 = 1$. In case a second floor level is also included then all the corresponding grids on this level will have $z_k = 2$. This grid representation will aid to explain the problem constraints and objective function, in a better way, as shown later. Each grid has the same side length, S_d, in the x and y coordinates (i.e. each grid is square). This assumption is necessary to state the rotation of equipment correctly. In order to model the problem accurately, the greatest common divisor of the size of all units must be used as the size of each grid. For example if there are 4 units of square shape with size 2, 4, 6 and 14 m^2 then the size of each grid will be 2 m^2.

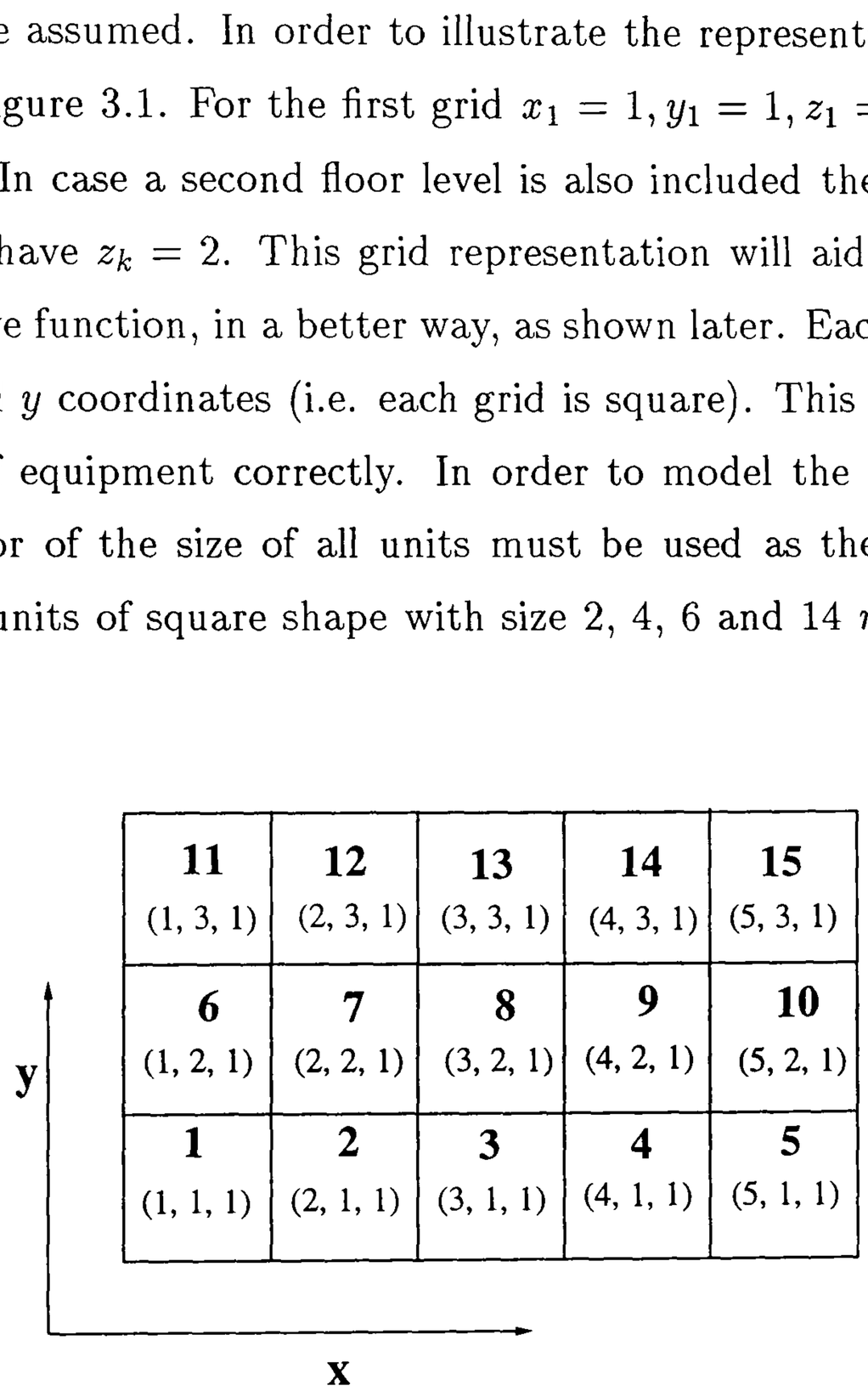


Figure 3.1: Grid representation in the layout area

The shape of each unit i, is specified using a set of sections s which are connected to form a rectangle. A rectangular shape is more appropriate for industrial problems than circular shapes (some extra space is included to allow access for maintenance, inspection etc). This discretization into sections is performed to enable the allocation of each section to a single grid.

For the example with four units presented in the previous paragraph, the equipment with size 6 m^2 will be divided into 3 sections and the one with 14 m^2 into 7 sections (see Figure 3.2). The smallest unit includes only one section with size 2 m^2. If all the equipment have only one section then the formulation presented here reduces to that of the previous chapter.

1	2	3	4	5	6	7
2 m^2	2 m^2	2 m^2	2 m^2	2 m^2	2 m^2	2 m^2

Figure 3.2: Equipment shape discretization

It should be emphasized here that in other approaches (Suzuki *et al.*, 1991a; Penteado and Ciric, 1996) the layout problem is formulated as a non-linear non-convex optimisation problem. This results in a very difficult mathematical problem with local optimal solutions. The UAD proposed here avoids the problem of the non-linearities and non-convexities by transforming the problem into an MILP which can be solved to global optimality using standard commercial MILP solvers. Obviously, if the discretisation used in the model is too coarse, the UAD will lead to a solution which could be further optimised by using more refined grids.

3.3 Mathematical Formulation

For each equipment one must specify which of the sections defining the shape are used for connectivity purposes. For example if a heat exchanger has a rectangular shape (3×1) sections, **X X X** with section numbering **1 2 3** one can define the connection sections as 1 and 3 (inlet and/or outlet). The definition of the connection sections is based on the physical form of the equipment and it is not a degree of freedom available for the optimizer. The optimization procedure will determine the optimal allocation of the connection sections but each equipment has to follow a well defined rectangular shape with all the relative sections allocated close to each other.

The connectivity between two units is represented by the following:

$$d_{isjt} = \begin{cases} 1, & \text{if transportation is from section } s \text{ of unit } i, \text{ to section } t \text{ of unit } j \\ 0, & \text{otherwise} \end{cases}$$

3.3.1 Basic Variables

The variables representing distances between sections are based on the grid representation and denote relative values expressed as integer numbers. For example, the horizontal distance between grid 1 and 3 in Figure 3.1 is 2 (*i.e.* two times the width of a grid). In order to calculate the actual distance, the horizontal distance variables (in the $x-y$ level) are multiplied by the grid side S_d. Similarly, the vertical distance variables are multiplied by the floor height, F_h. For all the connections between unit sections (*i.e.* $d_{isjt} = 1$), we introduce a set of variables representing the relative distance (in integer values) in the x, y and z coordinates:

R^x_{isjt}: relative distance in x-coordinates between section s of unit i and section t of unit j, if unit i is to the right of unit j

L^x_{isjt}: relative distance in x-coordinates between section s of unit i and section t of unit j, if unit i is to the left of unit j

R^y_{isjt}: relative distance in y-coordinates between section s of unit i and section t of unit j, if unit i is to the right of unit j

L^y_{isjt}: relative distance in y-coordinates between section s of unit i and section t of unit j, if unit i is to the left of unit j

U_{isjt}: relative vertical distance between section s of unit i and section t of unit j, if unit i is at a higher floor than unit j

D_{isjt}: relative vertical distance between section s of unit i and section t of unit j, if unit i is at a lower floor than unit j

In addition, a binary assignment variable y_{isk} is defined as:

$$y_{isk} = \begin{cases} 1, & \text{if section } s \text{ of unit } i \text{ is allocated to site area } k \\ 0, & \text{otherwise} \end{cases}$$

Note that all variables apart from y_{isk} are treated as continuous throughout the optimization.

3.3.2 Objective Function

The objective function is to minimize the total cost by considering

- the upward and horizontal transportation cost

- the capital cost of connections
- the floor construction cost (3-D problems)
- the land cost (2-D problems)

Cost coefficients are used to account for the direction and cost of transportation between connected units as in chapter 2. In summary, the following input data are required:

CF^{up}_{isjt}: upward transportation cost of unit i section s to unit j section t in $\$/m \cdot yr$

CF^{down}_{isjt}: downward transportation cost of unit i section s to unit j section t in $\$/m \cdot yr$

CF^{hor}_{isjt}: horizontal transportation cost of unit i section s to unit j section t in $\$/m \cdot yr$

CC_{isjt}: connection cost between unit i section s and unit j section t in $\$/m$

LCC: cost of land for the 2-D layout problems in $\$/m^2$

FCC: floor construction cost for the 3-D layout problems in $\$/m^2$

FA: area per floor for the 3-D layout problems in m^2

CCF: capital charge factor (Douglas, 1988)

F_h: floor heigh for the 3-D problems in m

S_d: length of each grid side in m

NF: number of floors

Thus the objective for the 3-D layout problem becomes:

$$\begin{aligned}\min OF \quad = \quad & \sum_{(is),(jt)|d_{isjt}=1} \Big[\Big(CF^{down}_{isjt} + CC_{isjt}\Big) \cdot U_{isjt} \cdot F_h + \Big(CF^{up}_{isjt} + CC_{isjt}\Big) \cdot D_{isjt} \cdot F_h \\ & + \Big(CF^{hor}_{isjt} + CC_{isjt}\Big) \cdot \Big(R^x_{isjt} + L^x_{isjt} + R^y_{isjt} + L^y_{isjt}\Big) \cdot S_d\Big] \\ & + CCF \cdot FCC \cdot FA \cdot NF \\ & + CCF \cdot LA \cdot LCC \end{aligned} \tag{3.1}$$

where LA is the land area in m^2 which is calculated explicitly as shown in section 3.7

If a 2-D layout is considered then the term representing the floor construction cost is neglected. In principle, the number of floors, NF, can be a variable and special constraints accounting for the calculation of the optimal number of floors must be added, as in our the

previous chapter. However, it is beyond the scope of this chapter to consider the problem of the optimal number of floors. Alternatively, and given that the number of floors is usually small, the problem presented here can be solved parametrically in terms of NF for the case of multilevel problems.

3.3.3 Assignment Constraints

Each unit i (and the corresponding sections) must be allocated to some of the given K locations. On the other hand, each location may be occupied at most by one unit. The following constraints are thus imposed:

$$\sum_{k=1}^{K} y_{isk} = 1 \quad \forall\, i, s \tag{3.2}$$

$$\sum_{i=1}^{n} \sum_{s=1}^{Nsec_i} y_{isk} \leq 1 \quad \forall\, k \in [1, K] \tag{3.3}$$

where $Nsec_i$ is the number of sections for unit i.

3.3.4 Distance constraints

The distance between connected units is taken to be rectangular which is more appropriate in industrial problems than straight-line distances. The following constraints calculate the relative distance between two connected units:

$$R^x_{isjt} - L^x_{isjt} = \sum_{k=1}^{K} x_k \cdot (y_{isk} - y_{jtk}) \quad \forall \Big[(is),(jt)\Big] | d_{isjt} = 1 \tag{3.4}$$

$$R^y_{isjt} - L^y_{isjt} = \sum_{k=1}^{K} y_k \cdot (y_{isk} - y_{jtk}) \quad \forall \Big[(is),(jt)\Big] | d_{isjt} = 1 \tag{3.5}$$

$$U_{isjt} - D_{isjt} = \sum_{k=1}^{K} z_k \cdot (y_{isk} - y_{jtk}) \quad \forall \Big[(is),(jt)\Big] | d_{isjt} = 1 \tag{3.6}$$

where x_k, y_k, z_k are the relative coordinates of grid k (see Figure 1). The distance between two connected units should always be not less than one (*i.e.* one grid size). The following constraint is thus added:

$$R^x_{isjt} + L^x_{isjt} + R^y_{isjt} + L^y_{isjt} + U_{isjt} + D_{isjt} \geq 1 \quad \forall \Big[(is),(jt)\Big] | d_{isjt} = 1 \tag{3.7}$$

Constraints (3.7) are redundant, however, they are added to obtain a tighter formulation. Note that all the above constraints are only defined for the connection sections of the two units.

3.3.5 Equipment shape constraints: single level

As mentioned before the geometric shape of each equipment is described by several sections s each of the size of one grid in the $x-y$ plane. Here we assume that each equipment is allocated to one floor. Special constraints must be added to describe the geometric shape of each unit. The orientation of the equipment can be modified to obtain an optimal process layout.

Basic linear shape

In order to take into account different equipment sizes we first consider simple forms which provide the building blocks to construct more complex ones. The simplest unit is described by just one section. Obviously, no constraints are required to describe this shape. The next simplest equipment shape consists of two sections **X X** with section numbering **1 2**. To enforce this shape in the layout area we must impose a set of constraints. First we introduce the following constraints:

$$\sum_{k=1}^{K}(x_k + y_k)(y_{i1k} - y_{i2k}) = 1 - 2o_i \tag{3.8a}$$

where o_i is an integer variable representing the orientation of the equipment parallel to either the x or y axis, and excluding the infeasible diagonal section allocation. For example, in Figure 3.1 the allocation of such a unit to grid one (section 2) and seven (section 1) is prohibited since the above constraint is violated. The meaning of o_i is better described graphically in Figure 3.3.

The above constraint does not avoid geometries with $\Delta x = 2$ and $\Delta y = -1$. For example allocation to grid three (section 1) and six (section 2) (see Figure 3.1). Thus, we need to ensure that the relative distance in the x and y coordinates does not exceed one, so as to exclude these prohibited allocations. The following constraints are then imposed:

$$-1 \leq \sum_{k=1}^{K} x_k \cdot (y_{i1k} - y_{i2k}) \leq 1 \quad |x^{dim} > 2 \tag{3.8b}$$

$$-1 \leq \sum_{k=1}^{K} y_k \cdot (y_{i1k} - y_{i2k}) \leq 1 \quad |y^{dim} > 2 \tag{3.8c}$$

where x^{dim} and y^{dim} is the total number of grids on the same floor in the x and y coordinate respectively. For example in Figure 3.1, $x^{dim} = 5$ and $y^{dim} = 3$. Note that these constraints are only written if x^{dim} and y^{dim} are greater than two. In that case it is possible to have the absolute difference in the x or y coordinate greater than one. In any other case these constraints are satisfied automatically by (3.8a).

Each section of the equipment has to be allocated on the same floor, *i.e.* $\Delta z = 0$:

$$\sum_{k=1}^{K} z_k \cdot (y_{i1k} - y_{i2k}) = 0 \qquad |z^{dim} > 1 \tag{3.8d}$$

where z^{dim} is the number of floors. The above constraints will be only imposed if more than one floor is considered.

Now using this basic shape we can easily derive the constraints for related shapes, the most common of which are presented as follows.

The third case is **X X X** with section numbering **1 2 3** : Constraints (3.8a)-(3.8d) need to be extended by the following set to link section 3 correctly with section 2:

$$\sum_{k=1}^{K} x_k \cdot (2y_{i2k} - y_{i1k} - y_{i3k}) = 0 \tag{3.9a}$$

$$\sum_{k=1}^{K} y_k \cdot (2y_{i2k} - y_{i1k} - y_{i3k}) = 0 \tag{3.9b}$$

Since the distance between section 1 and 2 due to (3.8b) and (3.8c) is equal to the side of one grid, the above constraints describe the unique geometric shape of the equipment. Note that the orientation has been already determined by (3.8a). In addition we need to ensure that section 3 is on the same level with sections 1 and 2:

$$\sum_{k=1}^{K} z_k \cdot (y_{i2k} - y_{i3k}) = 0 \qquad |z^{dim} > 1 \tag{3.9c}$$

The fourth case is **X X X X** with section numbering **1 2 3 4** : Constraints (3.8a)-(3.8d) and (3.9a)-(3.9c) need to be extended in order to link section 4 correctly with section 3. The following constraints are thus imposed:

$$\sum_{k=1}^{K} x_k \cdot (2y_{i3k} - y_{i2k} - y_{i4k}) = 0 \tag{3.10a}$$

$$\sum_{k=1}^{K} y_k \cdot (2y_{i3k} - y_{i2k} - y_{i4k}) = 0 \tag{3.10b}$$

Now we need to ensure that the distance between section 3 and 4 is the side of one unit grid by considering similarly to (3.8b) and (3.8c) the following two constraints:

$$-1 \leq \sum_{k=1}^{K} x_k \cdot (y_{i3k} - y_{i4k}) \leq 1 \qquad |x^{dim} > 4 \tag{3.10c}$$

$$-1 \leq \sum_{k=1}^{K} y_k \cdot (y_{i3k} - y_{i4k}) \leq 1 \qquad |y^{dim} > 4 \tag{3.10d}$$

It is clear that if all equipment sections have the same x coordinate then (3.8b) and (3.10c) become redundant, and similarly if they have the same dimension in the y coordinate then (3.8c) and (3.10d) become also redundant.

Note that sections 1 and 3 are forced on the same floor by constraint (3.9c) and similar constraints are needed for sections 3/4:

$$\sum_{k=1}^{K} z_k \cdot (y_{i3k} - y_{i4k}) = 0 \qquad |z^{dim} > 1 \tag{3.10e}$$

It should be noted here that every additional section for the linear shape requires three constraints each of the form (3.9a), (3.9b) and (3.9c).

Two-dimensional shapes:

Using the previously presented base-forms it is possible to construct two dimensional shapes by using a new binary variable l_i. This variable links the basic shapes in order to achieve proper orientation of the equipment. The idea is to describe the 2-D shape as a link of more than one simple one dimensional shapes.

Consider the square shape

X X
X X with the section numbering

3 4
1 2 : First one describes the geometrical shape of base sections 1/2 and 3/4 by applying the previously presented type of constraints (3.8a)-(3.8d). A unique binary variable o_i is used for each unit i forcing an identical orientation of these sections. Next the two basic shapes are linked as follows:

$$\sum_{k=1}^{K}(x_k + y_k)(y_{i3k} - y_{i1k}) = 1 - 2l_i \tag{3.11a}$$

$$-1 \leq \sum_{k=1}^{K} x_k \cdot (y_{i3k} - y_{i1k}) \leq 1 \quad |x^{dim} > 2 \tag{3.11b}$$

$$-1 \leq \sum_{k=1}^{K} y_k \cdot (y_{i3k} - y_{i1k}) \leq 1 \quad |y^{dim} > 2 \tag{3.11c}$$

$$\sum_{k=1}^{K}(x_k + y_k)(y_{i4k} - y_{i2k}) = 1 - 2l_i \tag{3.11d}$$

$$-1 \leq \sum_{k=1}^{K} x_k \cdot (y_{i4k} - y_{i2k}) \leq 1 \quad |x^{dim} > 2 \tag{3.11e}$$

$$-1 \leq \sum_{k=1}^{K} y_k \cdot (y_{i4k} - y_{i2k}) \leq 1 \quad |y^{dim} > 2 \tag{3.11f}$$

where the new binary variable l_i is defined similar to o_i, to allow proper orientation of sections 1/3 and 2/4. The above constraints ensure that the equipment will be allocated in such a way so as to follow its specific geometric shape.

In addition, all sections should be allocated to the same floor and this is guaranteed by the following constraints between sections 1/3 and 2/4:

$$\sum_{k=1}^{K} z_k \cdot (y_{i3k} - y_{i1k}) = 0 \quad |z^{dim} > 1 \tag{3.11g}$$

$$\sum_{k=1}^{K} z_k \cdot (y_{i4k} - y_{i2k}) = 0 \quad |z^{dim} > 1 \tag{3.11h}$$

Similarly, other shapes can be modelled such as

X X X
X X X

with the section numbering

4 5 6
1 2 3

First constraints (3.8a)-(3.8d) and (3.9a)-(3.9c) are used to describe the geometrical form of the two base shapes given by sections 1/2/3 and sections 4/5/6. Then these two forms are linked using constraints similar to (3.11a)-(3.11h) for the link between sections 1/4, and 5/2.

A similar approach can be followed to describe a 3x3 square given as:

X X X 7 8 9
X X X with the section numbering 4 5 6 This is modelled by using con-
X X X 1 2 3

straints (3.8a)-(3.8d) and (3.9a)-(3.9c) to describe the geometrical form of the three base shapes given by sections 1/2/3, 4/5/6 and 7/8/9. Then these three base shapes are linked together using constraints analog to (3.11a)-(3.11h) for linking *any two pairs* of sections 1/4 to 3/6 and similarly of sections 4/7 to 6/9.

Constraints similar to (3.11g) and (3.11h) are imposed to ensure that all the equipment sections are allocated to the same floor.

3.3.6 Equipment Constraints: Multi-Level

The model presented in the previous section considers the case where each equipment item is not allowed to occupy more than one floor. However, in many practical application an equipment (*e.g.* distillation column) must be allocated space on more than one floor.

If an equipment uses more than one floor, it is straightforward to link the previously described shapes in the $x-y$ coordinates together with the shape description in the z coordinate. Since we do not allow rotation in the z coordinates we know from the section enumeration, which sections are going to be allocated to higher floors and which have the same $x-y$ coordinates.

The simplest equipment consists of 2 sections one above the other,

X
X with numbering

2
1 : For this equipment the following constraints describe its geometric shape:

$$\sum_{k=1}^{K} x_k \cdot (y_{i2k} - y_{i1k}) = 0 \tag{3.12a}$$

$$\sum_{k=1}^{K} y_k \cdot (y_{i2k} - y_{i1k}) = 0 \tag{3.12b}$$

$$\sum_{k=1}^{K} z_k \cdot (y_{i2k} - y_{i1k}) = 1 \tag{3.12c}$$

where (3.12a) and (3.12b) ensure that the x and y coordinates of section 1 and 2 are identical. while (3.12b) that section 2 is on top of section 1.

If the equipment has the shape:

X X
X X with the section numbering

3 4
1 2 where sections 1 and 2 are to be allocated to a lower floor than sections 3 and 4 then in addition to the basic equations (3.8a) to (3.8d) for sections 1/2 and 3/4 the following constraints must be imposed:

$$\sum_{k=1}^{K} x_k \cdot (y_{i3k} - y_{i1k}) = 0 \qquad (3.13a)$$

$$\sum_{k=1}^{K} x_k \cdot (y_{i4k} - y_{i2k}) = 0 \qquad (3.13b)$$

$$\sum_{k=1}^{K} y_k \cdot (y_{i3k} - y_{i1k}) = 0 \qquad (3.13c)$$

$$\sum_{k=1}^{K} y_k \cdot (y_{i4k} - y_{i2k}) = 0 \qquad (3.13d)$$

where constraints (3.13a) and (3.13b) ensure that the x coordinates of sections 1 and 3 and sections 2 and 4 are identical while constraints (3.13c) and (3.13d) that the y coordinates of all sections are also identical.

Finally the following constraints are added to ensure that section 3 and 4 are above 1 and 2.

$$\sum_{k=1}^{K} z_k \cdot (y_{i3k} - y_{i1k}) = 1 \qquad (3.14a)$$

$$\sum_{k=1}^{K} z_k \cdot (y_{i4k} - y_{i2k}) = 1 \qquad (3.14b)$$

If the equipment consists of 3 sections the one above the other,

X
X with the numbering
X

3
2 : For this equipment further to the constraints (3.12a) to (3.12c) the following are also
1

imposed to connect section 3 with the other two:

$$\sum_{k=1}^{K} x_k \cdot (y_{i3k} - y_{i2k}) = 0 \tag{3.15a}$$

$$\sum_{k=1}^{K} y_k \cdot (y_{i3k} - y_{i2k}) = 0 \tag{3.15b}$$

$$\sum_{k=1}^{K} z_k \cdot (y_{i3k} - y_{i2k}) = 1 \tag{3.15c}$$

In a similar fashion one can describe more complex 2-D and 3-D shapes.

3.3.7 Calculation of the Land Area

In many countries, land is expensive and a compact plant layout is preferable to minimize its cost. Here, it is assumed that the required area is defined by the minimum rectangular which includes all the allocated units. This approach is restricted to the 2-D layout problems. For example, consider the 2-D plant layout in Figure 3.4 where the area is discretized into 15 equal grids each with a shape of 100 m^2. If process units are allocated to grids 1, 2, 8, 9, 11, 12 and 14, it is clear that the required area is determined by a rectangle of length w and width d. The extra area by grids 5, 10 and 15 is not really required.

The idea is to determine the optimal area of land based on the unique grid that describes the above rectangle. In order to do so, to each grid in the 2-D space we assign an area AR_k defined by the area of the rectangle with respect to the origin of the axis. For example (see figure 3.4) for grid 1 this area will be 100 m^2, for grid 8, 600 m^2 (*i.e.* 6 internal grids) and for grid 14, 1200 m^2. It is clear that grid 14 is the one that will determine the required area. Now a new integer variable is defined for each grid as follows:

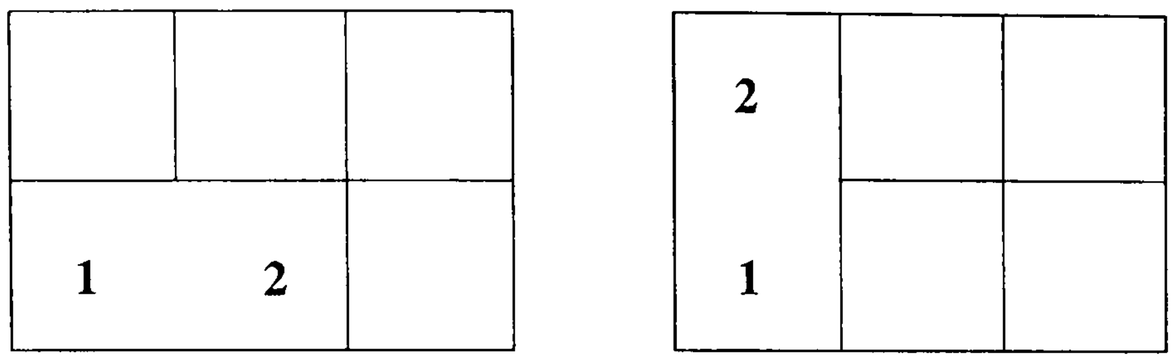
$$q_k = \begin{cases} 1, & \text{if grid } k \text{ determines the rectangular area required} \\ 0, & \text{otherwise} \end{cases}$$

The following set of constraints is added to the mathematical model.

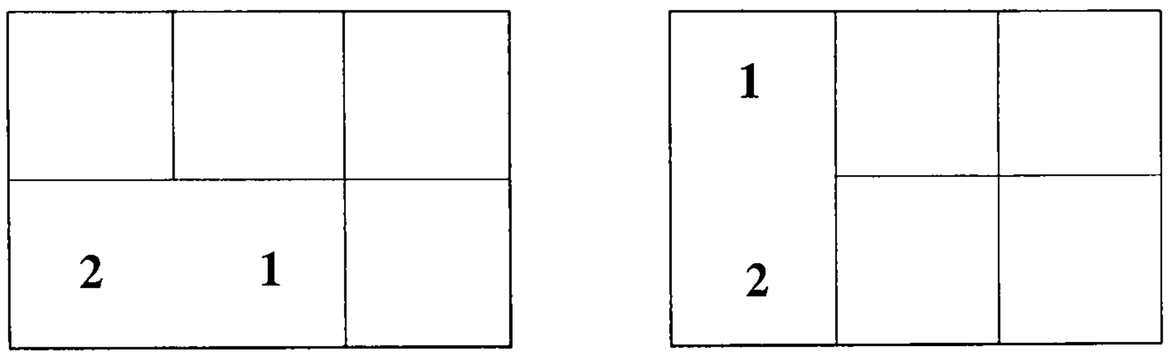
$$\sum_{k} q_k = 1 \tag{3.16a}$$

$$\sum_{k} x_k \cdot q_k = w \tag{3.16b}$$

$$\sum_{k} y_k \cdot q_k = d \tag{3.16c}$$



Equipment orientation for $o_i = 1$



Equipment orientation for $o_i = 0$

Figure 3.3: Equipment orientation in the $x - y$ level

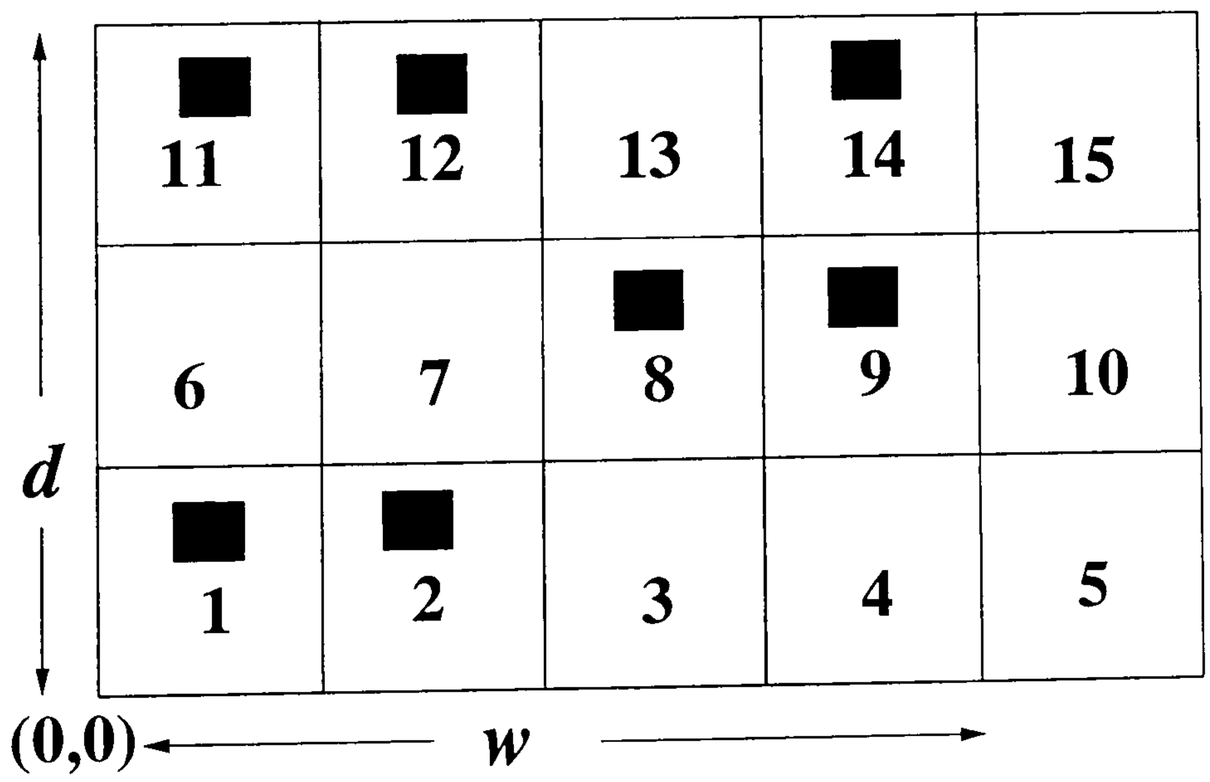


Figure 3.4: Determination of the required land in the 2-D problems

$$\sum_i \sum_s y_{isk} \cdot x_k \leq w \qquad \forall k \tag{3.16d}$$

$$\sum_i \sum_s y_{isk} \cdot y_k \leq d \qquad \forall k \tag{3.16e}$$

Finally the required land LA is given by the following equation:

$$LA = \sum_k AR_k \cdot q_k \tag{3.16f}$$

The above formulation can be easily extended to non equal grids. Note that the cost of land area, LA, can also be included in 3-D layout problems. In this case LA will be equal to the floor area, FA, and thus optimally decided by the problem. Clearly, no modification is required for constraints (3.16a) to (3.16f).

3.3.8 Degeneracy Reduction Constraints

The proposed formulation presents many degenerate solutions: given any solution, one may generate others with exactly the same value of the objective function. The source of this problem is that the formulation relies on relative distances between the units. For instance, equivalent solutions may often be obtained from the previous one by shifting its allocation by one column or row in the discretized area (i.e. a 3×2 area is the same as a 2×3 area). The existence of degenerate solutions may have adverse effects on the efficiency of the search procedure. To avoid it without any loss of optimality, one can introduce the following constraints, similar to those proposed the previous chapter.

$$\sum_i \sum_s \sum_{k \in L_m(k)} y_{isk} \leq \sum_i \sum_s \sum_{k \in L_{m-1}(k)} y_{isk} \cdot \mathrm{MNU} \tag{3.17}$$

3.3.9 Comments

The objective function and all constraints are linear including binary variables. Thus, the formulation presented in this section is a MILP problem which can be solved using standard MILP solvers. A number of equipment shapes have been modelled and proper orientation in the $x-y$ level is allowed to achieve the optimal layout. Equipment orientation on the z coordinate is not considered here. Although the above general formulation considers the 3-D layout, 2-D

problems are a special sub-case where the continuous variables related with the z dimension are zero.

It is clear that any equipment size and rectangular shape can be straightforwardly modelled for single or multi level units by imposing constraints similar to the above and/or suitable combinations of them. For the sake of simplicity and without loss of generality it is considered that there is no need to model more equipment shapes here.

The equipment discretization into sections greatly affects the size of the above MILP. If there is a big difference between the size of the smallest and largest equipment then a fine discretization is required an the problem will be large even for small process flowsheets (since the largest equipment will be discretized into many sections). One way to avoid this difficulty is to use *aggregate equipment modules* as discussed in chapter 2. For example a distillation column and its associated condenser, reboiler, pumps and reflux drum can form a module. In practice, further simplification to the problem can be achieved due to safety or operational constraints which may prohibit the allocation of some units to special areas or impose their allocation to fixed areas. In that case the corresponding integer variables y_{isk} will be set either to zero (exclude allocation) or to one (impose allocation). In the special case where two units must be allocated on the same floor (due to operating considerations) their vertical distance in the z direction should be set to zero. Furthermore, if two units must be allocated adjacent or close to each other then the total distance in the $x - y$ level between the two connection sections will be set to the size of one grid. Finally, constraints to impose a minimum distances between units which are considered source of hazard can be easily imposed.

3.4 Examples

The above MILP formulation has been implemented in a C++, object-oriented environment and is solved using a standard solver-in this case the CPLEX V4.0 mixed integer linear programming package (CPLEX Optimization, 1994). Once the decision of the layout area discretization into grids and equipment into sections has been made, the user can easily define in an input file the number of grids in the x and y direction, the number of floors (for 3-D problems), the size of each grid and height of floors and the geometric shape of each process unit. Each process unit is described by a vector the elements of which are the number of sections in each directions. For example a unit described as **[2, 2, 1]** consists of two sections along the x coordinate, two along the y coordinate and will be allocated to a single floor (square shape). The grid coordinates

are then automatically generated. Constraints such as allocation of process units to specific areas or floors can be easily imposed. The connectivities between units, the corresponding connection sections and cost data are also easily defined. A brief description of the solution procedure is given as follows:

1. Read input file into the data structure
2. Setup the MILP with the current data
3. Solve the MILP
4. Read the solution of the MILP solver and produce output file

The output file includes the exact allocation of each unit, the distances between connected units and the value of the objective function. Graphical input and outputs could be easily interfaced to this data structures. For all the case studies presented below an optimality margin of 1% has been used.

3.4.1 Example 1

Consider again the small instant coffee process taken from Jayakumar and Reklaitis (1996) and shown in Figure 2.2. The equipment sizes in terms of rectangular footprints and cost data are given in Table 3.1 and 3.2 respectively. The geometric shape of each process unit is shown in Figure 3.5. The size of each grid is defined to be 10 m^2 and each equipment is divided into a number of sections each of the size of one grid. Note that these data are only used for illustrative purposes. Here the objective function considers only the transportation and piping cost in order to illustrate the effect of the number of floors on the operating cost. It is beyond the scope of this example to consider trade-offs between capital and operating cost. The following cases are considered:

Case A. 2-D layout

The layout area is discretized into 36 grids (6×6) each with a size of 10 m^2. The objective function comprises land, transportation and piping cost (clearly, upward transportation costs are not present here). Since the land cost is uncertain and may differ significantly from one country to another (or even for different areas within the same country) we consider three sub-cases:

Equipment	Size, m^2
1	50
2	10
3	50
4	40
5	30

Table 3.1: Equipment sizes (rectangular footprint) for example 1

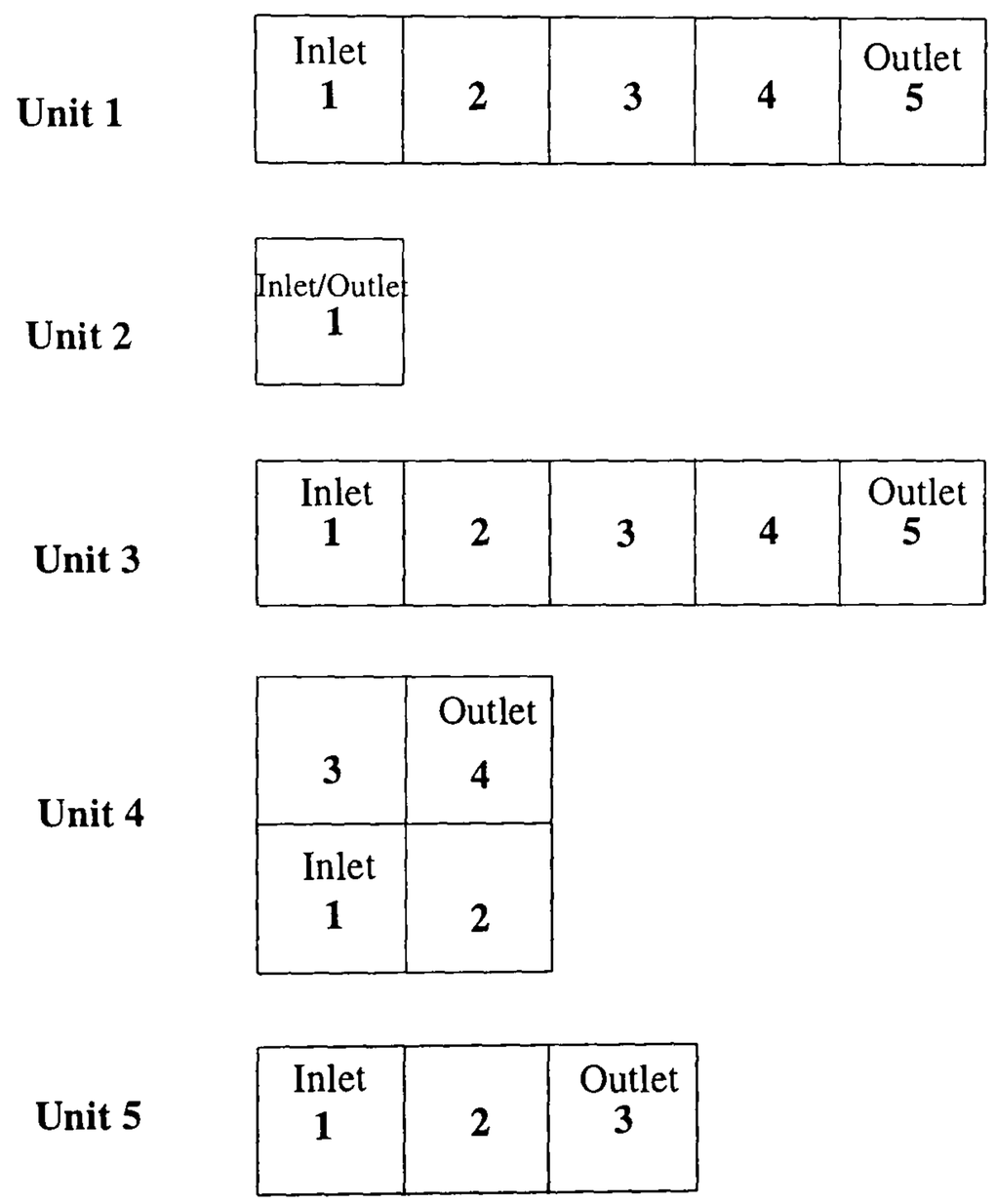


Figure 3.5: Process units shapes for example 1

Stream	CF_{ij}^{up} $\$/m \cdot yr$	CF_{ij}^{hor} $\$/m \cdot yr$	CC_{ij} $\$/m$
(1,2)	25250	2520	600
(1,3)	37820	3720	800
(2,3)	6300	630	350
(2,4)	18820	1880	400
(4,5)	14190	1410	500

Table 3.2: Cost data for example 1

A1. Zero land cost. In that case only transport and piping costs are considered. The optimal layout is shown in Figure 3.6. Although the transport cost is minimized the obtained layout is not compact. The total cost is 178,100 \$/yr and the layout area 300 m^2.

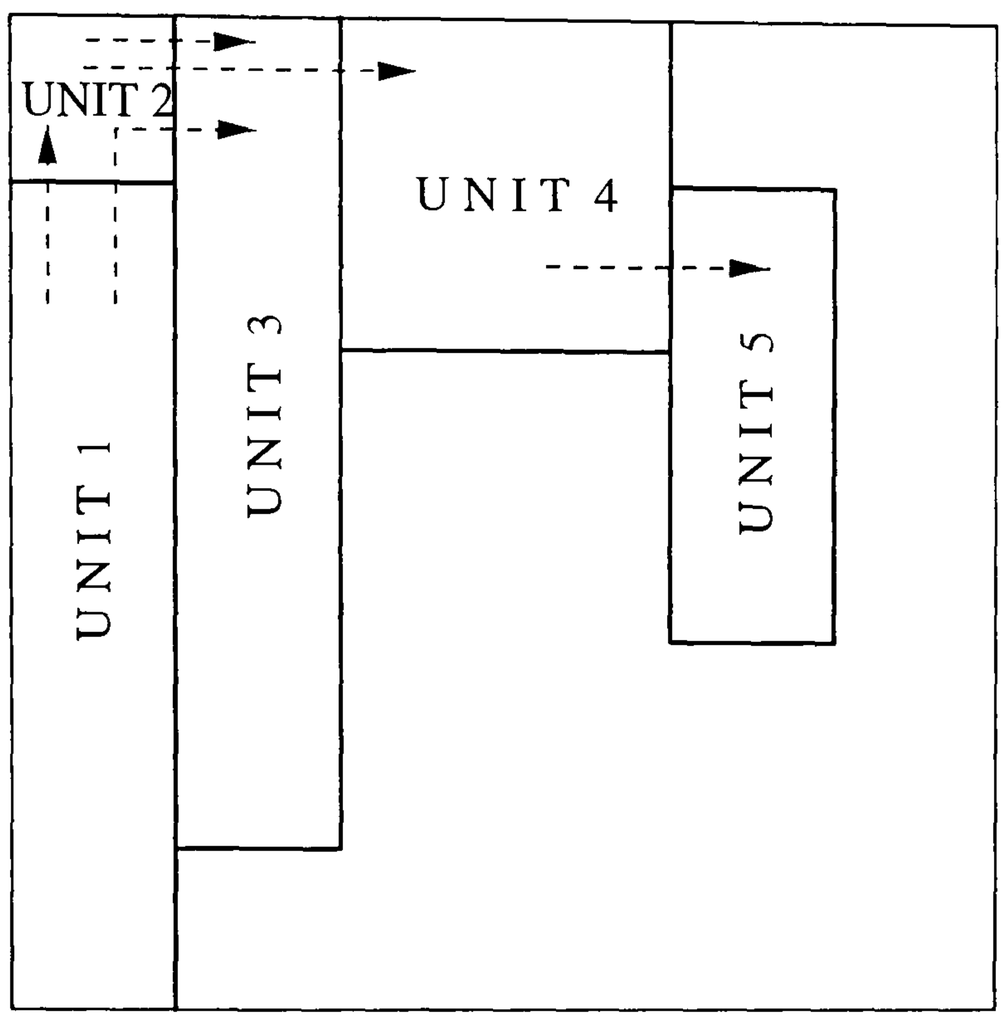


Figure 3.6: Optimal 2-D layout for example 1-case A1

A2. the land cost coefficient is taken to be 300 $\$/m^2$. Here the optimal layout is depicted in Figure 3.7. As we can see the units are allocated in such a way that the horizontal transport cost is minimized and the layout obtained is more compact than the previous case due to the land cost. The total layout cost is 202,000 $\$/yr$ and the layout area 240 m^2 (20% less than in the previous scenario).

A3. the land cost coefficient takes the value of 1000 $\$/m^2$. A different layout is obtained and shown in Figure 3.8. It is clear that a more compact layout is obtained, minimizing the cost of land (and increasing the pumping cost) which represents a significant factor in the objective function. The area required is now 200 m^2 and the layout cost 262,700 $\$/yr$.

Details of the optimisation results are given in Table 3.3.

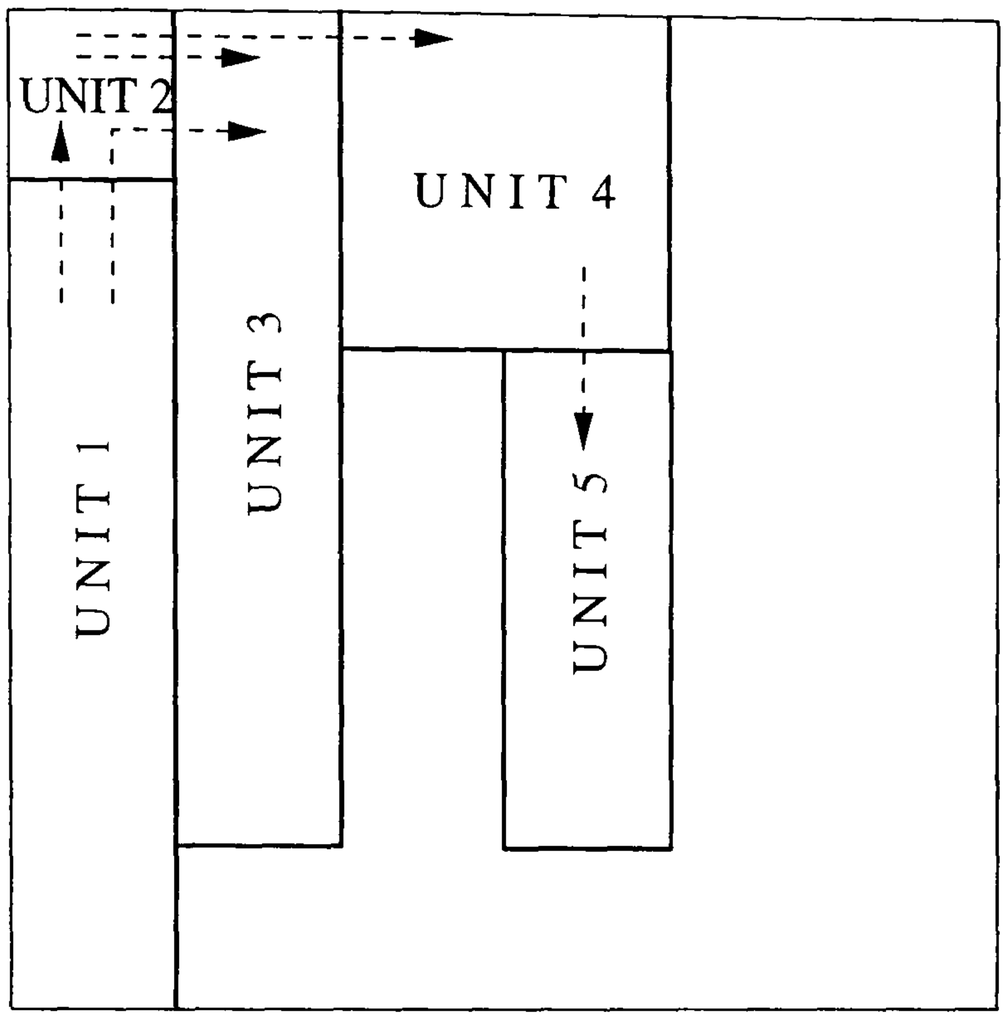


Figure 3.7: Optimal 2-D layout for example 1-case A2

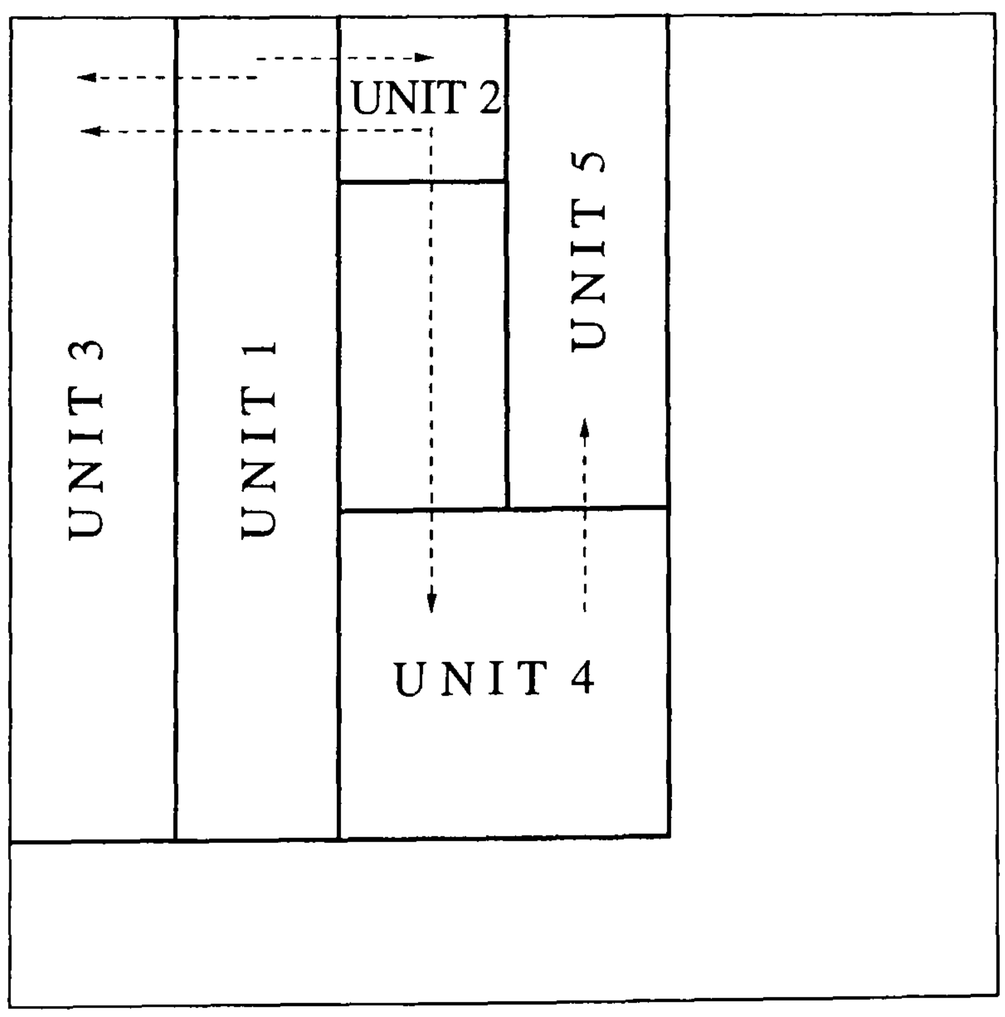


Figure 3.8: Optimal 2-D layout for example 1-case A3

Case B. 3-D layout

B1. Two floor levels.

The layout area is discretized into 30 grids (15 grids on each floor). There are 5 grids in the x and 3 grids in the y dimension. The height of each floor is taken to be 5 m. The optimal process layout is depicted in Figure 3.9. We observe that the units are allocated in such a way that a compact layout is obtained eliminating the high upward transport cost. An important information from the resulting layout is that only 100 m^2 are required for the second floor while the first floor is totally utilized. The total cost of layout is 87,000 $\$/yr$ and there are three horizontal transport flows (between units 1/2, 2/3 and 4/5). Note that unit 1 is exactly allocated on top of unit 3.

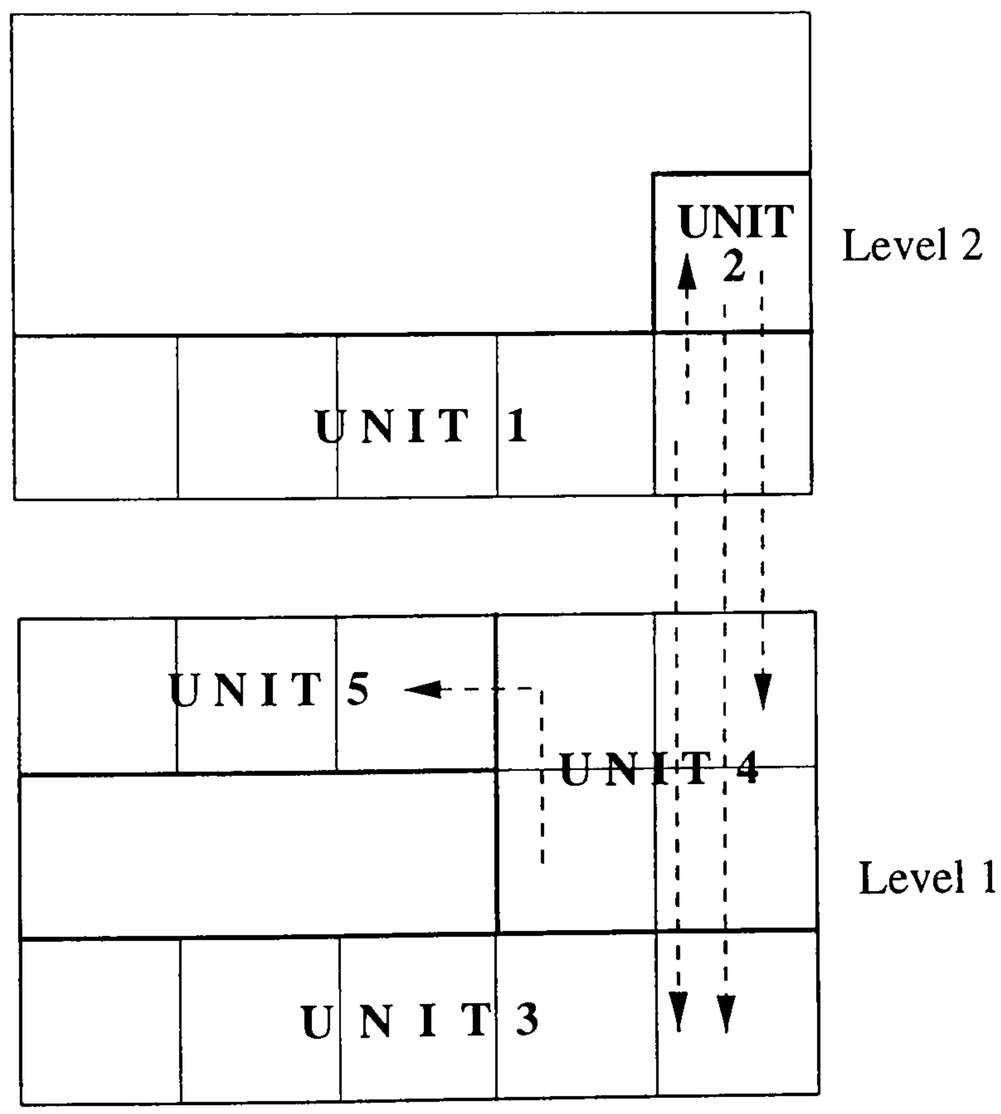


Figure 3.9: Optimal layout in two levels for example 1

B2. Three floor levels

Here the layout area is discretized into 45 grids ($5 \times 3 = 15$ grids on each floor). The optimal layout is depicted in Figure 3.10. The process units are allocated one below the other in a compact way, so that as many as possible flows are aided by the gravity. The cost of layout is 51,300 $\$/yr$ and it is lower compared with the two level problem since there are two horizontal transport costs (between units 1/2 and 2/3) and all the others

are zero due to gravity flows. It is interesting to note that process unit 5 is now oriented along the the y axis.

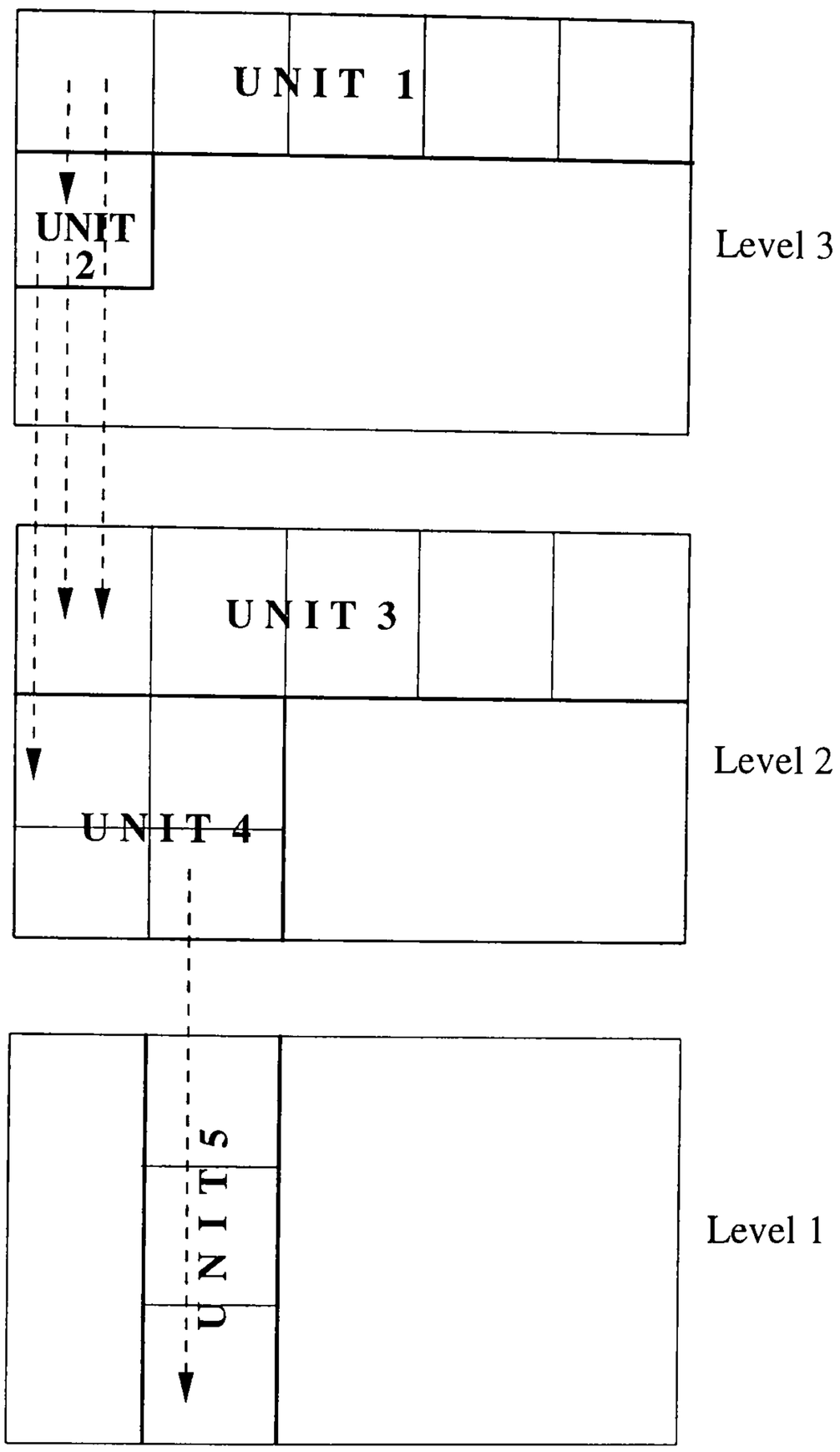


Figure 3.10: Optimal layout in three levels for example 1

B3. Four floor levels

Now there are 60 grids (15 grids on each floor). The optimal layout is shown in Figure 3.11. The same trend as in the previous cases holds. The process units are allocated so as to make the high upward transportation cost to be zero. There is now only one horizontal transport cost between units 4/5. This results in a lower operating cost of 33,800 $\$/yr$ comparing with the three floor levels case. The resulting layout indicates also the required area for each floor. Thus, level one requires 100 m^2, level two, 50 m^2, level three, 10 m^2 and level four 50 m^2.

Case	Piping Cost, $/yr	Transportation Cost, $/yr	Land Cost $/yr	Total Cost $/yr
A1	38,000	140,100	0	178,100
A2	38,000	140,100	23,900	202,000
A3	38,500	157,600	66,600	262,700

Table 3.3: Results for example 1-2D Layout

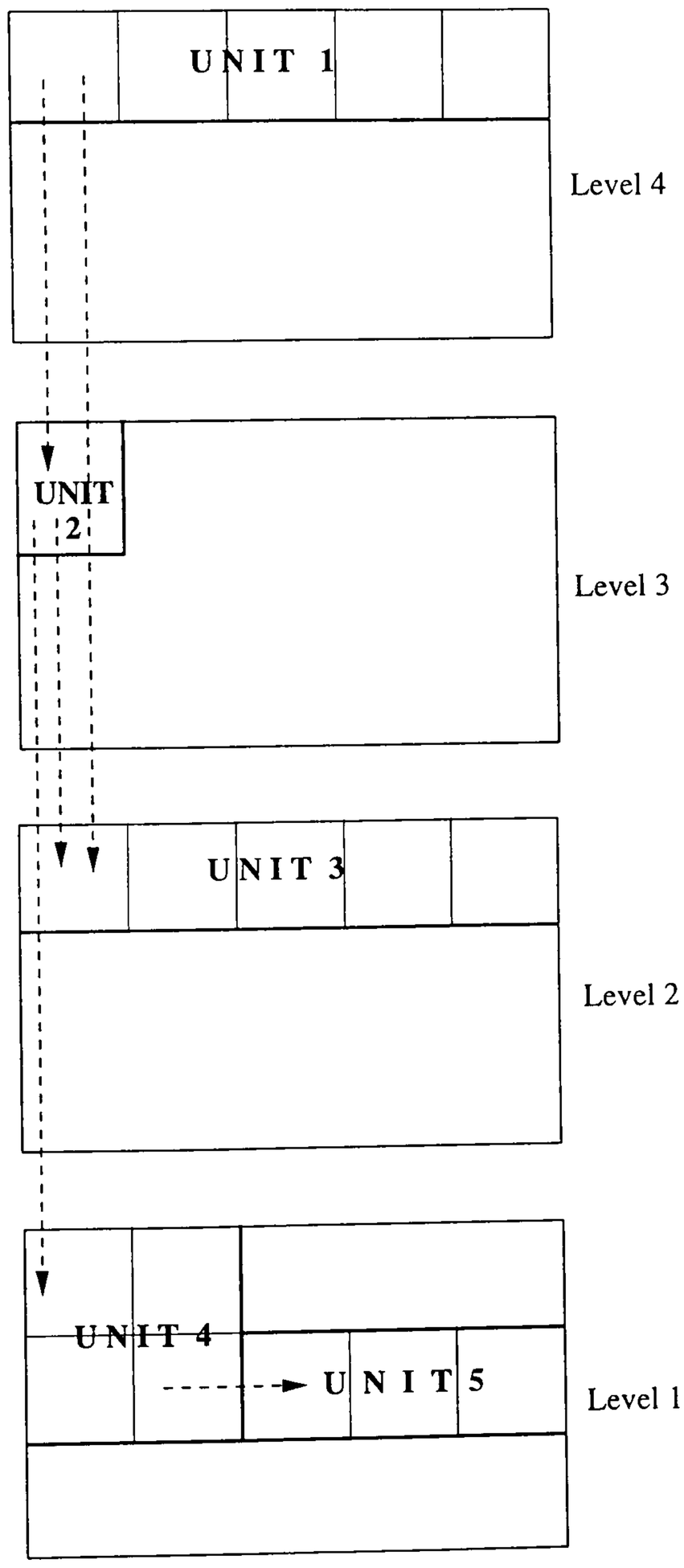


Figure 3.11: Optimal layout in four levels for example 1

It should be emphasised that the constructions cost of a multifloor building will offset some of the economic savings resulting from the reduction of the transport cost. This can lead in the optimal number of floors as illustrated in chapter 2.

Case C. Three floor levels-multilevel equipment

Here a multilevel equipment layout is considered. Unit 5 is assumed to be vertically arranged occupying 3 floors with a footprint of 1×3 grids. Similarly unit 4 occupies two floors with a footprint of 2×2 grids. The optimal layout is shown in Figure 3.12. It is clear that unit 5 is allocated to all floors and unit four to the first and second floor. Again, the upward transport cost is minimized to zero but there is a substantial horizontal pumping cost compared with the other cases which results in a higher layout cost (97,600 $\$/yr$). This is due to limitations imposed by the multilevel nature of the two units. It should be emphasized that the requirements of multilevel equipment are dictated only by their physical shape and not economic considerations. For example a batch distillation column by its nature must use more than one floor. The computational time for the solution of this example was 150-450 CPU sec on a SUN ULTRA workstation.

The results for all the multifloor case considered are summarised in Table 3.4.

Case	Connection Cost, \$/yr	Horizontal transportation Cost, \$/yr	Upward transportation Cost, \$/yr	Area, m^2	Total Cost \$/yr
B1	27,300	59,700	0	250	86,900
B2	19,700	31,500	0	310	51,200
B3	19,700	14,100	0	210	33,800
C	33,200	64,400	0	400	97,600

Table 3.4: Results for example 1-3D Layout

3.4.2 Example 2

The process flowsheet shown in Figure 3.13 is used as the second case study. It has been derived from the example considered by Suzuki *et al.* (1991*c*). The geometric shape of each process unit is depicted in Figure 3.14. Multilevel equipment is not considered. Each floor has a height of 5 m and is discretized into 18 grids (6×3). The size of each grid as determined by the smallest equipment is 10 m^2 (see Table 3.5). The connectivity matrix along with transportation and connection costs are given in Table 3.6.

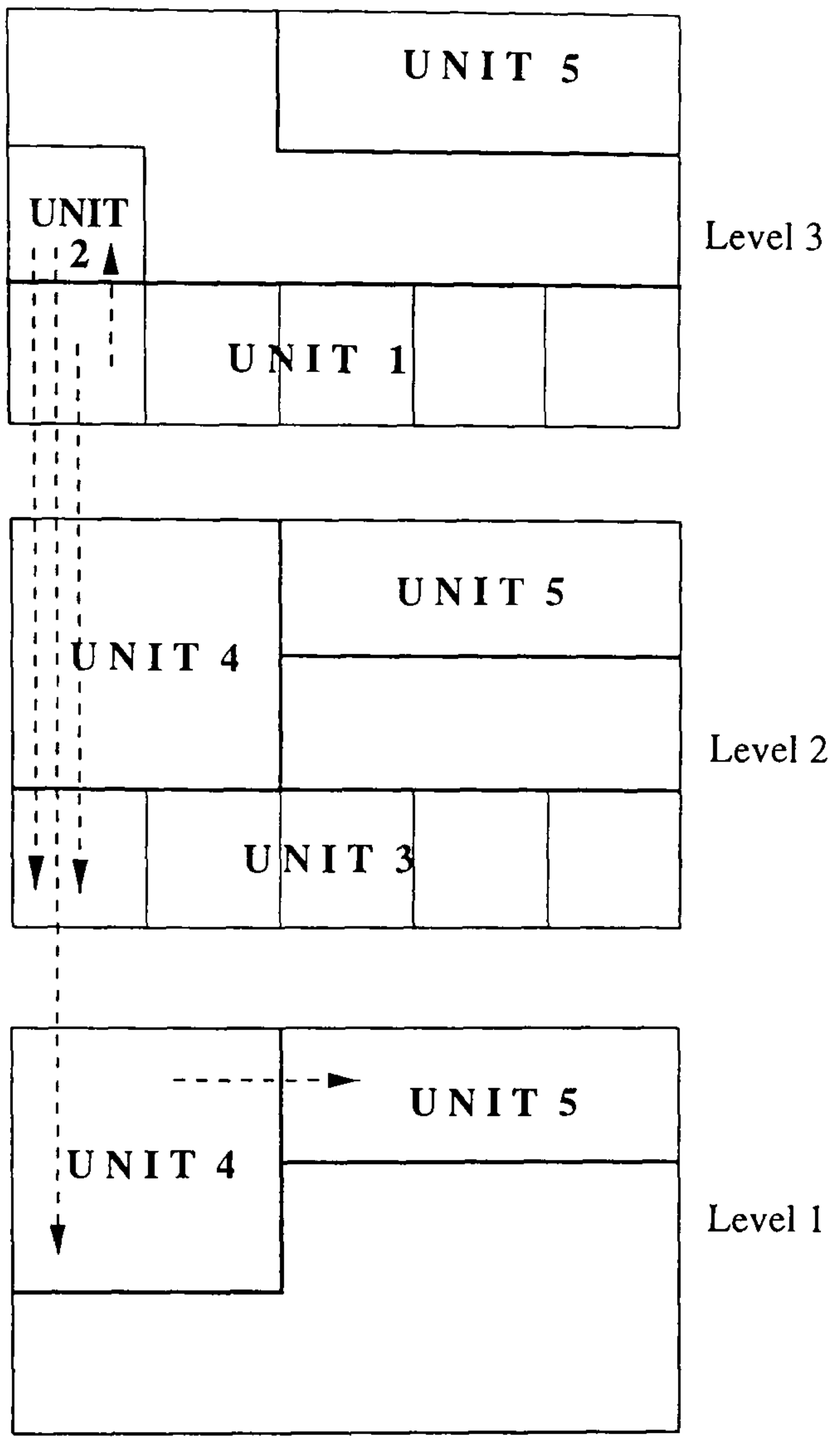


Figure 3.12: Optimal layout in three levels with multilevel units for example 1

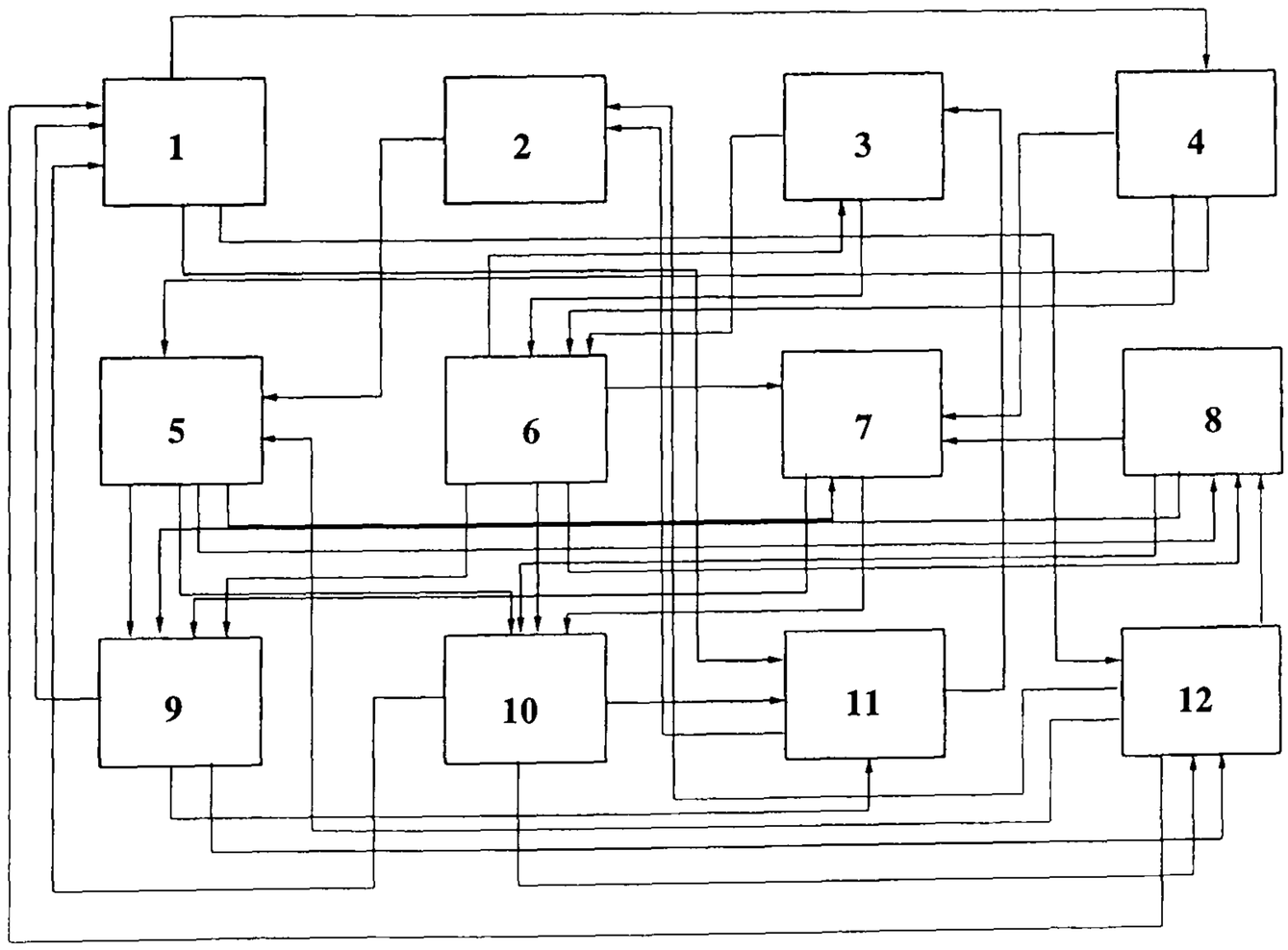


Figure 3.13: Process flowsheet for example 2

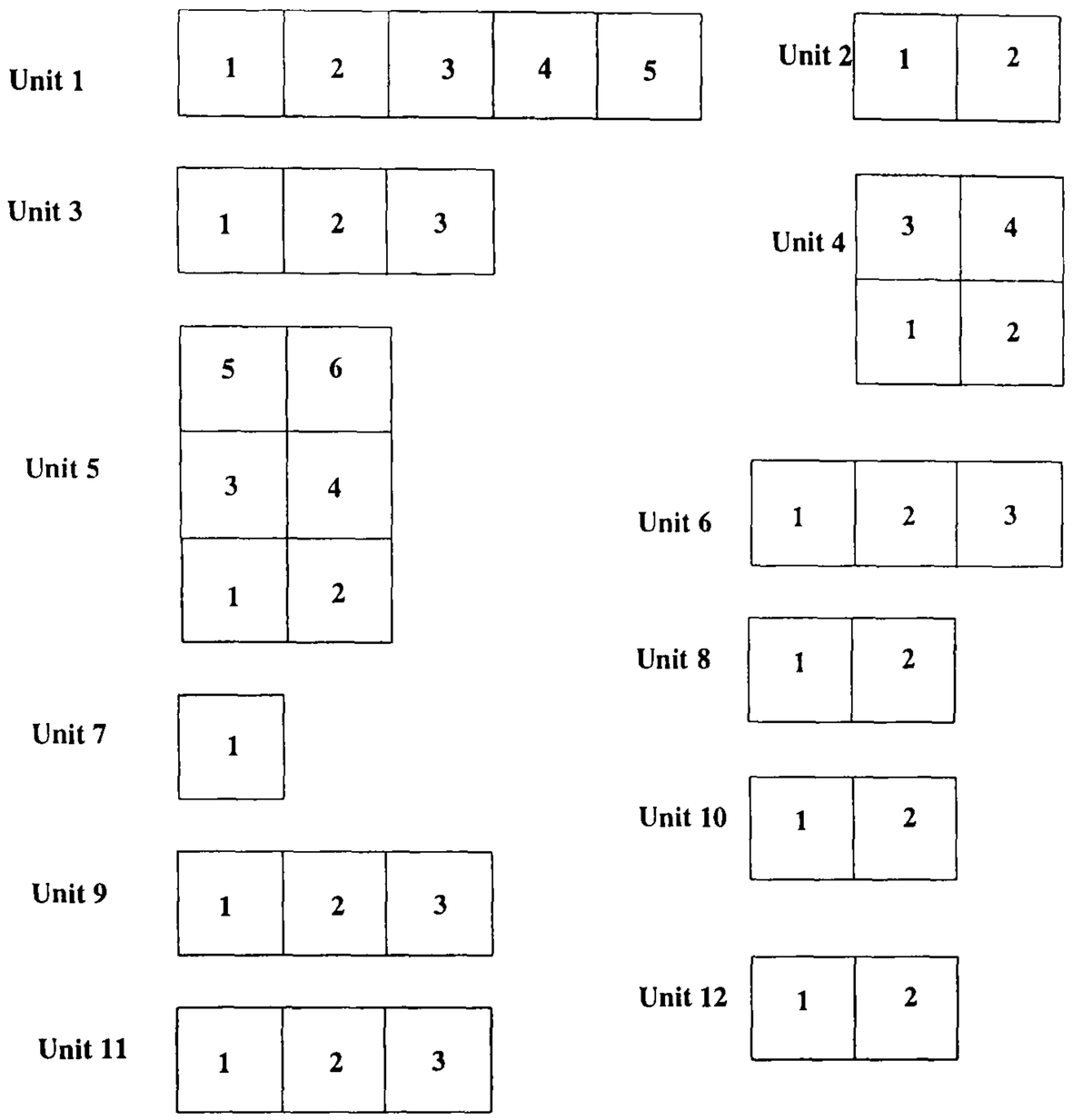


Figure 3.14: Process units shapes for example 2

Equipment	Size, m^2
1	50
2	20
3	30
4	40
5	60
6	30
7	10
8	20
9	30
10	20
11	30
12	20

Table 3.5: Equipment sizes for example 2

Stream (unit from, to)	CF_{ij}^{up} $\$/m \cdot yr$	CF_{ij}^{hor} $\$/m \cdot yr$	CC_{ij} $\$/m$	Stream	CF_{ij}^{up} $\$/m \cdot yr$	CF_{ij}^{hor} $\$/m \cdot yr$	CC_{ij} $\$/m$
(1,4)	2000	200	200	(7,4)	2000	200	200
(1,11)	2000	200	200	(7,9)	2000	200	200
(1,12)	2000	200	100	(7,10)	2000	200	250
(2,5)	4000	400	400	(8,5)	4000	400	400
(2,11)	2000	200	260	(8,7)	2000	200	300
(2,12)	2000	200	340	(8,9)	2000	200	230
(3,5)	4000	400	170	(8,10)	2000	200	300
(3,6)	4000	400	310	(9,1)	2000	200	200
(3,9)	2000	200	260	(9,6)	4000	400	300
(3,10)	2000	200	200	(9,7)	2000	200	370
(4,5)	4000	400	110	(9,11)	2000	200	160
(4,6)	4000	400	230	(9,12)	2000	200	100
(4,7)	2000	200	290	(10,1)	2000	200	400
(4,8)	2000	200	370	(10,5)	4000	400	200
(5,7)	4000	400	400	(10,11)	2000	200	190
(5,8)	4000	400	440	(11,1)	2000	200	300
(5,9)	4000	400	230	(11,2)	2000	200	300
(5,10)	4000	400	150	(11,3)	2000	200	300
(5,3)	4000	400	100	(11,7)	2000	200	240
(6,7)	4000	400	360	(11,9)	2000	200	230
(6,8)	4000	400	220	(12,1)	2000	200	400
(6,9)	4000	400	500	(12,2)	2000	200	260
(6,10)	4000	400	310	(12,5)	2000	200	190
(12,8)	2000	200	130	(12,10)	2000	200	220

Table 3.6: Connectivity matrix and costs for example 2

The optimal layout is depicted in Figure 3.15. We can see that a compact layout is obtained in an attempt to minimize the high upward transport cost. It is interesting to note again that some of the units have been oriented along the x axis and others along the y axis. The optimal layout has an annualized cost of 480,000 $\$/yr$. The computation time required on an SUN ULTRA workstation was 3200 CPU sec.

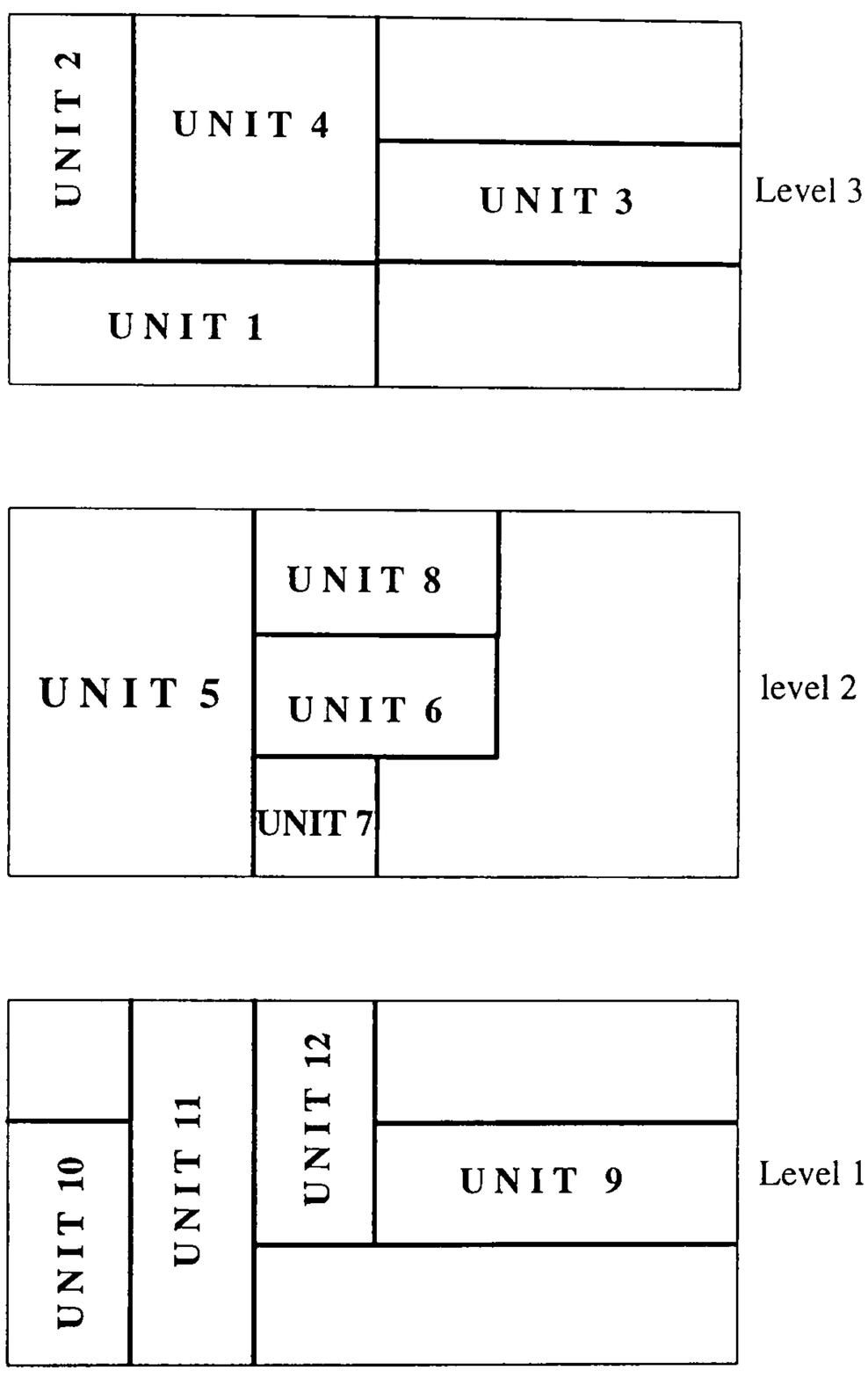


Figure 3.15: Process layout for example 2

3.4.3 Example 3

Consider the case study from Barbosa-Povoa and Macchietto (1994) shown in Figure 2.9. It is a multipurpose batch plant, with a high degree of connectivity and 18 processing units. The size and shape of each process unit are shown in Table 3.7 and Figure 3.16 respectively. The transportation and connection costs are given in Table 3.8. A five floor process layout is considered. Each floor is discretized in 10 equal grids with size 10 m^2. There are 5 grids in

the x coordinate and 2 in the y coordinate. Each floor is taken to have a height of 5 m. Units *still*, v9 and v5 have a vertical dimension of 10 m^2, and hence must occupy two floors.

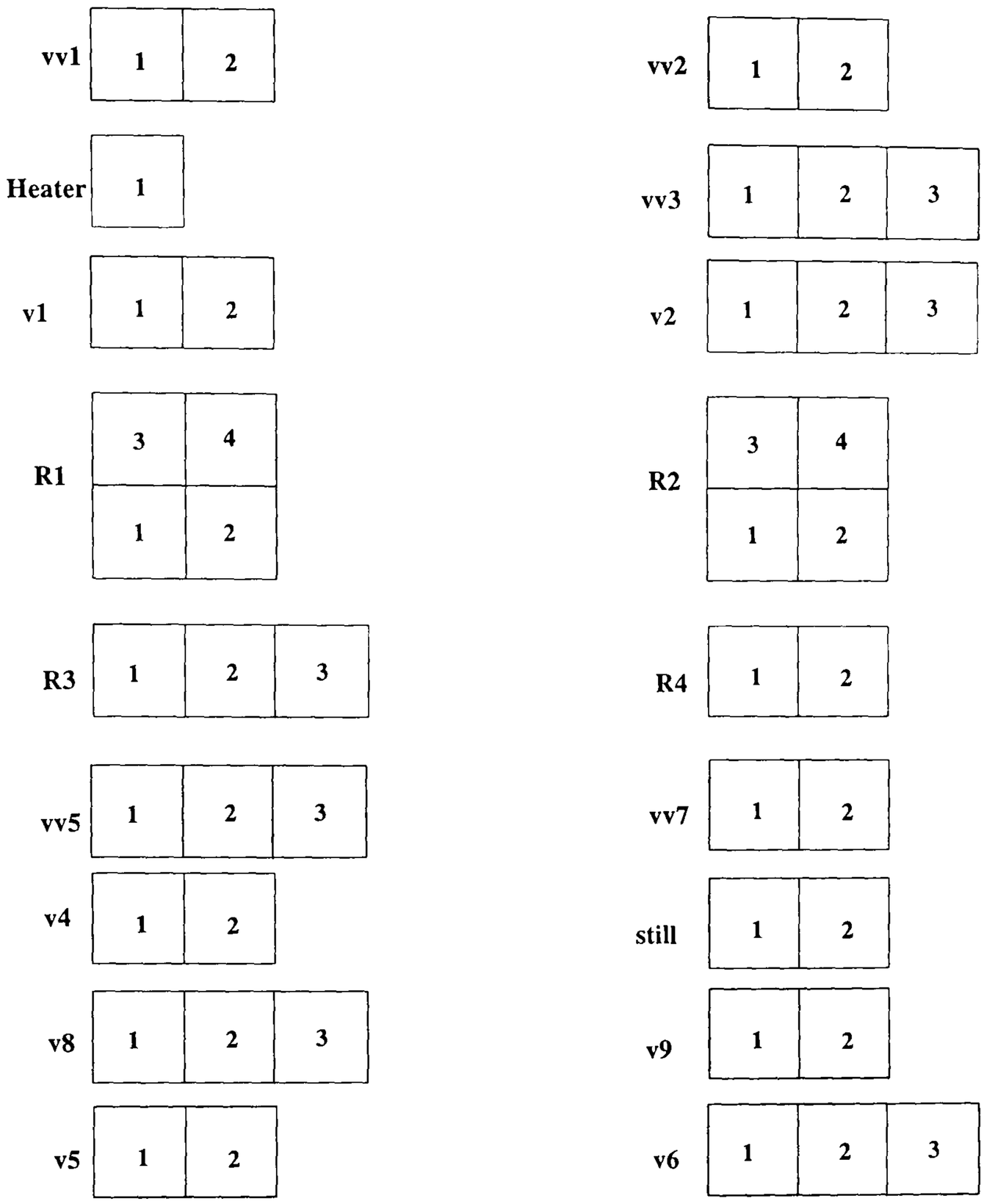


Figure 3.16: Process units shapes for example 3

The optimal layout is shown in Figure 3.17. We can see that a compact layout is obtained minimizing the upward pumping cost. Unit *still* is allocated to the second and third floor and units v9 and v5 to the first and second floor. The cost of this layout is 111,000 \$/yr comprising transport and connection costs. The computational time for the solutions was 9100 CPU sec on an ULTRA workstation.

Equipment	Size, m^2	Equipment	Size, m^2
vv1	20	vv5	30
vv2	20	vv7	30
vv3	30	v4	30
v1	20	still	20
v2	30	v8	30
R1	40	v9	20
R2	40	v5	20
R3	30	v6	30
R4	20	Heater	10

Table 3.7: Equipment sizes (floor space) for example 3

Stream	CF_{ij}^{up} $\$/m \cdot yr$	CF_{ij}^{hor} $\$/m \cdot yr$	CC_{ij} $\$/m$	Stream	CF_{ij}^{up} $\$/m \cdot yr$	CF_{ij}^{hor} $\$/m \cdot yr$	CC_{ij} $\$/m$
(vv1,Heater)	3250	325	200	(vv3, R2)	2540	254	230
(Heater, R1)	3680	368	240	(v1, R4)	2690	269	160
(vv2, R2)	3540	354	230	(v2, R1)	3680	368	250
(vv3, R1)	3680	368	400	(v2, R4)	2690	269	160
(R1, R2)	3540	354	230	(R1, R3)	2800	280	170
(R2, vv5)	5300	530	270	(R2, v8)	5300	530	270
(R1, vv7)	5500	550	280	(vv7, still)	5500	550	300
(still, vv5)	2760	276	170	(still, v9)	2760	276	170
(vv5, R1)	8100	810	300	(R3, vv5)	4100	410	250
(R3, v6)	4100	410	250	(R4, R3)	2800	280	175
(R4, v4)	2690	269	170	(v4, R3)	2800	280	175
(vv5, R3)	1200	120	140				

Table 3.8: Cost data for example 3

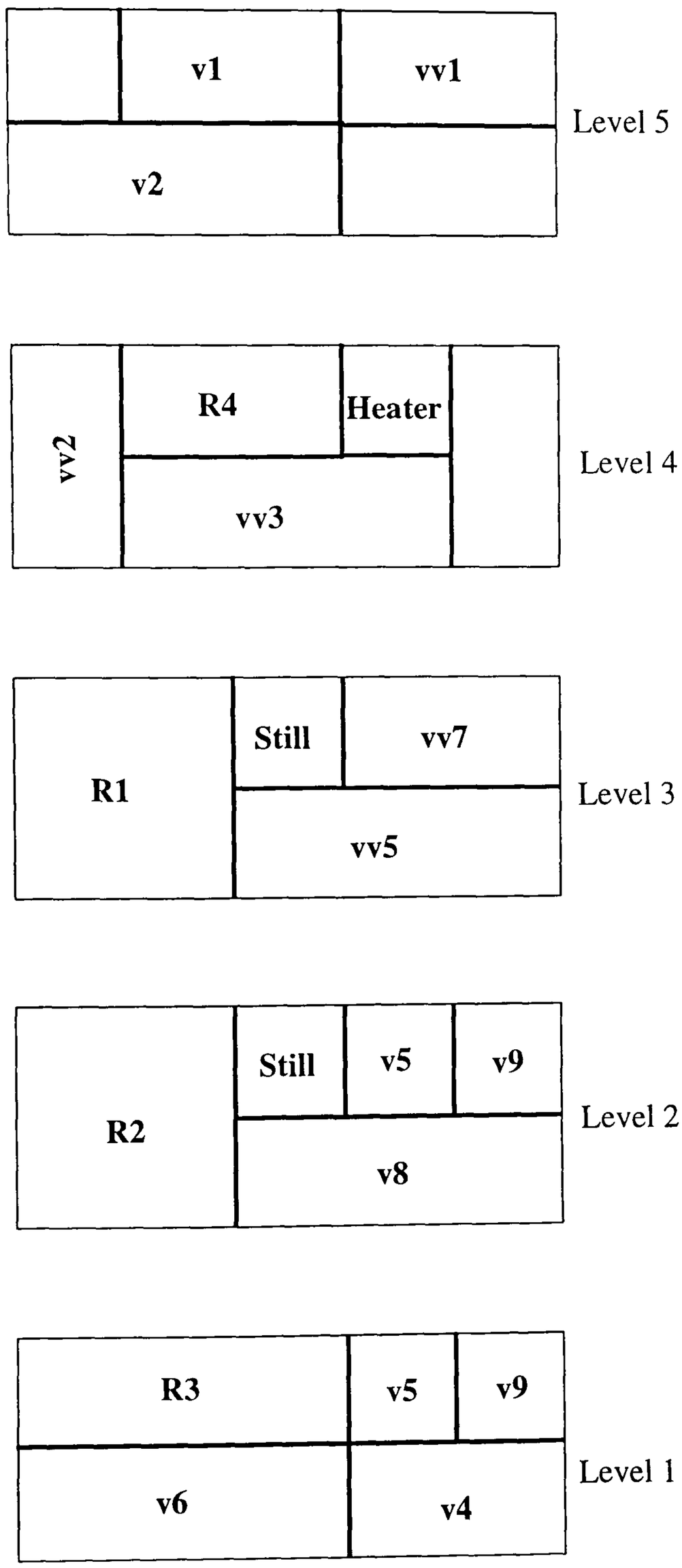


Figure 3.17: Process layout for example 3

3.5 Conclusions

A novel MILP formulation is developed for the the 2-D and 3-D process plant layout based on a uniform area discretization approach. The formulation results in a problem which can be solved using standard MILP solvers. The objective function represents the total transportation, piping, land and floor construction cost using detailed cost models and incorporating the aspect of direction dependent flow costs. The effect of land cost on the plant layout has been investigated with a small process example. Here, high land cost may result in more compact layouts. A salient feature of the formulation is that equipment sizes and geometries based on rectangular shapes are considered when solving the problem of finding the optimal allocation. Both single level and multilevel equipment geometries have been modelled. Orientation of the equipment in the 2-D level is allowed in order to obtain optimal layouts. Different types of constraints, for example due to safety considerations (*e.g.* minimum distance between units) can be easily incorporated. A way to handle degenerate solutions is also presented. The effectiveness of the presented approach is demonstrated with the attainment of global optimality for 3 case studies with up to 18 units.

It should be emphasized, however, that for problems with more than 20 units and for cases where many different equipment sizes and geometries exist the presented approach generates a formulation with a potentially very large number of binary variables. This may lead to the solution of an MILP problem requiring high computational costs (more than 10,000 CPU sec). In that case the problem can be considerable simplified if the optimal partitioning of units to floors is given (for example using the approach presented in the previous chapter). Once the optimal partitioning has been decided, the problem can take the form of deciding about the optimal exact allocation of process units (incorporating their sizes and geometries) using the approach presented in this paper. Thus, even for very large problems a good initial layout can be obtained during the conceptual design stage.

Part II-Modelling, Simulation and Optimisation of Heat Treatment Processes in Batch Plants

Chapter 4

Modelling and Simulation of Tubular Heat Exchangers under Milk Fouling

A mathematical model for single tubular heat exchangers under milk fouling is presented. A fouling model based on a reaction/mass transfer scheme is detailed where the main factors during milk heat treatment are quantified in a formal way. An analytical procedure for the calculation of key parameters is discussed, and provides the means to achieve more accuracy. The simulation results obtained show good agreement with available experimental work. Four different heat exchanger arrangements are then considered to illustrate the impact of design on the fouling behaviour.

4.1 Introduction

A variety of heat treatments are employed in the food batch industries. A typical and important example is dairy pasteurization where, when milk is heated and as the result of its instability, a deposit of milk solids is formed on the heat exchanger surface. Although this deposit is not sufficient to affect milk composition significantly, it results in hydraulic and thermal performance degradation and creates the need for cleaning operations which have to be carried out to bring the exchanger surface back to its original state. Fouling in food plants is a severe problem compared with other industries. For example, while in the petrochemical refineries heat exchangers may only be cleaned annually, in the dairy industry it is common practice to clean them every 5-10 hours. It should be noted here that the operating cost of fouling in the USA fluid milk industry (for pasteurized milk production, i.e. no sterilized and

ultra high temperature milk) has been estimated in $140 millions per year, approximately at current prices (Sandu and Singh, 1991).

Milk fouling has been studied for a number of years. The composition of the deposit is known and the chemical changes that occur when heating milk are fairly well understood. There are two key contributions in this area. The work of Fryer and co-workers (Fryer *et al.*, 1996) and the work at the food technology and food process engineering laboratory in France (Lalande *et al.*, 1989).

The key role played by proteins and especially β–lactoglobulin has been recognized in most recent milk fouling studies. Lalande *et al.* (1985) were the first who investigated the effect of β-lactoglobulin denaturation in milk fouling and showed that heat denaturation of this protein governs the milk deposit formation on the heat transfer area. Jong *et al.* (1992) applied the kinetics of the β-lactoglobulin reaction to analyze fouling in plate heat exchangers, and found that the amount of deposit could be correlated with protein reaction rates.

In their initial work Fryer and Slater (1985, 1986) modelled fouling using a dimensionless number, known as the Biot number (Bi) and a very simple reaction scheme. This model was able to predict the typical fouling behaviour according to which fouling builds up to an asymptotic level. However, milk fouling may not reach an asymptote as the same authors pointed out later (Paterson and Fryer, 1988). On the other hand, its main drawback is that it is not able to capture the effect of some very important parameters such as milk composition. The protein reaction scheme is not taken into account and fouling is controlled by reaction at the interface layer. Mass transfer operations are also omitted.

An interesting analysis concerning the chemical reactions governing fouling is presented by Paterson and Fryer (1988). They proved, following some principles of reaction engineering, that milk fouling is generated by chemical reaction(s) and the reaction(s) occur throughout the region of the fluid which is hot enough to support significant reaction rates. This means that there is no reason to assume that the rate controlling step in reaction fouling is the surface reaction. It also implies that bulk reactions could be significant together with mass transfer from the bulk region to the hot sublayer. Building upon this analysis Belmar-Beiny *et al.* (1993) studied the effect of Reynolds Number and fluid temperature in whey protein fouling. They showed that fouling is significantly increased as the fluid is heating up. Two possible mechanism were considered: (i) Fouling is mass transfer controlled and (ii) Fouling is reaction controlled. Fryer *et al.*, (1996) developed a statistical model for fouling of a plate heat exchanger. Based on a statistically-designed series of experiments they studied and quantified the significance of

a number of factors, including β-lactoglobulin reaction rate, on fouling within an ultra high temperature process. Recently, Toyoda and Fryer (1997) presented a very detailed fouling model which takes account of mass transfer between bulk and layer.

Sandu (1989) presents a considerable amount of work on milk fouling in plate heat exchangers. He developed a detailed physicomathematical model where fouling kinetics and dynamics were defined based on experimental results. Sandu and Lund (1982) developed a general model for fouling dynamics for the simple case of an inverse-solubility salt under the assumption that the deposition rate is entirely mass transfer controlled. This model was extended under more assumptions for fluids which are multicomponent systems. No simulation results were presented.

So far, in most cases, fouling has been modelled with a simple representation of the hydrodynamics of heat exchanger. However, it is known that there are strong interactions between the physiochemical, hydro-and thermo-dynamic fundamentals involved in fouling. For example, if mass transfer operations are important these are determined by the boundary layer thickness which depends on the fluid velocity. It is therefore important to consider all the relevant transport phenomena which take place during milk heat treatment along with the fouling kinetics.

Accurate prediction and analysis of fouling dynamics for a given system would pave the way for obtaining the optimal design and operating policies for industrial heat exchangers. The need for optimizing dairy plants suffering severe fouling problems has been long recognized (Sandu and Lund, 1983; Fryer, 1989). It is clear that the use of realistic and detailed models to optimize the equipment design and control can result in substantial economic benefits.

In this chapter we use fundamental kinetic theories to perform a comprehensive study of milk fouling as a process affected by momentum, heat and mass transfer phenomena. For this purpose, a fouling model taken from Toyoda and Fryer (1997) is coupled with a detailed dynamic heat exchanger model, where transport phenomena are taken into account in detail. Four different types of heat exchangers are considered to illustrate how the fouling behaviour is affected. The simulation results are verified against available experimental data and current industrial techniques for fouling mitigation.

4.2 Mathematical Model

4.2.1 Description of the Fouling Model

A fouling model must take into account all the relevant factors during milk heat treatment, such as fluid velocity, milk composition and temperature. It is generally agreed now that fouling is controlled by reactions, but still not clear if these are bulk or layer reactions or a combination of both. Mass transfer between the bulk and layer may be also important. Here the β-lactoglobulin reaction scheme is used for the fouling model. When milk is heated above 65 °C, β-lactoglobulin becomes thermally unstable and it (i) unfolds in molecular *denaturation* exposing reactive sulphydry (-SH) groups and (ii) polymerises irreversibly to give insoluble particles in *aggregation* (Jong *et al.*, 1992). The key step in studying fouling is to capture the interrelationship between the chemical reactions which give rise to deposition and the fluid mechanics associated with the heat transfer equipment.

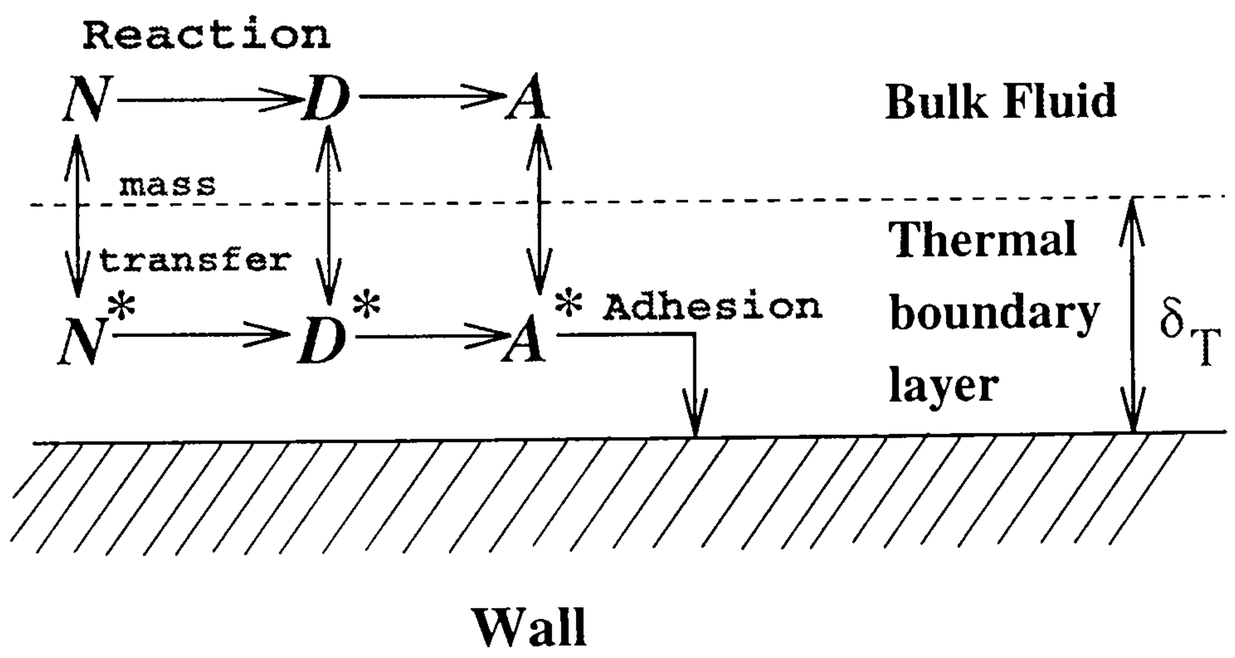


Figure 4.1: The protein reaction scheme

The reaction/mass transfer scheme is shown in Figure 4.1 and is the most detailed in the literature. It was adopted from Toyoda and Fryer (1997) and was first proposed by Jong *et al.*, (1992). The reaction scheme is described as follows:

- Proteins react in both the bulk and the thermal boundary layer in the milk. Native protein N is transformed to denaturated protein D, in a first order reaction. The denaturated protein then reacts to give aggregated protein A in a second order reaction.
- Mass transfer between the bulk and the thermal boundary layer takes place for each protein.

- Only the aggregated protein is deposited on the wall. The deposition rate is proportional to the concentration of aggregated protein in the thermal boundary layer.
- The fouling resistance to heat transfer is proportional to the thickness of the deposit.

The reaction rate constants are expressed in the common form as:

$$k = k_o \exp\left(\frac{-E}{RT}\right)$$

The pre-exponential factors k_o and the activation energies for the two reactions are taken from Jong *et al.* (1992) and given in Table 4.1 where the subscripts N and D refer to the first and second reaction respectively.

k_{No}, kJ/mol	k_{Do}, 1/sec	E_N, kJ/mol	E_D kJ/mol	Temperature, ^oC
261	312	$3.37 \cdot 10^{37}$	$1.36 \cdot 10^{43}$	70-90
-	-	56	$1.83 \cdot 10^{6}$	90-150

Table 4.1: Kinetic data for the reactions of β-lactoglobulin

4.2.2 Shell and Tube Heat exchanger Model under Fouling

In previous work on heat exchangers under fouling very simple models were used to account for the hydro and thermo-dynamic characteristics of the fluid. Two common assumptions were:

- The fluid temperature in the bulk and thermal boundary layer are radially uniform, i.e. the temperature in the bulk and thermal boundary layer are equal and do not change with the tube radius.
- The fluid flows in plug flow at uniform velocity. The velocity in the thermal boundary layer is assumed negligible in comparison to that in the bulk.

The above assumptions simplify the conservation laws expressed by partial differential equations describing the hydrodynamics, the reactions, and mass transfer between the bulk and the layer. However, under turbulent flow conditions velocity is not uniform and a profile exists (Brodkey and Hershey, 1988).

It is then apparent that the physical behavior may change significantly in the radial direction. The radial velocity profile may affect considerably both the heat and the mass

transfer operations. Furthermore, a radial temperature profile in the bulk exists which also affects the rate of the reactions and mass transfer. If these profiles are ignored, potential differences between bulk and boundary reaction rates are not captured. Note that milk fouling is determined by reactions rates which are strong functions of temperature.

Here we present a detailed model for shell and tube heat exchangers under fouling by relaxing the above assumptions and taking into account the radial dependency of velocity, temperature and concentrations. In order to be consistent with the proposed reaction scheme, where mass transfer operations occur between the bulk and the thermal boundary layer, we distinguish the bulk from the boundary layer based on the conservation laws. The velocity in the thermal boundary layer which is small but not negligible is taken into account.

The following assumptions are considered:

- The variation of the physical properties of milk with temperature are neglected and the properties are taken as those of milk at inlet conditions (McKetta, 1984). However transport properties are calculated in detail.
- The overall heat transfer resistance is determined by that on the tube side fluid (milk).
- The concentration and temperature of proteins in the boundary layer are assumed not to be radially dependent.

In the reference operating scenario considered, a stream of skimmed milk (0.25 kg/s) is to be heated from 333 K to a target temperature of approximately 370 K. Tables 4.2 and 4.3 give the specification of several heat exchangers prior to the initiation of the fouling. Four cases are examined (Figure 4.2). Cases (i) and (ii) represent constant wall temperature: (i) the heating medium is steam at temperature 374 K (ii) the heating medium is steam at temperature 390 K. In cases (iii) and (iv) the wall temperature varies along the length of the exchanger: (iii) the heating medium is hot water at 385 K in co-current flow with milk (iv) the same as in case (iii) but in a counter current operation. Similar data for the steady-state milk inlet and outlet temperatures were used by Fryer and Slater (1985) and approximately correspond to industrial conditions. Clearly, alternative scenarios could be easily included. The model described in the following section apply to a wide range of operating conditions.

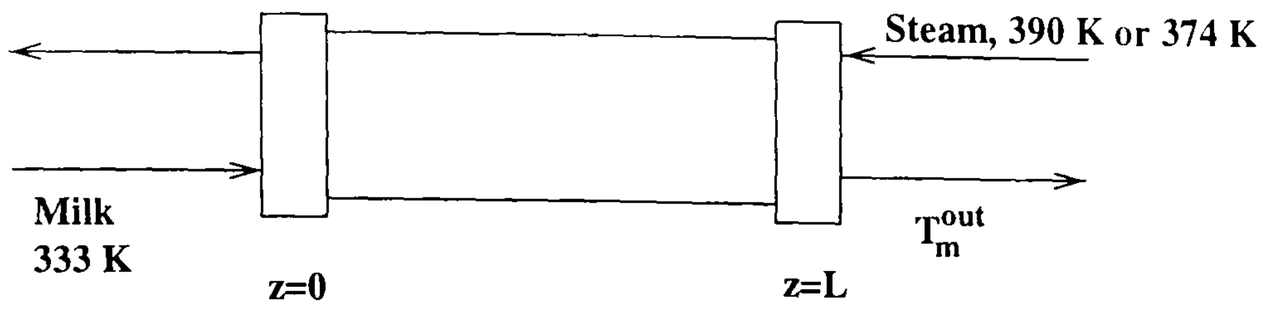


Figure 4.2: Shell and tube heat exchangers for milk heat treatment

4.2.3 Fundamental Equations

Consider a differential element in a circular tube, where r_o is the inner radius, and L is the length of the tube (Figure 4.3). The main variables used are given in the nomenclature section 4.5. Then material balances of proteins in the bulk are given by the following equations:

Native protein:

$$\frac{\partial C_N}{\partial t} + u_z(r)\frac{\partial C_N}{\partial z} = -k_{No}\exp\left(\frac{-E_N}{RT_f(r)}\right)\cdot C_N + \frac{1}{r}\frac{\partial}{\partial r}\left(r\cdot D_N\frac{\partial C_N}{\partial r}\right) + \frac{\partial}{\partial z}\left(D_N\frac{\partial C_N}{\partial z}\right) \tag{4.1}$$

Denaturated protein:

$$\frac{\partial C_D}{\partial t} + u_z(r)\frac{\partial C_D}{\partial z} = k_{No}\exp\left(\frac{-E_N}{RT_f(r)}\right)\cdot C_N - k_{Do}\exp\left(\frac{-E_D}{RT_f(r)}\right)\cdot C_D^2 + \frac{1}{r}\frac{\partial}{\partial r}\left(r\cdot D_D\frac{\partial C_D}{\partial r}\right) + \frac{\partial}{\partial z}\left(D_D\frac{\partial C_D}{\partial z}\right) \tag{4.2}$$

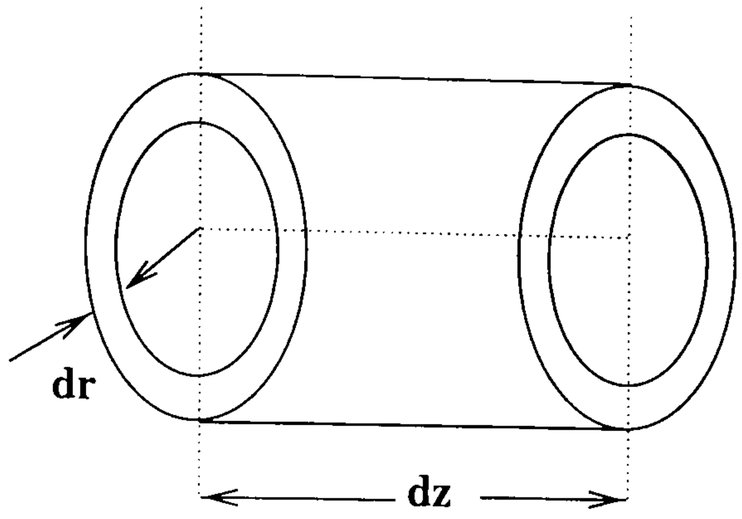


Figure 4.3: A differential element in a shell and tube heat exchanger

Aggregated protein:

$$\frac{\partial C_A}{\partial t} + u_z(r)\frac{\partial C_A}{\partial z} = k_{Do}\exp\left(\frac{-E_D}{RT_f(r)}\right)\cdot C_D^2 + \frac{1}{r}\frac{\partial}{\partial r}\left(r\cdot D_A\frac{\partial C_A}{\partial r}\right) + \frac{\partial}{\partial z}\left(D_A\frac{\partial C_A}{\partial z}\right) \tag{4.3}$$

The last two right hand side terms express the rate of diffusion into the control volume with respect to the radial and axial distance. In the above equations, $u_z(r)$ is the fluid velocity as a function of the tube radius and D_N, D_D and D_A are the diffusion coefficients of the three proteins.

For the proteins in the boundary layer radial gradients of the concentrations are not considered but terms are included to account for radial mass transfer with the bulk phase via mass transfer coefficients. In order to distinguish between bulk and surface reactions rates the last are assumed to take place at the interface temperature T_i which is radially independent and given by equation (4.63) or (4.65). The assumption of constant T_i provides an approximate way to distinguish bulk and surface reaction rates. On the other hand, diffusion in the axial direction is considered. Thus, the material balances of the proteins in the thermal boundary layer are given by:

Native protein:

$$\frac{\partial C_N^*}{\partial t} + u_z(r)\frac{\partial C_N^*}{\partial z} = -k_{No}\exp\left(\frac{-E_N}{RT_i}\right)\cdot C_N^* - \frac{k_{mN}}{\delta_T}(C_N^* - C_N) + \frac{\partial}{\partial z}\left(D_N\frac{\partial C_N^*}{\partial z}\right) \tag{4.4}$$

Denaturated protein:

$$\frac{\partial C_D^*}{\partial t} + u_z(r)\frac{\partial C_D^*}{\partial z} = k_{No}\exp\left(\frac{-E_N}{RT_i}\right)\cdot C_N^* - k_{Do}\exp(\frac{-E_D}{RT_i})\cdot C_D^{*2} - \frac{k_{mD}}{\delta_T}(C_D^* - C_D) + \frac{\partial}{\partial z}\left(D_D\frac{\partial C_D^*}{\partial z}\right) \tag{4.5}$$

Aggregated protein:

$$\frac{\partial C_A^*}{\partial t} + u_z(r)\frac{\partial C_A^*}{\partial z} = k_{Do}\exp\left(\frac{-E_D}{RT_i}\right)\cdot C_D^{*2} - \frac{1}{\delta_T}\cdot\left[k_{mA}(C_A^* - C_A) + k_w C_A^*\right] + \frac{\partial}{\partial z}\left(D_A\frac{\partial C_A^*}{\partial z}\right) \tag{4.6}$$

where C_N, C_D and C_A are the values of the bulk protein in contact with the boundary layer and δ_T is the thickness of the thermal layer. Finally k_{mN}, k_{mD}, k_{mA} are the protein mass transfer coefficients.

The rate of deposition is related to the concentration of aggregated protein in the boundary layer by the mass transfer coefficient k_w. The dimensionless Biot number is used to express the change of heat transfer due to fouling and it is related to the rate of deposition by a constant β (Toyoda and Fryer, 1997):

$$\frac{\partial Bi}{\partial t} = \beta k_w C_A^* \tag{4.7}$$

The energy balance on the milk side can be written as:

$$\rho C_p\frac{\partial T_f(r)}{\partial t} + \rho C_p\cdot u_z(r)\frac{\partial T_f(r)}{\partial z} = \frac{\partial}{\partial z}\left(k_f\frac{\partial T_f(r)}{\partial z}\right) + \frac{1}{r}\frac{\partial}{\partial r}\left(rk_f\frac{\partial T_f(r)}{\partial r}\right) \tag{4.8}$$

where $T_f(r)$ is the milk temperature. For the utility side, one assumption is that a heating fluid, here hot water is adopted for counter current and co-current operation. It is assumed that its temperature and velocity are radially uniform. Under this assumption the energy balance for the heating medium takes the following form:

- Co-current operation with milk

$$\frac{\partial T_s}{\partial t} + v_s \frac{\partial T_s}{\partial z} = -\frac{1}{\rho_w C_{pw}} \cdot U \cdot \alpha_s (T_s - T_f) \tag{4.9}$$

- Counter-current operation with milk:

$$\frac{\partial T_s}{\partial t} - v_s \frac{\partial T_s}{\partial z} = -\frac{1}{\rho_w C_{pw}} \cdot U \cdot \alpha_s (T_s - T_f) \tag{4.10}$$

where T_s and u_s are the heating medium temperature and velocity respectively and α_s is the shell heat transfer area per unit volume and can be taken equal to $4/d$ where d is the tube diameter.

Another alternative explored was the use of steam as heating medium. In this case it is assumed that steam enters and exits the exchanger at the same temperature (*i.e.* flowrate is high enough for the given thermal duty) providing its heat of condensation for the heating purposes. The steam temperature is thus function of its pressure only.

4.2.4 Boundary Conditions

Proteins in the Bulk:

The integration in the radial direction should be carried out from $r = 0$ (center of the tube) to $r{=}r_o - \delta_T$ where δ_T is the thermal boundary layer (see figure 4.1). However, the thickness of the boundary layer is very small compared with the tube radius (a typical value for the constant wall temperature operation is 0.023 mm). It is then reasonable to assume, that the mass balance equations are integrated over the entire range of the tube radius.

Danckwerts (1953) boundary conditions are utilized at the inlet and outlet of the tube:

$$-D_N \cdot \frac{\partial C_N}{\partial z} = u_z(r)(C_N^{in} - C_N) \qquad z = 0, \quad r \in [0, r_o] \tag{4.11}$$

$$-D_A \cdot \frac{\partial C_A}{\partial z} = u_z(r)(C_A^{in} - C_A) \qquad z = 0, \quad r \in [0, r_o] \tag{4.12}$$

$$-D_D \cdot \frac{\partial C_D}{\partial z} = u_z(r)(C_D^{in} - C_D) \qquad z = 0, \quad r \in [0, r_o] \tag{4.13}$$

$$\frac{\partial C_N}{\partial z} = 0.0 \qquad z = L, \quad r \in [0, r_o] \tag{4.14}$$

$$\frac{\partial C_D}{\partial z} = 0.0 \qquad z = L, \quad r \in [0, r_o] \tag{4.15}$$

$$\frac{\partial C_A}{\partial z} = 0.0 \qquad z = L, \quad r \in [0, r_o] \tag{4.16}$$

The values of the inlet protein concentrations, $C_{N,in}$, $C_{D,in}$ and $C_{A,in}$ are given in Table 4.4 (McKetta, 1984).

The main transfer rate balance at the interface between the bulk and the boundary layer yields:

$$-D_N \frac{\partial C_N}{\partial r} = k_{mN}(C_N - C_N^*) \qquad r = r_o, \quad z \in (0, L) \tag{4.17}$$

$$-D_D \frac{\partial C_D}{\partial r} = k_{mD}(C_D - C_D^*) \qquad r = r_o, \quad z \in (0, L) \tag{4.18}$$

$$-D_A \frac{\partial C_A}{\partial r} = k_{mA}(C_A - C_A^*) \qquad r = r_o, \quad z \in (0, L) \tag{4.19}$$

while radial symmetry dictates that:

$$\frac{\partial C_N}{\partial r} = 0.0 \qquad r = 0, \quad z \in (0, L) \tag{4.20}$$

$$\frac{\partial C_D}{\partial r} = 0.0 \qquad r = 0, \quad z \in (0, L) \tag{4.21}$$

$$\frac{\partial C_A}{\partial r} = 0.0 \qquad r = 0, \quad z \in (0, L) \tag{4.22}$$

Boundary Layer proteins:

$$-D_N \cdot \frac{\partial C_N^*}{\partial z} = u_z(r)(C_{N^*}^{in} - C_N^*) \qquad z = 0 \tag{4.23}$$

$$-D_D \cdot \frac{\partial C_D^*}{\partial z} = u_z(r)(C_{D^*}^{in} - C_D^*) \qquad z = 0 \tag{4.24}$$

$$-D_A \cdot \frac{\partial C_A^*}{\partial z} = u_z(r)(C_{A^*}^{in} - C_A^*) \qquad z = 0 \tag{4.25}$$

$$\frac{\partial C_N^*}{\partial z} = 0.0 \qquad z = L \tag{4.26}$$

$$\frac{\partial C_D^*}{\partial z} = 0.0 \qquad z = L \tag{4.27}$$

$$\frac{\partial C_A^*}{\partial z} = 0.0 \qquad z = L \tag{4.28}$$

The values of the inlet ($z = 0$) concentrations $C_{N^*}^{in}$, $C_{D^*}^{in}$ and $C_{A^*}^{in}$ are given in Table 4.4.

Energy Balance:

The boundary conditions for all the heat exchanger arrangements considered are as follows:

$$-k_f \frac{\partial T_f(r)}{\partial z} = \rho C_p u_z(r)(T_f^{in} - T_f(r)) \qquad z = 0, \quad r \in [0, r_o] \tag{4.29}$$

$$\frac{\partial T_f(r)}{\partial z} = 0 \qquad z = L, \quad r \in [0, r_o] \tag{4.30}$$

$$\frac{\partial T_f(r)}{\partial r} = 0 \qquad r = 0, \quad z \in (0, L) \tag{4.31}$$

$$k_f \cdot \frac{\partial T_f(r)}{\partial r} = U \cdot (T_w - T_f(r)) \qquad r = r_o, \quad z \in (0, L) \tag{4.32}$$

$$k_f \cdot \frac{\partial T_f(r)}{\partial r} = U \cdot (T_s(z) - T_f(r)) \qquad r = r_o, \quad z \in (0, L) \tag{4.33}$$

Equations 4.32 is for the constant wall temperature case only (*i.e.* steam as the heating medium), while equation 4.33 is for the counter current (or co current) case. U is the overall heat transfer coefficient which is a function of the fouling resistance (Biot number) and T_f^{in} is the milk inlet temperature (see Table 4.2). Finally T_w and $T_s(z)$ is the wall and the heating medium temperature respectively.

The boundary conditions for the heating medium are given below:

$$\text{Co-current operation} \quad T_s(z) = T_s^{in} \text{ K}, \qquad z = 0 \tag{4.34}$$

$$\text{Counter current operation} \quad T_s(z) = T_s^{in} \text{ K}, \qquad z = L \tag{4.35}$$

where the heating medium inlet temperature is given in Table 4.2.

4.2.5 Initial Conditions

It is assumed that prior to the circulation of milk (*e.g.* initiation of fouling) the exchanger was operating at steady state with a non fouling fluid on the tube site. This is justified since pasteurizers are preheated and sterilized with hot water before the milk fluid is processed.

$$\frac{\partial T_f(z,r,t)}{\partial t} = 0 \qquad t = 0, \quad \forall z \in (0, L) \quad \forall r \in (0, r_o)$$

$$\frac{\partial T_s(z,t)}{\partial t} = 0 \qquad t = 0, \quad \forall z \in (0, L)$$

$$C_N(z, r, t) = C_D(z, r, t) = C_A(z, r, t) = 0.0 \qquad t = 0, \quad \forall z \in (0, L) \quad \forall r \in (0, r_o)$$

$$C_N^*(z, t) = C_D^*(z, t) = C_A^*(z, t) = 0.0 \qquad t = 0, \quad \forall z \in (0, L)$$

$$Bi(z, t) = 0.0 \qquad t = 0, \quad \forall z \in (0, L)$$

Case of operation	Type of exchanger	Length, m	T_f^{in}, K	T_f^{out}, K	T_s^{in}, K	T_s^{out}, K
1	Steam, $T_w = 374$K	10	333	370.4	-	-
2	Steam, $T_w = 390$K	5	333	370.4	-	-
3	Hot water, co-current flow	10	333	370.4	385	374
4	Hot water, counter-current flow	7	333	370.4	385	374

Table 4.2: Details of heat exchangers used in simulation (steady state)

Milk flowrate, kg/s	Hot water flowrate, kg/s	diameter m	α_s, 1/m	v_s, m/s
0.25	1.5	0.025	160	4.08

Table 4.3: Heat exchanger data used in simulation

Parameter	Value, kg/m^3	Parameter	Value, kg/m^3
C_N^{in}	3.8	$C_{N^*}^{in}$	3.8
C_D^{in}	0.0	$C_{D^*}^{in}$	0.0
C_A^{in}	0.0	$C_{A^*}^{in}$	0.0

Table 4.4: Parameter values used in simulation

4.2.6 Calculation of the Transport Phenomena Variables

The model of a shell and tube heat exchanger under fouling includes a number of variables such as the thickness of the thermal boundary layer δ_T, the mass transfer coefficients k_{mN}, k_{mD}, k_{mA}, k_w,and the fluid velocity $u_z(r)$. Here, detailed expressions are used for the calculation of these variables.

The thickness of the thermal boundary layer δ_T is related to that of the laminar boundary layer δ using the following expression:

$$\frac{\delta_T}{\delta} = Pr^{1/3} \tag{4.36}$$

where Pr is the Prandtl number given by:

$$Pr = \frac{C_p \cdot \mu}{k_f} \tag{4.37}$$

The above two expressions derive from the analogy between the momentum and heat transfer in turbulent flow conditions. Physical property data are given in Table 4.5

Viscosity, μ $kg/(m \cdot s)$	Thermal Conductivity, k_f $J/(s \cdot m \cdot K)$	Heat Capacity, C_p $J/(kg \cdot K)$
$1.5 \cdot 10^{-3}$	0.59	3930

Table 4.5: Physical property data used in simulation

In order to calculate δ, one can assume (Brodkey and Hershey, 1988) that it is equal to the thickness of the viscous sub-layer. It is known that during milk heat treatment the flow is turbulent (i.e. Reynolds number greater than 2100). Therefore, the velocity profile within the flow can now be expressed as:

$$\text{Viscous sub-Layer:} \quad u^+ = y^+ \quad \text{for} \quad 0 < y^+ \leq 5 \tag{4.38}$$

$$\text{Generation zone:} \quad u^+ = 5 \ln y^+ - 3.05 \quad \text{for} \quad 5 < y^+ < 30 \tag{4.39}$$

$$\text{Turbulent core:} \quad u^+ = 2.5 \ln y^+ + 5.5 \quad \text{for} \quad 30 \leq y^+ \tag{4.40}$$

where u^+ is a dimensionless velocity and y^+ the dimensionless distance from the wall defined as:

$$u^+ = \frac{u_z(r)}{U^*}, \qquad y^+ = \frac{y \cdot U^* \cdot \rho}{\mu} \tag{4.41}$$

where U^* the friction velocity, is a function of the wall shear stress τ_w and given by the following equations:

$$U^* = \sqrt{\left(\frac{\tau_w}{\rho}\right)} \tag{4.42}$$

It is now possible using equations 4.38 and 4.41 to calculate δ for y^+ equal to 5 (by setting δ equal to y since it is equal to the thickness of the boundary layer).

The wall shear stress τ_w can be calculated using the following expressions which holds for the case of turbulent flow:

$$f = 0.079 N_{Re}^{1/4} \tag{4.43}$$

$$f = \frac{\tau_w}{\frac{1}{2}\rho u_{z,aver}^2} \tag{4.44}$$

$$Re = \frac{d \cdot u_{z,aver} \cdot \rho}{\mu} \tag{4.45}$$

where f is the friction factor and $u_{z,aver}$ is the average velocity which can easily be calculated from the fluid flowrate w_f as follows:

$$u_{z,aver} = \frac{w_f}{\rho \cdot Area} \qquad Area = \frac{\pi \cdot d^2}{4} \tag{4.46}$$

Finally, the mass transfer coefficients for the three proteins are related to the diffusion coefficients by:

$$k_{mi} = \frac{D_i}{\delta} \qquad i = N, D, A \tag{4.47}$$

When the diameter of the particles is known, the diffusion coefficients can be estimated by the Wilke-Chang equation (Perry and Green, 1984):

$$D_i = 1.310^{-17} \frac{T_i}{\mu V_i^{0.6}} \qquad i = N, D, A \tag{4.48}$$

with V_i as the molecular volume of the absorbed particles:

$$V_i = N_{AV} \frac{1}{6} \pi d_i^3 \qquad i = N, D, A \tag{4.49}$$

where N_{AV} is the Avogadro constant, $6.023 \cdot 10^{23}$, and d_i is the particle diameter which must be determined experimentally. Unfortunately, their values for the proteins in milk are

not reported in the literature. Jong *et al.*, (1992) performed a regression analysis with several assumed particle diameters and they concluded that the highest correlation coefficients were obtained with particle diameters smaller than 10 nm and very close to 10^{-10} m; mean diameters above 50 nm did not give satisfactory agreement with the experimental results. Here the values of the particles diameters are estimated using optimal regression methods in order to achieve a good agreement with experimental work, while taking into account the size limitations reported by the above researchers (Table 4.6). This is discussed in more detail in section 4.3.1.

Native particle, d_N	Denaturated particles,d_D	Aggregated particles, d_A
$7.5 \cdot 10^{-11}$ m	$7.5 \cdot 10^{-11}$ m	$4.2 \cdot 10^{-10}$ m

Table 4.6: Values of particle diameters for the three proteins from optimal fit of experimental data

A key assumption made in the calculation of the transport properties is that the turbulent contribution as expressed by the eddy diffusivity of mass and heat transfer is neglected. For the transport properties in the boundary layer the turbulent contribution is indeed small ($\sim 10^{-8}$) compared with the values of the Fickian diffusivities ($\sim 10^{-6}$). On the other hand, for the bulk this contribution may be considerable. A sensitivity analysis has been performed using approximate values for the eddy diffusivities in the bulk. The analysis indicates that there is a less than 2% change in the simulation results which can be considered acceptable within the experimental error.

The value of the mass transfer coefficient from the boundary layer to the deposit, k_w is given by Toyoda and Fryer (1997) and it is equal to 10^{-7} m/sec. Finally, the proportionality constant β can be determined only by experimental data. Here, a value of 58 m^2/kg was obtained from a parameter estimation analysis (see section 4.3.1).

Radial velocity profile

Although equations 4.38 to 4.40 provide a good description of the velocity distribution for flow in the tubes, they introduce discontinuities in the model which may cause numerical difficulties in the simulation. Alternatively it is possible to use the Pai's continuous model for the radial velocity distribution, under turbulent flow conditions, described by the following equations (Brodkey and Hershey, 1988).

$$\frac{u_z(r)}{u_{z,max}} = 1 + \alpha_1 \left(\frac{r}{r_o}\right)^2 + \alpha_2 \left(\frac{r}{r_o}\right)^{2m} \tag{4.50}$$

where the terms α_1 and α_2 are given as follows:

$$\alpha_1 = \frac{(s-m)}{(m-1)} \tag{4.51}$$

$$\alpha_2 = \frac{(1-s)}{(m-1)} \tag{4.52}$$

and m can be expressed as the whole integer closest up or down to the value given by :

$$m = -0.617 + (8.211 \times 10^{-3})(N_{Re})^{0.786} \tag{4.53}$$

Finally the quantity s can be correlated in terms of the Reynolds number, N_{Re}:

$$s = 0.585 + (3.172 \times 10^{-3})(N_{Re})^{0.833} \qquad 2800 < N_{Re} \tag{4.54}$$

Note that the maximum velocity $u_{z,max}$ is a function of the average velocity:

$$\frac{u_{z,\max}}{u_{z,aver}} = 1 + \frac{\alpha_1}{2} + \frac{\alpha_2}{(m+1)} \tag{4.55}$$

The above model equations provide a continuous model of the velocity radial profile which is quite accurate for Reynolds number less than 100,000 (Brodkey and Hershey, 1988). Since due to pressure drop limitations it is not possible to exceed this value for the problem considered here, these equations were adopted for the simulation results presented in the next section.

4.2.7 Quantifying Fouling

Additional variables allow us to quantify fouling. Since the Biot number is a function of the tube distance z (it is determined by the aggregated protein concentration), an average Biot number can be defined over the heat exchanger as:

$$\bar{Bi} = \frac{1}{L}\int_o^L Bi(z)dz \tag{4.56}$$

The thickness of the deposit, x_d, at each position z along the heat exchanger can be defined using the Biot number as:

$$x_d(z) = \frac{\lambda_d \cdot Bi(z)}{U_o} \tag{4.57}$$

where λ_d is the deposit thermal conductivity equal to 0.5 $W/m \cdot K$ (LeClercq-Perlat and Lalande, 1991) and the overall heat transfer coefficient under clean conditions, U_o, can be easily determined for a given thermal duty and heat transfer area.

An average deposit thickness is defined over the tube by the following equation

$$\bar{x}_d = \frac{1}{L}\int_o^L x_d(z)dz \tag{4.58}$$

The deposit mass at each position z along the heat exchanger, expressed in kg/m^2 is defined as:

$$mass(z) = \frac{\lambda_d \cdot Bi(z) \cdot \rho_d}{U_o} \tag{4.59}$$

where ρ_d is the deposit density equal to 1030 kg/m^3.

Similarly, the average deposit mass over the tube is:

$$\overline{mass} = \frac{1}{L}\int_o^L mass(z)dz \tag{4.60}$$

Another way to quantify fouling is by the "fictitious" efficiency of the heat exchanger given by the following equation:

$$\epsilon_{fic} = \frac{\text{Heat exchanged during operation without control}}{\text{maximal heat exchanged}} = \tag{4.61}$$

$$\frac{T_f^{outlet}(t) - T_f^{in}}{T_f^{out}(0) - T_f^{in}} \quad \forall t \in (0, t_{heat}] \tag{4.62}$$

where $T_f^{out}(0)$ is the milk outlet temperature at steady state (before fouling), which is specified to be 370.4 K, $T_f^{outlet}(t)$ is the same temperature during the heating operation and t_{heat} is the total heating period.

The overall heat transfer coefficient U and the interface temperature T_i are given by the following expressions (Fryer and Slater, 1985)

$$U = \frac{U_o}{1+Bi} \tag{4.63}$$

$$T_i = \frac{T_w + BiT_f}{1+Bi} \text{ steam as heating fluid} \tag{4.64}$$

$$T_i = \frac{T_s + BiT_f}{1+Bi} \text{ hot water as heating fluid} \tag{4.65}$$

4.3 Numerical Simulation and Results

The model of a shell and tube heat exchanger under milk fouling described by equations 4.1 to 4.65 comprises a set of integral, partial differential, and algebraic equations (IPDAEs). It is simulated using the simulation package *gPROMS* (Barton and Pantelides, 1994; Oh and Pantelides, 1996; *gPROMS* Technical Manual, 1998c). The solution method is based on a two-phase method-of-lines approach (see Figure 4.4). In the first phase, the spatial dimensions (axial and radial) are discretized in terms of finite dimensional representations, and this reduces the IPDAEs into sets of differential algebraic equations (DAEs) with respect to time. In the second phase, the DAEs are integrated over the time horizon of interest using appropriate integration techniques. Here, the axial domain is discretized using 2nd order orthogonal collocation on 20 uniform finite elements, whereas the radial domain is approximated by 3rd order orthogonal collocation on 5 finite elements. This number of elements and order of approximation over the two spatial domains provides the best accurate results. A number of simulations tests has been performed which indicated that if less than 10 elements are used for the axial domain discretization there is a 5-10% change in the results. On the other hand, the discretization over the radial domain is sensitive if less than 3 elements and/or a 2nd order approximation are used. The data used in simulation are given in Tables 4.1 to 4.5.

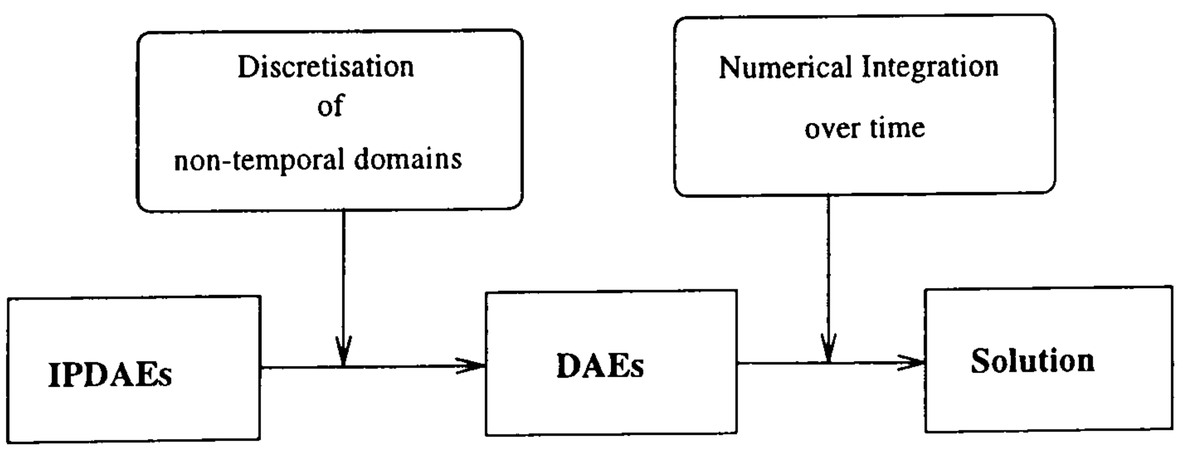


Figure 4.4: Solution strategy of the model

4.3.1 Parameter Estimation and Verification of the Simulation Results with Experimental Data

There are a few publications in the literature where experimental results of milk fouling in a tube are reported. Verification of the simulation results is an important step in order to:

- Check the validity of the model presented here.
- Determine appropriate values for certain parameters (*e.g.* particle diameters)

There are four unknown parameters in the model presented in section 4.2. These are the diameters of the three protein particles, d_N, d_D, d_A and the deposition rate constant β. Only size ranges for the particles are reported in the literature (see section 2.6). Taking into account these limits, a parameter estimation analysis was performed based on the solution of a dynamic optimization problem. To this purpose, the dynamic parameter estimation facility (*gEST*) within *gPROMS* was used directly. This problem was solved in order to take into account the constraints on the particles diameters. It should be emphasized here that the mass transfer coefficient is taken as constant (from Toyoda and Fryer, 1997) since the are no data concerning even the approximate order of its magnitude. Therefore, any attempt to find its optimal value may lead to unrealistic values. A brief description of the mathematical problem being solved is given in Appendix A. The optimal values of the particle diameters are given in Table 4.6 while the constant β was found to be 58. It is worthwhile to notice that the values obtained are very close to the experimental conclusions of Jong *et al.*, (1992).

Here for the purpose of parameters estimation and verification we use the experimental results of Belmar-Beiny *et al.* (1993). The experimental conditions are: 1% whey protein; Reynolds number 6250; heating period 1 hour, length of the tube 1.5 m and two sets of fluid inlet and outlet temperature: (i) inlet temperature 69^oC and outlet temperature 81^oC and (ii) inlet and outlet temperature 61^oC and 76^oC respectively. The variable fitted is the amount of deposit at different positions along the tube, at the end of heating period. A comparison between the best fit and experimental results is shown in Figure 4.5, for the two experimental sets. There is a good agreement of the simulation results with the experimental data. It can be seen that the total amount of deposition increases with the inlet temperature and that fouling is at a low level in the inlet region and then increases significantly at some point down the tube. It should be emphasized here that in the parameter estimation problem the two sets of experimental conditions (different inlet and outlet temperatures) are analyzed simultaneously.

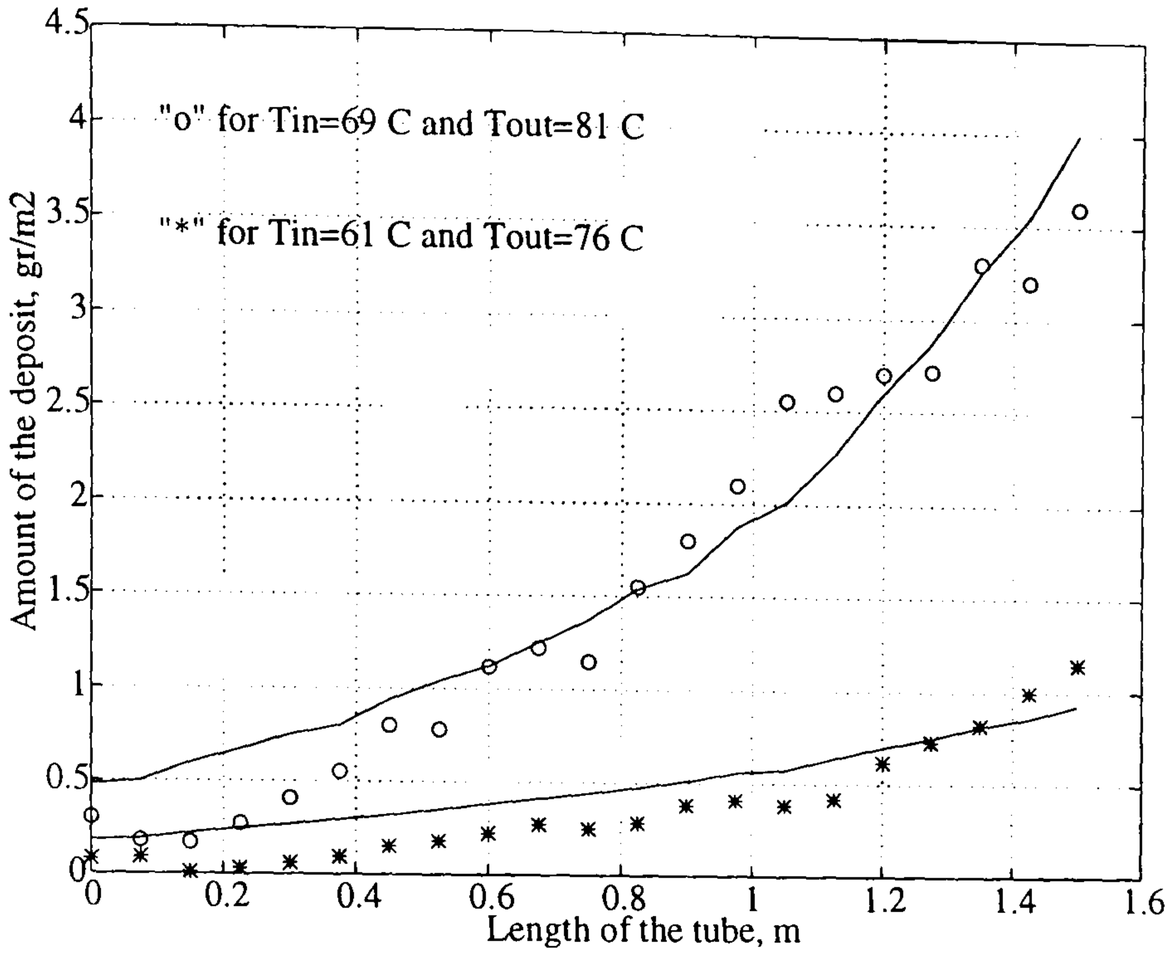


Figure 4.5: Comparison between simulation and experimental results

An independent check of the validity of the model is obtained by plotting the effect of Reynolds number on fouling and comparing with other experimental results (independently measured and not used for parameter estimation). This is shown in Figure 4.6. Again the experimental results were taken from Belmar-Beiny *et al.* (1993). The experimental conditions are 1% whey protein, milk inlet and outlet temperature $73°C$ and $83°C$ respectively and heating time 1 hour. We observe that as the Reynolds number increases the total amount of deposit down the tube decreases. There is a quite good agreement with the experimental work although fouling is overestimated at low Reynolds number.

4.3.2 Simulation Results and Discussion

The fouling behavior of four different heat exchanger configurations was then investigated (see Table 4.2). The inlet native protein concentration in all cases is 3.8 kg/m^3 (for skimmed milk). The key role of some of the model's parameters is also illustrated. The main results are summarized as follows:

- Figure 4.7 shows a 3-D representation of the milk bulk temperature with respect to tube length and radius at time 5.55 hours for the constant wall temperature case (steam as heating medium, 374 K). Clearly, milk temperature increases along the tube while a radial temperature profile is also observed. Figures 4.8 shows the evolution of layer

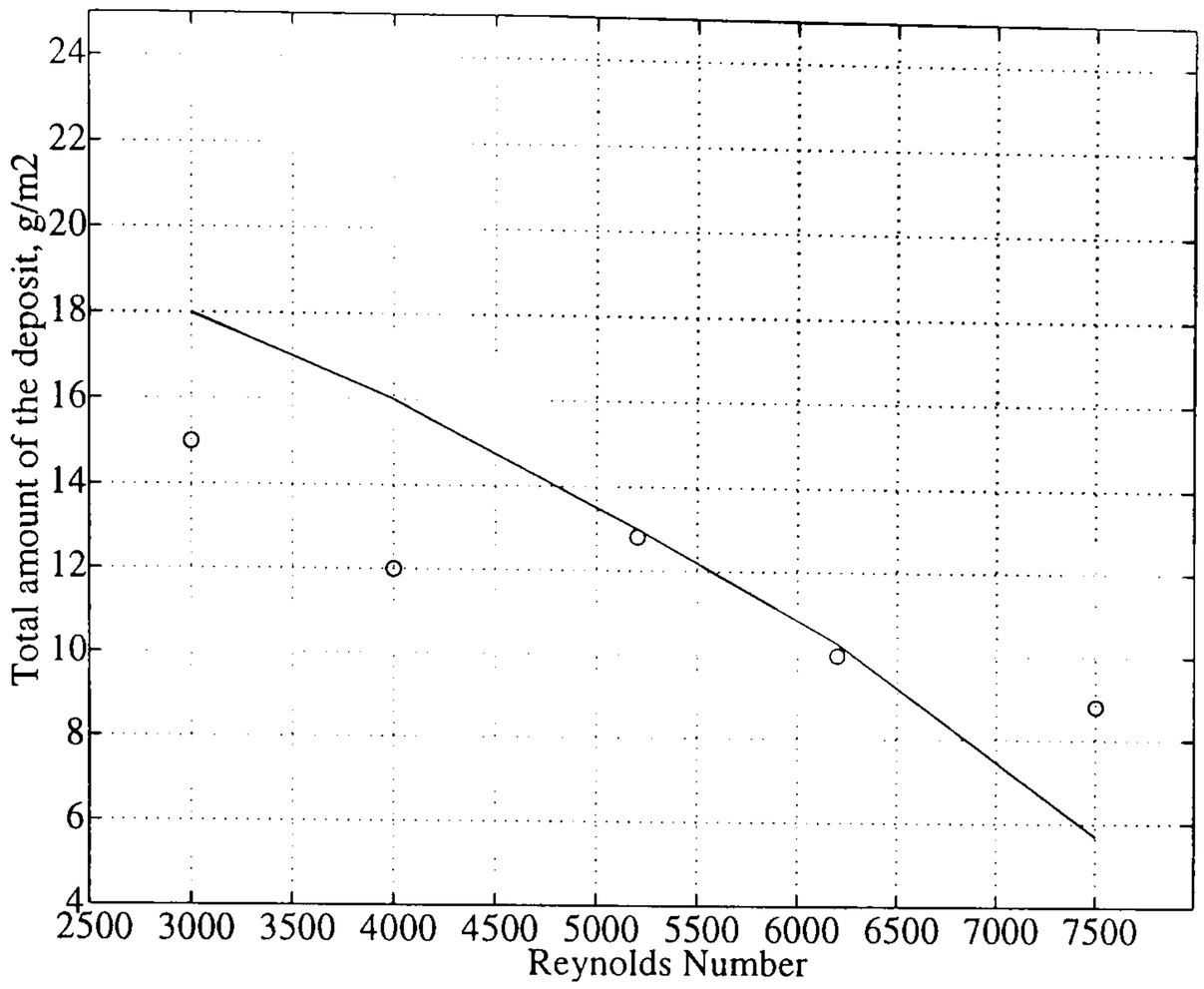


Figure 4.6: Effect of Reynolds number and comparison with experimental results

proteins along the tube. We observe, as expected from the reaction mechanism, that the concentration of the native protein decreases, while denatured protein initially increases and then decreases along the tube. Finally, the concentration of the aggregated protein is initially small and then increases significantly. The bulk aggregated protein concentration profile at different times is depicted in Figure 4.9. It is worth noting here that since the milk bulk temperature decreases with time (due to fouling) the protein reaction rates decrease and thus the concentration of aggregated protein also decreases.

- Figure 4.10 depicts the profile of Biot number (fouling resistance) at different times for case (i) (constant wall temperature operation, $T_w = 374$ K). The Biot number increases with respect to time and along the tube. This indicates that fouling is greatly affected by reactions. Since the bulk and interface temperature increase along the tube, this also increases the rate of the protein reactions and therefore the concentration of layer aggregated protein and finally the Biot number.

- The deposit thickness follows a similar pattern to that of the Biot number, increasing its value along the tube (Figure 4.11). Here, again the first case of operation is studied. Similar profiles are obtained for the mass of the deposit as shown in the comparison with the experimental results (see Figure 4.5).

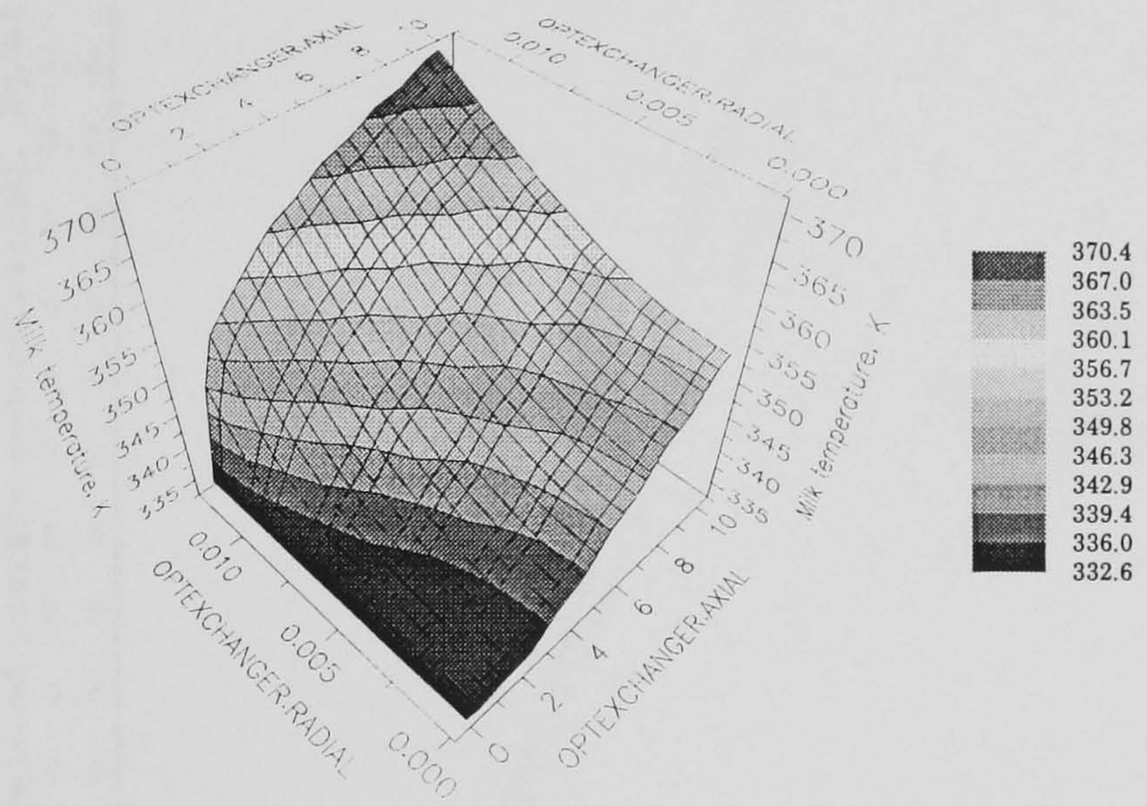


Figure 4.7: 3-D representation of milk temperature for constant wall temperature, T_w=374 K

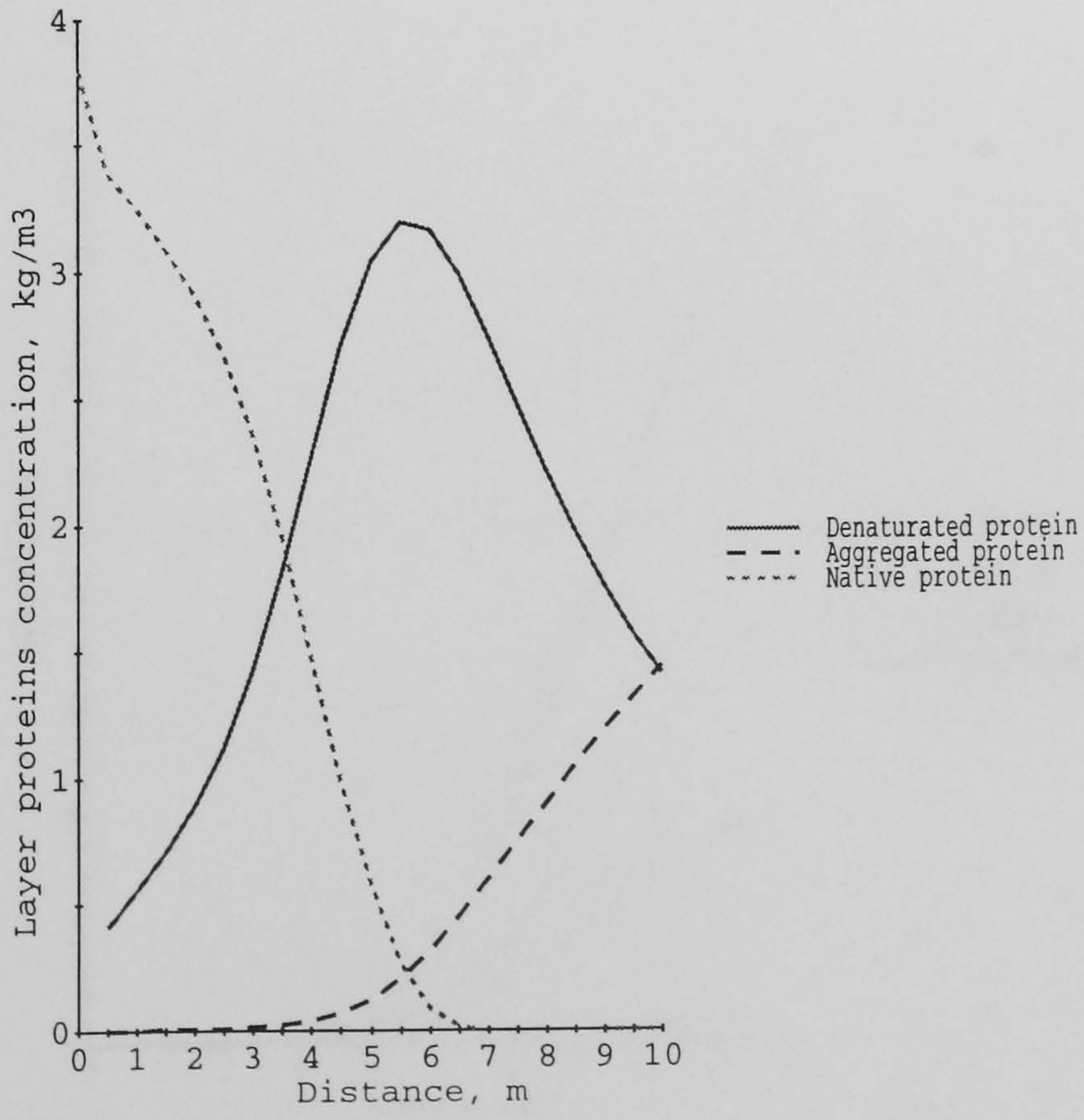


Figure 4.8: Layer proteins concentrations at $t = 20,000$ sec (case i)

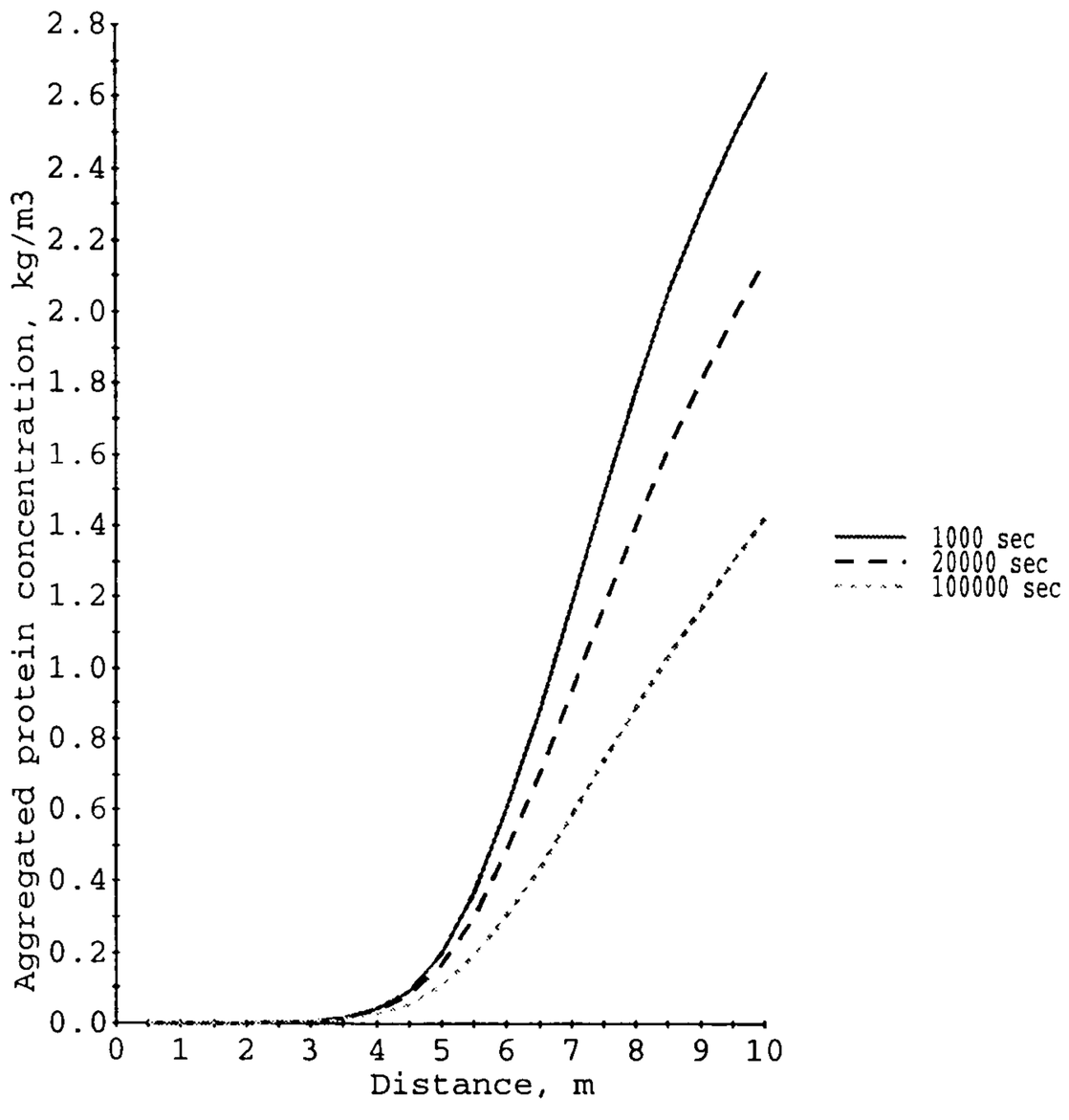


Figure 4.9: Bulk aggregated protein concentration profiles at different times (case i)

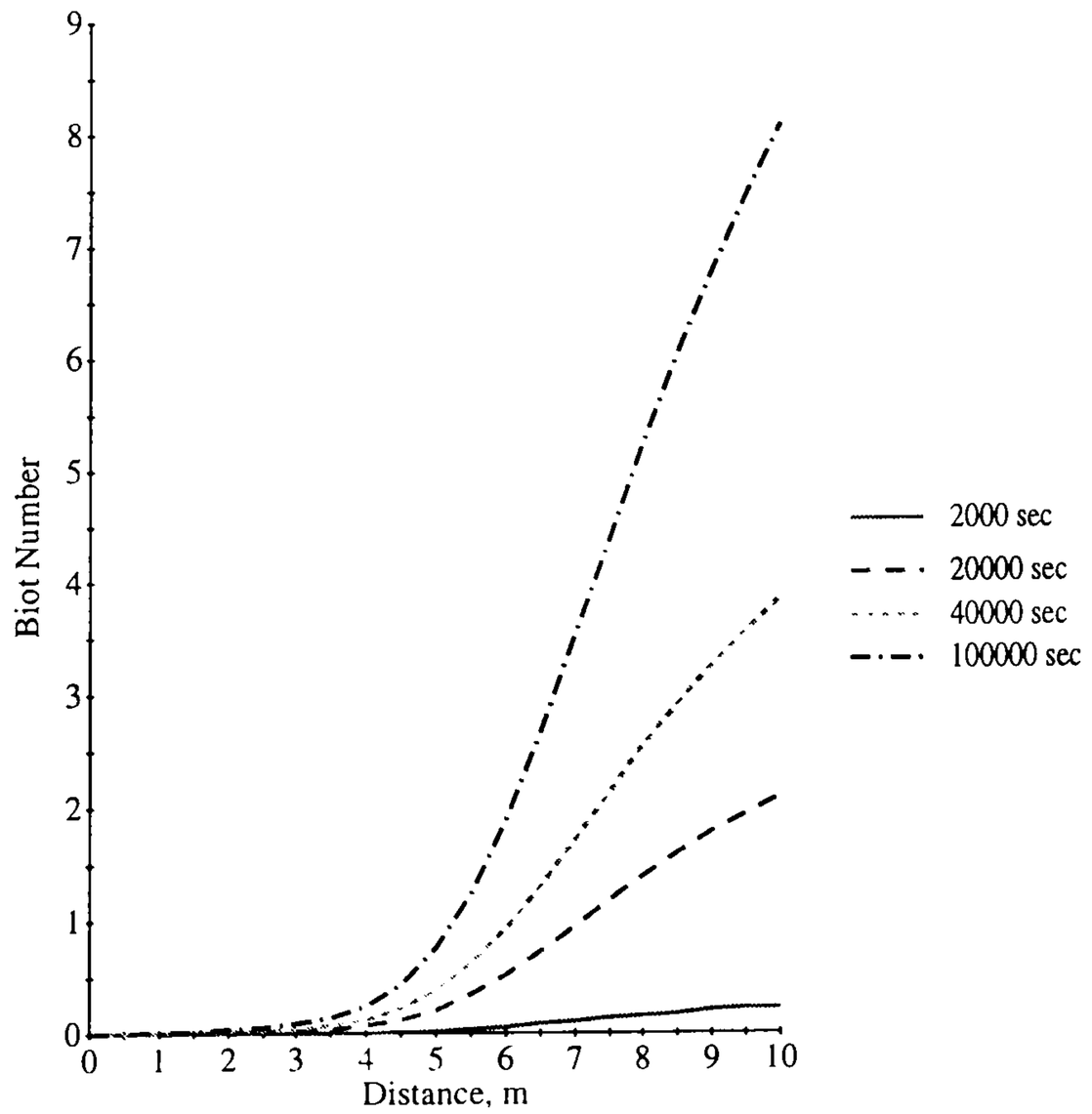


Figure 4.10: Biot number profile for constant wall temperature, T_w=374 K at different times

- As expected, the overall heat transfer coefficient decreases with time (Figure 4.12). This refers to the 374 K uniform wall temperature. The overall heat transfer coefficient at the end of the time horizon reaches the value of 1500 W/m^2K and the corresponding value under clean conditions is 3100 W/m^2K. Similarly the milk outlet temperature reaches a final value of 362 K (Figure 4.13 for case i). It should be noted here that the rate of fouling decreases with time following the decrease in milk outlet temperature. However, if control action is applied (i.e. increasing steam temperature) this may not be the case since more heat will be provided to the system in order to maintain milk outlet temperature close to its target value.

- Finally the four cases of operation are compared in Figure 4.13. We observe that case (ii), constant wall temperature 390 K, results in the most severe drift in milk outlet temperature. Counter-current operation also causes a significant decrease in the heat exchanger thermal performance. The final results are summarized in Table 4.7. We note that a heat exchanger operating at constant wall temperature of 374 K will suffer a 8 K drop outlet temperature after 27.5 hours while the corresponding value for one operating at 390 K is just 1.4 hours. Thus, although the higher temperature option has a lower capital cost, the downtime for cleaning will be significantly higher.

Case of operation	Type of exchanger	Drift in milk outlet temperature, K
1	Steam, $T_w = 374$K	8.3
2	Steam, $T_w = 390$K	13.9
3	Hot water, co-current flow	9.4
4	Hot water, counter-current flow	12

Table 4.7: Effect of fouling on milk outlet temperature for four cases of operation

4.3.3 Sensitivity Analysis

The mathematical model presented in section 2 includes a number of parameters such as the initial protein concentrations. The values of these parameters are uncertain due to variability in the milk quality. For example, there is a seasonal variation of the inlet native protein (Grandison, 1988). Here we investigate the impact of these parameters on the milk outlet temperature by simulation. The results for the constant wall temperature case (374 K) are summarized as follows:

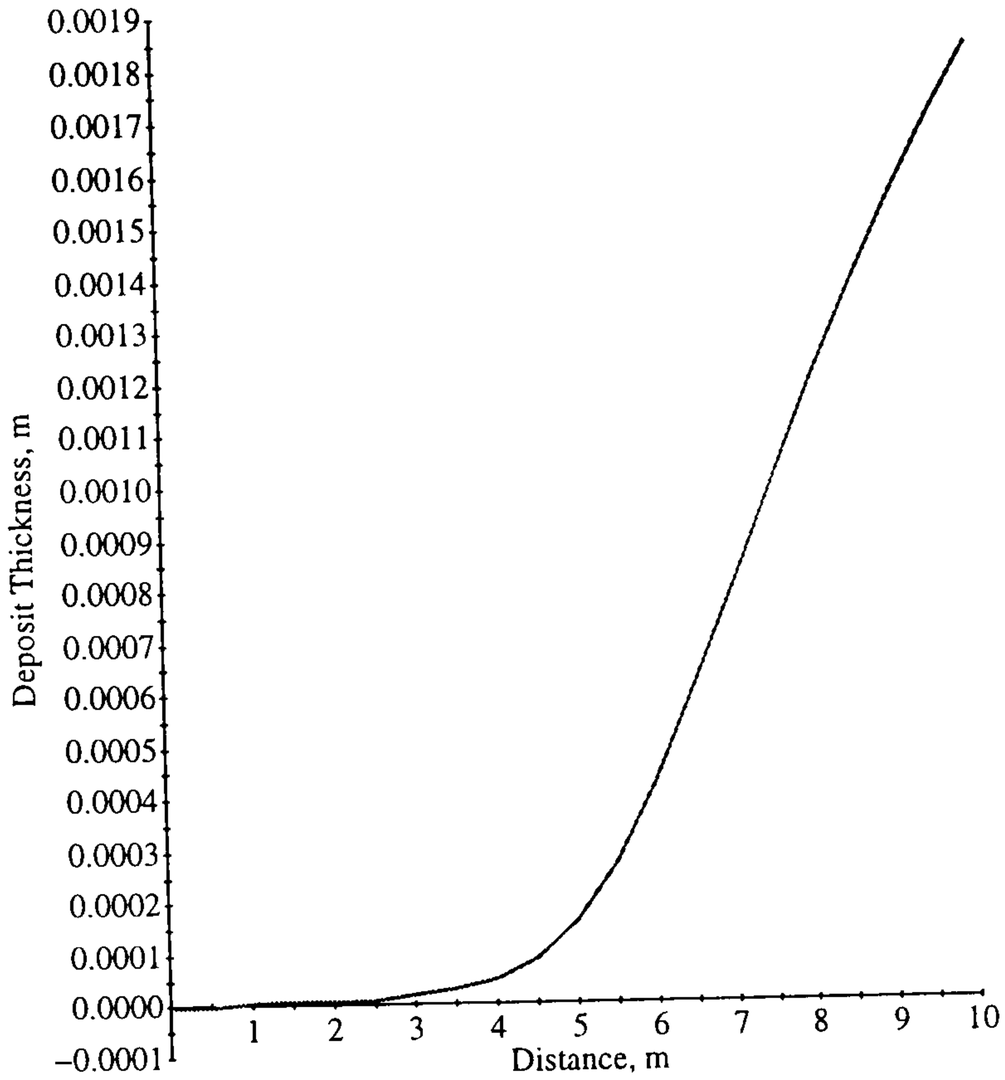


Figure 4.11: Deposit thickness profile for heating time 100,000 sec (case i)

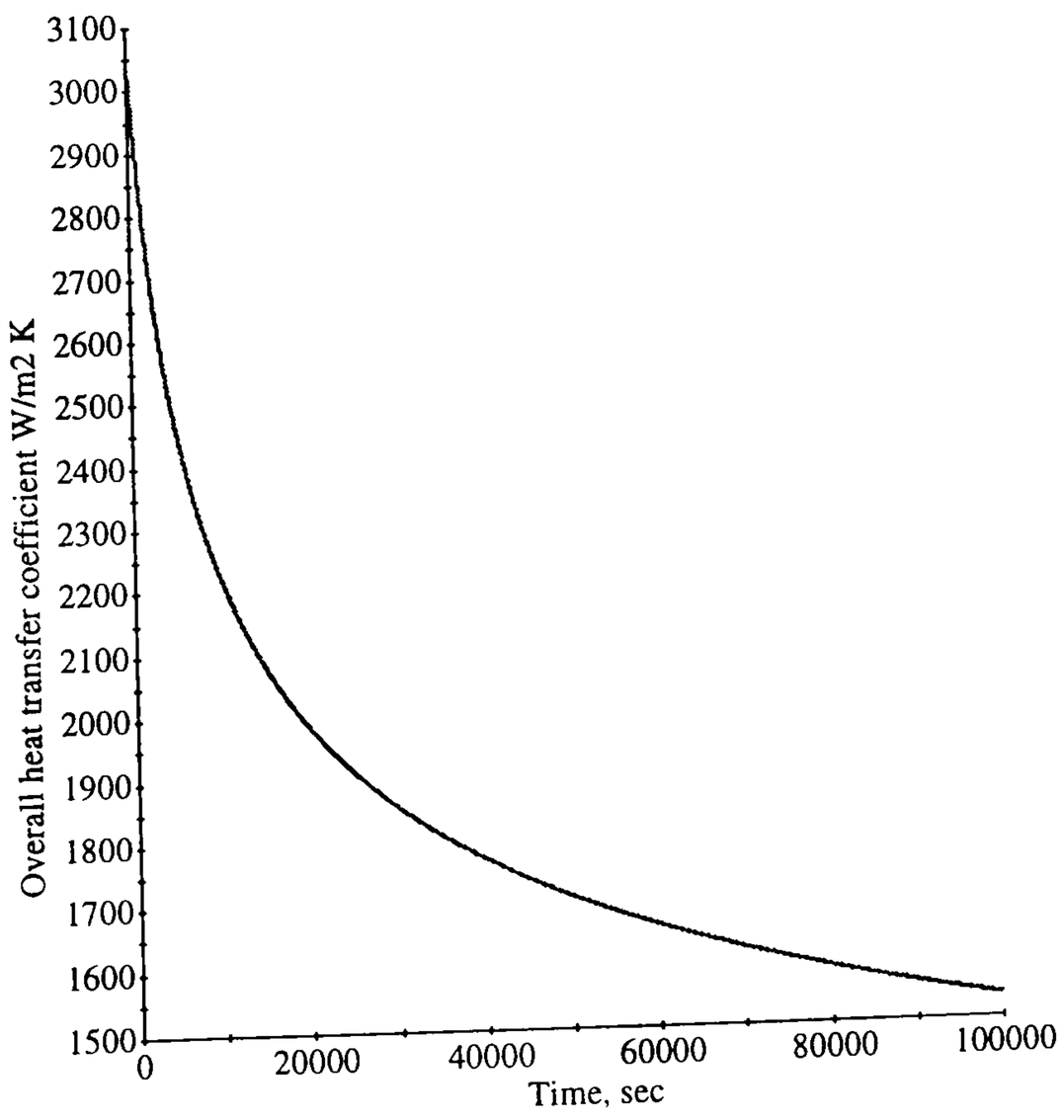


Figure 4.12: Overall heat transfer coefficient (case i)

- Figure 4.14 depicts the effect on fouling of a 32% change in the initial native protein concentration. The total drift in the milk outlet temperature when the initial protein concentration is 2.5 kg/m^3 decreases by 30% compared to the nominal case where the concentration was 3.8 kg/m^3. Clearly there is a significant effect of milk composition on fouling.

- In Figure 4.15, the Reynolds number is increased to the value of 14,000 (by decreasing tube diameter), from 8800 (nominal case). We observe that substantial mitigation of fouling is achieved (almost 60% reduction). This result provides some justification for the current industrial practice that milk should be processed at the highest possible velocity. A similar effect of Reynolds number on fouling was also illustrated experimentally by Belmar-Beiny *et al.* (1993) and Toyoda and Fryer (1997).

- The effect of having a fraction of denaturated protein at the inlet of the heat exchanger is depicted in Figure 4.16 ($C_{D,in} = 1\ kg/m^3$). We observe higher fouling compared to the nominal case where there is no denaturated protein. The existence of this protein at the inlet may arise from a previous thermal milk treatment.

The simulation results are intuitively correct and show that changes in important parameters lead to the expected conclusions. The presented model describes all the important heat and mass transport phenomena occurring during fouling in a realistic way, while current industrial practice for milk fouling mitigation is qualitatively supported. It should be noted here that if a control action will be applied by increasing steam or hot water inlet temperature (in order to maintain milk outlet temperature close to its target value) fouling will become more severe. This is due to the increased wall temperature which will give rise to faster reaction rates.

An important conclusion is that, for a given thermal duty, short exchangers appear to give the most severe drift in milk outlet temperature. This view supports the operating heuristic commonly employed in dairy plants that in order to minimize fouling, milk should be heated as gradually as possible.

In general, the mathematical models presented in this paper are based on fundamental physical laws (under the specified assumptions) to capture and quantify the effect of milk fouling on the heat exchanger performance. The results obtained may be extrapolated to unexplored regions, in other words help in solving the scale up problem which implies extrapolation. In this context the models presented here may also allow the design of optimal control strategies

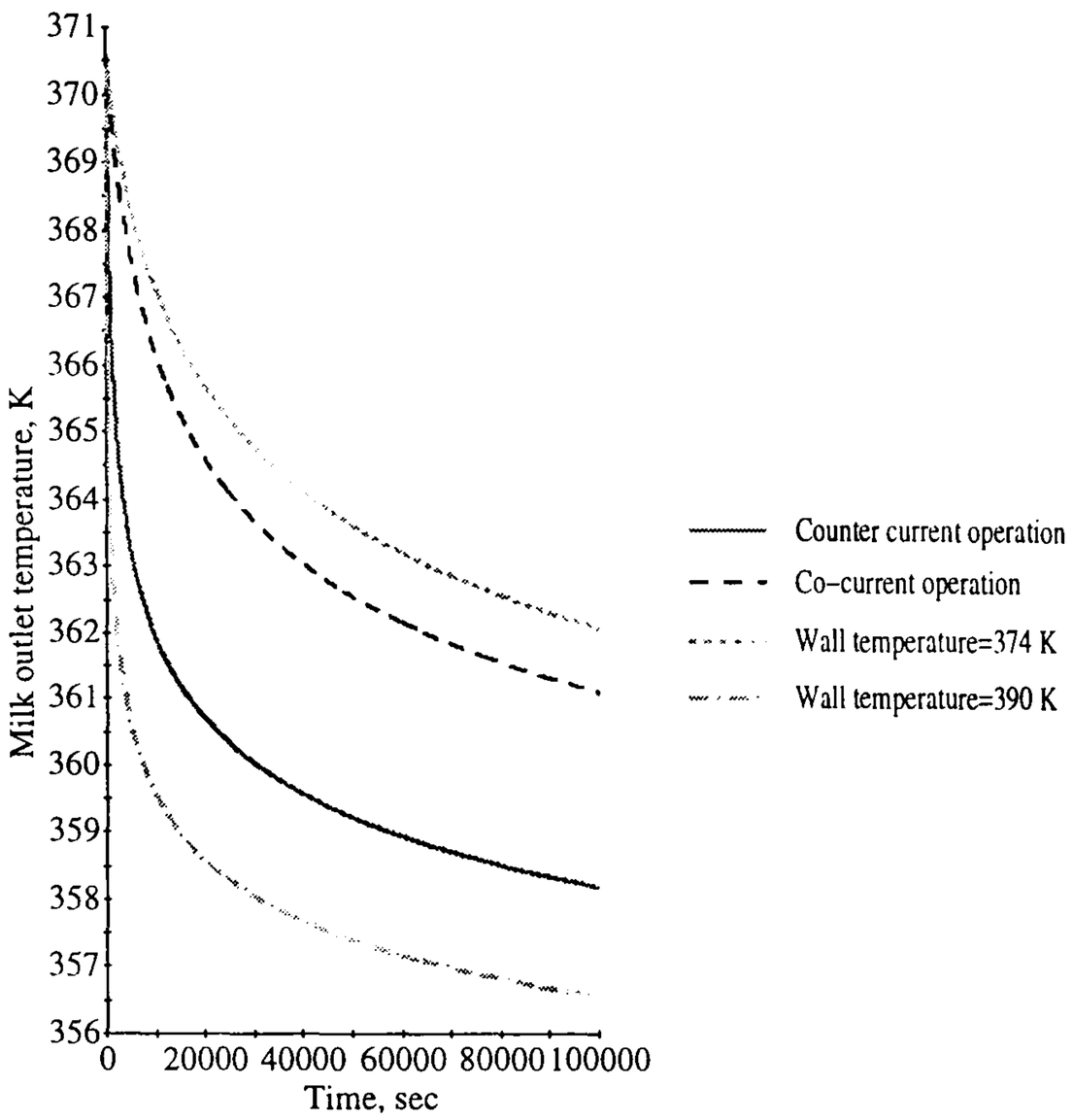


Figure 4.13: Effect of all cases of operation on milk outlet temperature

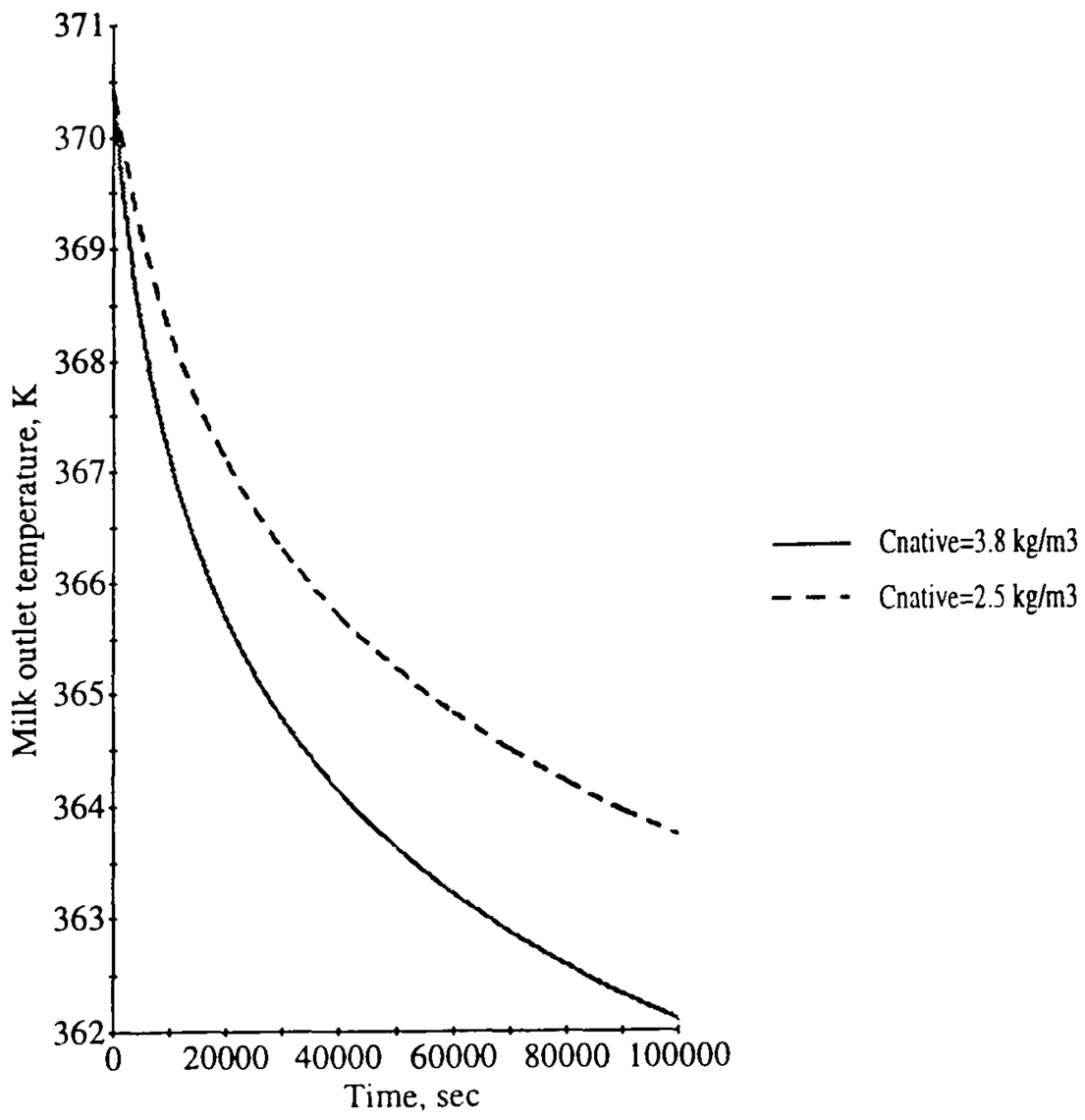


Figure 4.14: Effect of native protein concentration on fouling (case i)

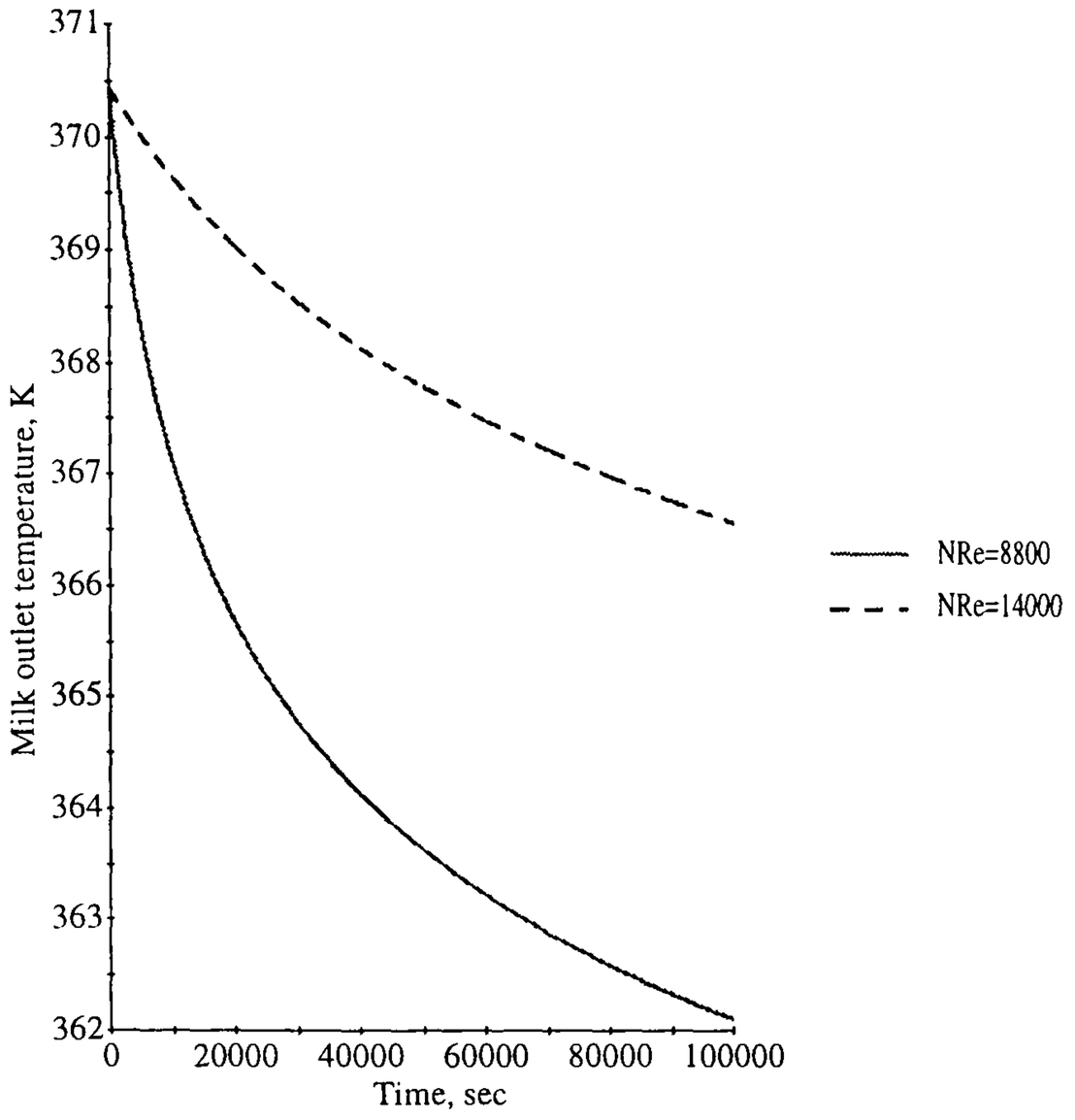


Figure 4.15: Effect of Reynolds number on fouling

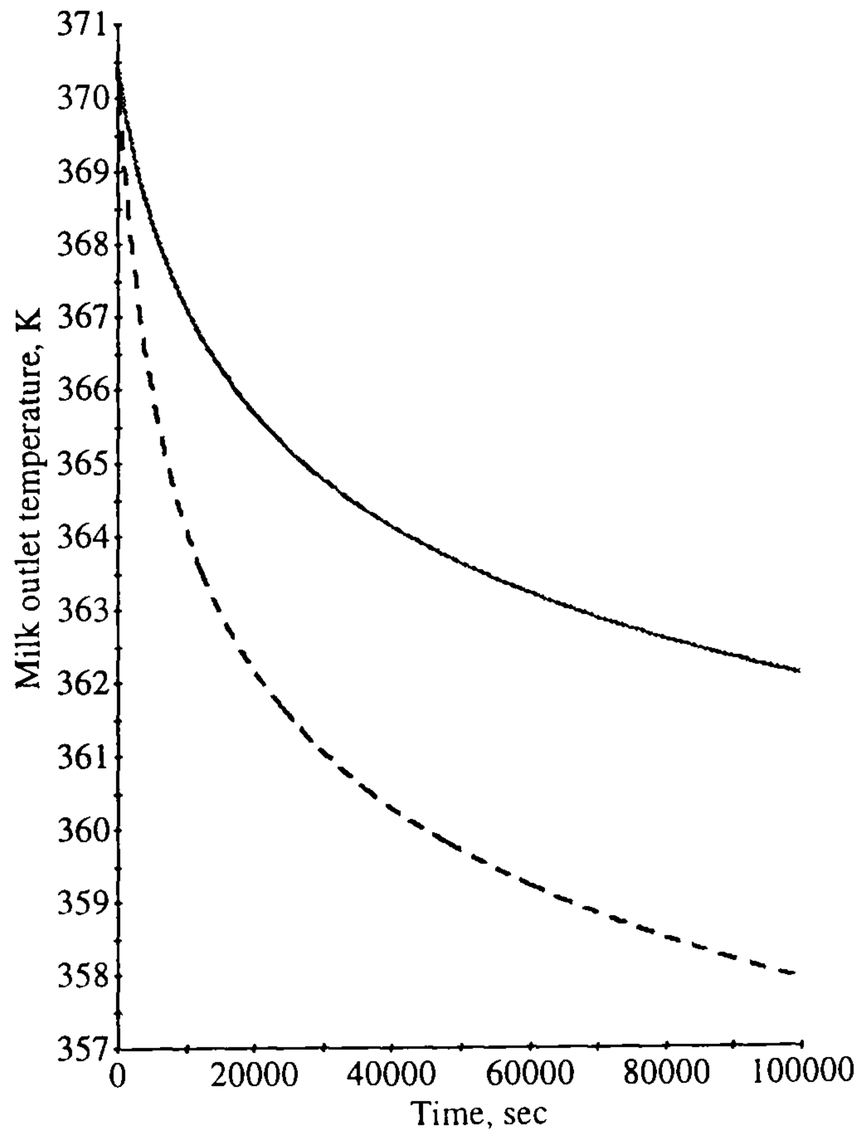


Figure 4.16: Effect of initial denaturated protein on fouling

and/or operations to be studied. It would be useful, however, to further validate the models against experimental data in other conditions. Such data are not easily available in the public domain.

4.4 Concluding Remarks

We have developed a general mathematical model of single shell and tube heat exchangers under fouling. The model was developed in particular for a milk heat treatment, however it can also be used for heat exchangers which are subjected to fouling caused by chemical reaction(s) on the tube side. All transfer phenomena which take place during milk heat treatment were quantified in a formal way and a large number of variables were monitored to study the behaviour and effect of fouling on the heat exchanger performance. Despite its complexity, the model can be simulated successfully using currently available modelling tools such as *gPROMS*. Good agreement of the simulation results with experimental data has been achieved based on the solution of a dynamic parameter estimation problem. Typical industrial operating techniques for fouling mitigations were verified. Examples have been presented to illustrate the behavior of fouling for four different configurations of tubular heat exchangers.

There exists a trade-off between operating costs such as cleaning and capital costs. A larger heat exchanger area will decrease the cleaning duties but will simultaneously increase capital costs. As mentioned by Fryer (1989), for any given thermal duty, an optimum heat exchanger size exists that balances the reduced operating cost and fouling afforded by large heat exchangers against their increased capital cost. Furthermore, the switching time from heating to cleaning and the control policy (in order to maintain milk temperature close to its target value) must also be optimally selected. So far, no attempt has been made to optimise heat exchangers under fouling taking into account all the cost factors related to the milk heat treatment and using rigorous dynamic models. The model presented here can provide the basis for such an exercise and this is considered in chapter 6.

4.5 Nomenclature

$Area$ cross sectional area of the tube, m

C_N bulk native protein concentration, kg/m^3

C_D bulk denaturated protein concentration, kg/m^3

C_A bulk aggregated protein concentration, kg/m^3

C_N^* layer native protein concentration, kg/m^3

C_D^* bulk denaturated protein concentration, kg/m^3

C_A^* bulk aggregated protein concentration, kg/m^3

C_p Milk specific heat capacity, $J/(kg \cdot K)$

C_{pw} heating medium specific heat capacity, $J/(kg \cdot K)$

k_f milk thermal conductivity, $J/(m \cdot s \cdot K)$

T_s^{out} heating medium steady state outlet temperature, K

T_s^{in} heating medium steady state inlet temperature, K

$T_f(r)$ milk temperature, K

T_f^{out} milk steady state outlet temperature, K

T_f^{in} milk steady state inlet temperature, K

T_w wall temperature, K

u_s heat medium velocity, m/s

$u_z(r)$ milk velocity as a function of radius, m/s

Greek Letters

β deposition rate constant

μ milk viscosity, $kg/(m \cdot s)$

ρ milk density, kg/m^3

ρ_w heating medium density, kg/m^3

Chapter 5

Modelling and Simulation of Complex Plate Heat Exchanger Arrangements under Milk Fouling

This chapter presents the detailed mathematical modelling and simulation of complex plate heat exchangers under milk fouling. A general dynamic thermal model of plate heat exchangers is first developed and coupled with the milk fouling model presented in chapter 4. The simulation results are in a good agreement with experimental data. Three different industrial configurations are considered to illustrate aspects of fouling behaviour.

5.1 Introduction

Plate heat exchangers (PHEs) are widely used for different process applications. They exhibit excellent heat transfer characteristics which allow more compact designs than achievable with conventional shell and tube heat exchangers. Along with their easy maintenance and other advantages, this factor has made the PHEs the prime choice for many engineering applications involving liquid-liquid heat transfer duties. PHEs are most common in the dairy, beverage, general food processing, and pharmaceutical industries due to their ease of cleaning and their thermal control characteristics required for thermal sterilization/pasteurization purposes (Shah *et al.*, 1988).

A plate heat exchanger consists of a number of parallel flow channels formed by metal plates which are separated by gasket material around the perimeter of each plate (see Figure

5.1). Nozzles for the flow of fluids extend through the frames to the plate packages. Heat is transferred through these plates from one fluid to another.

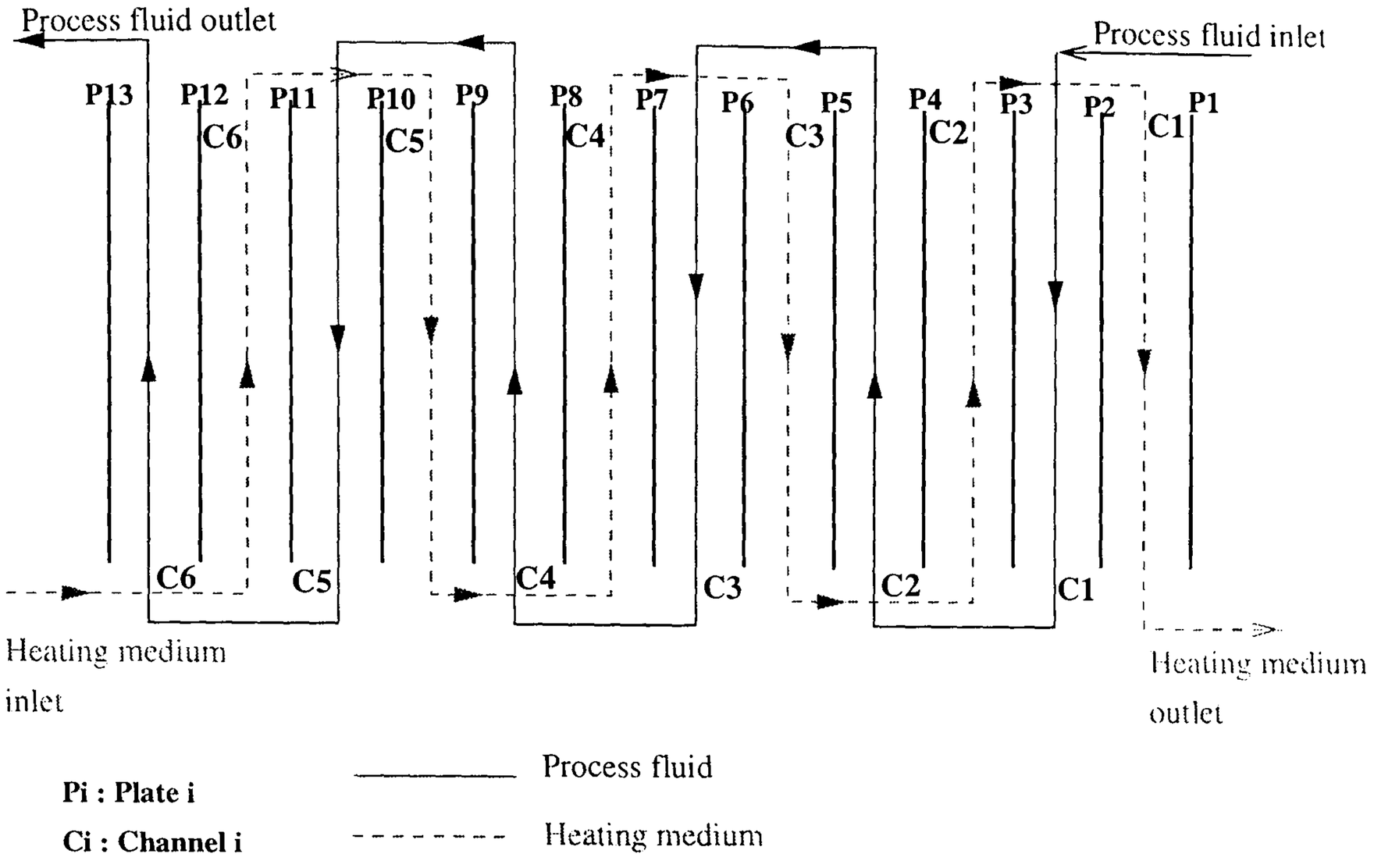


Figure 5.1: PHE arrangement-1

Previous work on the modelling and simulation of PHEs under milk fouling has mainly been carried out at the Food Technology and Process Engineering Laboratory in France. Delplace *et al.* (1994) performed experiments in a PHE with complex flow arrangement consisting of 13 plates. The overall heat transfer coefficient and pressure drop were measured as a function of time. Based on steady-state numerical simulation, the temperature profiles for each channel were determined. These profiles were able to explain the uneven deposit formation in each channel and/or plate. The maximum quantity of deposit was observed in those channels where the maximum temperature difference takes place. Delplace and Leuliet (1995) studied milk fouling of several PHEs flow arrangements by measuring both the heat transfer coefficient and dry mass of deposit. They developed an empirical model to predict the dry mass of deposit in each channel by calculating the heat denaturation of β-lactoglubulin protein. The proposed empirical model relies on steady-state numerical simulation for the prediction of temperature profiles. Delplace *et al.* (1995) carried out experiments in PHEs equipped with two plate geometries: (i) straight corrugation plates with corrugation angle 90^o and (ii) herringbone plates with corrugation angle 60^o. The results obtained showed that herringbone plates are less prone to fouling than straight corrugation plates. Based on steady-state temperature profiles and a simple protein kinetics they proposed two empirical models for the prediction of deposit mass

in each channel.

Most of the previous work on PHEs modelling has been concentrated on steady-state simulation. There are a few publications in the literature where dynamic modelling is considered and these are restricted to specific geometries. Lakshmanan (1990) considered dynamic simulation of PHEs using a numerical method known as "cinematic" model. The procedure was applied to two types of PHEs requiring a small amount of numerical calculations. However, the proposed approach cannot be applied to any arrangement and variations with respect to the axial domain were ignored. Zaleski and Klepacka (1992) presented an approximated method of calculating the thermal efficiency and temperature distribution in PHEs based on an approximation of the temperature in channels by means of linear exponential functions. Their approach was illustrated in three PHE arrangements. It is restricted to a specific range of thermal parameters and cannot be applied to other types of multichannel plate heat exchangers. Das and Roetzel (1995) presented an extensive analysis, based on a dispersion model, to predict the response due to temperature transients in counter-current plate heat exchangers.

The main drawback of the existing methods and models for PHEs under dynamic behaviour is that they are limited to a certain class of geometries and often very simple models are used. The difficulties arise primarily due to the existence of both counter current and co-current flows, the strong energy interactions between fluids in neighbouring channels, and the great variety of complex geometries that can be found in industrial applications.

5.2 A General PHE Dynamic Model

For the purpose of modelling, consider a differential element of the PHE in channel j (see Figure 5.2). The modelling assumptions are defined as follows:

- No heat is conducted in the direction of flow in channels and also in the plates.
- The flowrate and temperature profiles are uniform across the channel and plate width
- Each fluid is split equally between all related channels
- Heat losses to surrounding are negligible
- The head and follower parts of the PHE are assumed to be insulated and serve as adiabatic plates

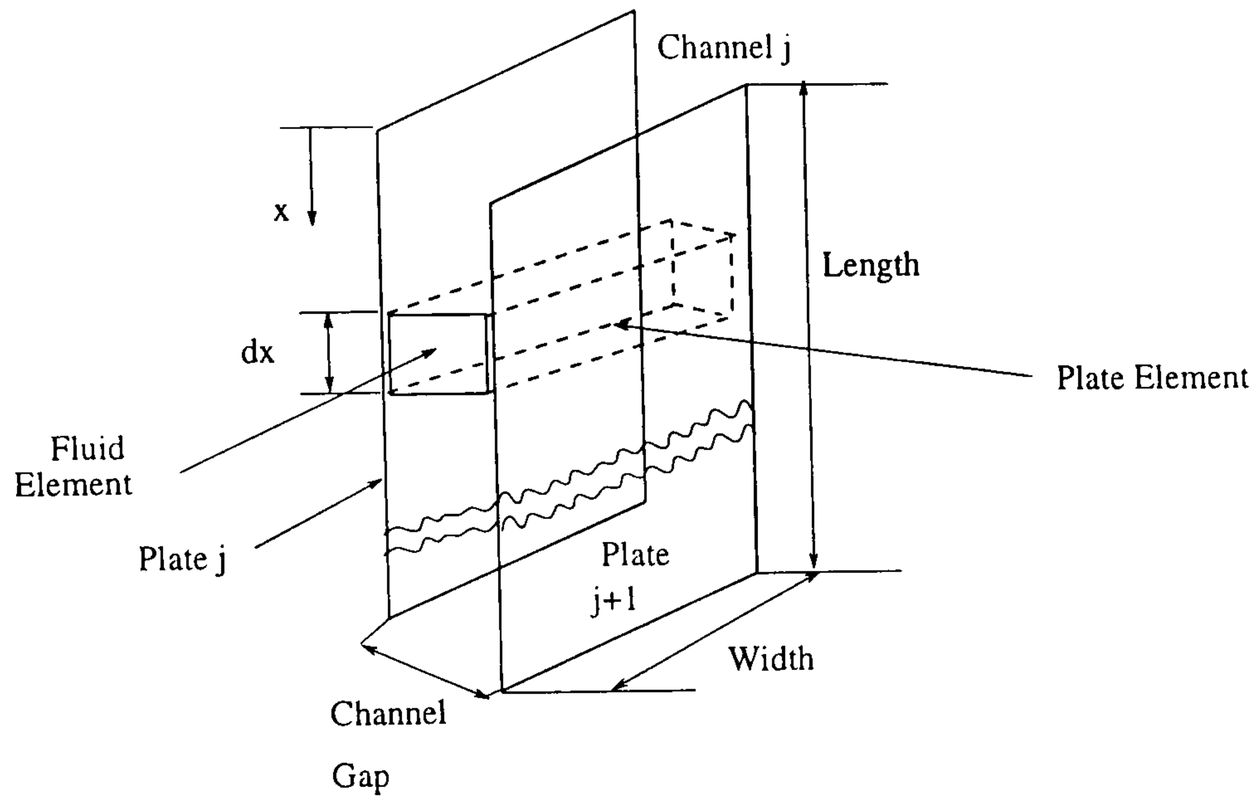


Figure 5.2: A differential element in a Plate Heat Exchanger

Based on the fundamental energy conservation law the following equations describe the heat transfer between process fluid or heating medium in a channel j and its neighbouring plates p_j and p_{j+1}:

$$A_x \rho_j Cp_j \left(\frac{\partial T_j}{\partial t} + n_j u_x \frac{\partial T_j}{\partial x} \right) = U_j A_j (T_{p_{j-1}} - T_j) + U_j A_j (T_{p_j} - T_j) \tag{5.1}$$

Plate j:

$$\rho_j Cp_p A_{x_p} \frac{\partial T_{pj}}{\partial t} = U_j A_j (T_j - T_{pj}) + U_{j+1} A_j (T_{j+1} - T_{pj}) \tag{5.2}$$

For the first and last channel, equation 5.1 takes the following form:

Channel 1:

$$A_x \rho_1 Cp_1 (\frac{\partial T_1}{\partial t} + n_1 u_1 \frac{\partial T_1}{\partial x}) = U_1 A_1 (T_{p_1} - T_1) \tag{5.3}$$

Last Channel:

$$A_x \rho_m Cp_m (\frac{\partial T_m}{\partial t} + n_m u_m \frac{\partial T_m}{\partial x}) = U_m A_m (T_{p_{m-1}} - T_m) \tag{5.4}$$

where t denotes time, x axial position and m the total number of channels. $T_j(x,t)$ is the fluid temperature in channel j, T_{pj} the temperature of plate j, U_j the overall heat transfer coefficient

in channel j,u_x is the average fluid velocity and A_j the heat transfer area of channel j. All the other variables/parameters are explained in the nomenclature section 5.6. The quantity n_j takes a value of $+1$ or -1 depending of the direction of the flow in channel j. The main advantage of the above model is that it can be used to simulate the transient behaviour of several types of PHEs, including counter-current, co-current, multi-channel etc. This model is based on energy balances where the synergistic effects between neighbouring channels and plates are formally quantified. Temperature profiles with respect to the axial distance are also considered. However, temperature dependence with respect to the channel width is neglected since it is small in comparison. The complete nomenclature is given in section 5.6. Detailed algebraic expressions are used to calculate all the necessary thermal parameters as follows:

The overall heat transfer coefficient under clean conditions, U_o, can be calculated from the Nusselt number (Nu) which is a function of the Reynolds (Re) and Prandtl (Pr) numbers:

$$Nu = 0.214(Re^{0.662} - 3.2)Pr^{0.4} \tag{5.5}$$

$$Pr = \frac{C_p \cdot \mu}{\lambda} \tag{5.6}$$

$$Re = \frac{D_e \cdot u_x \cdot \rho}{\mu} \tag{5.7}$$

$$Nu = \frac{h \cdot D_e}{\lambda} \tag{5.8}$$

The equivalent diameter, D_e, is given as follows:

$$D_e = 2e_j \tag{5.9}$$

where e_j is the spacing between plates given by the design of the heat exchanger. The overall heat transfer coefficient can be then calculated by the following expression:

$$\frac{1}{U_o} = \frac{1}{h_{hot}} + \frac{1}{h_{cold}} + \frac{tp_j}{\lambda_p} \tag{5.10}$$

where λ_p and tp_j is the thermal conductivity and thickness of plates respectively. The heat transfer coefficient, U, is then defined as in equation 4.63.

5.3 Material Balances

For milk pasteurization, the fouling model described in chapter 4 is used to quantify the effect of milk fouling on the overall equipment performance. It is assumed that bulk reactions take place in each channel (where milk flows) at the channel temperature, T_j, whereas boundary

layer reactions take place at the plate temperature, T_{pj}. Therefore, the rate of milk deposition will be different for the two plates delimiting the same channel due to the different temperature and protein concentration conditions on each of them. Thus, material balances of proteins in the bulk are given by the following set of equations for each channel j where milk flows:

Native protein:

$$\frac{\partial C_{Nj}}{\partial t} + n_j u_x \frac{\partial C_{Nj}}{\partial x} = -k_{No} \exp\left(\frac{-E_N}{RT_j}\right) \cdot C_{Nj} + \frac{k_{mN}}{\epsilon_j} \cdot (C_{Nj} - C^*_{Np}) \tag{5.11}$$

Denaturated protein:

$$\frac{\partial C_{Dj}}{\partial t} + n_j u_x \frac{\partial C_{Dj}}{\partial x} = k_{No} \exp\left(\frac{-E_N}{RT_j}\right) \cdot C_{Nj} k_{Do} \exp\left(\frac{-E_D}{RT_j}\right) \cdot C^2_{Dj} + \frac{k_{mD}}{\epsilon_j} \cdot (C_{Dj} - C^*_{Dp}) \tag{5.12}$$

Aggregated protein:

$$\frac{\partial C_{Aj}}{\partial t} + n_j u_x \frac{\partial C_{Aj}}{\partial x} = k_{Do} \exp\left(\frac{-E_D}{RT_j}\right) \cdot C^2_{Dj} + \frac{k_{mA}}{\epsilon_j} \cdot (C_{Aj} - C^*_{Ap}) \tag{5.13}$$

Material balances of the proteins in the thermal boundary layer for the side of plate p delimiting channel j are: given by:

Native protein:

$$\frac{\partial C^*_{Np}}{\partial t} + n_j u_x \frac{\partial C^*_{Np}}{\partial x} = -k_{No} \exp\left(\frac{-E_N}{RT_{pj}}\right) \cdot C^*_{Np} - \frac{k_{mN}}{\delta_T}(C^*_{Np} - C_{Nj}) \tag{5.14}$$

Denaturated protein:

$$\frac{\partial C^*_{Dp}}{\partial t} + n_j u_x \frac{\partial C^*_{Dp}}{\partial x} = k_{No} \exp\left(\frac{-E_N}{RT_{pj}}\right) \cdot C^*_{Np} - k_{Do} \exp(\frac{-E_D}{RT_{pj}}) \cdot C^{*2}_{Dp} - \frac{k_{mD}}{\delta_T}(C^*_{Dp} - C_{Dj}) \tag{5.15}$$

Aggregated protein:

$$\frac{\partial C^*_{Ap}}{\partial t} + n_j u_x \frac{\partial C^*_{Ap}}{\partial x} = k_{Do} \exp\left(\frac{-E_D}{RT_{pj}}\right) \cdot C^{*2}_{Dp} - \frac{1}{\delta_T} \cdot \left[k_{mA}(C^*_{Ap} - C_{Aj}) + k_w C^*_{Ap}\right] \tag{5.16}$$

Initial conditions are specified as in chapter 4. Typically it is assumed that prior to the circulation of milk (*e.g.* initiation of fouling) the exchanger was operating at steady-state with a non-fouling fluid. However, other conditions can easily be imposed. Boundary conditions depend on the specific geometry and are presented in the next sections. Finally, all the transport properties and algebraic variables to describe fouling are calculated as in section 4.2.6.

5.4 Numerical Simulation and Results

The model described in the previous section comprises a set of integral, partial differential and algebraic equations (IPDAEs). It is simulated using the simulation package *gPROMS* (Barton and Pantelides, 1994; Oh and Pantelides, 1996; *gPROMS* Technical Manual, 1998c). The idea of hierarchical model building is employed. Each channel is modelled as a sub-model. All the sub-models are eventually connected to a general model through appropriate boundary conditions. The PHE thermal model is also defined independently and suitably connected with all the other sub-models so as to define the temperatures required by the protein reaction scheme (see Figure 5.3). Different numerical methods are used for the discretization of PDAEs according to the flow direction. If the flow direction is in the positive x direction (from zero to the exit of the channel) then a second order backward finite difference method with 20 elements is used. For the reverse flows a second order forward finite difference method is used. The PHE thermal model is approximated by a second order centered finite difference method with 20 elements. These discretization schemes and orders where chosen so as to obtain accurate results.

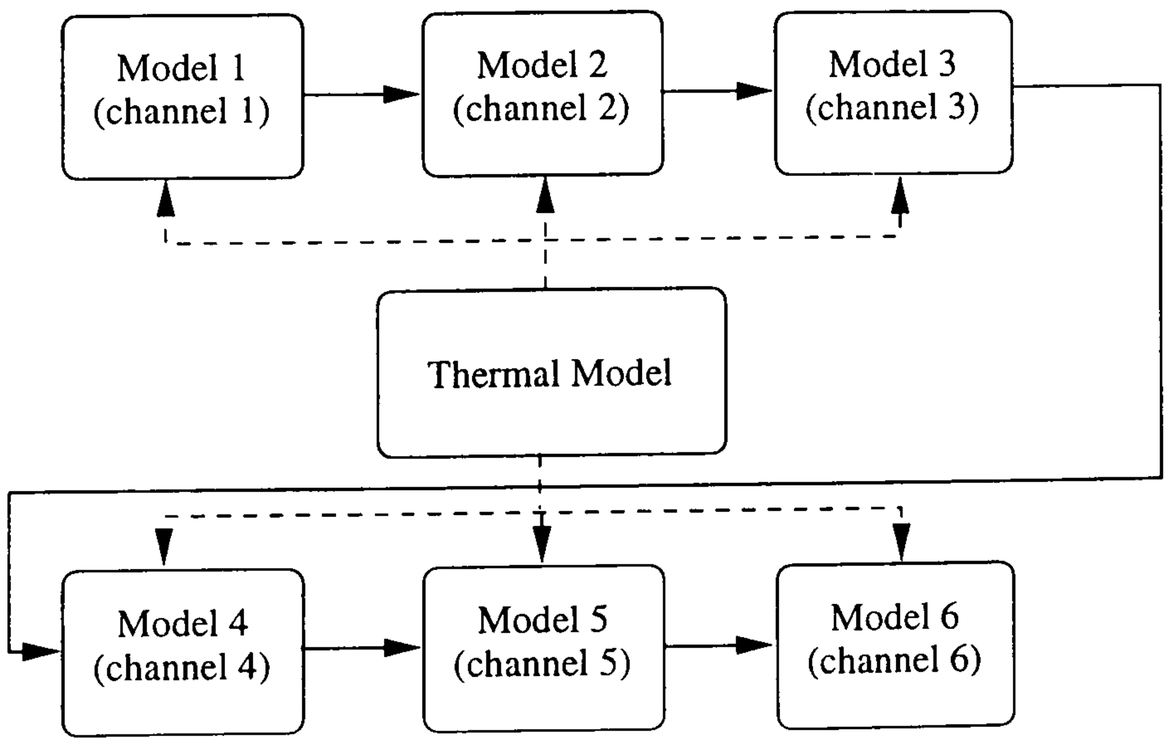


Figure 5.3: Model decomposition for PHE–arrangement 1

5.4.1 Arrangement 1

This arrangement is shown in Figure 5.1 and it is one channel per pass with total six passes. The heat exchanger consists of 13 plates and both counter-current and co-current flows exists. Milk (process fluid) enters the PHE at 60 °C and its flowrate is $0.833 \cdot 10^{-4} m^3/s$. The technical details of this exchanger are given in Table 5.1. Hot water is assumed to be the heating medium at a flowrate of $2.4 \cdot 10^{-4} m^3/s$ and inlet temperature 97 °C. The inlet protein concentration is 5 kg/m^3. All these details were taken from Delplace *et al.* (1994). Milk properties are assumed to be identical to those of water as in Delplace *et al.* (1994). Based on the given technical characteristics the heat transfer and cross sectional areas can be easily calculated (see Table 5.1). All plates are assumed to have the same geometric characteristics.

L, length of plates, m	0.75
Width of plates, m	0.20
p_j, thickness of plates, m	$7.45 \cdot 10^{-4}$
e_j, gap between plates, m	$4.0 \cdot 10^{-3}$
λ_p, thermal conductivity of plates, $J/(m \cdot s \cdot K)$	16.3
Cp_j, specific heat capacity of plates, $J/(kg \cdot K)$	502
A_j, heat transfer area, m^2	0.1875
A_x, cross sectional area, m^2	$1 \cdot 10^{-3}$

Table 5.1: Technical details of the PHE-arrangement 1

Boundary Conditions:

For the geometry considered here special boundary conditions have to be imposed between channels to ensure continuity of temperature:

$$T_{fluid}(1,0) = T_{fin} \tag{5.17}$$

$$T_{fluid}(j,L) = T_{fluid}(j-1,L) \qquad j = 2,4,6 \tag{5.18}$$

$$T_{fluid}(j,0) = T_{fluid}(j-1,0) \qquad j = 3,5 \tag{5.19}$$

$$T_s(6,L) = T_{sin} \tag{5.20}$$

$$T_s(j,0) = T_s(j-1,0) \qquad j = 2,4,6 \tag{5.21}$$

$$T_s(j,L) = T_s(j-1,L) \qquad j = 3,5 \tag{5.22}$$

where T_{fluid} and T_s are the milk and heating medium temperature respectively. The first domain corresponds to the number of channels and the second to the inlet or outlet point. For example, $T_{fluid}(1,L)$ is the milk temperature at the outlet (L) of channel 1 which must be

equal to the inlet temperature of channel 2, $T_{fluid}(2, L)$. Finally T_{fin} and T_{sin} are the milk and heating medium inlet temperatures respectively.

Appropriate boundary conditions are imposed for the protein concentrations between connected channels. For example, between channel 1 and 2 the following boundary conditions are imposed to ensure continuity of concentration:

$$C_N(2, L) = C_N(1, L) \tag{5.23}$$

$$C_D(2, L) = C_D(1, L) \tag{5.24}$$

$$C_A(2, L) = C_A(1, L) \tag{5.25}$$

$$C_N^*(2, L) = C_N^*(1, L) \tag{5.26}$$

$$C_D^*(2, L) = C_D^*(1, L) \tag{5.27}$$

$$C_A^*(2, L) = C_A^*(1, L) \tag{5.28}$$

Similar boundary conditions are considered for all the other channels.

In order to check the validity of the thermal model the steady-state temperature profile (clean conditions) inside the channels were first determined. The simulation results are depicted in Figure 5.4. Note that the channel bulk temperature increase is maximum in the first three channels while it remains almost constant in the last two channel. The results are in a very good agreement with the experimental work of Delplace *et al.*, (1994)(not shown here).

An important step is the parameter estimation analysis. As in chapter 4 there are four unknown parameters to be estimated. These are the particle diameters for the three protein and also the constant β to quantify the Biot number. The parameter estimation analysis is performed based on the solution of a dynamic optimization problem where the objective is to minimize the deviation between experimental data and predicted values (see Appendix A). All the model equations are considered in this problem. Experimental data are available in the form of dry deposit masses in each channel and overall heat transfer coefficient values over time, taken from Delplace *et al.*, (1994). For the purpose of our analysis only the dry deposit masses data were used. The parameter estimation problem is solved using *gEST*, the parameter estimation tool of *gPROMS*. Results are shown in Table 5.2.

Based on the parameter estimation results a comparison of the predicted mass deposit values at each plate with experimental data is shown in Table 5.3. It is clear that a good agreement exists between the theoretical results, based on our model, and the experimental values, within the experimental error (which was $\pm$ 10 %). The results indicate that fouling is

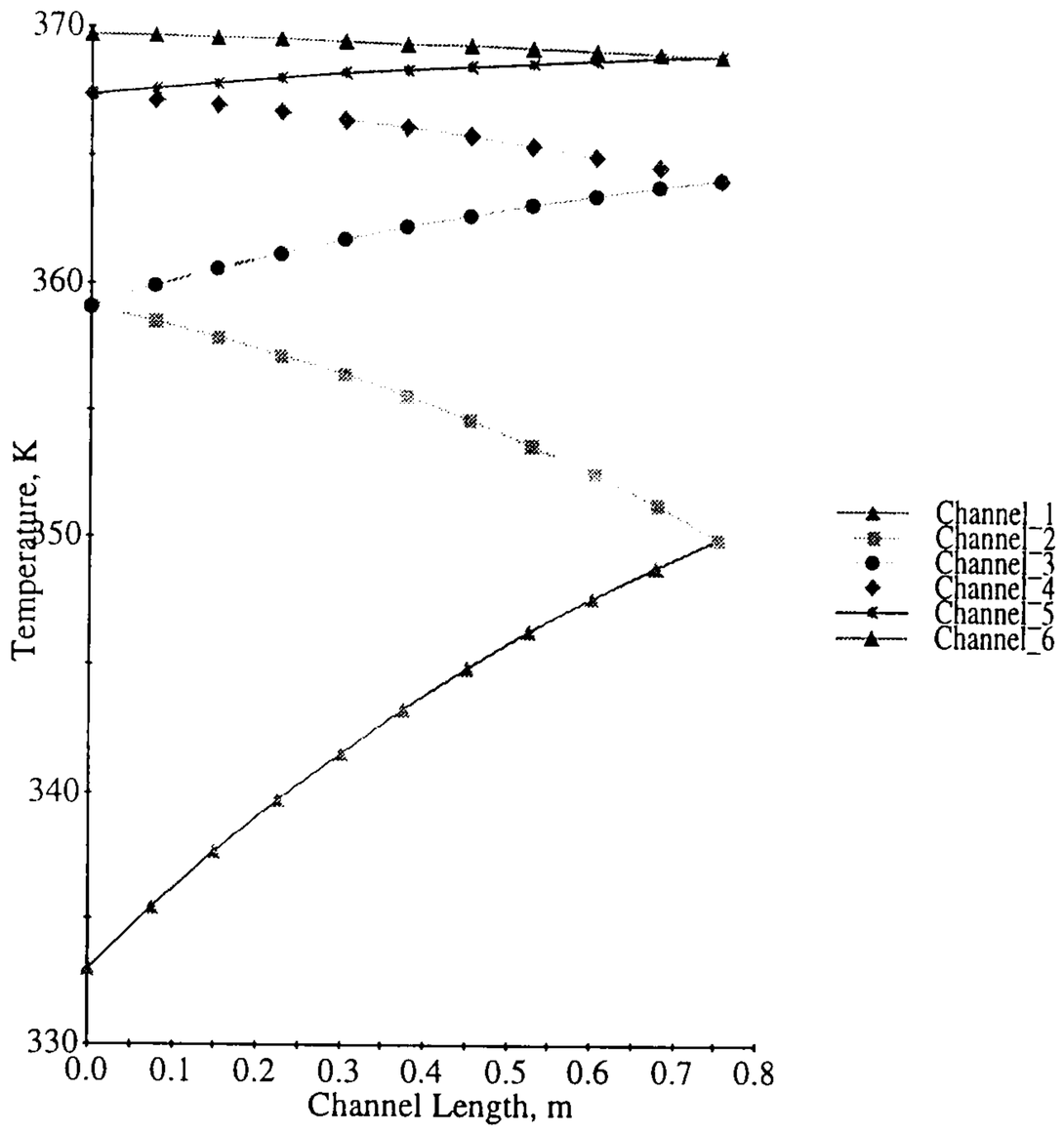


Figure 5.4: Steady state temperature profile of the process fluid for PHE–arrangement 1

Native protein particles diameter, m	$9.8 \cdot 10^{-11}$
Denaturated protein particles diameter, m	$9.3 \cdot 10^{-11}$
Aggregated protein particles diameter, m	$9.91 \cdot 10^{-10}$
Constant β	129

Table 5.2: Parameter Estimation Results-arrangement 1

low in the first channel. This can be explained due to temperature distribution. It is known that fouling appears at temperatures greater than 68 °C and the temperature in this channel changes from 60 °C to 78 °C. Thus, only temperatures greater than 68 ° C were sufficient to cause fouling, based on the reaction scheme. The same results were observed experimentally by Delplace *et al.*, (1994). The maximum quantity of deposit is in channels 3 and 4 and a decrease in channel 5 (holding zone) is observed. Such a decrease in the holding zone has been observed by several authors and it is difficult to explain (Lalande *et al.*, 1985; Jong and Linden, 1992). A possible explanation is based on the low native protein concentration remaining in the last channels. Another important conclusion is that mass deposit increases almost linearly with time. The parameter estimation results are also verified independently by considering the calculated overall heat transfer coefficient profile with time against the results by Delplace *et al.*, (1994). The comparison is shown in Figure 5.5. Note that the simulation results underestimate the heat transfer coefficient in the first 3.8 hours of operation while there is a good agreement in the last stages of fouling. The initial induction period, in which the overall heat transfer coefficient is constant is very difficult to be predicted by our model and by any other model in the literature. Overall the agreement with experimental work can be considered satisfactory.

Plate Number	Experimental Value, gr	Predicted Value, gr
1	6.0	5.85
2	7.5	10.4
3	12.3	11.6
4	14.0	13.9
5	18.8	18.2
6	20.0	18.9
7	20.0	18.1
8	19.5	18.0
9	18.5	17.0
10	17.0	16.9
11	13.0	11.6
12	11.8	11.6

Table 5.3: Comparison of experimental with predicted mass deposit values-arrangement 1

Typical profiles of the deposit masses for plates 1 to 8 are shown in Figures 5.6 and 5.7 over a simulation time of 6.66 hours. Note that fouling is not uniform and increases with the plate number (according to the numbering in Figure 5.1). This can be explained based on the temperature profile. It is worthwhile to notice that fouling is not the same even for plates

delimiting the same channel (*e.g.* plates 1 and 2).

Dynamic Simulation Results

Based on the dynamic model and the same base conditions it is interesting to investigate the effect of fouling on the milk outlet temperature. The latter is depicted in Figure 5.8 as a function of time for two different values of the inlet protein concentration. As expected milk outlet temperature decreases with time. Over a period of operation of 6.66 hours the overall decrease is 2.4 °C. Comparing with the shell and tube heat exchangers fouling seems to be less severe in PHEs (in terms of the outlet temperature). This can be explained since a PHE can be viewed as a series of co-current and counter-current shell and tube exchangers with strong thermal interactions between channels. Due to fouling, milk temperature in one channel decreases and the heat losses are recovered by the heating medium in the neighbouring channels. This also affects milk temperature in all the other channels providing, in such a way, extra heat for partial mitigation of fouling. Figure 5.9 shows the heating medium outlet temperature for the first and third channel. Due to fouling, the heating medium temperature increases with time providing in such a way part of the required heat to overcome fouling resistance in the next channels.

The effect of Reynolds number on milk outlet temperature is illustrated in Figure 5.10. Note that there is a considerable fouling mitigation at higher Reynolds numbers. The same results were obtained for the shell and tube heat exchanger case. Unfortunately, no experimental results are available for the effect of Reynolds number. Finally, the effect of inlet protein concentration on fouling is shown in Figure 5.8 for two values of 2.5 and 5 kg/m^3 respectively and in Figure 5.11 for a value of 2.5 kg/m^3. As expected lower inlet protein concentrations results in less fouling. Figure 5.11 presents also a comparison with experimental results. Comparing with Figure 5.5 (for which $C_{N,in} = 5\ kg/m^3$) the evolution of the overall heat transfer coefficient with time is lower if a first milk thermal treatment is applied (in order to reduce concentration from 5 to 2.5 kg/m^3). We can see that fouling is underestimated by the simulation results but the accuracy is within the range of 3-15% which can be considered satisfactory.

5.4.2 Arrangement 2

This arrangement is shown in Figure 5.12 and it is two channel per pass with total four passes. The heat exchanger consists of 17 plates and both counter-current and co-current flows exists. Milk enters the PHE at 60 °C and the steady state outlet temperature should be 97 °C. The

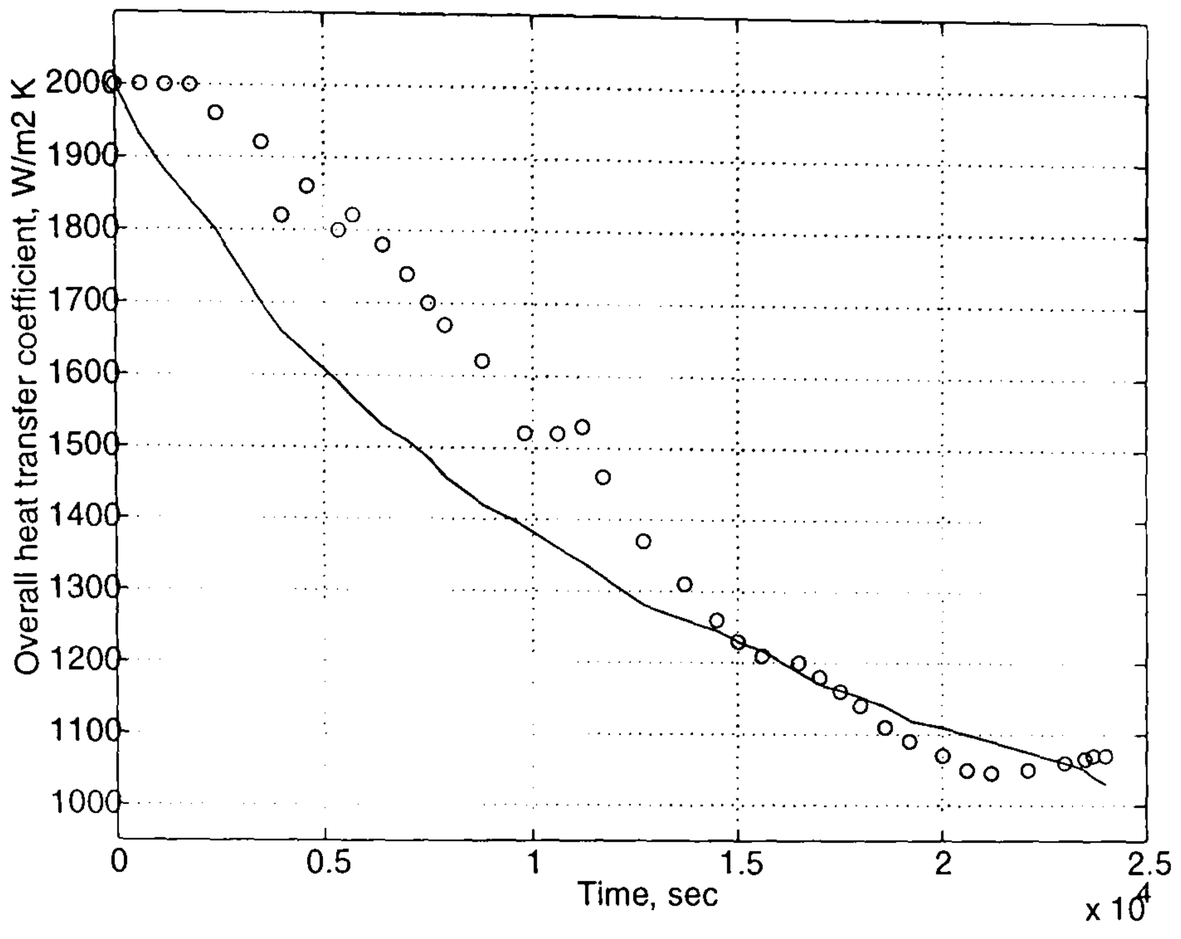


Figure 5.5: Comparison of predicted and experimental values of overall heat transfer coefficient-arrangement 1

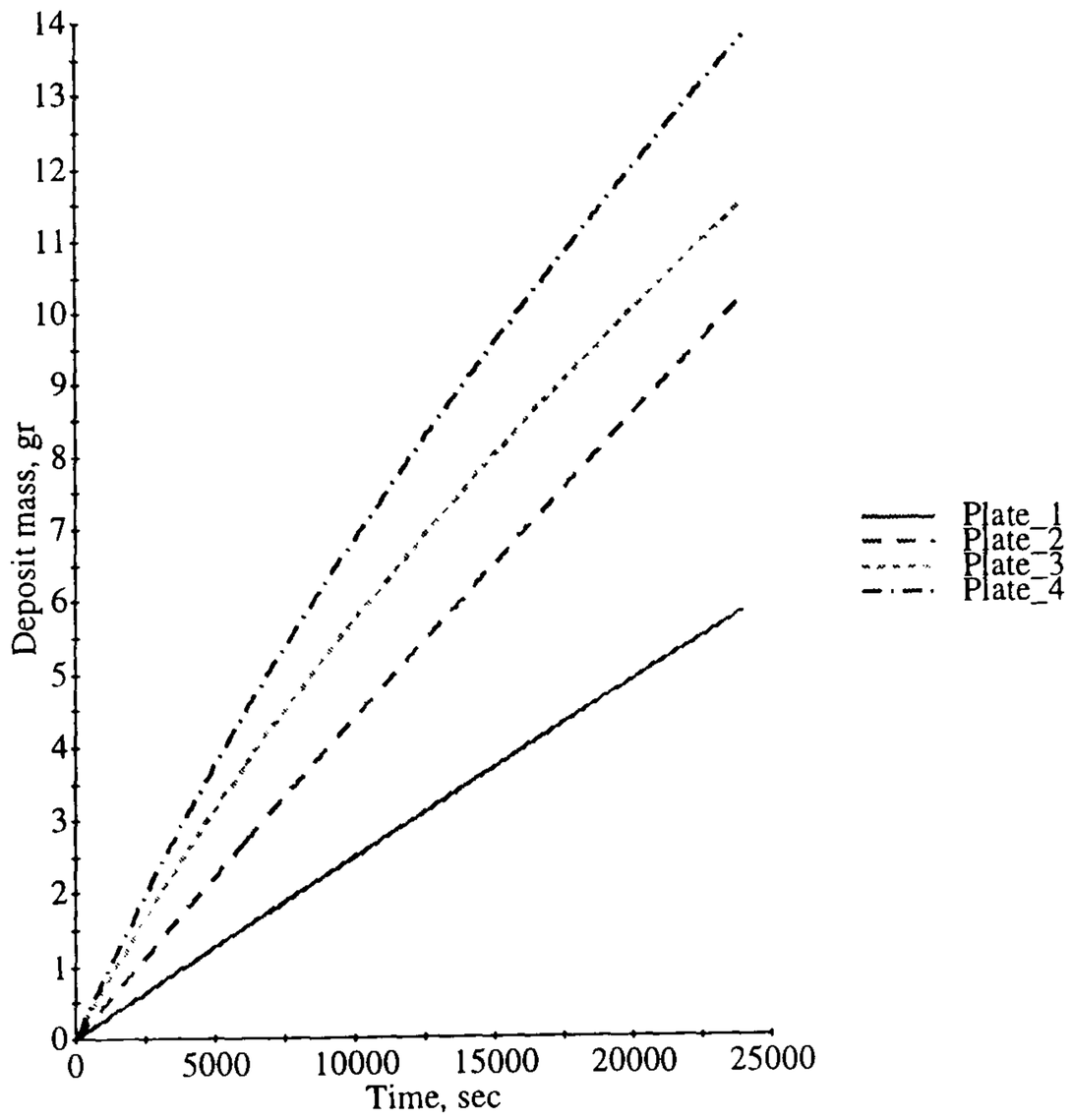


Figure 5.6: Deposit profiles for plates 1-4-arrangement 1

heating medium is taken to be hot water at a flowrate of $0.833 \cdot 10^{-4} m^3/s$ and inlet temperature 106 °C. Milk flowrate is $0.833 \cdot 10^{-4} m^3/s$. The inlet protein concentration is 5 kg/m^3. All the details were taken from Delplace *et al.* (1994). It is assumed that milk flow is the same in each channel and since there are 2 channels per pass it will be $0.4165 \cdot 10^{-4} m^3/s$.

Boundary Conditions:

For this geometry there is a mixing of milk at the outlet of each pass. Since milk is split equally, the inlet temperature for the next pass will be the mean outlet temperature of the channels belonging to the previous pass. The following boundary conditions are then imposed.

$$T_{fluid}(1,0) = T_{fin} \tag{5.29}$$

$$T_{fluid}(2,0) = T_{fin} \tag{5.30}$$

$$T_{fluid}(3,L) = \frac{T_{fluid}(1,L) + T_{fluid}(2,L)}{2} \tag{5.31}$$

$$T_{fluid}(4,L) = \frac{T_{fluid}(1,L) + T_{fluid}(2,L)}{2} \tag{5.32}$$

$$T_{fluid}(5,0) = \frac{T_{fluid}(3,0) + T_{fluid}(4,0)}{2} \tag{5.33}$$

$$T_{fluid}(6,0) = \frac{T_{fluid}(3,0) + T_{fluid}(4,0)}{2} \tag{5.34}$$

$$T_{fluid}(7,L) = \frac{T_{fluid}(5,L) + T_{fluid}(6,L)}{2} \tag{5.35}$$

$$T_{fluid}(8,L) = \frac{T_{fluid}(5,L) + T_{fluid}(6,L)}{2} \tag{5.36}$$

$$T_s(8,L) = T_{sin} \tag{5.37}$$

$$T_s(j,L) = T_s(j+1,L) \qquad j = 2,4,6 \tag{5.38}$$

$$T_s(j,0) = T_s(j+1,0) \qquad j = 1,3,5,7 \tag{5.39}$$

Similar boundary conditions are imposed for the protein concentrations between connected channels.

The model is simulated using *gPROMS* employing the same discretization scheme (using 25 elements) and a similar model decomposition as in the first arrangement. The final model after discretization comprises a set of about 8000 variables. The steady state temperature profile is depicted in Figure 5.13. The results are in very good agreement with the experimental work of Delplace and Leuliet (1995).

Experimental data are available in the form of deposit mass at each channel and overall

heat transfer coefficient values with time. Parameter estimation analysis has been performed using the deposit mass set of data from Delplace *et al.*, (1994) and the results are given in Table 5.4. Typical simulation results illustrating a comparison between model predictions and experimental data are shown in Figure 5.14. Note that there is a good agreement especially after the first 2 hours of operation.

Native protein particles diameter, m	$8.6 \cdot 10^{-11}$
Denaturated protein particles diameter, m	$8.1 \cdot 10^{-11}$
Aggregated protein particles diameter, m	$8.8 \cdot 10^{-10}$
Constant β	24.5

Table 5.4: Parameter Estimation Results-arrangement 2

Dynamic simulation result-change of operating conditions

For this geometry Delplace and Leuliet (1995) studied experimentally the effect on fouling when the initial protein concentration change from 5 to 3.2 kg/m^3. The fluid was passed through the PHE and the same solution was reprocessed in the same conditions of flowrate and temperatures. The PHE was not cleaned between the two runs in order to observe any potential change on the fouling rate. The results of this change are illustrated in Figure 5.15 together with comparison with experimental data. A change in the slope of curve is noted due to the discontinuity at time 24000 sec. The comparison with the experimental results is good and the change in the system's behaviour is predicted with an error less than 4%. As is clear in both simulation and experimental results the overall heat transfer coefficient rate of decrease with time was lower after the first heat treatment of the simulation. It can be concluded that fouling is lower when milk has been pre-processed in the plant whatever the fouling level of the PHE (clean or dirty). Note that the same behaviour is illustrated for a clean PHE with lower protein concentration (see Figure 5.11).

5.4.3 Arrangement 3

This arrangement is shown in Figure 5.16 and it is six channel per pass with total one pass. The heat exchanger consists of 13 plates and both counter-current and co-current flows exists. Milk enters the PHE at 60 °C and the steady state outlet temperature is about 90 °C. The heating medium is taken to be hot water at a flowrate of $0.92 \cdot 10^{-4} m^3/s$ and inlet temperature 110 °C. Milk flowrate is $0.833 \cdot 10^{-4} m^3/s$. The inlet protein concentration is 5 kg/m^3. All the details were taken from Delplace *et al.* (1994). It is assumed that milk flowrate is homogeneously distributed in the channels and thus the flowrate in each channel is $0.1533 \cdot 10^{-4} m^3/s$.

For the sake of simplicity the boundary conditions are not presented here but are imposed in a similar way as in the previous arrangements. In fact, no special boundary conditions are required for the milk channels since there are no connected channels. However, for the heating medium channels the same type of boundary conditions as in arrangement 1 are taken into account. Milk outlet temperature is taken as the mean value of the channels outlet temperatures.

The model is simulated using *gPROMS*. The partial differential equations are discretized using a centered finite difference method with 30 elements for each channel. This number of elements was found to be sufficient for the numerical approximation of PDEs. As in the other two arrangement a hierarchical model building approach was followed. The final model after the discretization comprises a set of about 5000 variables. The steady state temperature profiles (clean conditions) depicted in Figure 5.17 are in the very good agreement with the experimental results of Delplace and Leuliet (1995) (not shown here). The results can also be explained intuitively based on the thermal pattern.

Experimental data are available in the form of time profiles of deposit masses in each channel. The results of the parameter estimation problem are shown in Table 5.5 and the comparison with experimental data is presented in Table 5.6. We can see that there is a very good agreement (accuracy of 3%) of the predicted values with the experimental work. This geometry results in lower fouling than the other two, however, this is expected since the heating load is lower (milk outlet temperature is 90 ^oC).

Typical profiles of the deposit mass over plates 9 to 12 are shown in Figure 5.18. The model also predicts the profiles of the milk outlet temperature with time and allows for the monitoring of a large number of variables to quantify fouling effects. For the sake of simplicity such simulation results are not presented here.

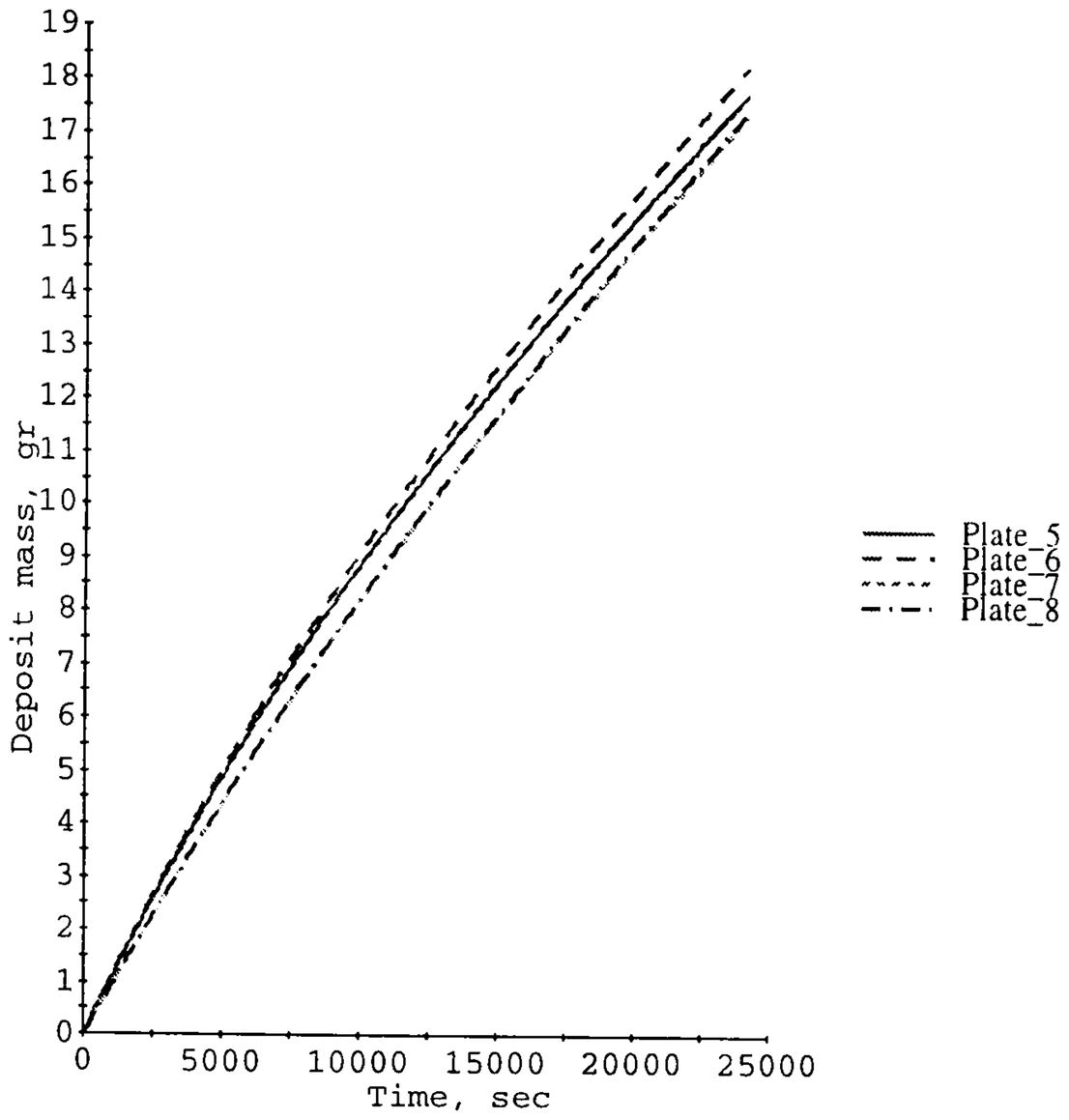


Figure 5.7: Deposit profiles for plates 5-8-arrangement 1

Native protein particles diameter, m	$4.8 \cdot 10^{-11}$
Denaturated protein particles diameter, m	$4.1 \cdot 10^{-11}$
Aggregated protein particles diameter, m	$5.3 \cdot 10^{-10}$
Constant β	0.54

Table 5.5: Parameter Estimation Results-arrangement 3

Channel Number	Experimental Value, gr	Predicted Value, gr
1	0.0	0.03
2	1.5	1.31
3	4.0	4.06
4	7.0	6.78
5	8.5	8.90
6	12.0	12.05

Table 5.6: Comparison of experimental with predicted deposit mass values-arrangement 3

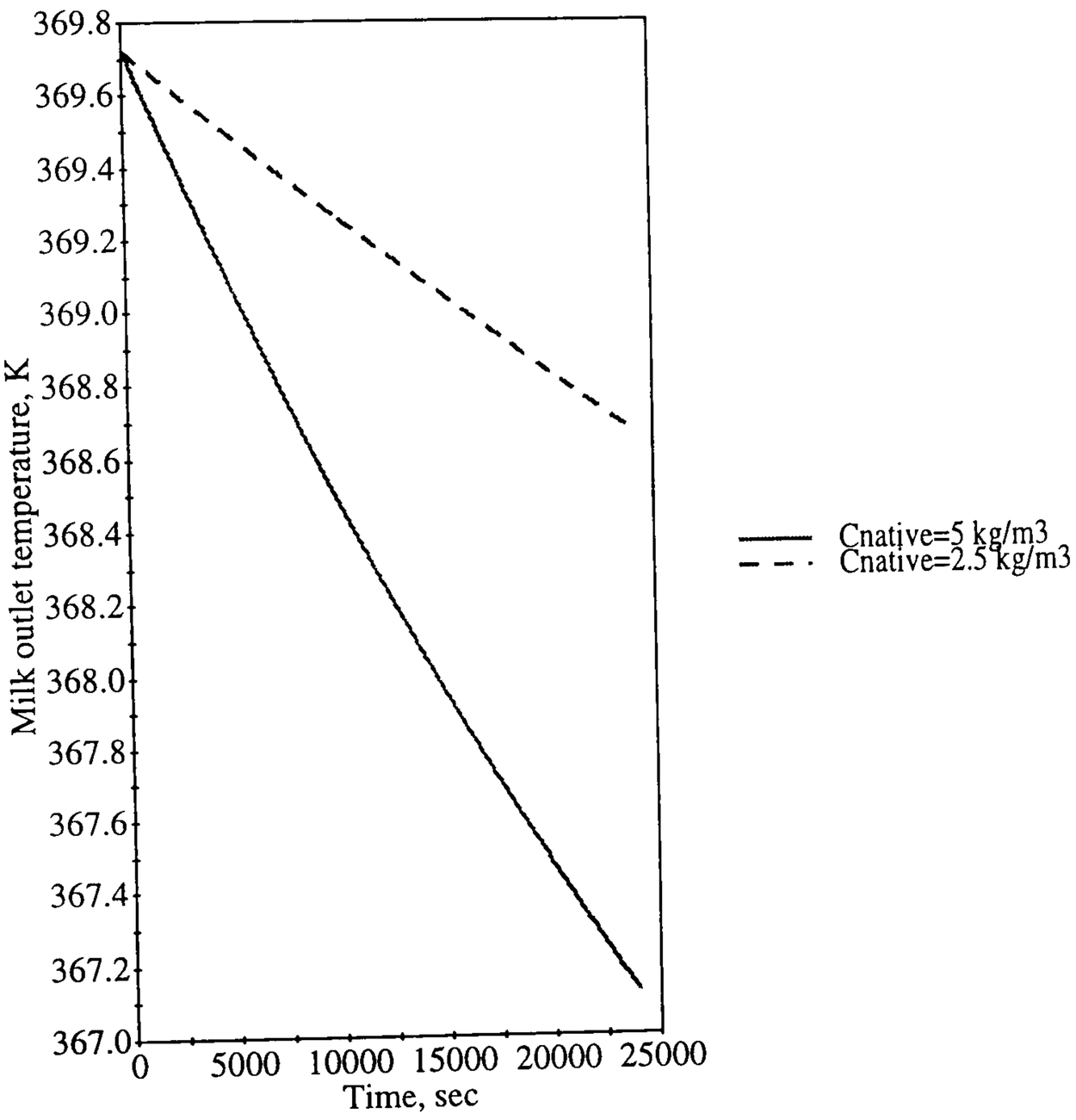


Figure 5.8: Milk outlet temperature profile for two values of inlet native protein concentration-arrangement 1

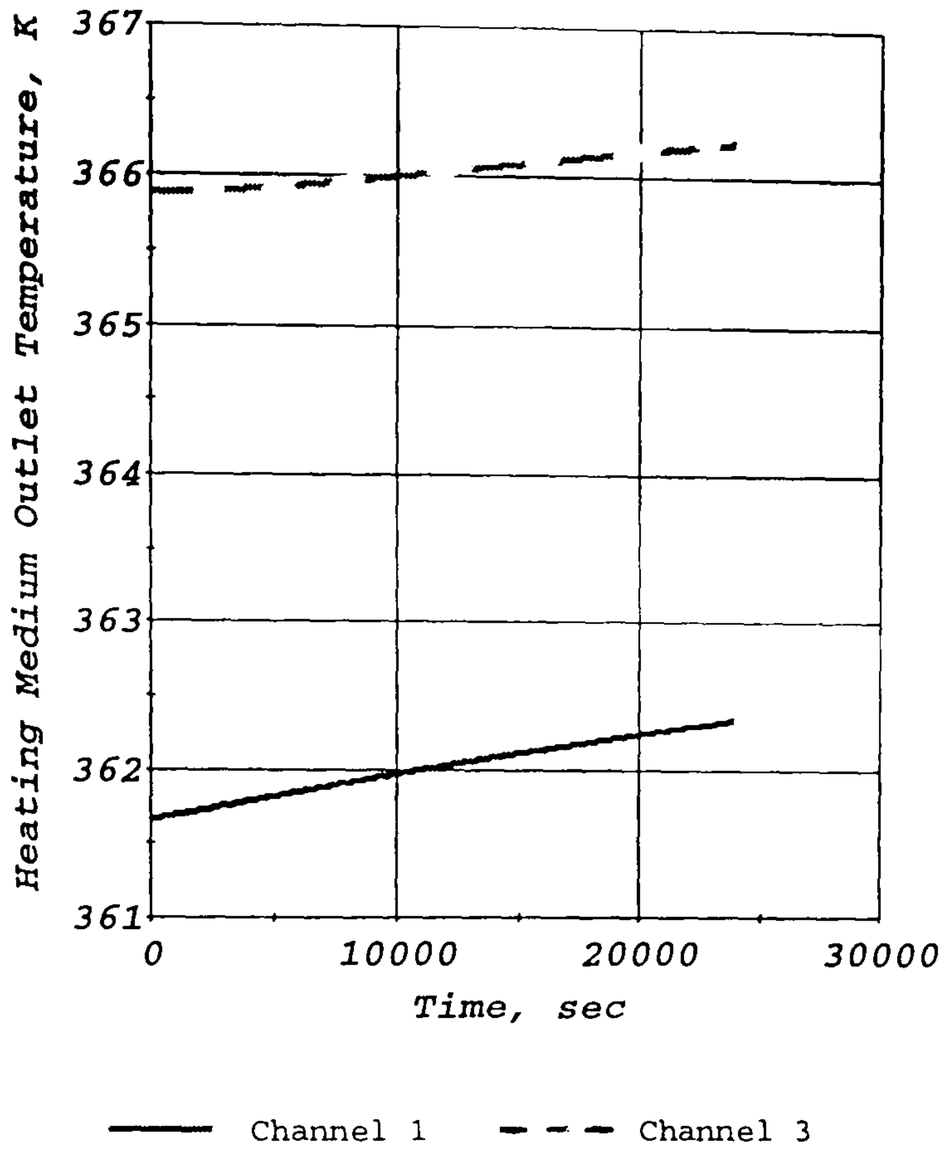


Figure 5.9: Heating medium outlet temperature profile-arrangement 1

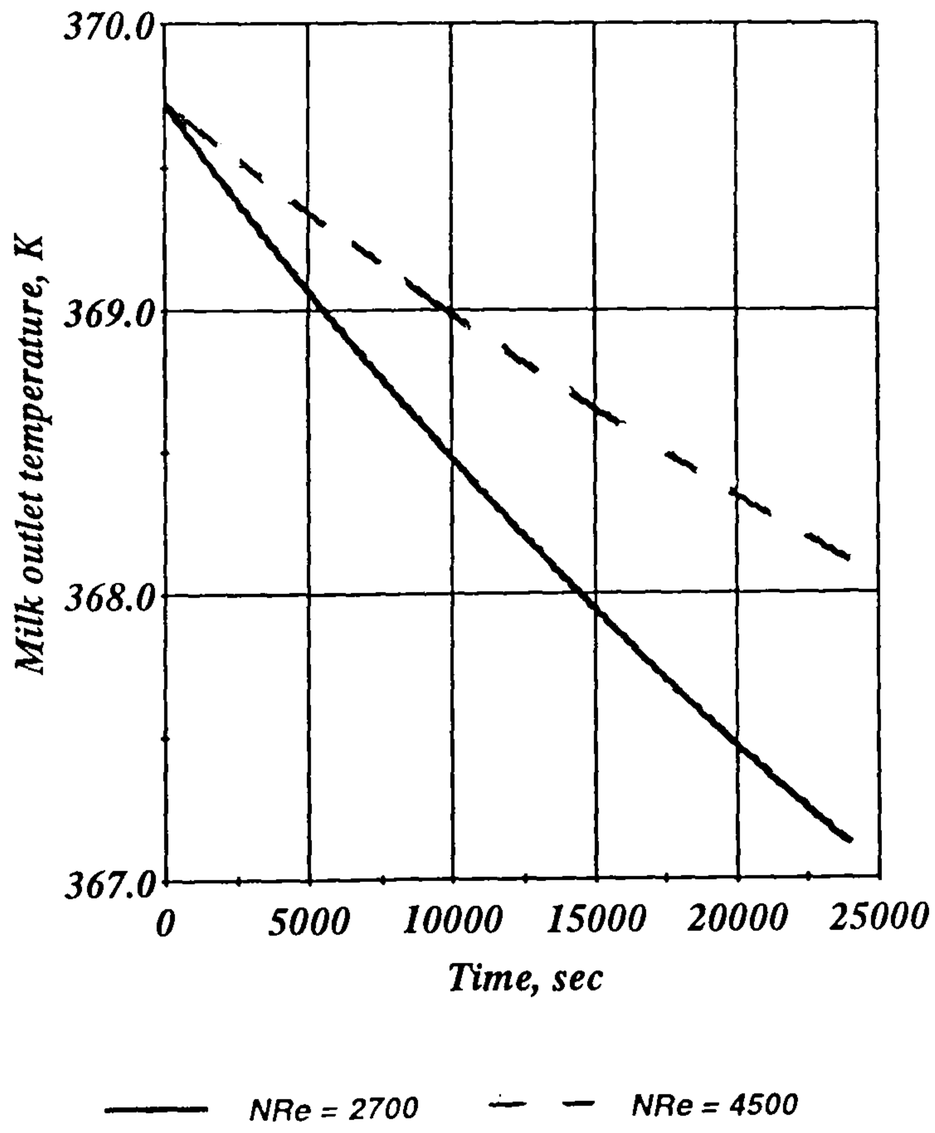


Figure 5.10: Milk outlet temperature for different Reynolds numbers-arrangement 1

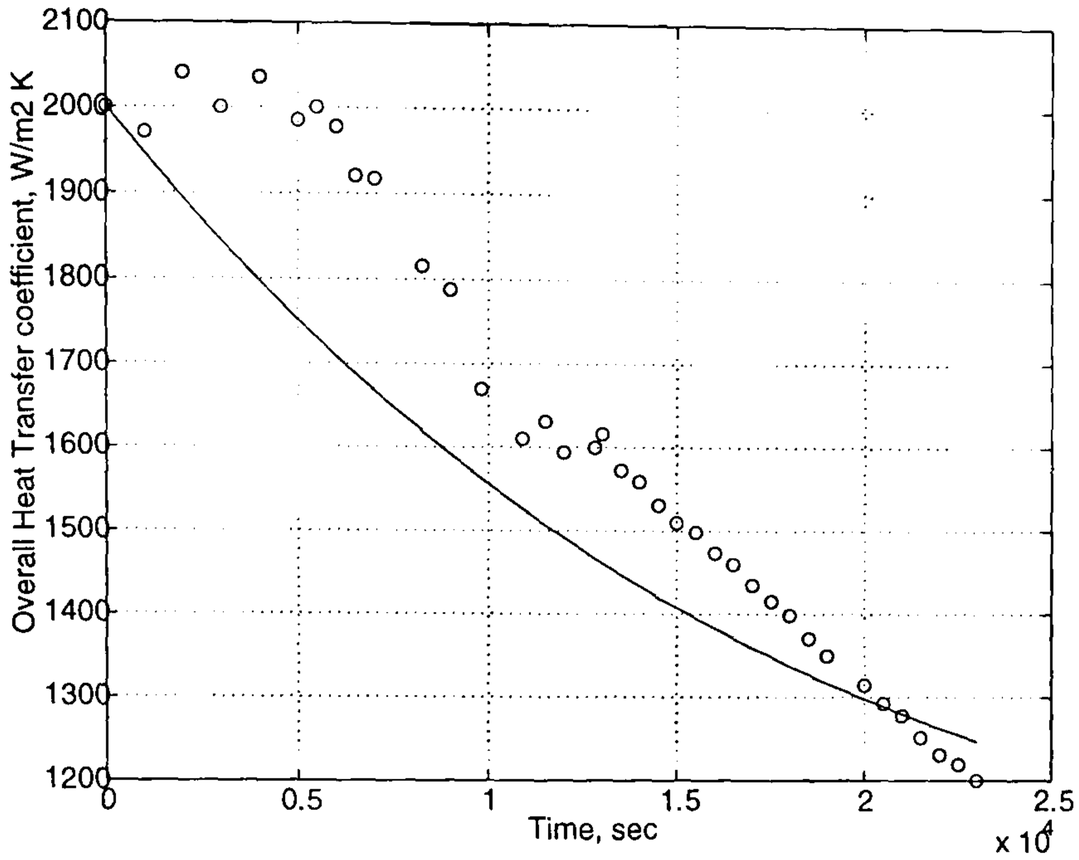


Figure 5.11: Effect of initial protein concentration and comparison with experimental data

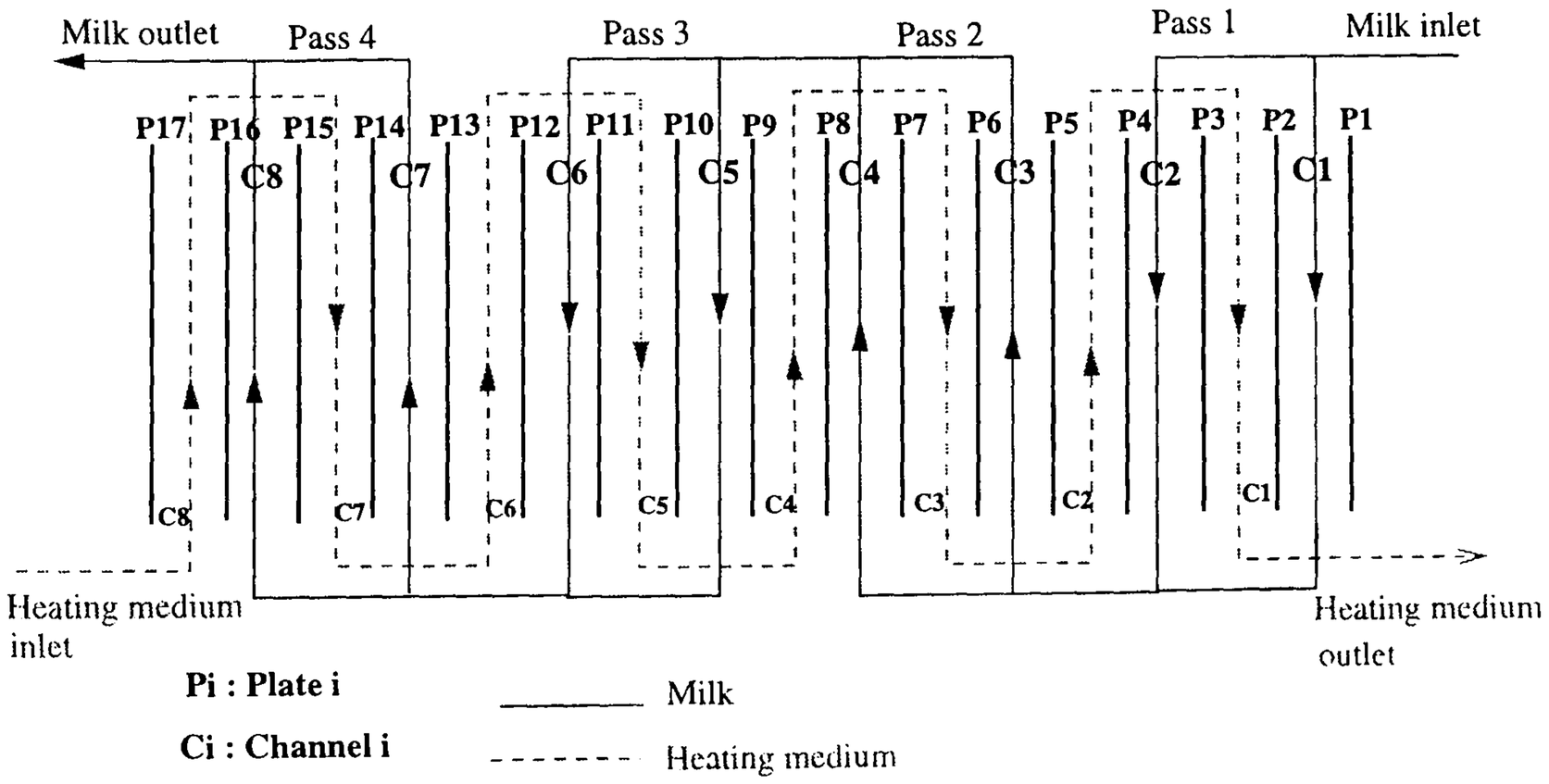


Figure 5.12: PHE-arrangement 2

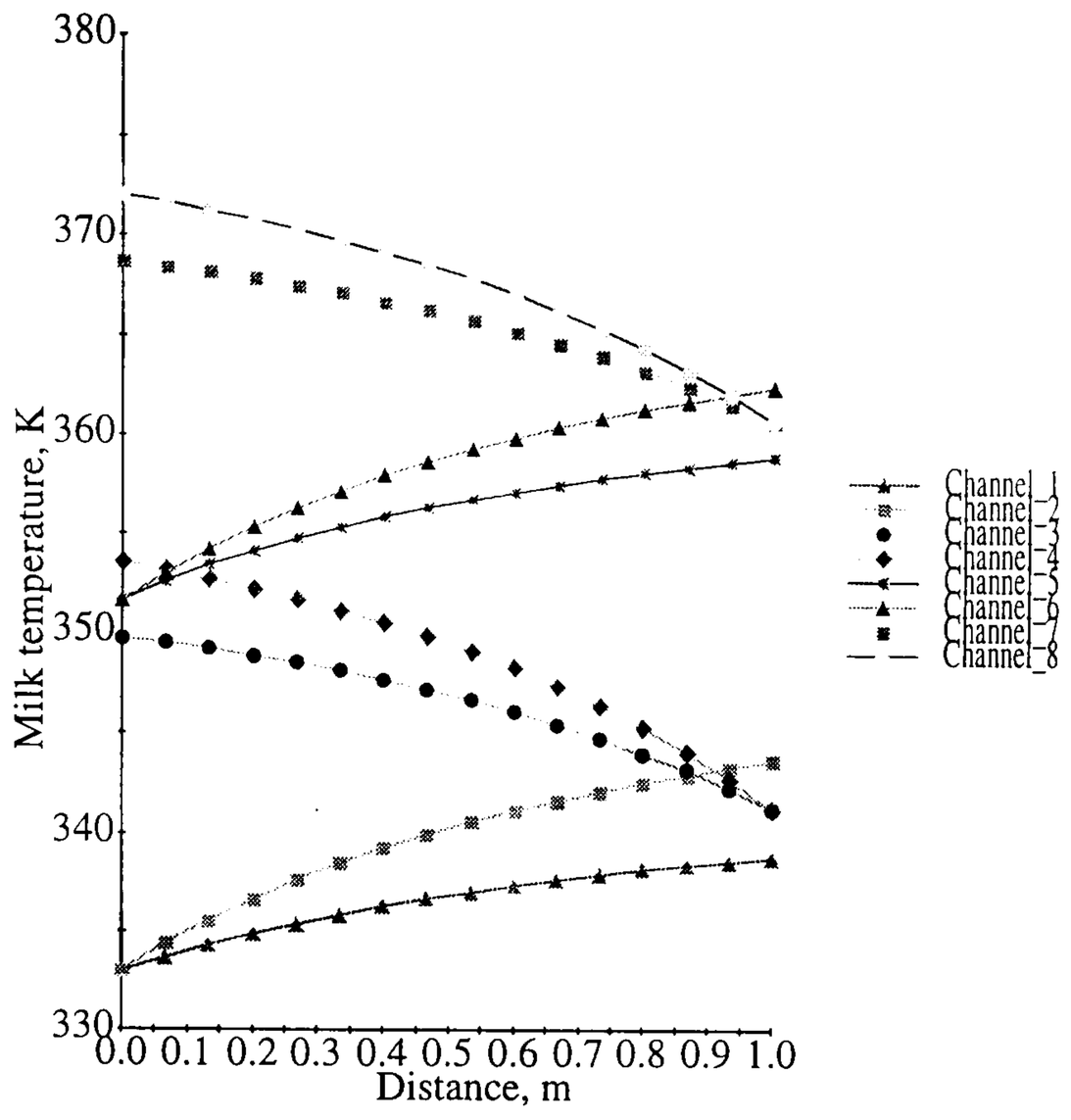


Figure 5.13: Steady state temperature profile for PHE-arrangement 2

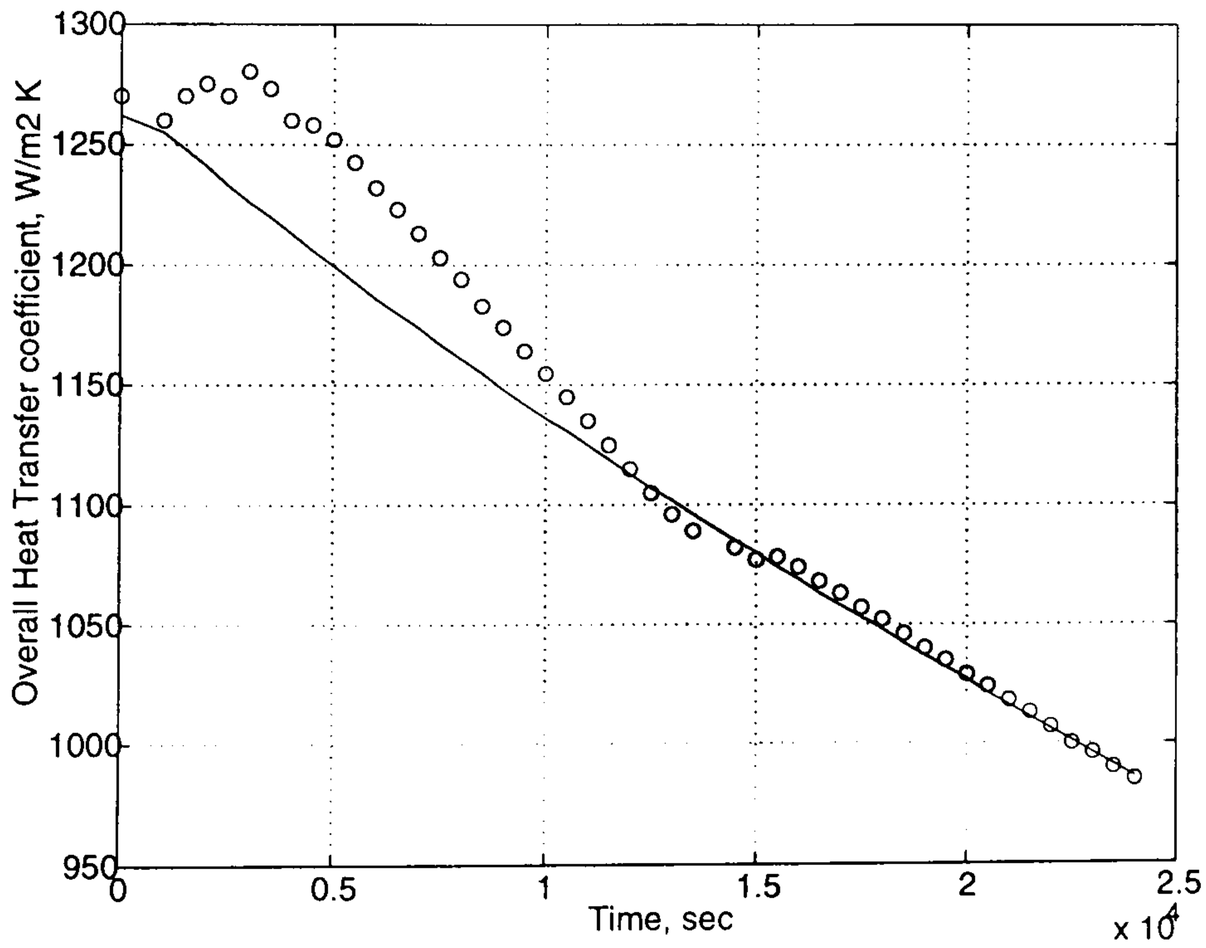


Figure 5.14: Comparison between experimental and predicted values-arrangement 2

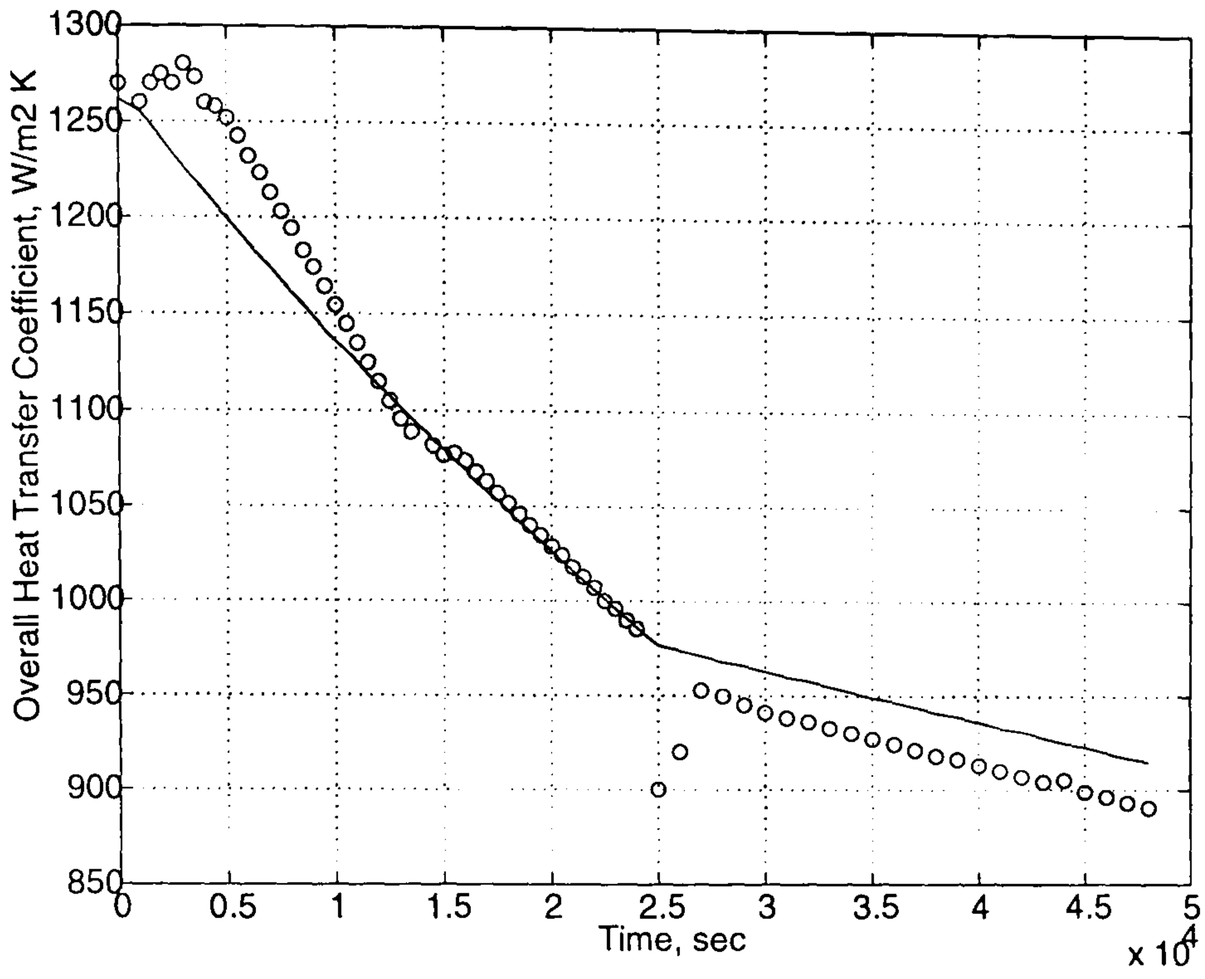


Figure 5.15: Effect of changing the initial protein concentration and comparison between experimental and predicted values-arrangement 2

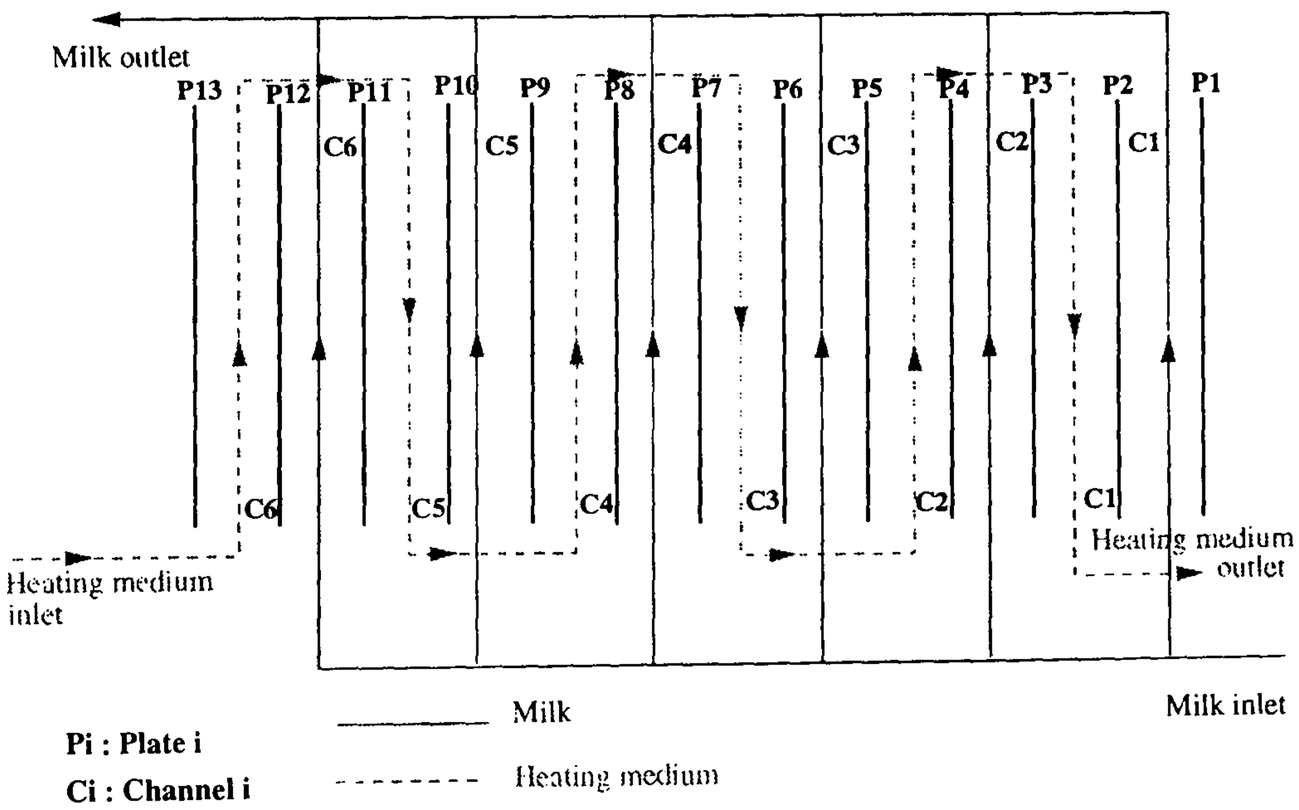


Figure 5.16: PHE-arrangement 3

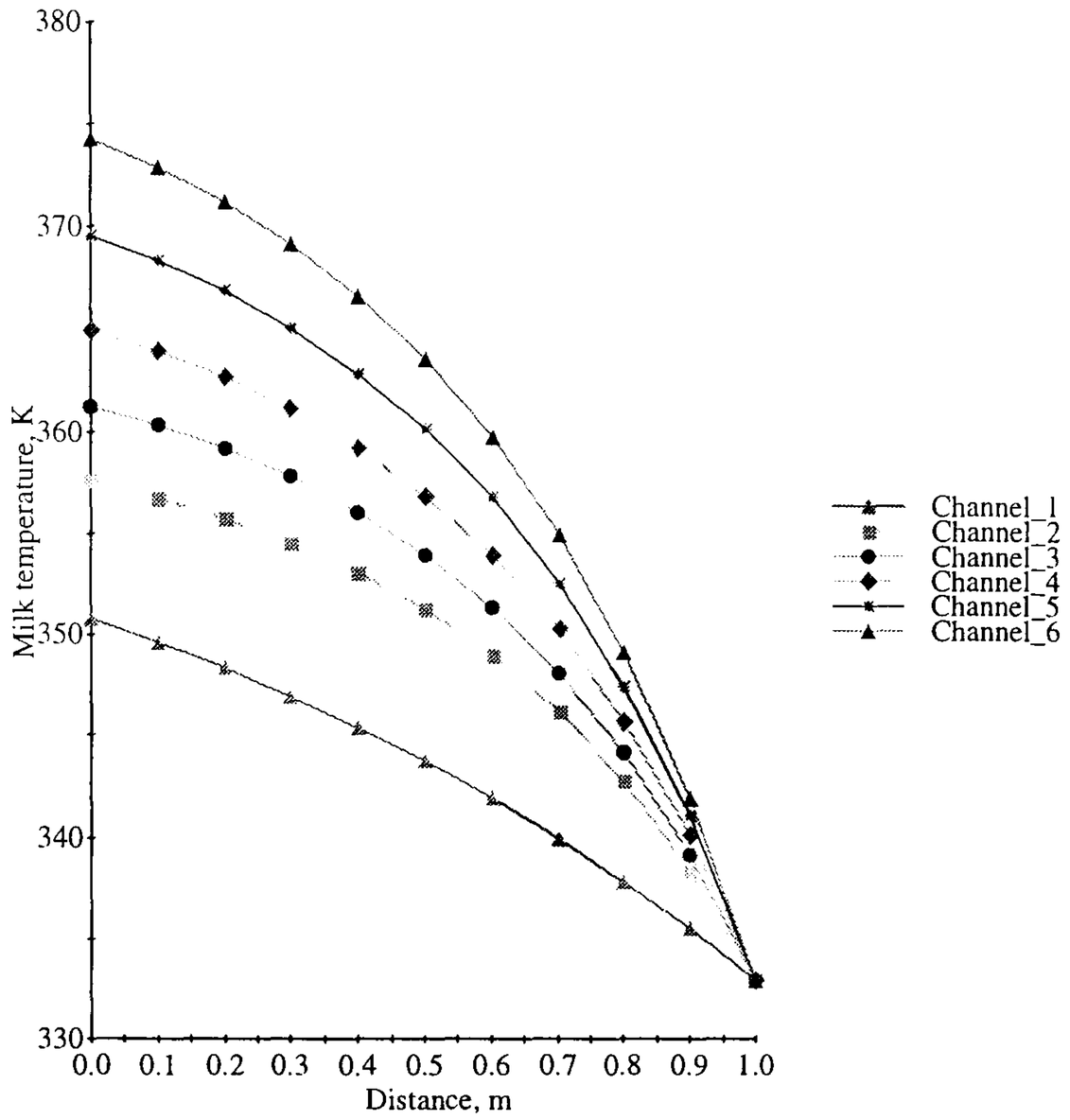


Figure 5.17: Steady state temperature profile for PHE–arrangement 3

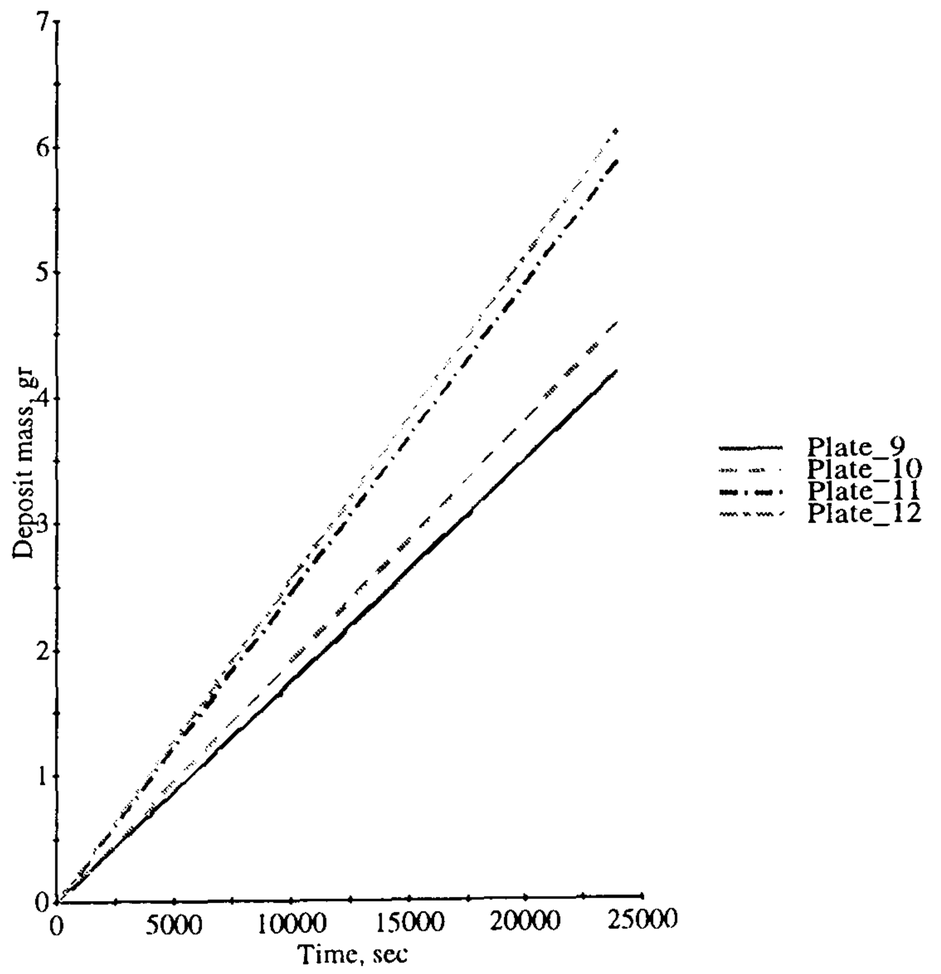


Figure 5.18: Deposit mass profiles for plates 9 to 12-arrangement 3

5.5 Concluding Remarks

In this chapter the detailed mathematical modelling and simulation of three PHEs arrangements under milk fouling, typically met in dairy plants, is presented. The simulation results agree well with experimental work. The effect of process conditions (*e.g.* initial protein concentration or flow conditions) has been investigated and compared with experimental data. The models developed provide significant insight into the key factors affecting milk fouling and can be used to identify ways in which its effects can be mitigated.

Based on the dynamic results an important conclusion is that fouling is not so severe (compared with the tubular case) in terms on the milk outlet temperature, due to the strong thermal interaction between channels and "self-correcting" behaviour. This may indicate that the main bottleneck is the pressure drop limitations due to the blockage of the channels and not the hot utility availability, as in the case of shell and tube exchangers. It is also important to notice that fouling is always lower after a first milk heat treatment and it is not uniform over the channels.

The simulation results presented here can aid in developing suitable cleaning policies in complex heat exchanger arrangements. This is considered in chapter 7.

5.6 Nomenclature

$A_x =$ channel cross sectional area, m^2

$A_{xp} =$ plate cross sectional area, m^2

$A_j =$ heat transfer area, m^2

$Cp_j =$ fluid heat capacity, $J/(kgK)$

$Cp_p =$ heat capacity of plate p, $J/(kgK)$

$h_{cold}, h_{hot} =$ local heat transfer coefficient in the cold and hot side respectively, $J/(m^2 \cdot sK)$

$p_j =$ fluid density in channel number j, kg/m^3

$T_{p_j} =$ temperature of plate j, K

$T_j =$ temperature of channel j, K

$\epsilon_j =$ gap between plates, m

k_{mN} = native protein mass transfer coefficient, m/s

k_{mD} = denaturated protein mass transfer coefficient, m/s

k_{mA} = aggregated protein mass transfer coefficient, m/s

k_w = mass transfer coefficient for the deposition, m/s

u_x = average fluid velocity, m/s

Chapter 6

Optimal Design and Operation of Heat Exchangers under Milk Fouling

The simultaneous optimisation of the design and operation of heat exchangers under milk fouling is considered in this chapter. The design and operating parameters determined by the dynamic optimisation include the length and diameter of the exchanger, the temperature control policy and the timing of the key operating steps (*e.g.* switching time from heating to cleaning). Three different heat exchanger configurations are considered to study the effect of fouling on the optimal plant design based on a comprehensive economic objective function. The optimization indicates that the cost factor due to the interruption of production is dominant while the increase in energy consumption due to fouling is not very important. The constant wall temperature configuration proved to be the most economical. The economic impact of different control structures has also been explored.

6.1 Introduction

Heat transfer plays an important role in industrial processing and heat exchangers are used in most stages of industrial transformations. Heat exchanger fouling is the major unresolved problem in this field and it is particularly acute for fluids, such as milk, which contain heat-sensitive components (Taborek *et al.*, 1972). The presence of fouling in heat exchanger equipment represents additional costs to the industrial sector in terms of extra capital, energy and labour. Specifically the cost of fouling include (Garett *et al.*, 1985):

- increased capital cost due to oversized or redundant equipment

- additional downtime for maintenance and repair
- loss of production
- cleaning equipment and services
- waste of energy and heat

In dairy plants *pasteurization* (a milk heat treatment) is an important process required to safeguard public health by destroying all pathogenic bacteria and also to ensure good quality dairy products (Hall, 1976). The common practice to overcome fouling in dairy plants is to implement cleaning-in-place (CIP) operations based on predetermined heating-cleaning cycles. These cycles are typically developed empirically, without direct knowledge of the actual fouling state of the system and without accounting for broad economical considerations. Furthermore, the design of the equipment and the control policies are also empirical. This results in additional operating and capital costs and unnecessary interruptions to the operation of the plant. In particular, from a design point of view, if the fouling effect is overestimated, the capital cost of the plant is too high, whereas if it is underestimated the resulting plant requires frequent cleaning and thus has high operating costs. In general, the greater the heat transfer area used to perform a given thermal duty, the less the control action required to maintain the process stream target temperature under fouling (Garett *et al.*, 1985).

It is clear that the size of the heat exchanger adopted for milk heat treatment should be determined by an economical balance between equipment capital cost and potential benefits arising from enhanced thermal efficiency and reduced cleaning costs (Foumeny and Heggs, 1991). Although fouling may eventually settle down to a constant value, in the food industry it is generally so severe that cleaning is necessary before this happens. To cope with the changing fouling resistance, process control is needed. If this control is applied incorrectly, for example by having wall temperature that is too high or product flowrate that is too low, fouling may become more severe (Fryer, 1989).

The need for optimising the economics of heat exchangers under fouling has long been recognized. Sandu and Lund (1983) discussed the potential for optimal design and operation of heat exchangers in order to mitigate fouling. They emphasized that the dynamics of fouling and the design and operation of heat exchangers used for pasteurization are strongly related and the key point is to quantify and optimize this relationship. These authors presented three basic procedures to minimize fouling cost: (i) economical suppression of fouling resistance (ii) optimum production-cleaning cycle and (iii) stand-by heat exchangers. They also noted

that practical experience shows that engineers improve the operation of heat exchangers under fouling when they are aware of the transient behaviour of fouling and take into account the design and operation parameters influencing its dynamics. Engineers need first to determine and understand the fouling dynamics and then decide whether it can be economically suppressed or not and what optimization procedure is suitable in each case (Sandu and Lund, 1985).

Although there is a considerable amount of experimental and theoretical work on milk fouling (Fryer *et al.*, 1996; Delplace *et al.*, 1994) to our knowledge, there has been no previous publication concerning optimal design and operation of heat exchangers under milk fouling using detailed models and taking into account comprehensive economic considerations. The dynamics of milk fouling are complex, making the process optimisation a difficult mathematical problem. As an attempt to explore aspects of the problem some authors studied the effect of different operating procedures on milk fouling. Yoon and Lund (1994) presented an experimental comparison of two different operating methods for controlling the temperature profile under milk fouling; (i) control by increasing the flow rate of the heating medium and (ii) control by increasing the inlet temperature of the heating medium. Jong and Linden (1992) presented a mathematical model defining the optimal operating conditions in heat treatment equipment for milk, assuming an analogy with a cascade of non isothermal plug flow and isothermal tank reactors. The problem of defining the optimal control policy in order to maintain milk temperature close to its target value was not considered. Furthermore, the whole analysis is based on simulation rather than on formal optimisation schemes.

Fryer and Slater (1986) used simplified models to simulate various alternative strategies for the control of heat exchangers subject to reaction fouling. Four different configurations of exchangers and control strategies were considered. Although the work is not based on an optimisation procedure and the design problem is not addressed, useful conclusions were obtained with respect to the effectiveness of different control strategies. Fryer *et al.* (1988) examined the optimal design of heat exchangers under reaction fouling for uniform wall temperature and fixed outlet fluid temperature. The objective was to minimise the amount of fouling in the system. Beyond the fact that a simple model was used, in order to quantify fouling, the problem of defining the optimal operating policies was not considered.

One of the weaknesses of the above approaches is that they are not based on optimisation techniques but on simulation. More importantly, simple and/or aggregated models were used, often neglecting fluid hydrodynamics and other important interactions. Also, the interactions between design and control decisions have been ignored. Finally, an explicit economic objective

function has never been used since the objective function (if there was one) was to minimise the amount of fouling.

In this chapter we present a mathematical approach for addressing the problem of optimal design and operation of heat exchangers under fouling. In particular, we consider tubular heat exchangers. The problem is posed as an optimal control problem, based on control vector parameterization (CVP) using the detailed non-linear process model presented in chapter 4. The optimisation procedure is demonstrated for three different heat exchanger configurations and a variety of control policies. It results in (i) the optimal switching time from heating to cleaning (ii) the optimal length and diameter of the tube and (iii) the optimal control policy (*e.g.* profile of the control variables with respect to time).

6.2 Mathematical Model

As discussed in chapter 4 the detailed mathematical modelling of the physical phenomena occurring within a tubular heat exchanger under fouling leads to a mixed set of partial differential and algebraic equations of the general form:

$$F(x, x_z, x_{zz}, \dot{x}, y, y_z, u) = 0 \qquad \forall z \in (0, L), \quad t \in (0, T] \tag{6.1}$$

$$\bar{F}(x, x_z, x_{zz}, y, y_z, u) = 0 \qquad \forall z \in (0, L), \quad t \in [0, T] \tag{6.2}$$

where z represents the spatial position in the exchanger, $\dot{x}$ denotes $\frac{\partial x}{\partial t}$, and F and $\bar{F}$ correspond to differential and algebraic equations respectively. Note that the distinction between the two types of equations is that $\bar{F}(.)$ do not involve time derivatives $\dot{x}$ and these equations also hold at $t = 0$. On the other hand, $F(.)$ do involve $\dot{x}$, they only hold for $t > 0$ and at $t = 0$ they are replaced by initial or other temporal conditions.

For the sake of notation simplicity, here we assume a singe spatial dimension corresponding to the axial position within the exchanger, *i.e.* $z \in [0, L]$ where L is the bed length. However, the models described in chapter 4 include also the radial dimension. The methodology presented here is entirely general and it is also applied to the radial domain.

We distinguish two classes of variables in the general model described by equations 6.1 and 6.2, namely differential variables $x(z, t)$ and algebraic $y(z, t)$, depending on whether or not their partial derivatives with respect to time also appear in the equations. The number

of differential (algebraic) variables is equal to the number of differential (algebraic) equations. The model also involves spatial derivatives (namely $x_z \equiv \frac{\partial x}{\partial z}, x_{zz} \equiv \frac{\partial^2 x}{\partial z^2}, y_z \equiv \frac{\partial y}{\partial z}$) arising from convective and dispersive phenomena. It also involves certain parameters u that do not vary with either time or spatial position such as for instance the friction factor or the molecular volume of the absorbed particles. We note also that the PDAEs system 6.1 and 6.2 has been written strictly for the interior of the spatial domain $z \in (0, L)$ and not for the boundaries conditions $z = 0$ and $z = L$. The phenomena taking place at the latter are described by the boundary conditions. These are given in more details in chapter 4.

6.3 A Comprehensive Objective Function

So far, there are no known assessments of heat exchanger fouling costs in food processing. One of the reasons is that food industries have design and operation features that distinguish their equipment from similar equipment in other industries (Sandu and Lund, 1985). Here a detailed objective function is proposed to account for all important economic considerations related to fouling. The cost objective function (to be minimised) not only has to take into account the cleaning cost (which is generated by fouling) but also the cost incurred due to the interruption of production. This is very important and represents the direct economic impact of fouling on the manufacturing plant. Other operating cost terms, such as the annualized capital and energy cost are also included in the objective function.

We assume that the pasteurizer is periodically cleaned (cyclic operation). In order to quantify the cost of cleaning a simple way to correlate cleaning time, t_{clean}, with heating time, t_{heat}, is proposed based on simulation of the cleaning operation (see Appendix B). The total *cycle* time is then given by the summation of heating and cleaning times.

6.3.1 Cost of Cleaning

There are several cost drivers in the cleaning operation. These drivers are the cost of water, the cost of product loss and effluent disposal, the cost of steam for heating the cleaning solution and the cost of detergent, typically NaOH. Bird and Espig (1994) reported the cost coefficients for the above drivers.

- *Water cost.*
  The total amount of water consumed during the cleaning operation is a function of the

tube cross sectional area and the cleaning time. The cost of water is \$0.6854/m^3. The total cost of water over the heating-cleaning *cycle* is given by the following expression:

$$C_{water} = \frac{0.1192 \cdot \pi \cdot d^2}{4} \cdot t_{clean} \qquad \$/cycle \tag{6.3}$$

- *Cost of NaOH.*

The solution is 1% w.t. and the cost is \$0.298/kg. In an analogy to the cost of water the final expression over the cleaning time is:

$$C_{NaOH} = \frac{0.51 \cdot \pi \cdot d^2}{4} \cdot t_{clean} \qquad \$/cycle \tag{6.4}$$

- *Cost of effluent disposal.*

The cost coefficient is \$1.355/m^3, and the total cost is:

$$C_{ef} = \frac{0.235 \cdot \pi \cdot d^2}{4} \cdot t_{clean} \qquad \$/cycle \tag{6.5}$$

- *Cost of steam.*

The cost of steam is \$0.0283/MJ and it is assumed that steam is used to heat the cleaning solution to the desired temperature (here 60 °C). The total cost is given by:

$$C_{steam} = \frac{0.824 \cdot \pi \cdot d^2}{4} \cdot t_{clean} \qquad \$/cycle \tag{6.6}$$

In the above expressions a constant cleaning solution velocity (0.174 m/s) was used for the necessary unit transformations while the cleaning time can be replaced by the heating time using equation B.5 in Appendix B. Therefore, the above expressions have as unknowns the heating time and the tube diameter, d (time invariant parameter for the optimisation). The total cleaning cost is given by the following equation:

$$C_{cleaning} = C_{water} + C_{NaOH} + C_{ef} + C_{steam} \qquad \$/cycle \tag{6.7}$$

If required the annualized capital cost of a CIP station could also be included.

6.3.2 Cost of Heating Medium

Three heating configurations are considered: (i) uniform wall temperature (ii) co-current operation with a heating medium and (iii) counter-current operation. For the *uniform wall temperature* case it is assumed that the wall temperature is determined by steam available from

the utility system in the plant. The amount of steam required is given by the following simple energy balance equation:

$$m_{steam} = \frac{w_{milk} \cdot C_{p,milk}(T_m^{out} - T_m^{in})}{\lambda_{steam}} \qquad kg/s \tag{6.8}$$

where the enthalpy of vaporization λ_{steam} is a function of its temperature (or tube wall temperature) and is given by:

$$\lambda_{steam} = 2537 - 2.8013 \cdot T_w \qquad J/kg \tag{6.9}$$

In this way, the optimization algorithm manipulates the wall temperature T_w as control variable and the corresponding steam cost can be easily calculated. The steam cost coefficient is taken approximately as \$0.062/kg and the total steam cost over the heating operation is given by the following expression:

$$C_{steam2} = \int_0^{t_{heat}} 0.062 \cdot m_{steam} dt \qquad \$/cycle \tag{6.10}$$

Note that T_m^{out} and T_m^{in} are the milk outlet and inlet temperature respectively and w_{milk} is the mass flowrate of milk equal to 0.25 kg/s.

For the *co-current* and *counter-current* operation the energy cost of the heating medium is also taken into account. Since its inlet temperature is a control variable it is assumed that this temperature is determined by steam from the utility system using an auxiliary exchanger. In order to be consistent with the economic analysis of the constant wall temperature case, the required amount of steam is calculated by a similar balance as follows:

$$m_{steam} = \frac{w_s \cdot C_{ps} \cdot (T_s^{in} - T_s^{out})}{\lambda_{steam}} \qquad kg/s \tag{6.11}$$

where T_s^{in} and T_s^{out} is the inlet and outlet heating medium temperature and w_s its flowrate (control variable). It is assumed that the heating medium is circulated between the auxiliary exchanger and the pasteurizer. The total cost over one heating cycle is given by an expression similar to equation 6.10.

6.3.3 Heating Medium Pumping Cost

The pumping cost of the heating medium (for the co-current and counter-current operation), due to frictional pressure drop, must also be included in the objective. This cost is a function

of the recirculating heating medium flowrate. After suitable unit transformations the following expression is added in the objective function to account for the pumping cost:

$$C_{pump} = \Delta P_s \cdot C_{pp} \cdot w_s \cdot 1.8 \cdot 10^{-8} \quad \$/sec \tag{6.12}$$

where C_{pp} is the cost coefficient equal to $\$0.54/MJ$ and ΔP_s is the pressure drop which is calculated using standard models (Peters and Timmerhaus, 1981). The pumping cost can then be easily calculated over the period of one heating cycle as shown for the other cost factors.

6.3.4 Cost of Heat Exchanger

The capital cost of the heat exchanger is represented by a depreciation rate, over a period of one year using a suitable charge factor (Douglas, 1988). The capital cost of a heat exchanger is a function of its material and heat transfer area. Here it is assumed that the construction material for the shell and tube is stainless steel. The capital cost approximately at current prices (1998) is given by:

$$\begin{aligned} CHEN &= 2403[10.75 \cdot Area]^{0.65} \quad \$ \\ Area &= \pi \cdot d \cdot L \qquad\qquad m^2 \end{aligned}$$

where L is the heat exchanger length. The above cost equation is multiplied by a capital charge factor of 1/3 (Douglas, 1988) and the final expression is as follows:

$$CHEN = 801[10.75 \cdot Area]^{0.65} \qquad \$/yr \tag{6.13}$$

6.3.5 Cost due to interruption of production

Another very important cost factor which must be added in the objective function is the interruption of production during the cleaning operation (heat exchanger downtime). The model must penalize system downtime because this disruption results in considerable loss of production.

The above can be illustrated by the following: consider the case where the duration of the heating operation is 1 hour. Using equation B.5 the corresponding time for the required cleaning will be 0.365 hours. Assuming full utilization over a period of one year the total

number of cycles (heating + cleaning) will be 5455 while the total duration of the heating periods is 5455 hours and downtime for cleaning is 1991 hours. On the other hand, if the heating time is 55.5 hours the cleaning time per cycle is 0.617 hours and the total heating periods over one year add up to 7364 hrs. In order to take into account the cost of disruption, production losses are represented by the following cost equation:

$$C_{losses} = w_{milk} \cdot S_{net} \cdot t_{clean} \quad \$/cycle \tag{6.14}$$

where S_{net} is a sales value which represent the net profit per unit of product. This value can be easily determined and for the purposes of our analysis is taken as \$0.25/kg. The above cost is expressed in \$ per cycle.

It is easy to see that the approach adopted provides results equivalent to those that would have been obtained by maximising the Net Present Value (NPV) of the design. This is because the production losses reduce the annual revenue per pasteurizer and therefore the NPV of the project. The adoption of a production losses term enables us to pose the problem as a cost-minimisation.

6.3.6 Summary of Objective Function

The objective function which represents the total cost over one year including production losses is given by the following expression:

$$CC = \text{NCL} \cdot \int_0^{t_{heat}} [C_{cleaning} + C_{steam2} + C_{losses} + C_{pump}]dt + C_{HE} \qquad \$/year \tag{6.15}$$

where the total number of cycles per year, NCL, is:

$$\text{NCL} = \frac{7446}{t_{heat} + t_{clean}} = \frac{7446}{0.353 + 1.01237 \cdot t_{heat} - 2.55 \cdot 10^{-4} \cdot t_{heat}^2 + 1.87 \cdot 10^{-6} \cdot t_{heat}^3}$$

where 7446 is the total working hours of the plant over one year. Cleaning time, t_{clean}, has been replaced by equation B.5 in Appendix B, leaving as unknown the heating time, t_{heat}.

Minimisation of this objective function clearly imposes a penalty due to the interruption of production and necessary cleaning operations.

6.4 The Optimisation Problem

The optimization procedures proposed determines: (i) the optimal heating time of the exchanger (or switching time from heating to cleaning), (ii) the optimal control profiles (time variation of either the wall temperature or the inlet heating medium temperature and flowrate) and *simultaneously* (iii) the optimal design (length and diameter) of the tube. The complexity of the dynamic optimisation problem arises primarily from the distributed and highly nonlinear nature of the system model.

There are two main issues which must be taken into consideration when establishing optimal control strategies for this problem. The first issue is to ensure that the milk outlet temperature is always kept close to its target value (within the capabilities of the hot utilities in the plant). The second issue is to seek for the best economic performance. However, because of the complexity of the underlying physical process, it is often difficult to define simple heuristic strategies in order to address these two issues and take into account all the operating constraints.

6.4.1 Optimisation Decision Variables

In this study, three heat exchanger configurations are optimized: (i) constant wall temperature using steam as the heating medium (ii) co-current operation of milk with any available heating medium (e.g. hot oil or water) (iii) the same as in case (ii) but in counter-current operation.

For the *constant wall temperature* configuration, the only available control variable is the wall temperature. This is assumed to be determined by steam available in the plant which enters and exit the tube at the same temperature. In a processing site, steam is usually available at a set of pressure conditions (and therefore a set of corresponding temperatures). However, for the purpose of our analysis steam is assumed to be available at any temperature below a predefined upper limit which represents its availability in the plant. For the *co-current* and *counter-current* operation both flowrate and inlet temperature of the heating medium are control variables which are also subject to similar upper bounds.

In pasteurization the selection of the residence time, which is a function of the flowrate and the length and diameter of the tube, is an important issue. In our analysis, the residence time is optimized through the length and diameter of the tube. However, requirements of minimum residence time arising from bacteriological and sterilisation reasons are not included here, but could be easily added if required.

6.4.2 Spatial Domain Normalization

A complication that arises in the context of optimisation is that the lengths of both the axial and radial domains are decision variables and these appear only implicitly in many of the equations determining their domain of definition (*e.g.* $z \in [0, L]$). We therefore define a normalized space co-ordinate $\zeta \in [0, 1]$ as follows:

$$\zeta \equiv \frac{z}{L} \tag{6.16}$$

All partial derivatives and integrals can then be expressed in terms of this new independent variable:

$$\frac{\partial}{\partial z} = \frac{1}{L}\frac{\partial}{\partial \zeta} \tag{6.17}$$

$$\frac{\partial^2}{\partial z^2} = \frac{1}{L^2}\frac{\partial^2}{\partial \zeta^2} \tag{6.18}$$

Following these normalizations, the general model equations 6.1 and 6.2 become:

$$F\left(x, \frac{1}{L}x_\zeta, \frac{1}{L^2}x_{\zeta\zeta}, y, \dot{x}, \frac{1}{L}y_\zeta, u\right) = 0 \qquad \forall \zeta \in (0,1) \;\; \forall t \in (0, t_{heat}] \tag{6.19}$$

$$\bar{F}\left(x, \frac{1}{L}x_\zeta, \frac{1}{L^2}x_{\zeta\zeta}, y, \frac{1}{L}y_\zeta, u\right) = 0 \qquad \forall \zeta \in (0,1) \;\; \forall t \in [0, t_{heat}] \tag{6.20}$$

Similar transformations are applied to the boundary conditions. A new normalized independent variable is also introduced for the radial domain. We note that all the transformed equations are now expressed over *fixed* domains of unit length while the quantity L (and similarly the quantity R for the radius) appears explicitly and can therefore be subject to optimization.

6.4.3 Constraints

Some constraints must be satisfied at all times during the heating operation and are known as "path" constraints. Here there are three types of path constraints. The first concerns the average pressure drop on the milk side which must be less than an upper bound. Following Kern (1965) this bound is set to 7 psi. The second type is the pressure drop at the heating medium side which must also be less than 7 psi. Finally, milk outlet temperature must be

maintained close to its target value. A lower bound of 369.5 ^oC is assumed. Note here that no upper bound in the exit temperature is required, since in order to minimize the energy consumption the optimisation algorithm will force this temperature close to the lower bound. These constraints can be mathematically stated as follows:

$$-\Delta P(t) \leq 7 \quad \text{psi} \quad \forall t \in [0, t_{heat}] \tag{6.21}$$

$$-\Delta P_s(t) \leq 7 \quad \text{psi} \quad \forall t \in [0, t_{heat}] \tag{6.22}$$

$$369.5 \leq T_m^{out}(t) \quad \forall t \in [0, t_{heat}] \tag{6.23}$$

Other typical constraints considered include upper and lower values on the time invariant parameters (tube length and diameter). The upper bound on the heating period (time horizon) is assumed to be defined by microbiological constraints equal to 70 hours. Specific attention should be given also to the control variables T_w, T_s^{in}, w_s for which an upper bound is imposed (derived from the plant data). Finally, the lower bound in the tube diameter, 0.018 m is defined by pressure drop limitations. The following inequalities express these constraints:

$$0.018 \leq \mathrm{d} \leq 0.030 \quad m \tag{6.24}$$

$$1 \leq \mathrm{L} \leq 20 \quad m \tag{6.25}$$

$$374 \leq T_w \leq 390 \ \ K \quad \text{constant wall temperature case} \tag{6.26}$$

$$380 \leq T_s^{in} \leq 400 \ \ K \quad \text{co-current or counter-current operation} \tag{6.27}$$

$$0.1 \leq w_s \leq 10 \ \ kg/sec \quad \text{co-current or counter-current operation} \tag{6.28}$$

$$3 \leq t_{heat} \leq 70 \quad hrs \tag{6.29}$$

The optimal control problem can then be formulated mathematically as follows:

$$\min_{t_{heat}, T_w(t), T_s^{in}(t), w_s(t), diam, L, t \in [0, t_{heat}]} CC(t_{heat})$$

subject to

- $CC(t_{heat})$ as given by equation 6.15

- the heat exchanger dynamic model under milk fouling:
  equations, initial and boundary conditions presented in chapter 4;
- control variable bounds: either constraints 6.26 for the constant wall temperature configuration, or constraints 6.27 and 6.28 for co-current or counter current operation;
- time horizon bounds, constraints 6.29;
- path constraints, 6.21 to 6.23;
- design parameters bounds, constraints 6.24 and 6.25.

6.5 Solution Approach

An important feature of the optimization problem defined in the previous section is that the model equations depend on the time t, axial and radial position. As in chapter 4 a spatial discretization method is applied to eliminate the last two independent variables, leading to an optimization problem described by differential algebraic equations only. Nonetheless, it remains a complex infinite dimensional, non linear optimization problem. The infinite dimensionality arises because the state and control variables (for instance, milk temperature and heating medium inlet temperature) are functions of time rather than simple scalar quantities. There are several numerical methods to solve such dynamic optimal control problems. A class of methods that is widely used, especially in chemical engineering applications, is control vector parameterization (Vassiliadis, 1994,a,b). This approach converts the infinite dimensional optimization problem into a finite dimensional one, allowing the use of standard non-linear programming (NLP) solution techniques for the solution of the latter. The reduction in dimensionality is performed by using a piecewise Lagrange polynomial to approximate the control vector. This allows the control variables to be approximated by polynomials of various degrees and orders of continuity such as piecewise constant, piecewise linear or quadratic functions.

Assume that $u(t)$ is a control variable (*e.g.* the wall temperature T_w). To make the dynamic optimization problem tractable the entire time horizon t_{heat} is first divided into N intervals with lengths $l_1, \cdots l_N$:

$$t_{heat} = \sum_{k=1}^{N} l_k \tag{6.30}$$

The values of l_k are not necessarily fixed or equal to each other. The control actions over each time interval are represented by:

$$u(t) = \Phi_k(t, v_k) \quad t \in [l_{k-1}, l_k),\ k = 1 \cdots N \tag{6.31}$$

where Φ_k are simple polynomial functions of time t (*e.g.* constant, linear or quadratic).

The number of intervals N depends on the practical problem to be solved. For piecewise constant specifications the parameterized control variable u in interval k at time t is given by:

$$u_k(t) = u_k \quad k = 1, \cdots N$$

In some cases additional constraints are imposed on the continuity of the values of the control variable at the boundaries of the intervals, or even their derivatives with respect to time. For example, if we consider piecewise linear control profiles with continuity the control variable T_w then the following expressions are added in the model

$$\frac{\partial T_w(t)}{\partial t} = \alpha \tag{6.32}$$

$$T_w(t) = 374, \qquad t = 0 \tag{6.33}$$

where α is a parameter determined by the optimization algorithm.

The precise form of Φ is determined by the finite set of parameters v and l. It is important to note that if an optimisation procedure determines the values for v and l, it will also have determined as a result the optimal control profile u within the space of the allowable functions. It is also important to emphasize that in many cases the choice of the form of the control variable is an engineering rather than a mathematical issue. It depends very much on the actual control strategy that one can or is willing to implement in practice.

In summary, the duration of each time interval and the parameterized control variable u_k are optimization decision variables with prespecified bounds:

$$u_k^{\min} \le u_k \le u_k^{\max} \quad k = 1, \cdots, N$$

$$l_k^{\min} \le l_k \le l_k^{\max} \quad k = 1, \cdots, N$$

The bounds l_k^{min} are set to a small value to avoid numerical problems that may occur if an interval k collapses to zero duration. The upper bounds u_k^{max} reflects the limitations of the hot utilities in the plant (*e.g.* maximum available steam pressure).

The aim of the optimisation is to determine the quantities u_k, l_k, t_{heat}, d and L so as to minimise the objective function while satisfying the constraints. Note here that both the design and control problems are simultaneously addressed.

So far, the control variable in the original problem has been reduced to a finite dimensional representation through control vector parameterization. However, the process model equations are still infinitely dimensional as they have to be enforced at all times $t \in [0, t_{heat}]$. To deal with this problem we note that if u_k, l_k, d, L and t_{heat} are given, the model equations with their initial conditions determine both the initial solution of the system and its subsequent behaviour for $t \in [0, t_{heat}]$. Once the final values of all the variables are determined in this fashion, then the values of the objective function and constraints can be simply calculated. Overall the infinite dimensional optimization problem in section 6.4.3 is now reduced to a finite dimensional problem which has a non-linear programming (NLP) form. For the path constraints and in order to avoid numerical difficulties a small cumulative violation is assumed over the entire time horizon and a special way to handle them is followed (Vassiliadis *et al.*, 1994b).

The dynamic optimization problem presented in section 6.4 is solved using *gOPT* an implementation of the CVP approach in the *gPROMS* modelling system (Vassiliadis, 1994a,b, *gPROMS* Technical Document, 1998b). The normalized axial domain is discretized using 2nd order orthogonal collocation on 20 finite elements, whereas the normalized radial domain is approximated by 3rd order orthogonal collocation on 5 elements. The equations that describe the model are generated by *gPROMS* as residual equations with symbolically generated partial derivatives (Jacobian) and used as inputs to *gOPT*. The latter employs:

- A sophisticated integrator, DASOLV (Jarvis and Pantelides, 1992) based on backward differentiation formulae methods for integrating the DAEs.

- The SRQPD non-linear programming code (Chen and Macchietto, 1988) implementing a reduced sequential quadratic programming algorithm. The NLP algorithm requires the gradients of the constraints and the objective function with respect to the optimization decision variables. These can be computed from the "sensitivities" of the state variables with respect to the optimization parameters.

The solution of the optimization problem is a two stage iterative procedure in *gOPT*. The first stage is the integration of the discretized model to obtain constraint residuals and/or gradients, and the second stage is the input of this information to SRQPD, as described below:

Given initial estimates for optimization variables $p \equiv \left(d, L, t_{heat}, u_k, l_k, k = 1, \cdots, N\right)$

REPEAT

1. Integrate DAEs to determine the objective function and constraints and if required their gradients with respect to p;

2. Call SRQPD to determine new estimates for p

UNTIL convergence (optimisation tolerance 10^{-3}).

The above algorithm is shown schematically in Figure 6.1. Initial points along with lower and upper bounds of all optimization variables are given in Table 6.1.

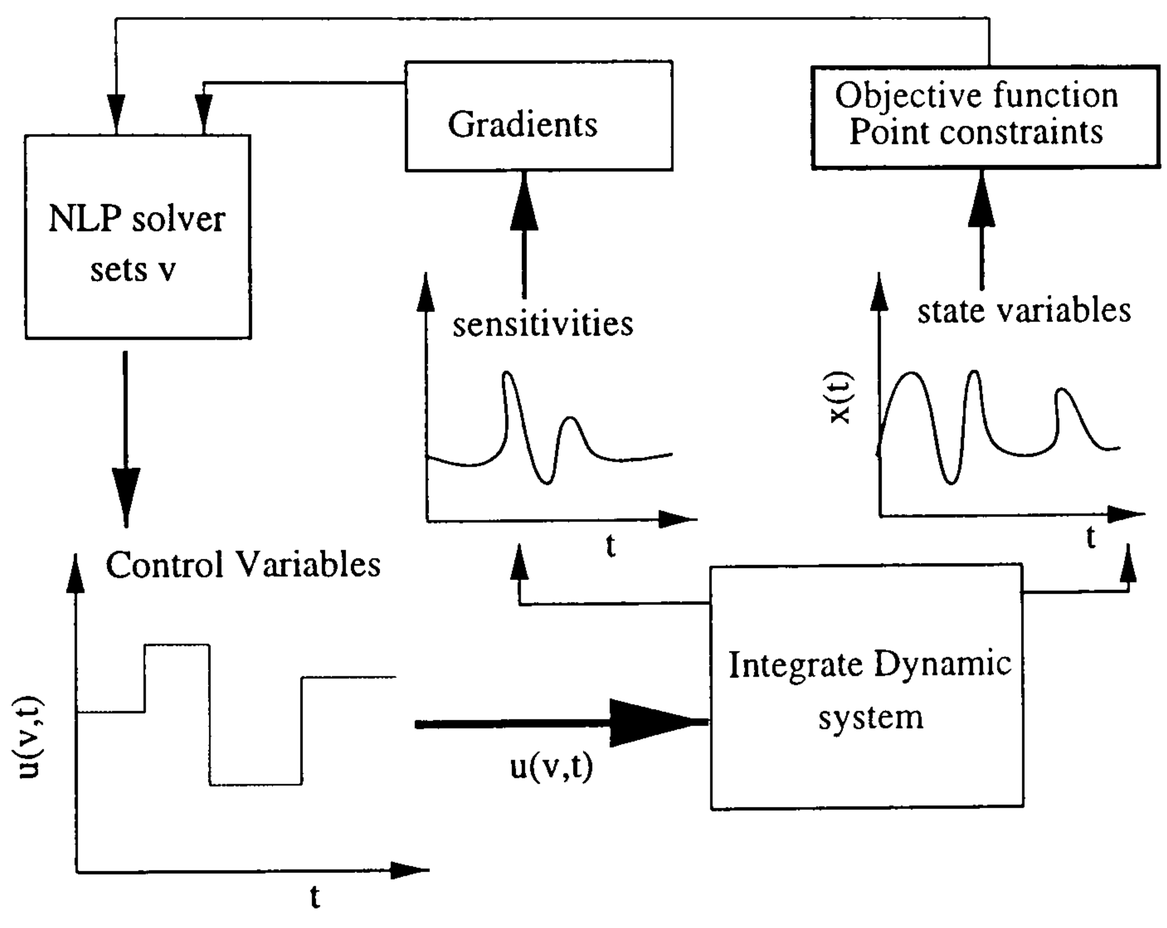


Figure 6.1: Algorithm of Dynamic optimization

6.6 Results and Discussion

The effect of time intervals and type of control profiles on the objective function is investigated for the three configurations being optimized. Two types of controls are considered: piecewise constant and piecewise linear controls.

6.6.1 Constant Wall Temperature Case

The results obtained for both the piecewise constant and linear profiles are shown in Table 6.2. Note here, that the control values for the piecewise linear case, are the optimal values of parameter α in equation 6.32.

The number of control intervals has a considerable impact on the objective function and four control intervals are not enough to fully optimize the problem. This is clearly shown in the case when 8 intervals are used resulting in a 10% improvement in the objective function. Finally, using 12 intervals the total improvement (compared with the case in which four intervals were used) is about 13% for both type of controls. If more than 12 intervals are used then there is no change in the objective function. Both type of control strategies result in the same value of the objective function for the case of 12 intervals. This is due to the fact that when the number of control intervals is large, piecewise linear profiles can be better approximated by piecewise constant profiles. It should be emphasized here that the cost factor due to the interruption of the production is dominant and thus the optimization algorithm is essentially trying to minimise the cleaning time. To illustrate this, a typical behaviour of the objective function with respect to heating time, t_{heat}, for 12 control intervals with piecewise constant control is shown in Figure 6.2. We can see that the operating cost is inversely proportional to the length of the heating cycle.

For illustration purposes, only the optimal piecewise constant control profile case with 12 intervals is shown. The milk outlet temperature as a function of time is shown in Figure 6.3 and the corresponding control profile is depicted in Figure 6.4. Clearly, the milk outlet temperature is kept above the lower limit in order to satisfy the temperature requirements of the pasteurization process.

6.6.2 Co-Current Operation

For this case, both the heating medium inlet temperature and flowrate are control variables. Here only piecewise constant control profiles are considered. The final results for 6 and 12 control intervals and the optimal design parameters are shown in Table 6.3.

For the optimal control policy and design the milk outlet temperature profile is shown in Figure 6.5 and the heating medium inlet temperature and flowrate in Figures 6.6 and 6.7. One can see that the milk outlet temperature satisfies the specified bounds over the entire heating

Optimization Variable	Lower Bound	Upper Bound	Initial Values
Control Intervals (sec)	200	30000	9000
Diameter, m	0.018	0.030	0.025
Length, m	1	20	8
Wall temperature, K	374	390	380
Heating medium inlet temperature, K	380	400	390
Heating medium flowrate, kg/s	0.1	10	3

Table 6.1: Bounds and Initial Points for the Optimization Variables

Type of control	Number of control intervals	Heating time hours (per cycle)	Objective function, $/yr	Diameter m	Length m
Piecewise constant	4	38.7	76600	0.018	10.7
Piecewise constant	8	52.7	69000	0.018	10.7
Piecewise constant	12	56.6	67200	0.018	10.7
Piecewise linear	4	35.7	79000	0.018	10.7
Piecewise linear	8	44.38	72000	0.018	10.7
Piecewise linear	12	56.8	67000	0.018	10.7

Table 6.2: Summary of optimization results for constant wall temperature case

Type of control	Number of control intervals	Heating time, hours (per cycle)	Objective function, $/yr	Diameter m	Length m
Piecewise constant	6	26.1	87500	0.018	11.8
Piecewise constant	12	24.8	85200	0.018	11.8

Table 6.3: Summary of optimization results for co-current operation

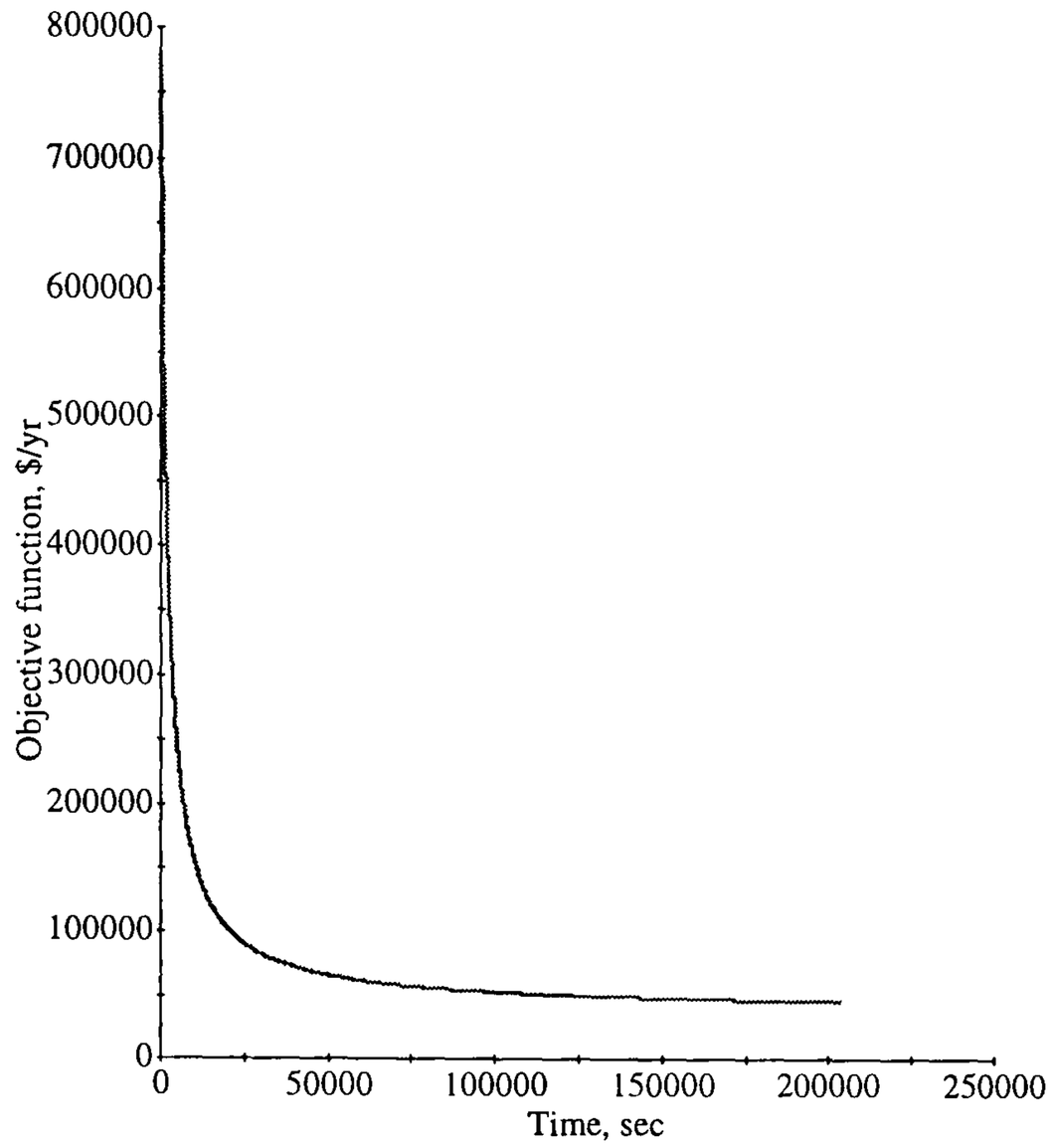


Figure 6.2: Profile of the objective function vs heating time

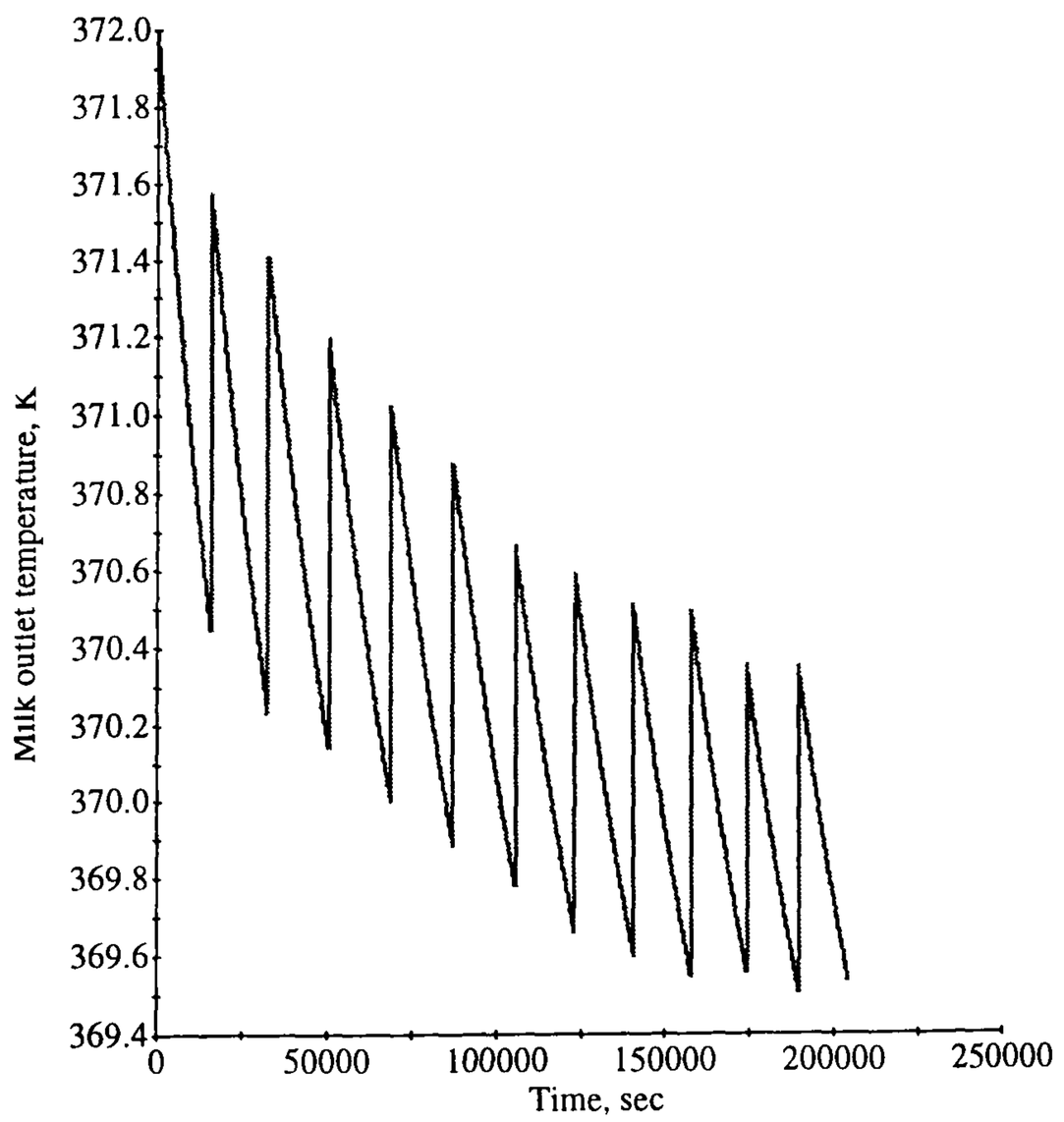


Figure 6.3: Milk outlet temperature under optimal control-constant wall temperature case

period. It is worth noticing here that during some of the time intervals the heating medium inlet temperature decreases while the flowrate increases. On the one hand, the algorithm is trying to minimise the energy consumption (keeping heating medium inlet temperature as low as possible) while the energy supply must increase to mitigate fouling effects. It is then possible for the inlet temperature to decrease if fouling can be mitigated by the proper manipulation (increase) of flowrate. It should also be noted that the observed "spike" in Figures 6.6 and 6.7 is due to the small values of the lower bound of the control intervals (200 sec).

The case of having only the heating medium inlet temperature as control variable is also investigated (flowrate is kept at its nominal value of 0.8 kg/s). The results for piecewise constant control profile and 12 intervals are shown in Table 6.4. It is worthwhile to notice here that this control scheme is not economical (100 % increase in the objective function) compared with the previous one. This is because the switching time to cleaning is significantly shorter. The case of having only the flowrate as control variable was also considered. Here, it was not possible to find even a feasible solution and both the optimisation and the integration/sensitivities stage was infeasible. This is due to the fact that the heating medium flowrate on its own is not an effective variable for control purposes.

Type of control	Number of control intervals	Heating time, hours	Objective function, \$/yr	Diameter m	Length m
Piecewise constant	12	7.22	166900	0.018	12.1

Table 6.4: Optimisation results for co-current operation with one control variable

6.6.3 Counter-Current Operation

Optimization results for piecewise constant control profiles with 6 and 12 intervals are summarized in Table 6.5. Again, the use of the heating medium inlet temperature as the only control variable is investigated leading to higher values of the objective function compared with the previous scenario (Table 6.6). The use of flowrate as the only control variable was proved to be infeasible.

The optimal milk outlet temperature and the control profiles are depicted in Figures 6.8 to 6.10.

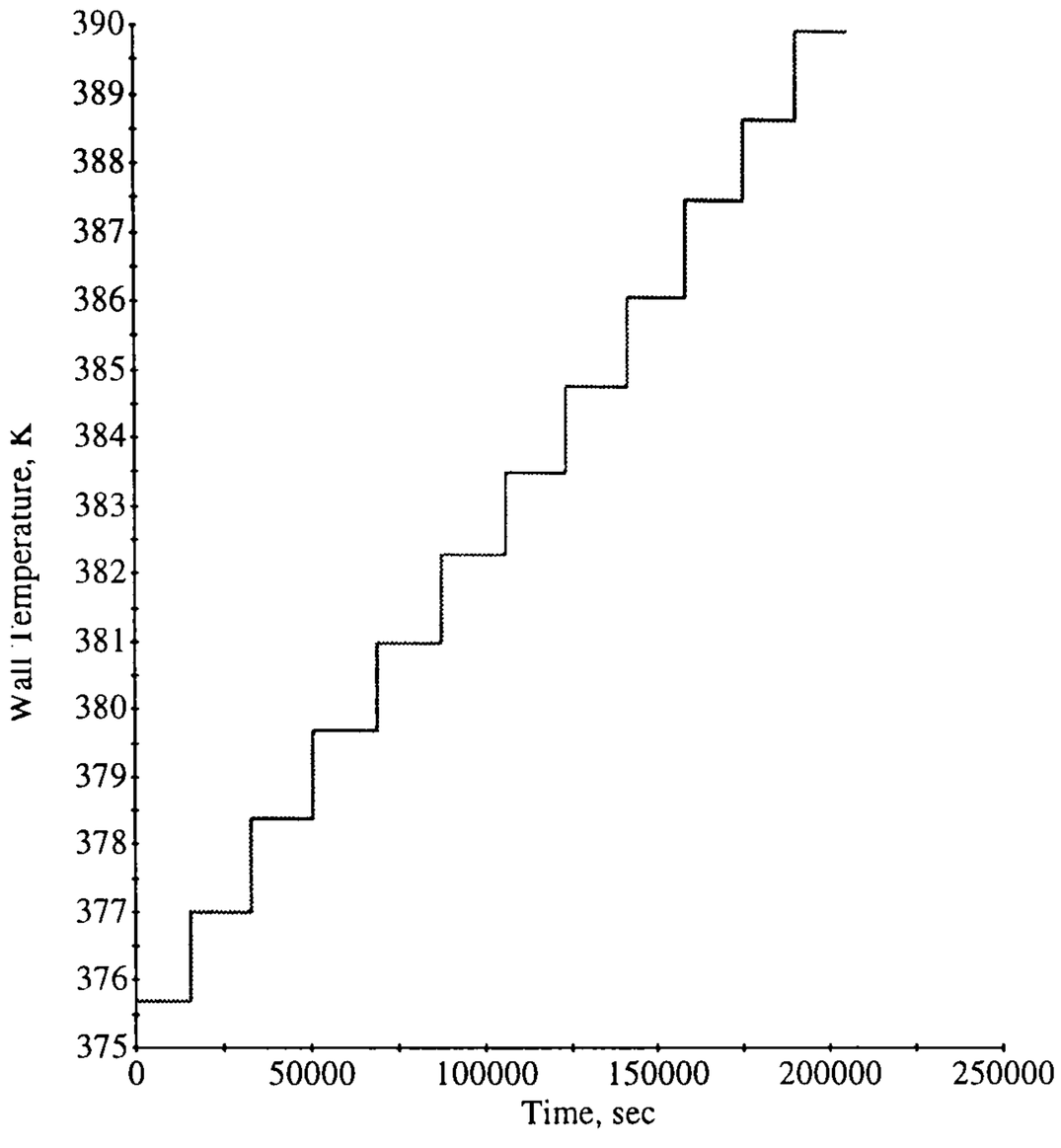


Figure 6.4: Optimal Control action (piecewise constant profile, 12 intervals)

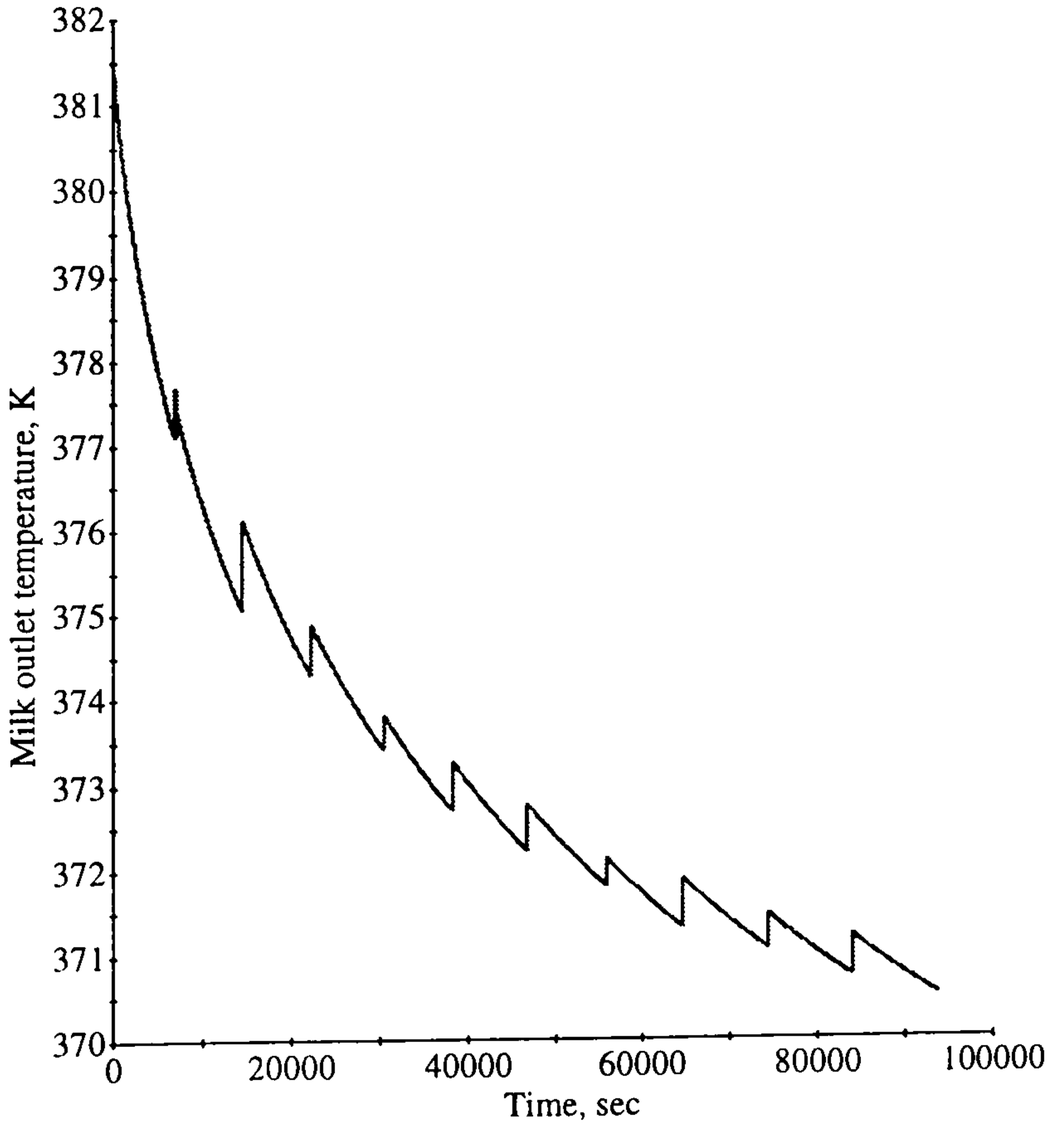


Figure 6.5: Milk outlet temperature profile under control for optimal co-current operation

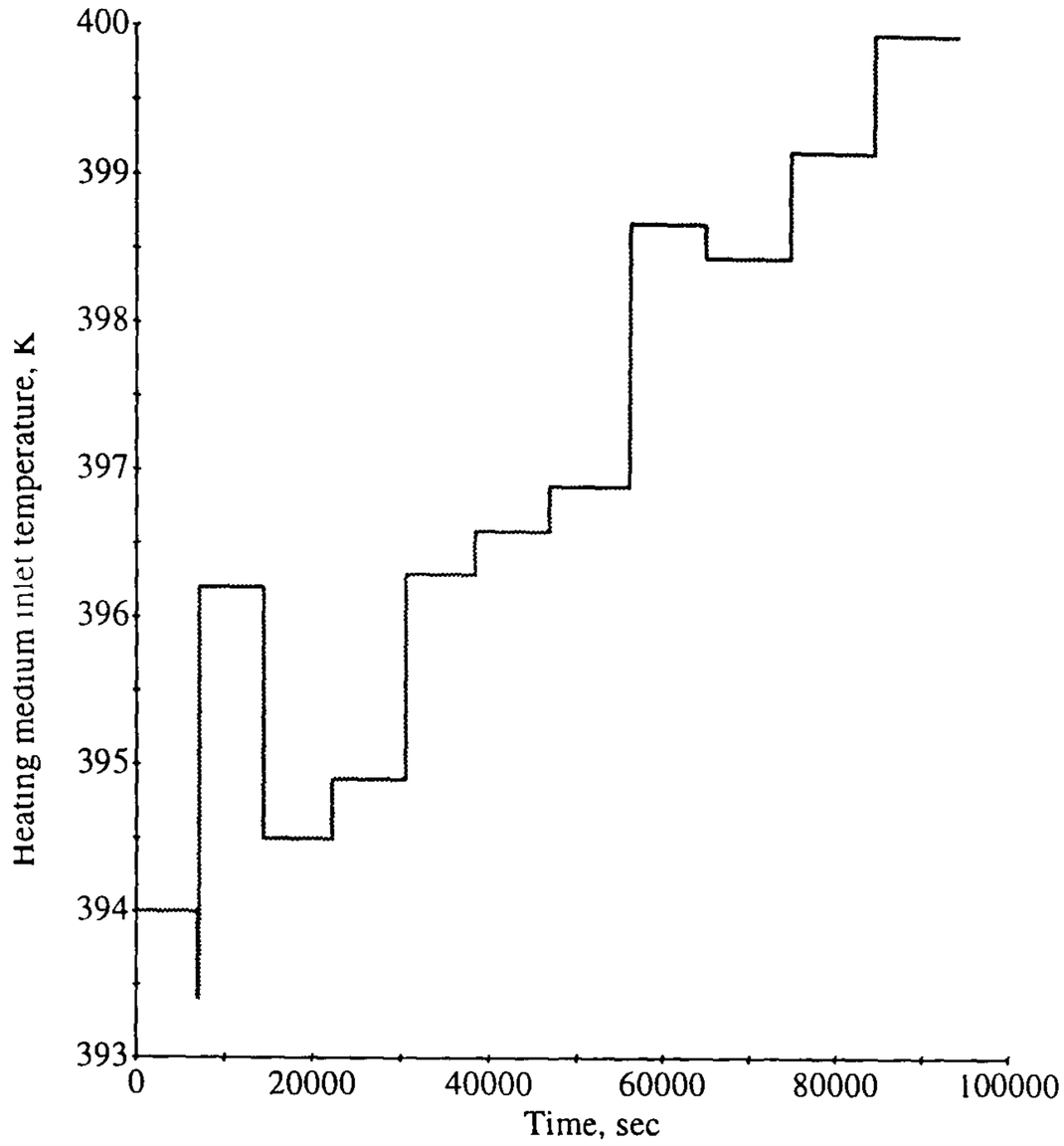


Figure 6.6: Heating medium inlet temperature profile for the co-current operation

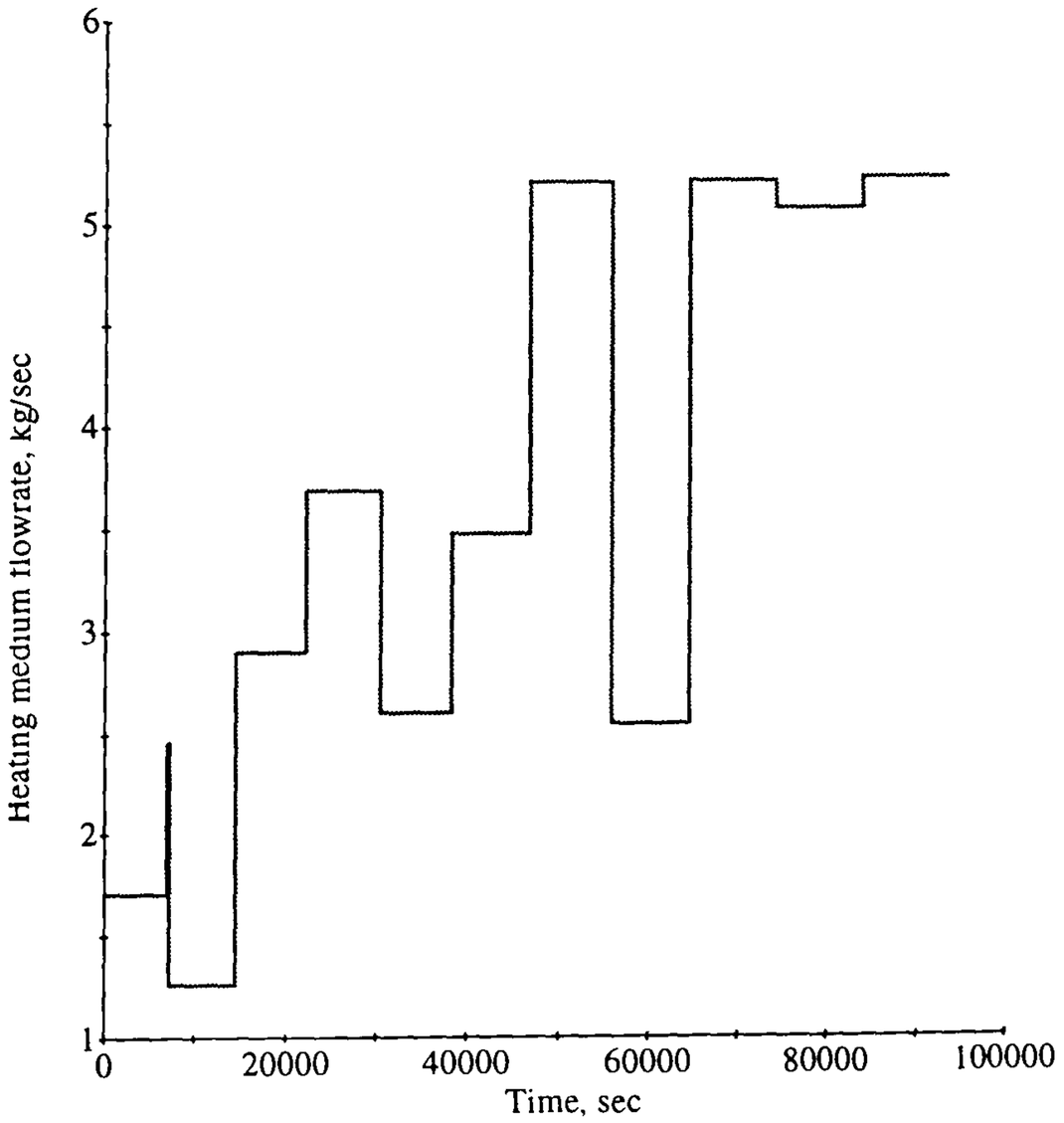


Figure 6.7: Heating medium flowrate profile for the co-current operation

Type of control	Number of control intervals	Heating time, hours (per cycle)	Objective function, $/yr	Diameter m	Length m
Piecewise constant	6	6.82	170000	0.018	13.6
Piecewise constant	12	7.84	158300	0.018	13.6

Table 6.5: Summary of optimisation results for the counter current operation

Type of control	Number of control intervals	Heating time, hours(per cycle)	Objective function, $/yr	Diameter m	Length m
Piecewise constant	12	6.3	182300	0.018	13.9

Table 6.6: Optimisation results for the counter current operation with one control variable

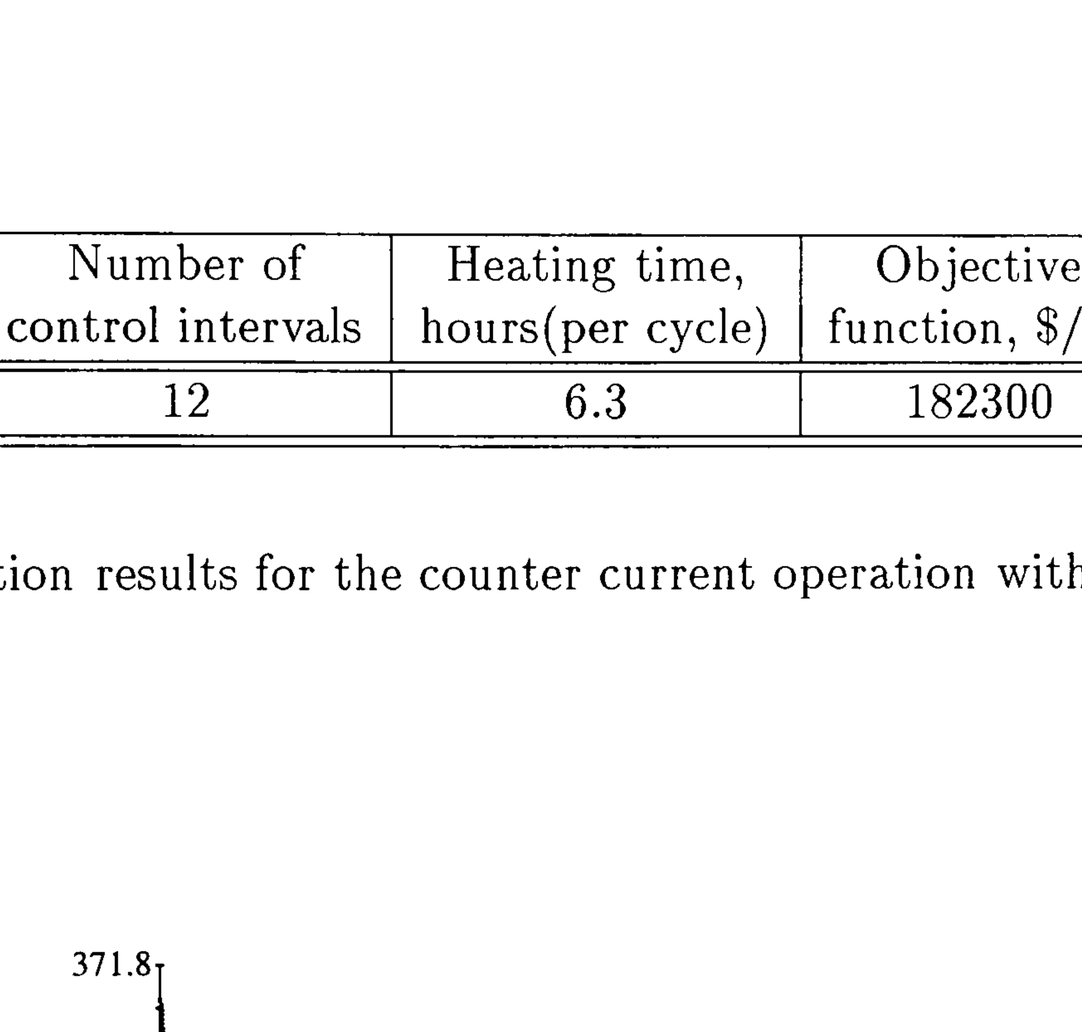


Figure 6.8: Milk outlet temperature profile under control for the counter-current operation

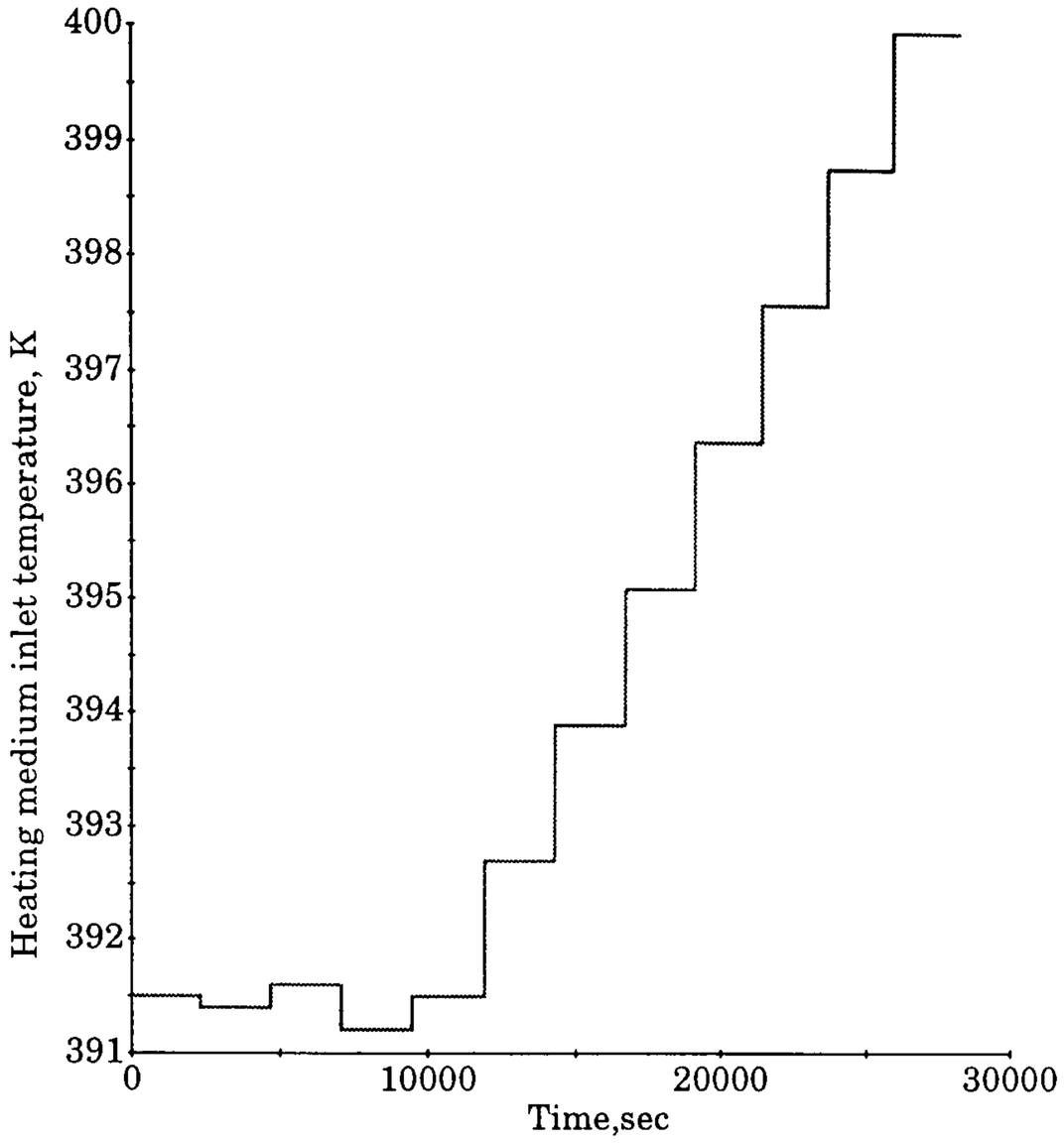


Figure 6.9: Optimal heating medium inlet temperature profile for the counter-current operation

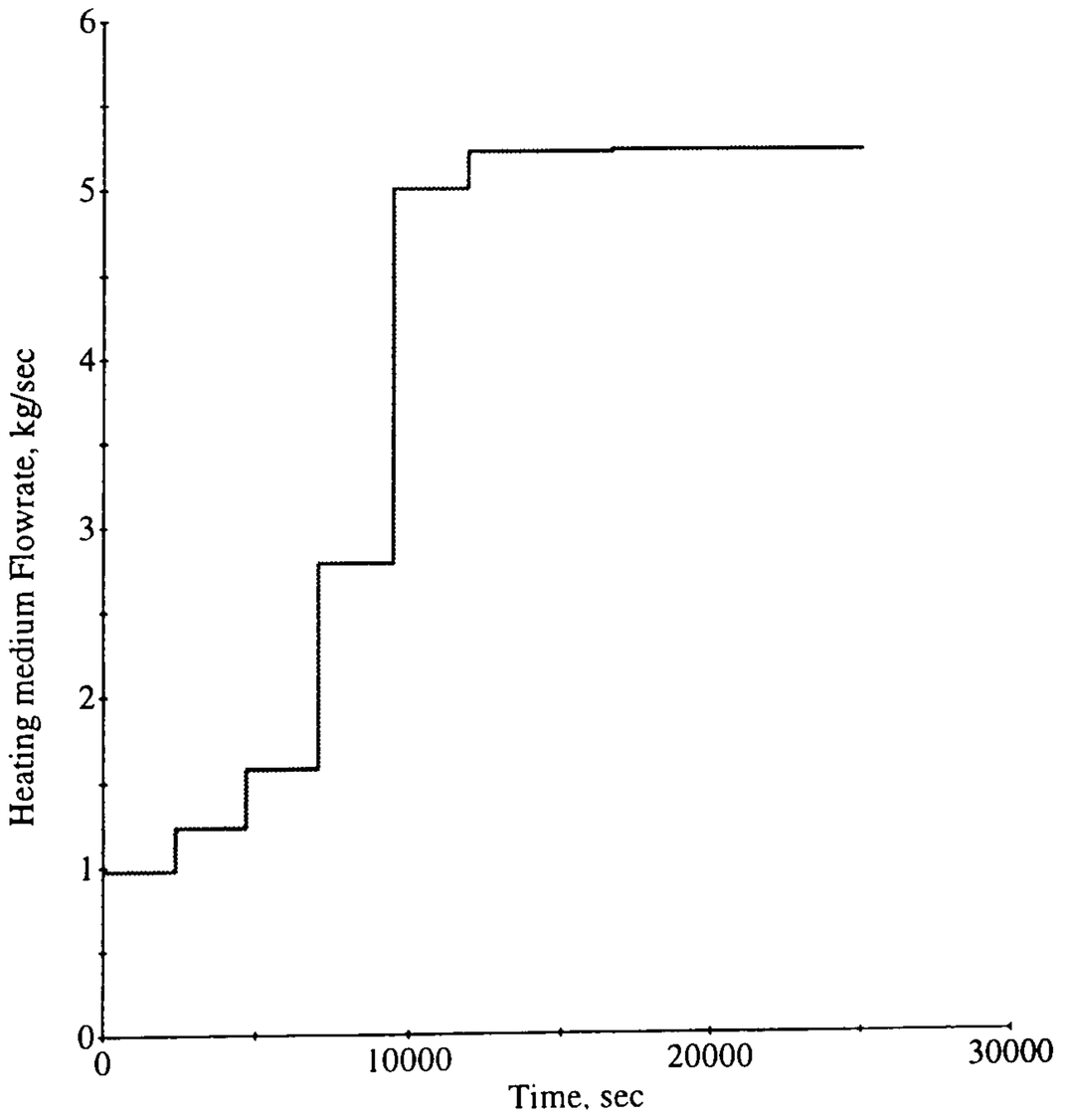


Figure 6.10: Optimal heating medium flowrate profile for the counter-current operation

6.6.4 Sensitivity Analysis of the Optimization Results

Sensitivity analysis is often useful in dynamic optimization problems to identify the sensitivity of the objective function with respect to some key parameters. The process model includes a number of parameters which are subject to uncertainty. This is especially true for parameters which are determined by experimental data such as the activation energies E_N and E_D in the fouling reaction scheme and for the constant β used to quantify the amount of fouling. Moreover, the initial milk protein concentration $C_{N,in}$ is also an uncertain parameter due to the variability of the raw milk concentration. Finally, the profit coefficient S_{net} can also be modified by market changes. In addition to the process parameters summarized above, the sensitivity with respect to design parameters such as tube diameter was also considered. The analytical values of the sensitivities are obtained directly from the DASOLV integrator (Jarvis and Pantelides, 1992) through the *gPROMS* modelling system.

The results of the sensitivity analysis are summarized in Table 6.7 and refer to the constant wall temperature case with piecewise constant control profile and 8 intervals. It is clear that the objective function is very sensitive to the tube diameter and the S_{net} parameter. The former affects both the heat exchanger capital cost and more importantly the amount of fouling, while the latter represents a considerable part of the objective function. The objective function is also quite sensitive to the milk composition $C_{N,in}$ and less to the parameter β. Finally it does not seem to change considerably with respect to the reactions activation energies E_N and E_D.

Parameter	Sensitivity of the objective function, absolute values
E_N	0.203
E_D	0.393
$C_{N,in}$	813.6
β	93.88
diameter	125700
S_{net}	156200

Table 6.7: Sensitivity analysis of the objective function for the constant wall temperature operation

6.6.5 Discussion

Based on the optimization results some general conclusions are summarized here:

- the interruption of the production has a great effect on the object function and represents approximately 65% of the total cost. The greater the heating time, the less the annual cost (Figure 6.2). It is clear that in all cases the optimisation procedure is trying to minimise downtime (*i.e.* maximise heating-cleaning cycle) under the specified constraints. It is worth noticing that in the work of Sandu and Singh (1991) it was emphasized that the energy increase due to heat exchanger fouling is about 8.3% of the total energy consumption and the associated costs represents only about 0.5% of the value of products shipments. Our results support these conclusions. The key issue is to minimise the production losses due to the interruption of the production (during the cleaning operation). Fryer (1989) also posed an important question. Are short but frequent cleans more efficient than infrequent but lengthly ones? From our results (under the assumptions and cost coefficients used) it is clear that lengthy heating cycles are more cost effective but control actions must be optimally chosen since they greatly affect fouling.

- the operability bottleneck in the optimal operation of heat exchangers under fouling is the availability of hot utilities in the plants. It seems that a higher maximum steam temperature would provide a more cost effective operation. Pressure drop limitation is also a bottleneck for the co-current and counter-current cases of operation.

- the constant wall temperature case results in longer heating times than the other two configurations. This is because milk is heated gradually (with respect to the axial domain) and at lower temperature and thus fouling is minimised (see also the analysis in chapter 4). The counter current operation results in shorter heating cycles where milk is heated quite rapidly with high mean temperature difference (counter current configurations provide maximum heat recovery) and thus fouling is favoured. These differences are apparent in Figures 6.3 and 6.5. The first scheme maintains milk temperature below 371.8 K while the second raises it up to 381 K.

- the heating medium inlet temperature is not an economic control variable if it is used on its own. The combination with the flowrate results in an improved control scheme. Control only by the flowrate does not seem to be feasible for constant inlet temperature. Similar conclusions were obtained by Yoon and Lund (1994) and Fryer and Slater (1986) in their experimental and simulation work respectively.

- the optimal tube diameter is relatively small (fixed at its lower bound) since high Reynolds number lead to longer heating cycles. As shown in the simulation results, substantial mitigation of fouling is achieved by increasing the Reynolds number. This validates

current industrial techniques for fouling mitigation. On the other hand, tube length in all cases is large enough to allow milk to be heated gradually. This also verifies current heat exchanger design techniques where most exchangers are oversized to mitigate the undesirable fouling effects. It is worth noticing however, that the optimal length of the tube is not at its upper bound. This shows that if larger heat exchangers are to be used the benefits from the extra fouling mitigation would be counterbalanced by the additional capital expenditure.

In general, the optimization approach presented in this work determines the optimal time programs for the control variables. These time programs can then be implemented in the control system of the plant to define optimal on-line control policies. However, extra work is required for the development of an integrated on-line approach.

6.7 Concluding Remarks

This chapter addresses the optimal design and operation of heat exchangers under milk fouling. The dynamic optimisation approach adopted, based on control vector parameterization, identifies simultaneously the optimal design parameters and operating policy of the exchanger. From the results it is clear that the cost factor due to the interruption of production (downtime) is dominant and the heating cycle should be as long as possible. The constant wall temperature configuration provides the best economical results compared with the co-current and counter-current operation. However, it should be emphasized that in practice, the implementation of a uniform wall temperature configuration may be technically difficult. In all cases, the main operability bottleneck is the hot utilities availability. The designs arising from optimization are characterized by small tube diameters and long heat exchangers. Control schemes based only on the heating medium inlet temperature were proved to be not economical while control only by the heating medium flowrate seems to be ineffective.

Beyond these practical conclusions the work also demonstrates the increasing ability to solve dynamic optimization problems involving fairly large models (described by thousands equations) with many interacting decisions and constraints. Moreover, the importance of using accurate dynamic models for this study cannot be overemphasized. This is especially true given the tight process economics and the tight operating constraints under which a pasteurizer operates.

The solution of the optimisation problems required large computational costs (in the range of 8-30 CPU hours on a SUN Ultra workstation). This is due to the high complexity and the nature of the models described by integral, partial differential and algebraic equations. However, current computer developments towards parallel architectures will provide a way to reduce dramatically such computational costs in the near future. Finally, it is worth pointing out that, because of the use of local optimization algorithms for the solution of the NLP, the global optimality of any solution obtained with our approach cannot normally be guaranteed. This is a common deficiency of optimization-based design methods which can only be overcome by the adoption of global optimization techniques.

6.8 Nomenclature

$cycle$ duration of the heating-cleaning cycle, secs

CC total annual operating cost in $\$/yr$

C_{ps} heating medium specific heat capacity, $J/(kg \cdot K)$

$C_{p,milk}$ specific heat capacity of milk, $J/(kg \cdot K)$

C_{NaOH} cost of NaOH for the cleaning operation, $\$/t_{clean}$

C_{ef} cost of the effluent disposal after the cleaning operation, $\$/t_{clean}$

C_{steam} cost of steam for the cleaning operation, $\$/t_{clean}$

$C_{p,milk}$ milk specific heat capacity, $J/(kg \cdot K)$

C_{pump} pumping cost in $\$/s$

C_{steam2} cost of steam for the heating operation, $\$/cycle$

C_{HE} heat exchanger operating cost, $\$/yr$

C_{losses} production losses, $\$/cycle$

CO_{water} water cost for the cleaning operation, $\$/t_{clean}$

d heat exchanger diameter, m

ΔP_s shell side pressure drop, psi

h_k duration of control interval k

l_k^{max} maximum duration of control interval k

l_k^{min} minimum duration of control interval k

L heat exchanger length, m

NCL number of heating and cleaning cycles per year

m_{steam} steam flowrate for the heating operation, kg/s

T_w wall temperature, K

T_s^{in} heating medium inlet temperature, K

T_s^{out} heating medium outlet temperature, K

T_m^{out} milk outlet temperature, K

T_m^{in} milk inlet temperature, 333 K

t_{clean} cleaning time, s

t_{heat} heating time, s

u_k parameterized control variable over interval k

w_{milk} milk flowrate, 0.25 kg/s

w_s heating medium flowrate, kg/s

Greek Letters

δ deposit thickness

ζ normalized axial domain

Chapter 7

Optimal Cleaning policies in Heat Exchanger Networks under Fouling

This chapter addresses the problem of optimising the short term cleaning scheduling in a special class of heat exchanger networks (HENs). A salient characteristic of this problem is that the performance of each heat exchanger decreases with time, due to fouling, which can then be restored to its initial state by performing cleaning operations. A mixed integer non-linear programming (MINLP) model is first presented incorporating general fouling profiles. This model is then linearized to a tight mixed integer linear programming (MILP) model which can be solved to global optimality. A number of complex heat exchanger networks examples is presented to illustrate the applicability of the proposed models together with comparative performance between the MINLP and MILP models.

7.1 Introduction

Fouling is the major unresolved problem of significant interest in the field of heat exchanger design and operation. Fouling affects nearly every plant relying on heat exchangers for its operation and introduces costs which are ultimately related to the conservation of energy, operation and capital investment. The common practice to mitigate fouling is to implement Cleaning-In-Place (CIP) operations. This is especially applicable to processes affected by rapid fouling, such as that caused by milk or fruit juice processing in the food industry.

Several methods for the optimization of cleaning schedules for a single heat exchanger have been proposed in the literature. Epstein (1979) presented an analytical method for the

calculation of the optimal evaporator cycle with scale formation. In a similar fashion, Casado (1990) used a detailed cost model to calculate the optimal cleaning cycle of a heat exchanger under fouling by exploring the major operating trade-offs. Based on this work, Sheikh *et al.* (1996) presented a reliability-based cleaning strategy by incorporating uncertainty in a linear fouling model. The effect of an acceptable risk level on the cleaning schedules was illustrated with a single heat exchanger used in a crude oil preheat train. In the same context, Zubari *et al.* (1992) and Zubari *et al.* (1997) considered different stochastic fouling models. Ahmad (1997) proposed a condition monitoring system to predict cleaning schedules for a single heat exchanger under milk fouling. The main drawback of these approaches is that they are restricted to a single equipment item. However, in process plants complex HENs exist with many interacting processing units. In that case, analytical methods for the determination of cleaning policies cannot be applied. The state of each equipment item (in operating or cleaning mode) affects the overall network performance.

Motivated by the above practical industrial problem, the simultaneous considerations of scheduling and process operations aspects seems to be promising. Scheduling and planning of batch and continuous plants has received considerable attention over the the last decade (Sahinidis and Grossmann, 1991; Kondili *et al.*, 1993). Several mathematical programming scheduling formulations have been presented using either continuous or discrete time representations (see for comprehensive reviews Reklaitis, 1992; Pantelides, 1994; Shah, 1998)

The exploitation of heat integration in the operation of multipurpose plants taking into account its interactions with production scheduling was considered by Corominas *et al.* (1993) and Papageorgiou *et al.* (1994). Both works assumed that the plant equipment performance remains unchanged over the time horizon.

Maintenance considerations in the scheduling of continuous and batch plants have recently received increasing attention. Dedopoulos and Shah (1995) presented a mathematical model for coordinating scheduling production and preventive maintenance activities within a multipurpose plant. They also extended this work in the long term combined production/maintenance planning problem, where the effect of equipment failures in the plant was taken into account (Dedopoulos and Shah, 1996). Thomaidis and Pistikopoulos (1995), and later Vassiliadis and Pistikopoulos (1998) explored the effect of maintenance considerations in the optimal operation of process plants under stochastic uncertainty. Maintenance decisions were also considered by Zhu *et al.* (1997) in the optimal design and scheduling of reverse osmosis networks under membrane fouling and scaling. The problem was formulated as an MINLP model and a num-

ber of operating constraints was incorporated. Recently, Jain and Grossmann (1998) studied the scheduling of multiple feeds on parallel units whose performance decreases with time and therefore requires shutdown for maintenance after regular intervals. An MINLP model was developed for determining the optimal cyclic schedules. The model yields a tight formulation and a proposed branch and bound method proved to be very effective for solving the example problems. Application in ethylene plants was the major motivation for this work. Muller-Steinhagen (1998) proposed an integrated approach for developing alternative fouling mitigation strategies based on both experimental and modelling work. The solution provided by the above approach is likely to be sub-optimal as detailed operating constraints (scheduling) and thermal interactions (energy balances) between equipment items were not considered. Finally, the objective function used does not include significant cost factors such as cost of cleaning and utilities.

In the previous chapter, we already presented a comprehensive method for the optimisation of production cycles of a single heat exchanger subject to time varying fouling, using detailed dynamic models. In this chapter, we consider the short-term cleaning scheduling of complex heat exchanger networks under fouling. Dairy plants constitute the motivation of this work where fouling is a severe problem with dramatic consequences such as significant production losses and increased energy requirements. In addition, product quality requirements are likely not to be met when utility provision bounds are present. Thus, CIP operations are necessary to be carried out every 4-8 hours so as to restore each heat exchanger area back to its original state. It is evident that the appropriate cleaning synchronization (scheduling) of multiple heat exchangers can have significant effects on the resulting process operating costs as there is a clear trade-off between a fixed cost term depending on the frequency of CIP operations and a variable cost term which is a function of the preceding heating time.

The problem is approached in a systematic fashion. First, a formulation for serial HENs is considered. Then, a new formulation for parallel arrangements of heat exchangers is proposed. Finally, we show how more complex arrangements can be built from these basic blocks. The case studies presented focus on rapid fouling arising in milk heat treatment process. The simulation results presented in chapter 4 and 5 are used to construct simple algebraic models in order to quantify the decaying performance of each exchanger. Special operating features of this problem (*e.g.* variable cleaning cost) are modelled in detail. An economic objective function is used to minimise the total cost incurred due to fouling taking into account utility provision and fixed and variable cleaning costs.

7.2 Description of the Problem

The milk sterilization process is the source of motivation for this work. This milk heat treatment is of critical importance as it is required to safeguard public health by destroying all pathogenic bacteria and ensuring good quality of final dairy products (Hall, 1976). When milk is heated, a deposit of milk solids is gradually formed in the heat exchanger surface as result of its instability (Fryer and Slater, 1987). Although this deposit is not sufficient to affect milk composition significantly, it results in hydraulic and thermal disturbances and cleaning operations have to be carried out in regular periods in order to restore the heat transfer coefficient to its original value.

The overall performance of each heat exchanger decreases dramatically with time as the heat transfer resistance increases due to the formation of the milk deposit. If the heating medium temperature is kept constant (*e.g.* high pressure steam) then the milk outlet temperature decreases and eventually violates sterilization requirements (see chapter 4). Thus, CIP operations are necessary to be applied to restore equipment performance. Alternatively, in order to satisfy sterilization requirements (*e.g.* constant milk outlet temperature) the heat exchanger can be operated by increasing the heating medium temperature (*e.g.* steam or hot oil) resulting in higher utility cost. Moreover, if the exchanger operates in production mode for a long period of time then the cleaning cost becomes larger since cleaning time increases with heating time due to larger deposit mass. In general, the profitability of the plant decreases with time and each exchanger has to be shut down in order to be cleaned so as to restart operation at a higher performance level. Furthermore, every time there is a changeover between production mode and cleaning mode all pipes must be flushed and rinsed, thus resulting in significant loss of valuable product. The time between successive cleaning operations must therefore be determined by considering the trade-off between cleaning costs, production losses, utility costs and also the state of each exchanger in the network.

In dairy plants, Plate-Heat-Exchangers (PHEs) are widely used for pasteurization and sterilization purposes. Due to fouling, the operation of the unit is interrupted and thus significant production losses take place. As it was illustrated in chapter 5 fouling is not uniform over different parts of the PHE and only a few channels are mainly responsible for the total interruption while other channels suffer less severe fouling and thus their operation can continue for longer processing times. Conceptually, it is possible to view a PHE as a complex arrangement of individual channels, each modelled as a shell and tube heat exchanger. It is then possible to think of an operation where different parts (channels) of a "smart" PHE operate in a produc-

tion mode while others are being cleaned at the same time. Thus, the optimal synchronization of cleaning and heating operation of different channels subject to product quality/sterilization requirements and utility availability, while maintaining continuous production, is of great interest. This is a generic representation which can efficiently capture the original PHE structure. It is then clear that each tubular exchanger may have different fouling rate according to the fouling state of each PHE channel.

Although the approach presented in this chapter is implemented for the synthesis of cleaning policies in PHEs, the models presented and solution approach are entirely general and applicable to various HENs subject to any type of fouling profile (*e.g.* in refineries as in Jain and Grossmann (1998)), to reactor networks where the catalyst undergoes deactivation with time, to reverse osmosis networks (Zhu *et al.*, 1997) etc. Next we describe a small quantitative example that highlights the underlying trade-offs as well as the need for systematic optimization approaches.

7.3 Motivating Example

Consider a small network with two heat exchangers in a serial arrangement with different fouling rates (see Figure 7.1). Each heat exchanger can be bypassed for cleaning if required. Steam is assumed to be the heating medium with a maximum available temperature in the plant of 600 K. The steam temperature is manipulated appropriately to ensure that the milk outlet temperature is kept above a specified bound of 369.5 K (quality requirements). The processing fluid flowrate is kept constant.

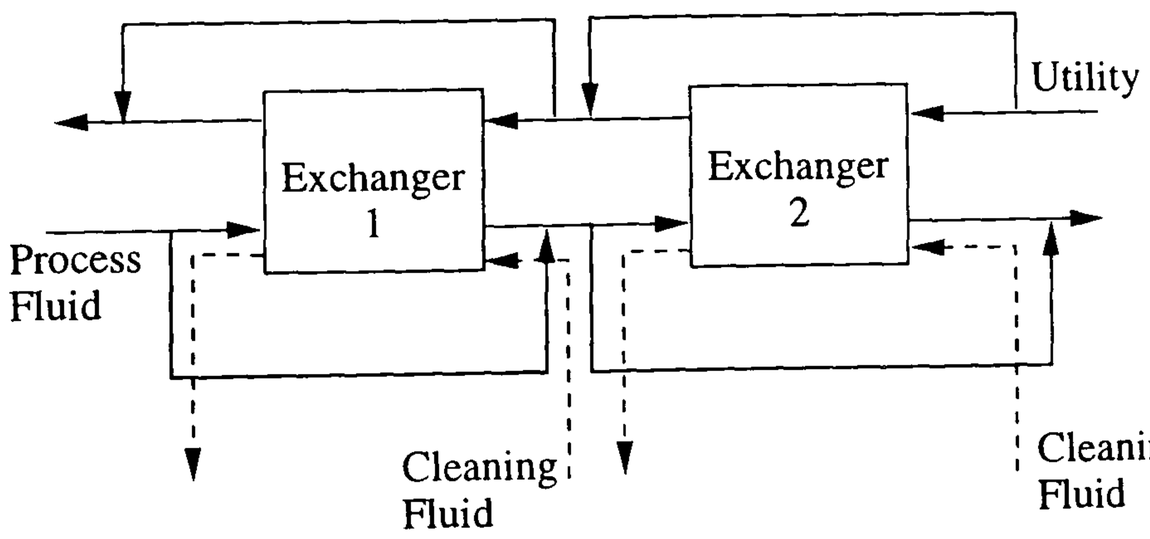


Figure 7.1: Serial Heat Exchanger Network with two processing units

We examine two alternative operating policies over a time horizon of 24 hours: (i) frequent and (ii) infrequent cleaning of each heat exchanger. Two feasible cleaning schedules for case

(i) and (ii) are shown in Figures 7.2 and 7.3, respectively.[1] For both cases the performance of each exchanger (*i.e.* the overall heat transfer coefficient) is assumed to decrease linearly with time. The cleaning cost comprises a fixed term (0.1 rmu^2) and a variable term (0.11 rmu/s) which is a function of the preceding heating period. The utility cost is assumed to be a linear function of its temperature (0.7 rmu/K). The resulting total operating costs for cases (i) and (ii) are 25500 rmu and 26100 rmu respectively.

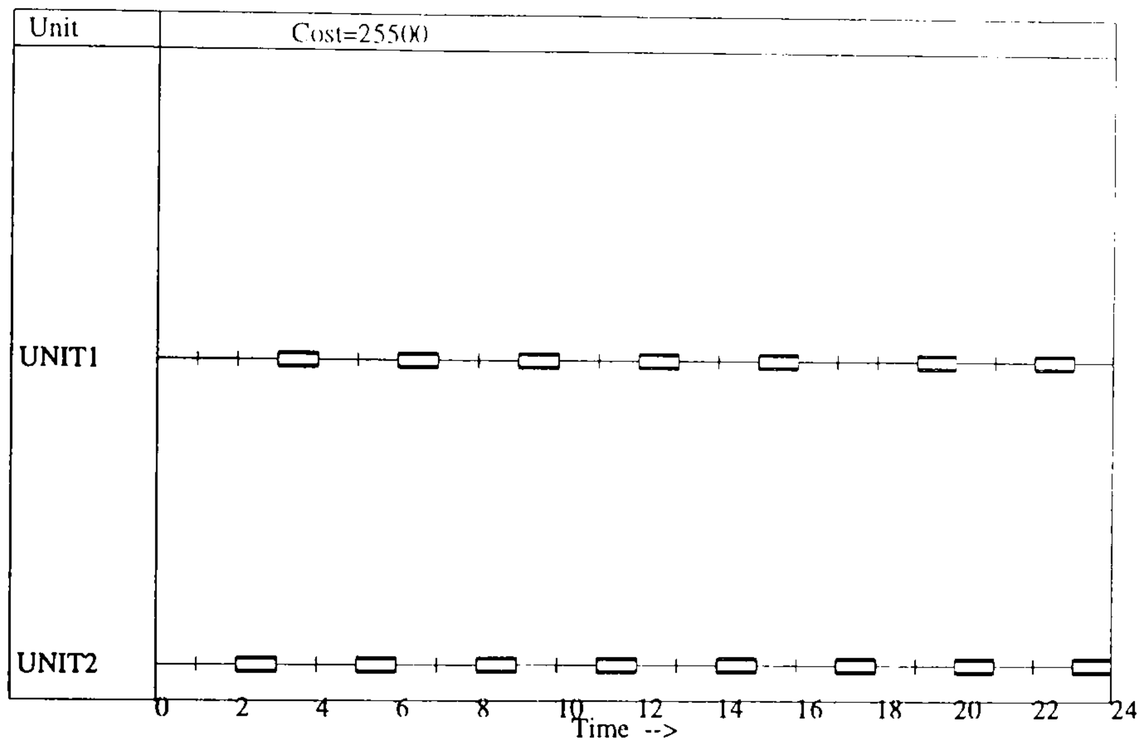


Figure 7.2: Schedule with frequent cleaning policy for two serial exchangers

However, another feasible schedule is to operate the network as shown in Figure 7.4 which involves a moderate number of cleaning operations. For this case, the total cost is 20400 rmu yielding up to 21% savings over the original operating scenarios. Clearly, there is a trade-off between frequent and infrequent cleaning and related utility costs. Moreover, the timing and synchronization of cleaning operations is also very important since their cost does not only depend on fixed terms but also on variable terms based on the preceding heating period. In addition, the timing of cleaning operations should be determined in such a way that the temperature of the final product is kept above a given lower value over the entire horizon of interest. The relation between the operating cost and the total number of cleaning tasks is

[1]The single horizontal bars in the figures declare unit operation (heating) while the double horizontal bars refer to cleaning tasks.

[2]rmu≡ relative money units

shown in Figure 7.5. We can notice that the operating cost decreases initially with the number of cleaning tasks because both variable cleaning and utility costs decrease, then reaches a minimum (optimal solution), and finally starts increasing as the fixed cleaning costs become dominant. The optimal solution (20400 *rmu*) was obtained using the model proposed in this chapter by performing 12 cleaning tasks.

The above analysis involved only two exchangers. If there are more exchangers with complicating network arrangements and operating limitations, the trade-offs are considerably more complex. In particular, an upper bound on the utility temperature may exist due to its availability in the plant. For example, if the steam is available up to 405 K, then the optimal schedule involves 14 cleaning tasks with a total cost of *rmu*21100, which is more expensive than the previous optimal solution without utility limitations. However, it should be noted that the final cost is not as high as in cases (i) and (ii) since the allocation of cleaning tasks is determined optimally by the model rather than based on arbitrary decisions.

In conclusion, the aim of this work is to develop mathematical models and a solution procedure that captures these complex interactions and trade-offs as well as to determine the optimal cleaning policies of complex HENs by optimizing a suitable economic criterion.

7.4 Problem Statement

For the sake of clarity we focus the discussion on cleaning scheduling of HENs under milk fouling over a short time horizon of interest (typically, 1 day). However, the models presented can be applied to any type of equipment with time-decaying behaviour.

The problem can be stated as:

Given:

- Fouling data (*e.g.* heat transfer coefficient profiles) for each heat exchanger
- time horizon of interest
- structure (*e.g.* serial) of the HEN
- utility bounds
- product quality requirements

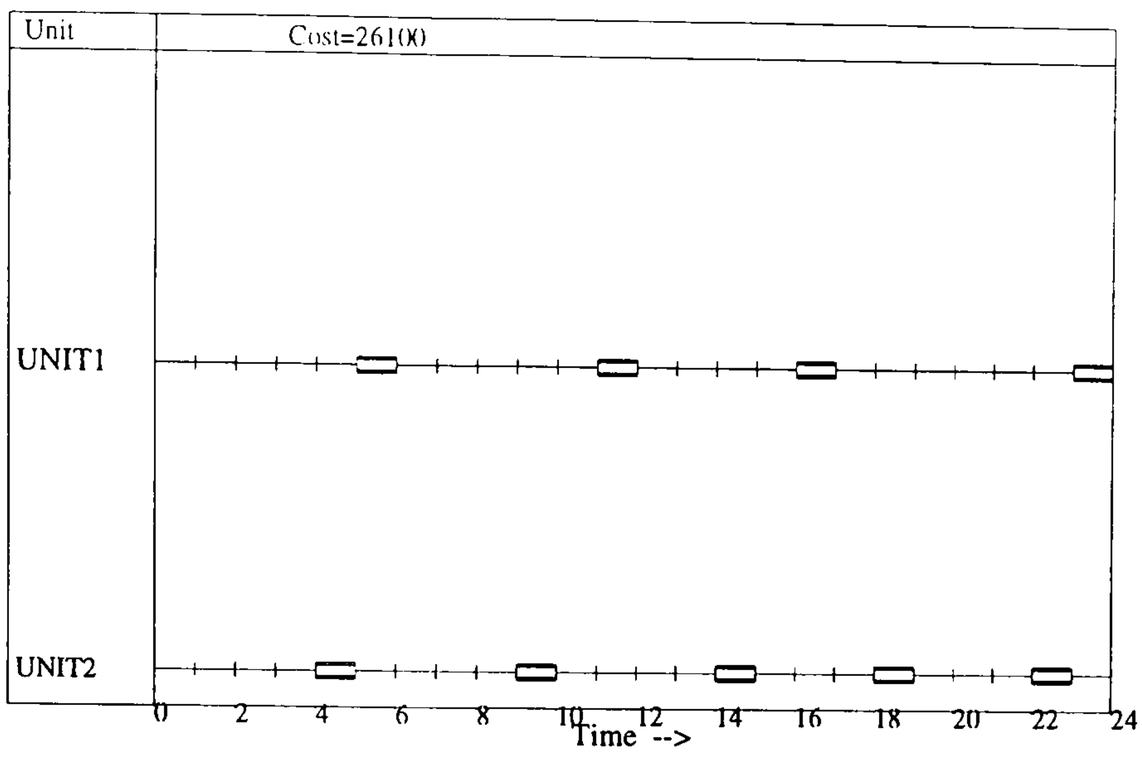


Figure 7.3: Schedule with infrequent cleaning policy for two serial exchangers

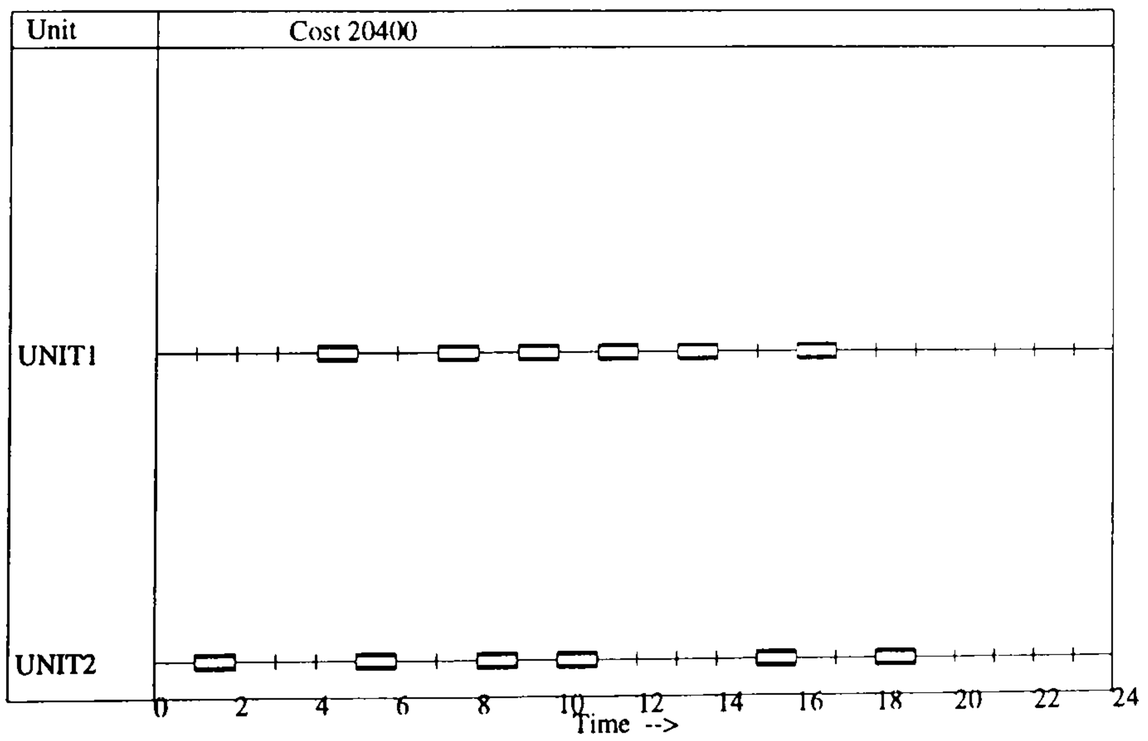


Figure 7.4: Optimal cleaning schedule for two serial exchangers

Determine:

- cleaning schedule
- utility utilization profile

So as to optimize an economic performance criterion.

It is assumed that the milk flowrate, F_m, is constant and the fluid is processed in a network which comprises a given number of heat exchangers ($i = 1..N$). As mentioned in the previous section, the fouling effects are different from exchanger to exchanger and consequently each of them is characterized by its own fouling profile. A maximum allowable (critical) value of the deposit mass, δ_i^{crit}, is taken into account to avoid pressure drop violations. This critical value predetermines the maximum operation time for each exchanger after which no heating is allowed and a cleaning task must take place. The heating medium of the plant (*e.g.* steam or hot oil) is usually constrained by a maximum available temperature. The cost of each cleaning operation includes two terms; a fixed term each time a cleaning task is performed (this includes for example, product losses upon changeover) and a variable term as a function of the preceding heating time.

A single hot utility is assumed to be available within a continuous temperature range while the utility cost is a linear function of its temperature level. The overall heat transfer coefficient, $U_i(t)$, in each heat exchanger i can be characterized by general decaying profiles (typical examples are exponential or linear decaying). It is assumed that at the beginning of operation the heat transfer coefficients have their largest values corresponding to *clean* exchanger conditions.

As illustrated in Figure 7.6 each exchanger includes two bypasses (one per stream) which are activated simultaneously according to current operating mode (*i.e.* heating or cleaning). It is assumed that each heat exchanger can be cleaned independently when required (cleaning circuits are not shown here and subsequent figures for simplicity). If the exchanger operates in the heating mode then both bypasses are forced to have zero flows. When the exchanger is cleaned then the process bypass flowrate equals the milk flowrate. In practice, activating these bypasses may be achieved by by using valves or similar mechanical devices which open and close during heating and cleaning, respectively. It is also assumed that cleaning capacity is not limited.

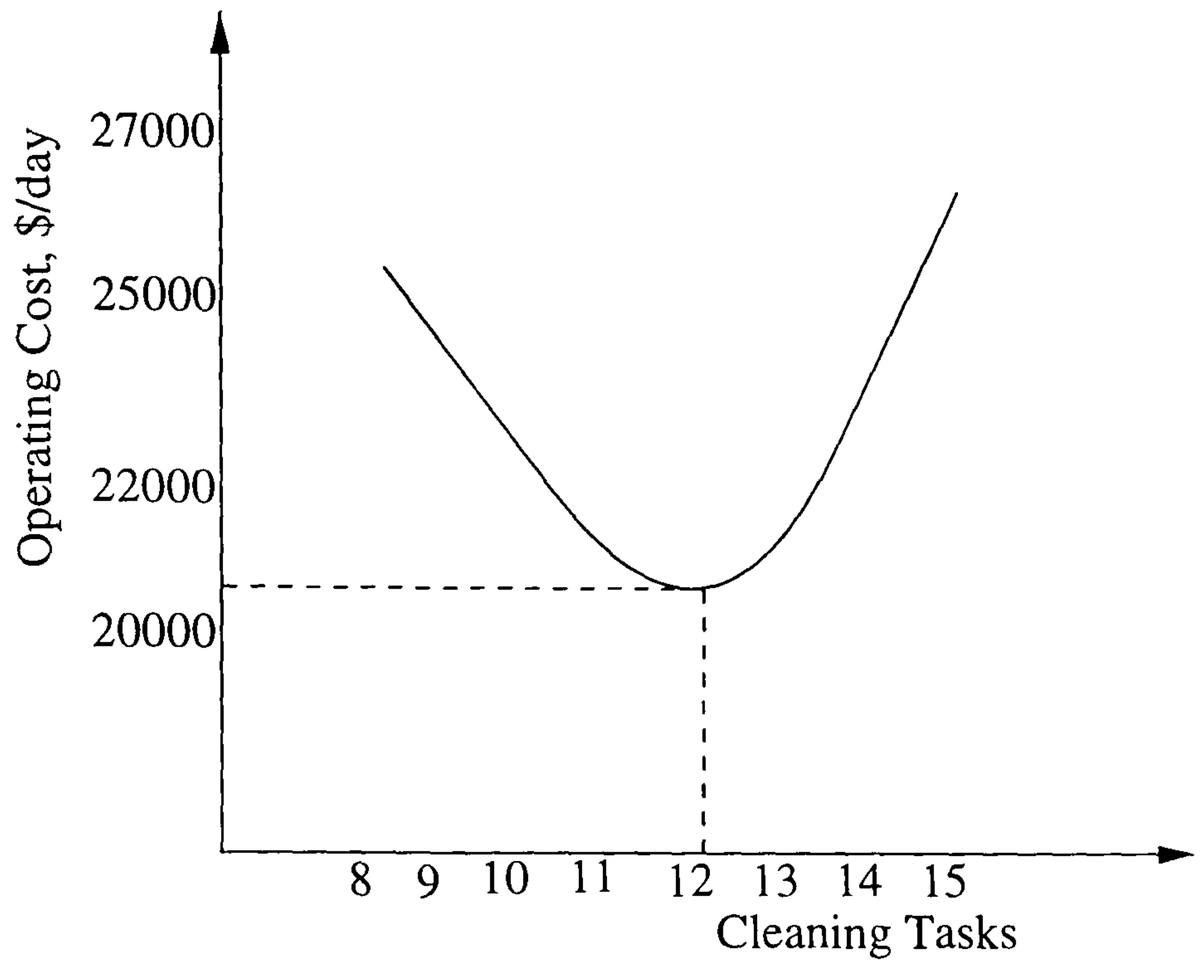


Figure 7.5: Operating cost as a function of the number of cleaning tasks

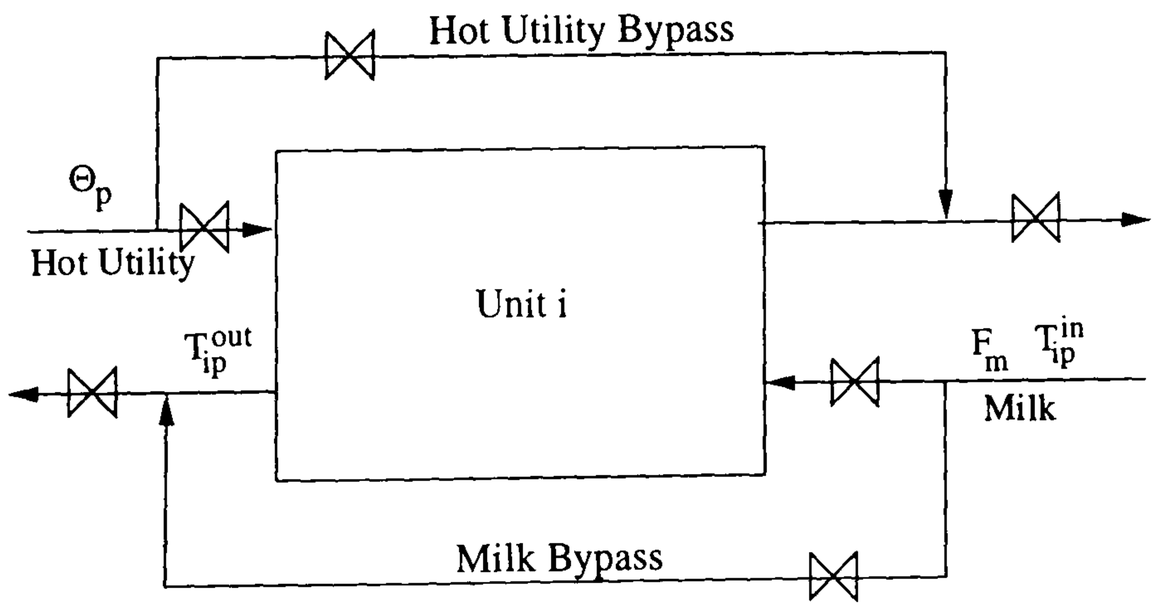


Figure 7.6: A unit representation with its bypasses for a serial HEN

It should be noted that the problem considered here is fairly general. Perhaps one of the limitations is that each heat exchanger is characterised by its own cleaning task (number of time periods during cleaning). In general, the duration of the cleaning operation may be a function of the preceding heating time. However, in this work this is approximately captured by taking into account the variable cleaning cost indicating that a more expensive and intensive cleaning operation is required as the preceding heating time increases. Furthermore, the feasibility of the mechanical aspects of the implemented cleaning policies is not considered. The approach for serial HENs relies on the existence of bypasses for each processing exchanger which may not exist in practice and their installation is thus required. Moreover, the dynamics of start-up and shut down is not considered in this work. Finally, we assume that the inlet flowrate is equally split to all parallel exchangers (see sections 7.6 and 7.7).

We adopt here a constructive approach. First, formulations for the basic building blocks related to serial and parallel arrangements of heat exchangers are studied. Then, we show how more complex networks can be described using these basic building blocks.

7.5 Serial Heat Exchanger Network Case

7.5.1 Mathematical Formulation

This case is concerned with a serial arrangement of heat exchangers (see Figure 7.7). In order to facilitate the mathematical description of the problem, the time horizon of interest is discretized into P periods (time intervals) with fixed duration. Piecewise constant profiles are assumed for all variables (*e.g.* heat transfer coefficients, temperatures *etc.*) as illustrated in Figure 7.8.

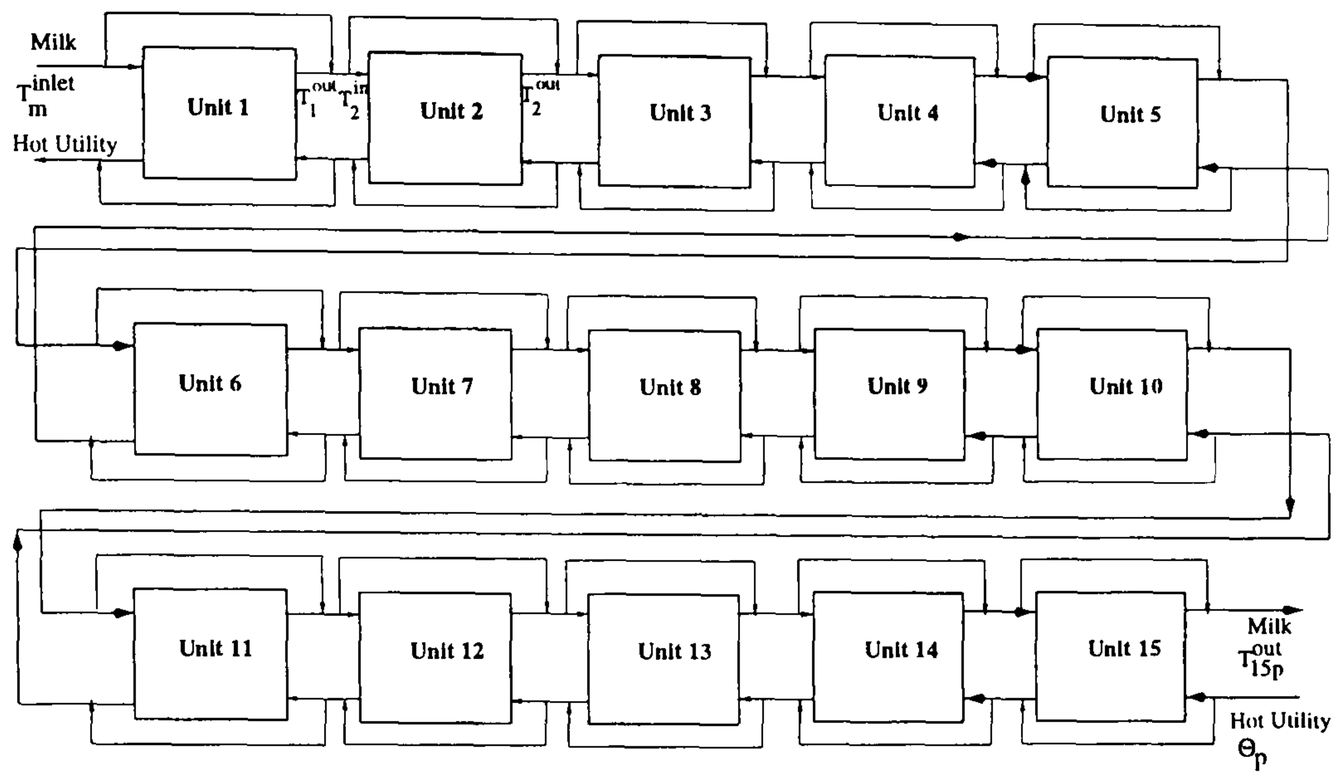


Figure 7.7: Serial heat exchanger network

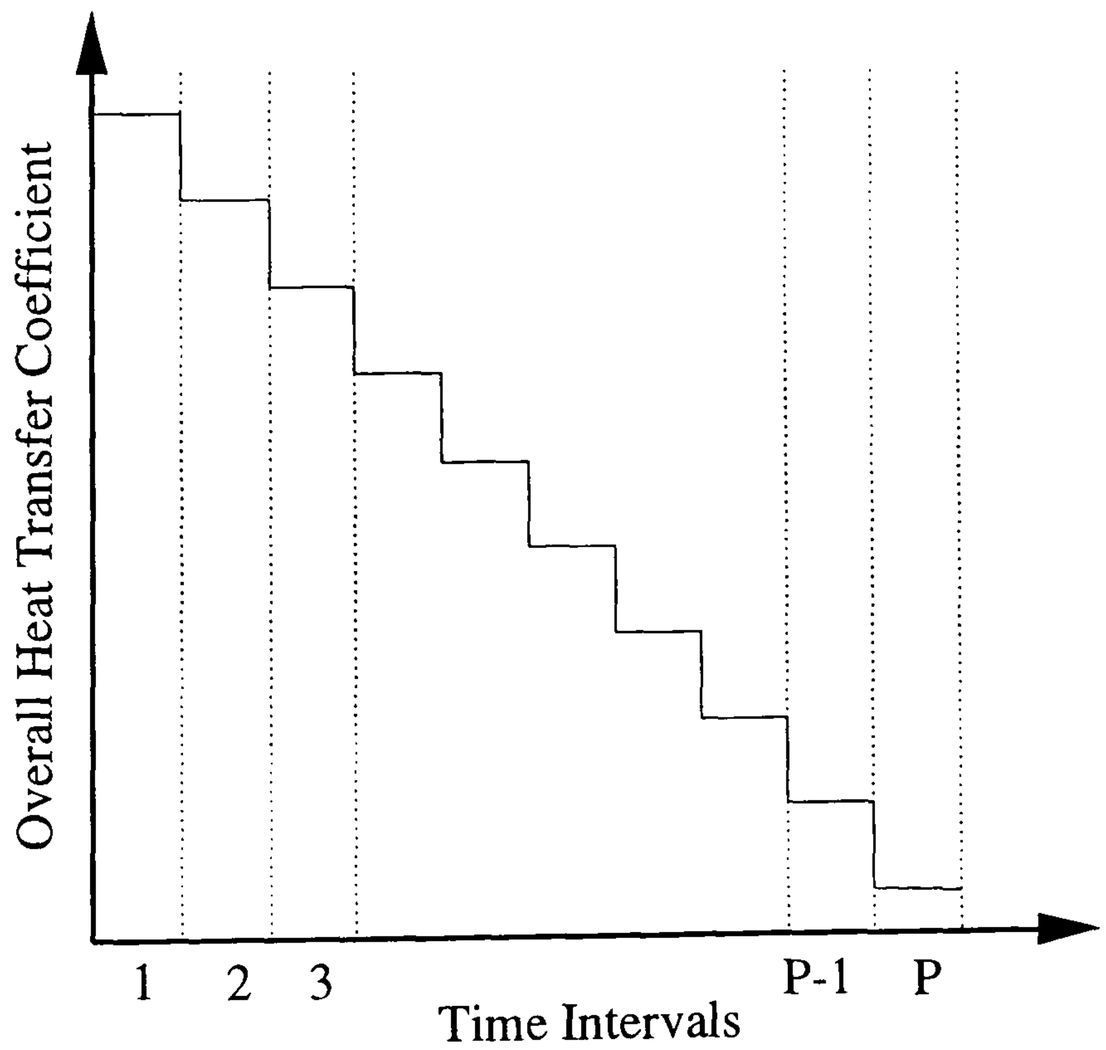


Figure 7.8: Piecewise constant approximation of the heat transfer coefficient

For the purpose of our analysis, the following notation is used:

Indices:

i heat exchanger

p, θ time period

Parameters:

N total number of heat exchangers in series

P total number of time periods

T_m^{inlet} process fluid inlet temperature, K

F_m process fluid flowrate, kg/s

Cp_m process fluid specific heat capacity, $J/(kg \cdot K)$

T_m^L lower bound on the milk outlet temperature, K

Each exchanger $i(i = 1..N)$ is characterized by:

A_i heat exchange area, m^2

ΔT_i^L minimum mean temperature difference, K

ΔT_i^U maximum mean temperature difference, K

Q_i^U maximum heating load, KJ/s

$\delta T_i^{\min}$ minimum temperature difference between process fluid and heating medium, K

$\zeta_{i\theta}$ value of the heat transfer coefficient after θ periods of operation, $W/(m^2 \cdot K)$

$\bar{C}_{ip}$ fixed cleaning cost coefficient over period p, rmu

$\hat{C}_{ip}$ variable cleaning cost coefficient over period p, rmu/hr

δ_i^{crit} critical deposit mass, kg/m^2

τ_i maximum heating period duration

The hot utility is characterized by:

C_p cost coefficient, rmu/K

Θ_p^L minimum temperature, K

Θ_p^U maximum temperature, K

The following *binary* variables are then introduced in the mathematical model:

$$y_{ip} = \begin{cases} 1, & \text{if exchanger } i \text{ operates in heating mode over period } p \\ 0, & \text{otherwise} \end{cases}$$

$$X_{ip\theta} = \begin{cases} 1, & \text{if the last cleaning of exchanger } i \text{ occurred in period } p-\theta \\ 0, & \text{otherwise} \end{cases}$$

We assume that if exchanger i does not operate over period p (*i.e.* $y_{ip} = 0$) then a cleaning task takes place to restore its performance.

The positive values of the following *continuous* variables over each period p ($p = 1..P$) have to be determined:

i) For each exchanger i

Q_{ip} heating load, J/s

T_{ip}^{in} milk inlet temperature, K

T_{ip}^{out} milk outlet temperature, K

U_{ip} heat transfer coefficient, $W/(m^2 \cdot K)$

ΔT_{ip} mean temperature difference, K

t_{ip} number of time intervals in heating mode at period p elapsed since the last cleaning

Δt_{ip} number of time intervals during cleaning at period p since the last cleaning

ii) The hot utility

Θ_p temperature, K

The difference between variables Δt_{ip} and t_{ip} is clarified in section 7.5.1.

Energy Balance Constraints

Continuity of the process fluid temperature is ensured by the following equations:

$$T_{ip}^{in} = T_m^{inlet} \qquad i = 1, \forall p \tag{7.1}$$

$$T_{ip}^{out} = T_{i-1,p}^{in} \qquad \forall i = 2..N, \forall p \tag{7.2}$$

where T_m^{inlet} is equal to 333 K for all the examples considered.

For each exchanger i the following energy balance is written for the process fluid side over each period p:

$$Q_{ip} = F_m \cdot Cp_m \cdot (T_{ip}^{out} - T_{ip}^{in}) \qquad \forall i, \forall p \tag{7.3}$$

In order to take into account the effect of CIP operations on the thermal behaviour additional constraints are included:

$$Q_{ip} \leq Q_i^U \cdot y_{ip} \quad \forall i, \forall p \tag{7.4}$$

The above constraint guarantees that if exchanger i is cleaned during period p (*i.e.* $y_{ip} = 0$) then the corresponding head load, Q_{ip}, is forced to zero. Consequently, the milk inlet and outlet temperatures will be equal by equation 7.3. On the other hand, if the exchanger i operates at period p (*i.e.* $y_{ip} = 1$) then a specific amount of heating load should be exchanged (as determined by the model) below a specified upper bound, Q_i^U.

The basic design equations for every exchanger i are as follows:

$$Q_{ip} = U_{ip} \cdot A_i \cdot \Delta T_{ip} \quad \forall i, p \tag{7.5}$$

$$\Delta T_{ip} = \frac{(\Theta_p - T_{ip}^{out}) + (\Theta_p - T_{ip}^{in})}{2} \quad \forall i, \forall p \tag{7.6}$$

The logarithmic mean temperature difference, ΔT_{ip}, has been approximated by the arithmetic mean temperature difference.

The process fluid outlet temperature of the last exchanger (*i.e.* $i = N$) should always lie above a specified bound according to the process (*i.e.* dairy sterilization) requirements. This is guaranteed by the following constraint:

$$T_{ip}^{out} \geq T_m^L \qquad i = N, \forall p \tag{7.7}$$

The value of T_m^L is defined by sterilization requirements to be 369 K for our analysis. The algorithm will force the process fluid outlet temperature close to its lower bound and not far above it, in order to minimize the energy consumption. Thus, no upper bound is required.

The steam temperature, Θ_p, is a degree of freedom which can be adjusted over time in order to mitigate fouling effects. It is assumed that Θ_p is available (in a piecewise constant mode) from the plant hot utility system between given lower and upper bounds:

$$\Theta_p^L \leq \Theta_p \leq \Theta_p^U \qquad \forall p \tag{7.8}$$

The following thermodynamic feasibility constraints are added to the formulation:

$$\Theta_p \geq T_{ip}^{in} + \delta T_i^{\min} \quad \forall i, \forall p \tag{7.9}$$

$$\Theta_p \geq T_{ip}^{out} + \delta T_i^{\min} \quad \forall i, \forall p \tag{7.10}$$

Fouling Constraints

A distinguishing feature is that the equipment fouling rates depend on the temperature and characteristics (in that case, milk protein concentration) of the process. Although in some cases the fouling rate may follow a linear profile, in the general case it will be a non-linear profile. The most common profile is the exponential one (monotonic decreasing) as illustrated in Figure 7.9.

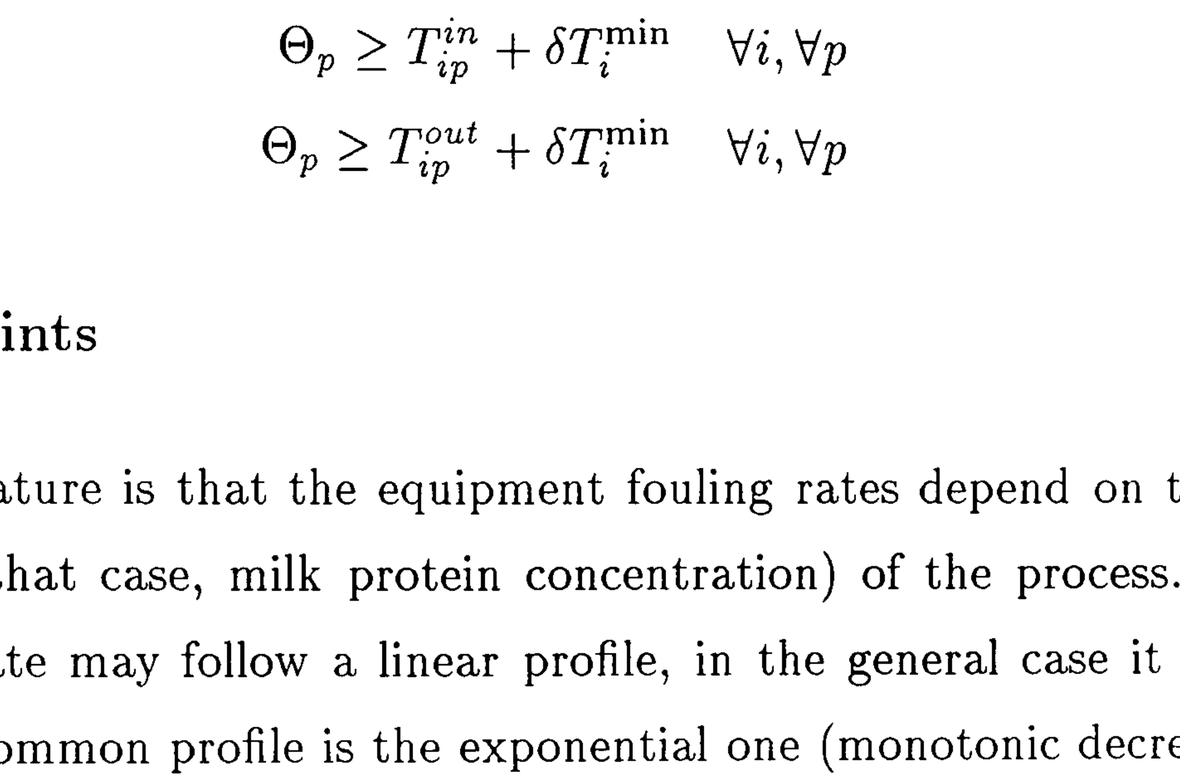


Figure 7.9: Non linear decaying profile

In this section a general monotonic decreasing non-linear fouling profile is modelled. The value of the overall heat transfer coefficient for exchanger i over period p after θ periods of

continuous operation since the last cleaning is given by parameter $\zeta_{i\theta}$ (see Figure 7.9). This parameter determines the value of the U_{ip} variable according to the following additional constraints:

$$U_{ip} = \sum_{\theta=1}^{\tau_i} \zeta_{i\theta} \cdot X_{ip\theta} \qquad \forall i, \forall p \tag{7.11}$$

$$X_{ip\theta} \leq 1 - y_{i,p-\theta} \qquad \forall i, \forall p, \forall \theta = 1..\tau_i \tag{7.12}$$

$$\sum_{\theta=1}^{\tau_i} X_{ip\theta} = y_{ip} \qquad \forall i, \forall p \tag{7.13}$$

where τ_i is the maximum number of periods over which exchanger unit i can operate continuously without being cleaned.

Note that if CIP takes place (*i.e.* $y_{ip} = 0$) then constraints 7.13 will force all $X_{ip\theta}$ variables to zero and consequently the corresponding U_{ip} variables take zero value through constraints 7.11. This in turn will force Q_{ip} to zero (from constraints 7.5) in agreement with constraints 7.4. On the other hand, if exchanger i in heating mode operates over period p and assuming that only *one* CIP task occurred at period $p - \theta^*$ ($\theta^* \leq \tau_i$) then all $X_{ip\theta}$ ($\theta = 1..\tau_i, \theta \neq \theta^*$) variables will take the value of zero (constraints 7.12) except $X_{ip\theta^*}$ which is forced to the value of one (constraints 7.13). This is turn will determine the value of U_{ip} being equal to $\zeta_{i\theta}$. Additionally, if exchanger i operates over period p and *more than one* CIP operation takes place over the last τ_i periods then the most *recent* cleaning task (smaller θ value) should be chosen to determine the correct U_{ip} value. This is guaranteed by the optimization algorithm as the smaller θ value (more *recent*) corresponds to a larger $\zeta_{i\theta}$ and consequently to a larger U_{ip} value thus minimizing energy consumption. It should be noted that the $X_{ip\theta}$ variables can be treated as continuous variables as they can obtain only zero or one values due to the monotonic decreasing nature of the fouling profile. Thus, the complexity of the problem is reduced significantly.

A serious problem that arises during milk heat treatment is blockage of the channels as a result of the deposit formation. This is due to extensive run times and results in significant pressure drop. One way to model this serious operating limitation is to monitor the value of deposit mass or thickness. In that case, a critical deposit thickness or mass, δ_i^{crit}, for each exchanger i can be defined, based on simulation results. This critical deposit mass corresponds to a maximum time period duration, τ_i (number of time intervals) after which exchanger i is not allowed to operate. This allows effectively to incorporate pressure drop limitations in the mathematical model.

For example if the deposit mass, $\delta_i(t)$ follows a linear profile:

$$\delta_i(t) = \gamma_i \cdot t$$

where γ_i is the slope of the linear profile and $\delta_i(t) \leq \delta_i^{crit}$, then τ_i will be determined by the upper bound of deposit mass (*i.e.* δ_i^{crit}) as follows:

$$\tau_i = \frac{\delta_i^{crit}}{\gamma_i} \tag{7.14}$$

Similarly, the values of τ_i can be easily determined for non-linear deposit mass profiles.

Timing Constraints

The cost of the CIP operations represents a major cost factor in dairy plants. While heat exchangers in refineries may only be cleaned annually, in the dairy industry it is common practice to clean them every 4-8 hours. The cost of cleaning comprises the cost of water, detergent, production losses, effluent disposal and required energy. It can be modelled (see also chapter 6) as a function of the preceding heating time and the number of periods during which the exchanger does not operate (*i.e.* $y_{ip} = 0$). Consequently, the effect of heating operation on the cleaning requirements is captured which is according to industrial practice since for long heating periods milk deposit requires intensive cleaning requirements to be removed. In this study, two cleaning costs are used: fixed and variable. The fixed cleaning cost represents the fixed expenses over the period of cleaning operation (*i.e.* periods at which $y_{ip} = 0$). On the other hand, the variable cost is a function of the preceding heating period.

In order to quantify the variable CIP cost factor, the number of elapsed time intervals, t_{ip}, since the last cleaning must be calculated for each operating exchanger i, (*i.e.* $y_{ip} = 1$) as follows:

$$t_{ip} + y_{ip} = \sum_{\theta=1}^{\tau_i} \theta \cdot X_{ip\theta} \qquad \forall i, p \tag{7.15}$$

It should be noted that variables t_{ip} monitor the number of time intervals during the whole period of heating operation. During cleaning periods the above timing variables, t_{ip} are reset to zero as both y_{ip} and the right-hand side summation of constraints 7.13 is zero.

In order to capture the elapsed time since the last cleaning, in the objective function (see section 7.5.1) the following additional variables, Δt_{ip}, are introduced along with the following constraints:

$$\Delta t_{ip} = t_{i,p-1} + y_{i,p-1} - t_{ip} \qquad \forall i, p \neq 1 \tag{7.16}$$

The above variables take non-zero values only if exchanger i is switched from operating in heating mode in period $p-1$ to being cleaned in period p (*i.e.* $y_{ip} = 0$ and $y_{i,p-1} \neq 0$). In all other cases, these variables are forced to zero by the optimization algorithm. Thus, Δt_{ip} is essentially a cleaning switch indicator.

The role of the above constraints and variables involved is illustrated in Figure 7.10.

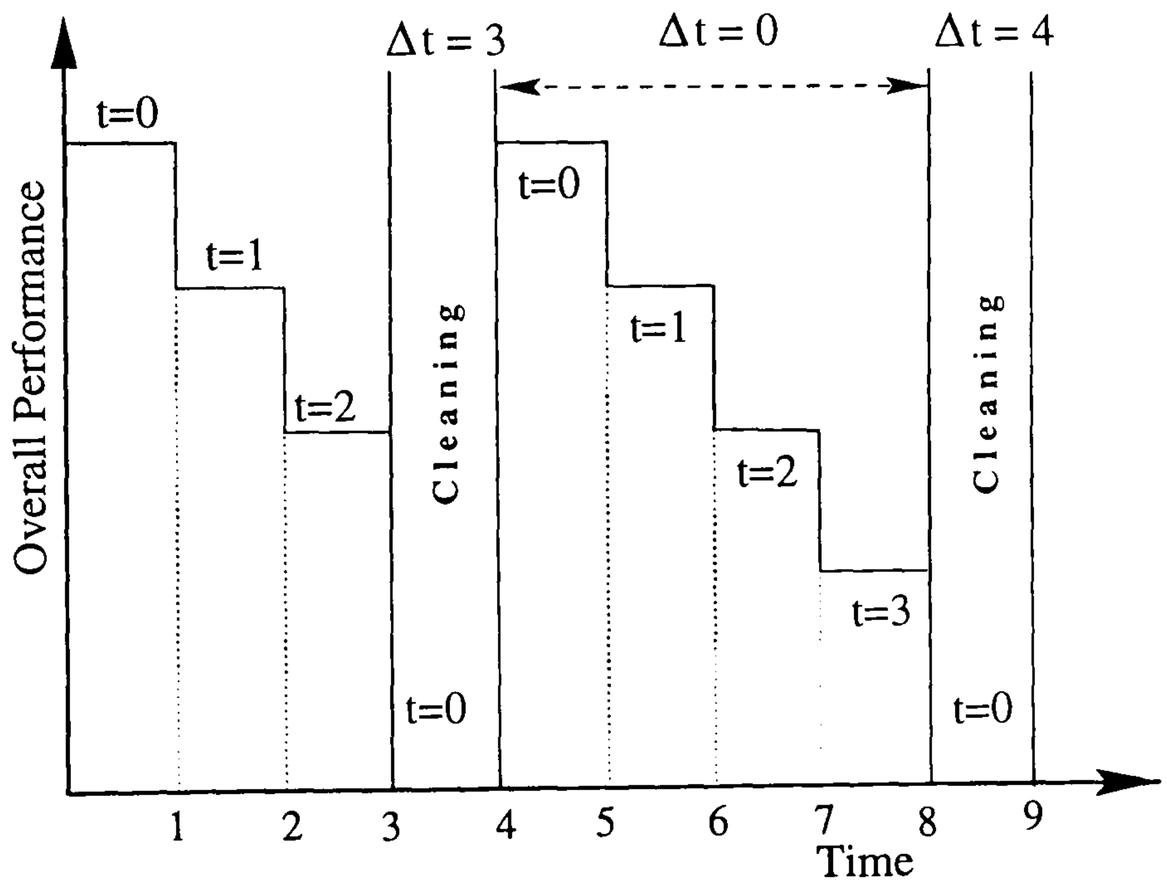


Figure 7.10: Graphical illustration of the cleaning constraints

Cleaning Constraints

Assume that each heat exchanger i is characterised by its own cleaning duration d_i. The following constraint is added in the formulation:

$$y_{i,p+\mu} \leq 1 - y_{i,p-1} + y_{ip} \qquad \forall i, p, \mu = 1..d_i - 1 : d_i > 1 \tag{7.17}$$

The above constraint is only applied when exchanger i starts being cleaned at period p Therefore, each exchanger is forced to be cleaned for d_i consecutive time periods.

A more aggregated form of the above constraint could be derived by summing over μ thus resulting in fewer constraints:

$$\sum_{\mu=1}^{d_i-1} y_{i,p+\mu} \leq (1 - y_{i,p-1} + y_{ip})(d_i - 1) \qquad \forall i, p : d_i > 1 \tag{7.18}$$

However, the above constraints exhibit looser linear programming relaxation.

Objective Function

Since the network operates continuously no term is included in the objective function to account for production losses during shut downs. Hence, the objective function includes just utility and cleaning costs. As mentioned before utility cost is assumed to be a linear function of utility temperature. This assumption is a simple approximation and can easily be relaxed by using more comprehensive models (for example taking into account the total enthalpy of the utility). Furthermore, it is assumed that the same utility source (and the same temperature) is used for all exchangers in the network. It should be emphasized that the models presented could be easily extended to account for multiple hot utility systems and temperature levels by introducing extra integer variables. Thus, utility cost is given by the following expression over the entire period of operation:

$$\text{Utility Cost} = \sum_p C_p \cdot \Theta_p \qquad rmu \tag{7.19}$$

The cost of CIP operation, as mentioned in section 7.5.1 involves two terms and given by the following expression:

$$\text{Cleaning Cost} = \sum_i \sum_p \left(\bar{C}_{ip} \cdot (1 - y_{ip}) + \hat{C}_{ip} \cdot \Delta t_{ip} \right) \qquad rmu \tag{7.20}$$

Again it is assumed that there is a single CIP utility, of infinite capacity. So, the objective function to be minimized is given by the following expression:

$$\min \sum_p C_p \cdot \Theta_p + \sum_i \sum_p \left(\bar{C}_{ip} \cdot (1 - y_{ip}) + \hat{C}_{ip} \cdot \Delta t_{ip} \right) \qquad rmu \tag{7.21}$$

7.5.2 Summary of Formulation

The overall formulation of the optimal cleaning scheduling problem for serial HENs under general milk fouling profiles is summarized as follows:

$$\min \sum_{p} C_p \cdot \Theta_p + \sum_{i} \sum_{p} \left(\bar{C}_{ip} \cdot (1 - y_{ip}) + \hat{C}_{ip} \cdot \Delta t_{ip} \right) \qquad [P1]$$

Subject to

Energy Balance Constraints:

$$T_{ip}^{in} = T_m^{inlet} \qquad \forall i = 1, p$$

$$T_{ip}^{out} = T_{i-1,p}^{in} \qquad \forall i = 2, p$$

$$Q_{ip} = F_m \cdot Cp_m \cdot (T_{ip}^{out} - T_{ip}^{in}) \qquad \forall i, p$$

$$Q_{ip} \leq \cdot Q_i^U \cdot y_{ip} \qquad \forall i, p$$

$$Q_{ip} = U_{ip} \cdot A_i \cdot \Delta T_{ip} \qquad \forall i, p$$

$$\Delta T_{ip} = \frac{(\Theta_p - T_{ip}^{out}) + (\Theta_p - T_{ip}^{in})}{2} \qquad \forall i, p$$

$$T_{ip}^{out} \geq T_m^L \qquad \forall i = N, p$$

$$\Theta_p^L \leq \Theta_p \leq \Theta_p^U \qquad \forall p$$

$$\Theta_p \geq T_{ip}^{in} + \delta T_i^{\min} \qquad \forall i, p$$

$$\Theta_p \geq T_{ip}^{out} + \delta T_i^{\min} \qquad \forall i, p$$

Decay Constraints:

$$U_{ip} = \sum_{\theta=1}^{\tau_i} \zeta_{i\theta} \cdot X_{ip\theta} \qquad \forall i, p$$

$$X_{ip\theta} \leq 1 - y_{i,p-\theta} \qquad \forall i, p, \theta = 1..\tau_i$$

$$\sum_{\theta=1}^{\tau_i} X_{ip\theta} = y_{ip} \qquad \forall i, p$$

Timing Constraints:

$$t_{ip} + y_{ip} = \sum_{\theta=1}^{\tau_i} \theta \cdot X_{ip\theta} \qquad \forall i, p$$

$$\Delta t_{ip} = t_{i,p-1} + y_{i,p-1} - t_{ip} \qquad \forall i, p \neq 1$$

Cleaning Constraints:

$$y_{i,p+\mu} \leq 1 - y_{i,p-1} + y_{ip} \qquad \forall i, p, \mu = 1..d_i - 1 : d_i > 1$$

The formulation presented above is an MINLP model where all the non-linearities arise from the bilinear equation 7.5. In general, for the solution of this problem, various two-level decomposition approaches can be employed. For example the Generalized Benders Decomposition (Geoffrion, 1972) or the Outer-Approximation method (Duran and Grossmann, 1986). An alternative way is to use a branch-and-bound method based on the solution of a series of NLP subproblem. This method has been employed by Jain and Grossmann (1998) and proved to be more efficient than the Outer Approximation method as implemented in the DICOPT++ modelling environment (Viswanathan and Grossmann, 1990).

Another option is to linearize the above model by using standard transformation techniques as discussed in the following section. Although such a linearization scheme increases the problem size, the resulting MILP can guarantee global optimality and be solved efficiently with commercial software.

7.5.3 MILP Reformulation

Standard transformations can be employed to linearize the model by introducing extra variables and constraints (Glover, 1975). However, a key issue is to explore any special structure of the model in order to reduce the size of the problem.

Thus, a new variable, $\overline{X\Delta T}_{ip\theta}$ is introduced defined as:

$$\overline{X\Delta T}_{ip\theta} \equiv X_{ip\theta} \cdot \Delta T_{ip} \qquad \forall i, p, \theta \leq p \tag{7.22}$$

where ΔT_{ip} is given by equation 7.6. The following constraints are then added in the model:

$$\Delta T_i^L \cdot X_{ip\theta} \leq \overline{X\Delta T}_{ip\theta} \leq \Delta T_i^U \cdot X_{ip\theta} \qquad \forall i, p, \theta = 1..\tau_i \tag{7.23}$$

$$\Delta T_{ip} - \Delta T_i^U \cdot (1 - X_{ip\theta}) \leq \overline{X\Delta T}_{ip\theta} \leq \Delta T_{ip} - \Delta T_i^L \cdot (1 - X_{ip\theta}) \qquad \forall i, p, \theta = 1..\tau_i \tag{7.24}$$

where ΔT_i^L and ΔT_i^U are lower and upper bounds of the mean temperature difference.

The design constraints 7.5 can then be rewritten as:

$$Q_{ip} = A_i \cdot \sum_{\theta=1}^{\tau_i} \zeta_{i\theta} \cdot \overline{X\Delta T}_{ip\theta} \tag{7.25}$$

Constraints 7.24 can be substituted by a more aggregated form similar to Voudouris and Grossmann (1992):

$$\Delta T_{ip} = \sum_{\theta=1}^{\tau_i} \overline{X\Delta T}_{ip\theta} + \xi_{ip} \qquad \forall i, p \tag{7.26}$$

$$\xi_{ip} \leq \Delta T_i^U \cdot (1 - y_{ip}) \qquad \forall i, p \tag{7.27}$$

where ξ_{ip} can be considered as a slack variable. Note that the above constraints are only defined over sets i and p and not over θ thus reducing significantly the number of linearization constraints.

7.6 Parallel Heat Exchanger Network Case

While the formulation presented in the previous section addresses the problem of serial heat exchangers, some modifications are required if parallel exchangers are involved (see Figure 7.11). This arrangement is widely used in dairy plants in the form of a one-channel per pass plate heat exchanger.

The process fluid flow is assumed to be split equally among all the active heat exchangers. Consequently, the process fluid inlet flowrate as well as the inlet and outlet temperatures for each exchanger will depend on its operating mode. If exchanger i is cleaned then the corresponding fluid flowrate and heating load is zero. Therefore, a new set k needs to be defined ($k = 1..N$) denoting the number of active exchangers at period p.

A new binary variable, W_{kp} is also introduced:

$$W_{kp} = \begin{cases} 1, & \text{if } k \text{ exchangers operate in heating mode over period } p \\ 0, & \text{otherwise} \end{cases}$$

During each period only a given number of exchangers (between 1 and N) can be active so as to provide continuity in fluid processing. This is expressed mathematically by the following constraints:

$$\sum_{k=1}^{N} W_{kp} = 1 \qquad \forall p \tag{7.28}$$

If F_m^* is the milk flowrate processed at each active heat exchanger, the energy balance constraints 7.3 must be replaced by:

$$Q_{ip} = F_m^* \cdot Cp_m \cdot (T_{ip}^{out} - T_{ip}^{in}) \tag{7.29}$$

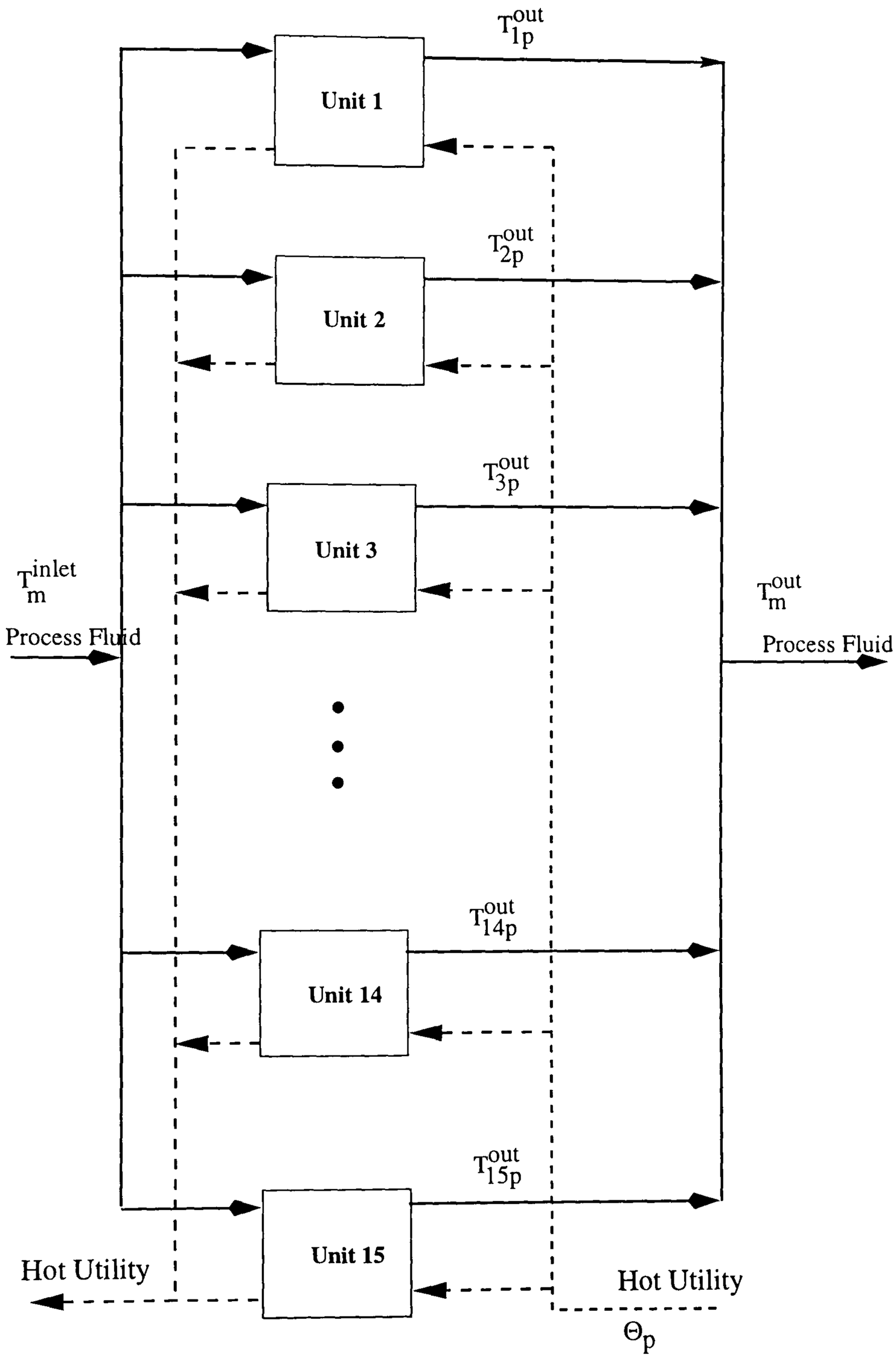


Figure 7.11: Parallel heat exchanger network arrangement

where F_m^* is given by the following equation:

$$F_m^* = \frac{F_m}{\sum_k \cdot W_{kp}} \tag{7.30}$$

Combining 7.29 and 7.30 we obtain:

$$Q_{ip} = \frac{F_m \cdot Cp_m}{\sum_k W_{kp}} (T_{ip}^{out} - T_{ip}^{in}) \tag{7.31}$$

and by exploiting constraints 7.28:

$$Q_{ip} = F_m \cdot Cp_m \cdot \sum_{k=1}^{N} \frac{W_{kp}}{k} \cdot (T_{ip}^{out} - T_{ip}^{in}) \qquad \forall i, p \tag{7.32}$$

where T_{ip}^{in} is equal to the milk inlet temperature T_m^{inlet}.

Constraint 7.32 involves non-linear terms which can be linearized by introducing new variables, $\overline{WT}_{kip}$, defined as follows:

$$\overline{WT}_{kip} \equiv W_{kp} \cdot (T_{ip}^{out} - T_{ip}^{in}) \qquad \forall k, \forall i, \forall p \tag{7.33}$$

These variables are calculated by the following constraints:

$$\overline{WT}_{kip} \leq T_i^U \cdot W_{kp} \qquad \forall k, \forall i, \forall p \tag{7.34}$$

$$\sum_{k=1}^{N} \overline{WT}_{kip} = T_{ip}^{out} - T_{ip}^{in} \qquad \forall i, p \tag{7.35}$$

where T_i^U is an appropriate bound on the process fluid temperature difference $(T_{ip}^{out} - T_{ip}^{in})$. In our dairy application, this difference is in the range 40-45 K. Thus, equation 7.32 can be written in a linear form as follows:

$$Q_{ip} = F_m \cdot Cp_m \cdot \sum_{k=1}^{N} \frac{\overline{WT}_{kip}}{k} \qquad \forall k, \forall i, \forall p \tag{7.36}$$

The number of active exchangers is related to the y_{ip} variables according to the following equation:

$$\sum_{k=1}^{N} k \cdot W_{kp} = \sum_{i} y_{ip} \qquad \forall p \tag{7.37}$$

Also, it may be possible, due to limitations such as pressure drop constraints, to enforce a minimum number of exchangers, $N^{\min}$, to be active (heating mode) over each period p. Then, constraint (7.37) are modified to:

$$\sum_{k=N^{\min}}^{N} k \cdot W_{kp} = \sum_{i} y_{ip} \qquad \forall p \tag{7.38}$$

Similar changes are applied to constraint (7.32). Apart from the engineering perspective, the above constraints to capture minimum number of operating exchangers result in smaller problem size since less binary variables (W_{kp}) and constraints are required.

The final process fluid outlet temperature, after mixing all streams can be calculated from the following overall energy balance equation:

$$T_m^{out} = T_m^{inlet} + \frac{\sum_i Q_{ip}}{F_m \cdot Cp_m} \qquad \forall p \tag{7.39}$$

It should be emphasized that the process fluid outlet temperature of each heat exchanger i, T_{ip}^{out}, will not take zero value if the exchanger does not operate. In that case it will be equal to T_m^{inlet} through constraint (7.32). However, it will not contribute to the overall energy balance since the final mixing temperature, T_m^{out}, is calculated based on the summation of heating loads of all active heat exchangers (see constraint (7.39)).

It is worth noticing that the underlying heat exchanger network will not include bypasses as in the serial one. It only requires suitable valves (*e.g.* on/off) of each end of exchanger, which may open (heating) or close (cleaning) depending on the operating mode. All the fouling constraints remain the same as the ones presented in section 7.5.1.

7.7 Block Heat Exchanger Network Case

Once formulations for the basic serial and parallel arrangements have been described, more complex configurations can be modelled by combining these basic cases. Here we examine for example a block HEN where different blocks of parallel exchangers are connected in series. Conceptually, we may consider such an arrangement to model a multi-pass PHE that is widely used in industrial food and pharmaceutical processing. Moreover, many industrial food HENs features combinations of parallel and serial networks (for example the plant for sugar manufacture at the Bury St Edmunds British Sugar factory, Smaili (1998)). A total number of 15

exchangers in 5 serial blocks is depicted in Figure 7.12. This case utilizes the modelling equations presented in the previous section with minor modifications to account for the continuity of temperature between successive blocks.

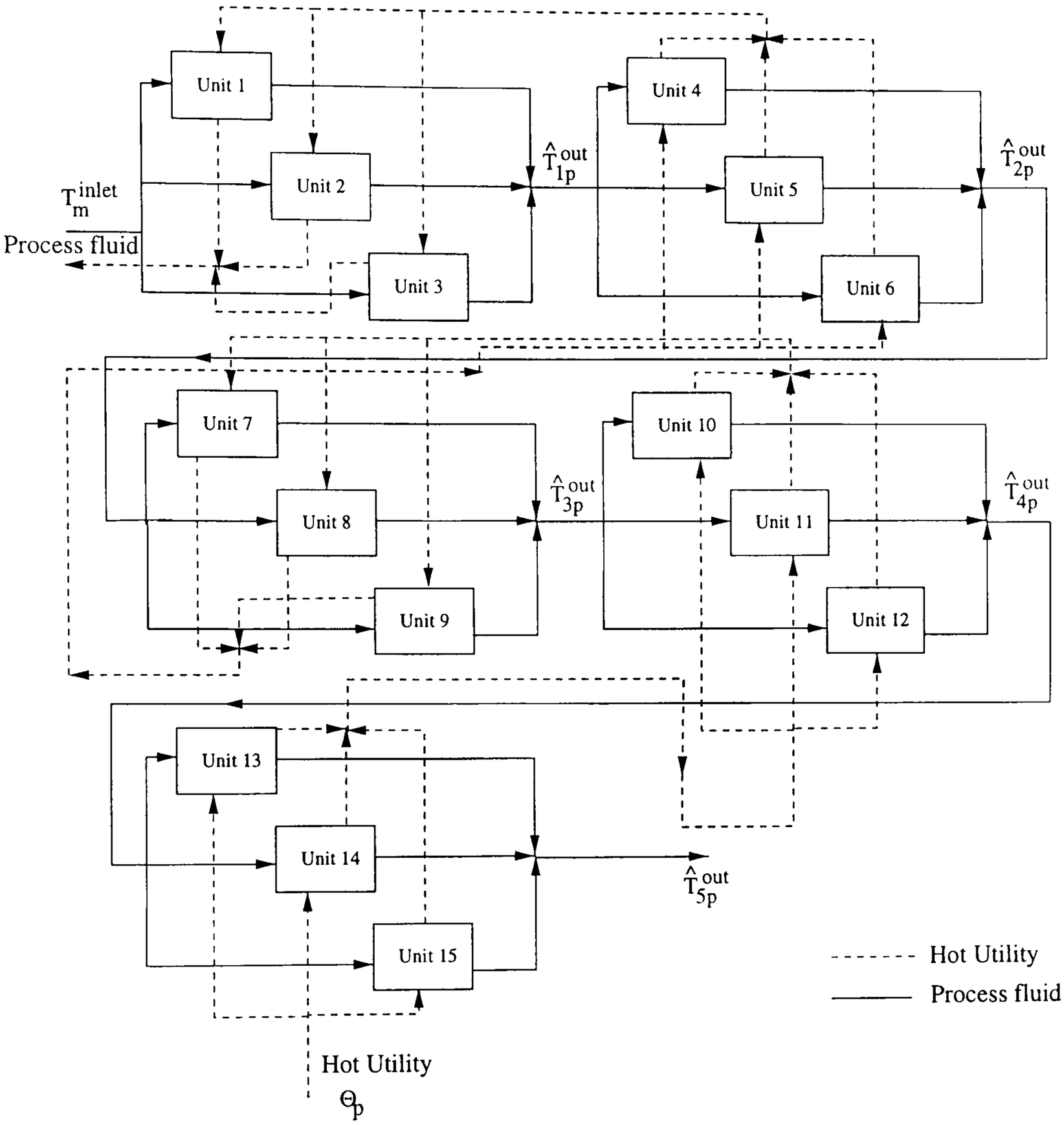


Figure 7.12: Complex HEN of serial blocks of parallel heat exchangers

The W_{kp} binary variables, in the case of parallel exchangers, are now redefined for each block b ($b = 1..B$). A new set I_b is defined to declare heat exchangers which belong to block b. The following energy balance is then imposed to calculate the milk outlet temperature, $\hat{T}_{bp}^{out}$, of block b:

$$\hat{T}_{bp}^{out} = \hat{T}_{bp}^{in} + \frac{\sum_{i \in I_b} Q_{bip}}{F_m \cdot Cp_m} \qquad \forall b, \forall p \tag{7.40}$$

where $\hat{T}_{bp}^{in}$ is the process fluid inlet temperature of block b.

The following constraints are also imposed to ensure temperature continuity between blocks.

$$\hat{T}^{out}_{bp} = \hat{T}^{in}_{b+1,p} \qquad \forall b = 1..B-1, \forall p \tag{7.41}$$

Clearly, for the first block $\hat{T}^{in}_{1p} = T^{inlet}_{m}$.

The heating load of exchanger i in block b, Q_{bip}, is calculated by the following constraints:

$$Q_{bip} = F_m \cdot Cp_m \cdot \sum_{k=1}^{N_b} \frac{W_{bkp}}{k} \cdot (T^{out}_{bip} - T^{in}_{bip}) \qquad \forall b, \forall i \in I_b, \forall p \tag{7.42}$$

where N_b is the total number of exchangers in block b (*e.g.* exchangers 1, 2, 3 in block 1) and T^{out}_{bip} is the milk outlet temperature from exchanger i in block b over period p. The resulting non-linearities are treated in a fashion similarly to section 7.6.

7.7.1 Fluid as Heating Medium

So far, we have considered the case of using saturated steam as heating medium. In general, any fluid heating medium (for example hot oil) can be used if available in the plant. The model in such a case requires minor changes in the formulation presented in the previous sections. The thermal energy balance constraints should also include the heating medium side contribution. Thus, similar to equation 7.42 the following one is added:

$$Q_{bip} = F_o \cdot Cp_o \cdot \sum_{k=1}^{N_b} \frac{W_{kp}}{k} \cdot (\Theta^{in}_{bip} - \Theta^{out}_{bip}) \qquad \forall b, i \in I_b, p \tag{7.43}$$

where Θ^{in}_{bip} and Θ^{out}_{bip} are the inlet and outlet temperatures of the heating medium respectively, for exchanger i in block b over period p. Finally, F_o and Cp_o are given parameters declaring the heating medium flowrate and thermal capacity, respectively. The above equations can then be linearized similarly to section 7.6.

Furthermore, the mean temperature difference constraint (7.6) is updated to include heating medium temperatures:

$$\Delta T_{ip} = \frac{(\Theta^{in}_{bip} - T^{out}_{bip}) + (\Theta^{out}_{bip} - T^{in}_{bip})}{2} \qquad \forall b, i \in I_b, p \tag{7.44}$$

It should be emphasized here that apart from the cleaning and heating timings the inlet temperature of the heating medium is an additional degree of freedom in the network which can be manipulated in order to meet the process thermal requirements.

7.7.2 Summary of the Mathematical Model

The mathematical model for the complex HENs involving serial blocks of parallel heat exchangers and steam as heating medium is summarized as follows:

$$\min \sum_{p} C_p \cdot \Theta_p + \sum_{b} \sum_{i \in I_b} \sum_{p} \left(\bar{C}_{bip} \cdot (1 - y_{bip}) + \hat{C}_{bip} \cdot \Delta t_{bip} \right) \qquad [P2]$$

Subject to

Energy Balance Constraints

$$Q_{bip} \leq Q_{bi}^{U} \cdot y_{bip} \quad \forall b, i \in I_b, p$$

$$Q_{bip} = A_i \cdot \sum_{\theta=1}^{\tau_i} \zeta_{bi\theta} \cdot \overline{X \Delta T}_{bip\theta} \quad \forall b, i \in I_b, p$$

$$Q_{bip} = F_m \cdot Cp_m \cdot \sum_{k=1}^{N_b} \frac{\overline{WT}_{bkip}}{k} \qquad \forall b, i \in I_b, p$$

$$\hat{T}_{bp}^{out} = \hat{T}_{bp}^{in} + \frac{\sum_{i \in I_b} Q_{bip}}{F_m \cdot Cp_m} \qquad \forall b, p$$

$$\hat{T}_{bp}^{out} = \hat{T}_{b+1,p}^{in} \qquad \forall b = 1..B-1, p$$

$$\hat{T}_{bp}^{in} = T_m^{inlet} \qquad \forall b = 1, p$$

$$\Delta T_{bip} = \frac{(\Theta_p - T_{bip}^{out}) + (\Theta_p - T_{bip}^{in})}{2} \qquad \forall b, i \in I_b, p$$

$$\hat{T}_{bp}^{out} \geq T_m^{L} \qquad \forall b = B, p$$

$$\Theta_p^{L} \leq \Theta_p \leq \Theta_p^{U} \qquad \forall p$$

$$\Theta_p \geq T_{bip}^{in} + \delta T_i^{\min} \qquad \forall b, i \in I_b, p$$

$$\Theta_p \geq T_{bip}^{out} + \delta T_i^{\min} \qquad \forall b, i \in I_b, p$$

Linearization Constraints

$$\overline{WT}_{bkip} \leq T_i^{U} \cdot W_{bkp} \qquad \forall b, k, i \in I_b, p$$

$$\sum_{k=1}^{N_b} \overline{WT}_{bkip} = T_{bip}^{out} - T_{bip}^{in} \qquad \forall b, i \in I_b, p$$

$$\sum_{k=1}^{N_b} k \cdot W_{bkp} = \sum_{i \in I_b}^{N_b} y_{bip} \qquad \forall b, p$$

$$\sum_{k=1}^{N_b} W_{bkp} = 1 \qquad \forall b, p$$

$$\Delta T_{bi}^{L} \cdot X_{bip\theta} \leq \overline{X\Delta T}_{bip\theta} \leq \Delta T_{bi}^{U} \cdot X_{bip\theta} \qquad \forall b, i \in I_b, p, \theta = 1..\tau_i$$

$$\Delta T_{bip} = \sum_{\theta=1}^{\tau_i} \overline{X\Delta T}_{bip\theta} + \xi_{bip} \qquad \forall b, i \in I_b, p$$

$$\xi_{bip} \leq \Delta T_{bi}^{U} \cdot (1 - y_{bip}) \qquad \forall b, i \in I_b, p$$

Fouling Constraints

$$U_{bip} = \sum_{\theta=1}^{\tau_i} \zeta_{bi\theta} \cdot X_{bip\theta} \qquad \forall b, i \in I_b, p$$

$$X_{bip\theta} \leq 1 - y_{bi,p-\theta} \qquad \forall b, i \in I_b, p, \theta = 1..\tau_i$$

$$\sum_{\theta=1}^{\tau_i} X_{bip\theta} = y_{bip} \qquad \forall b, i \in I_b, p$$

Timing Constraints

$$t_{bip} + y_{bip} = \sum_{\theta=1}^{\tau_i} \theta X_{bip\theta} \qquad \forall b, i \in I_b, p$$

$$\Delta t_{bip} = t_{bi,p-1} + y_{bi,p-1} - t_{bip} \qquad \forall b, i \in I_b, p \neq 1$$

Cleaning Constraints

$$y_{bi,p+\mu} \leq 1 - y_{bi,p-1} + y_{bip} \qquad \forall i \in I_b, \forall p, \mu = 1..d_i - 1 : d_i > 1$$

7.8 Case Studies

7.8.1 Serial Heat Exchangers

Consider the serial HEN shown in Figure 7.7 which comprises a total number of 15 heat exchangers. Linear fouling is assumed for all exchangers whose characteristics are given in Table 7.1 as derived from the simulation results in chapter 5. The overall heat transfer coefficient, $U_i(t)$, and deposit mass, $\delta_i(t)$, profiles are expressed by the following equations:

$$U_i(t) = \alpha_i + \beta_i \cdot t \qquad \forall i \tag{7.45}$$

$$\delta_i(t) = \gamma_i \cdot t \qquad \forall i \tag{7.46}$$

where α_i, β_i and γ_i are given parameters for exchanger i. It is assumed that within the temperature range of each heat exchanger fouling is only a function of time. In order to

guarantee that each exchanger operates (in heating mode) within a small temperature range a minimum number of exchangers in heating operation can been imposed using constraint (7.38). It should be noted that the equipment fouling rates differ from exchanger to exchanger with the maximum value observed in exchanger 9. The critical deposit mass is 16 gr/m^2. The heating medium is taken to be saturated steam with a minimum temperature availability of 550 K. The time horizon of interest is one day which is divided into 24 time intervals of equal duration. Milk is processed at a constant flowrate of 0.08583 kg/s and inlet temperature 333 K while the heat exchange area for each exchanger is 0.01101 m^2. The outlet temperature of milk is constrained to be above 369 K throughout process operation. All relevant cost data expressed in *rmu* are given in Table 7.2. The duration of the cleaning task for each heat exchanger is taken to be equal to the size of one time interval (one hour).

Exchanger Unit No	α W/m^2K	β W/m^2Ksec	γ kg/m^2sec
1	2000	-0.04166	10^{-5}
2	2000	-0.045	10^{-5}
3	2000	-0.048	10^{-5}
4	2000	-0.050	$5 \cdot 10^{-5}$
5	2000	-0.058	$5.5 \cdot 10^{-4}$
6	2000	-0.063	$6.0 \cdot 10^{-4}$
7	2000	-0.069	$9.2 \cdot 10^{-4}$
8	2000	-0.071	$9.5 \cdot 10^{-4}$
9	2000	-0.073	$9.8 \cdot 10^{-4}$
10	2000	-0.068	$9.4 \cdot 10^{-4}$
11	2000	-0.064	$9.3 \cdot 10^{-4}$
12	2000	-0.061	$9.1 \cdot 10^{-4}$
13	2000	-0.057	$8.92 \cdot 10^{-4}$
14	2000	-0.054	$8.1 \cdot 10^{-4}$
15	2000	-0.052	$7.5 \cdot 10^{-4}$

Table 7.1: Fouling data for the serial heat exchanger network case

C_p rmu/K	$\bar{C}_{ip}$ rmu	$\hat{C}_{ip}$ rmu/hr
2	900	360

Table 7.2: Cost data

The modelling system GAMS (Brooke *et al.*, 1992) was used to implement the mathematical models. The problem was first solved using the augmented penalty outer approximation method as implemented in DICOPT++ (Viswanathan and Grossmann, 1990) for the MINLP

model [P1], and the OSL MILP optimizer for the linearized model [P2]. An optimality gap of 1.5% was assumed for the solution of the MILP model.

Computational results are given in Table 7.3. This table highlights some interesting results regarding the computational features of the problem. The relaxation of model [P2] is very tight as the relative gap between the fully relaxed problem and the final MILP is 2.2 %. This example could not be solved using the MINLP model [P1] in reasonable computational time (10,000 CPU sec). On the other hand, the problem was solved very efficiently using the MILP model [P2]. Additionally, and in order to make a comparison between the two models another problem with 12 exchangers was also used. Although this example could be solved by using DICOPT++, the solution obtained was suboptimal (see Table 7.3). Once again, the MILP model [P2] performed more efficiently. Several tests have shown that the MINLP model [P1] for examples with more than 10-12 exchangers could not give any solution in reasonable time.

No of Units	Fouling Profile	Relaxation[1] *rmu*	Cost *rmu*	Model	Major iterations in OA or Branch-and-bound Nodes [2]	CPU[3]
12	Linear	111,604	116,700	MINLP	5	1910
			112,960	MILP	109	510
15	Linear	138,200	N/A[4]	MINLP	N/A[4]	N/A[4]
			141,100	MILP	23	750
15	General	138,700	N/A[4]	MINLP	N/A[4]	N/A[4]
			143,200	MILP	670	1630

Table 7.3: Computational results for the serial HEN case

So far, we have considered linear fouling profiles for all exchangers. The above problem with 15 heat exchangers has also been solved for the case of general fouling profile (decaying behaviour close to linear). Again no solution was obtained in reasonable computational time using the MINLP model [P1]. On the other hand, the linearized MILP model [P1] was solved with modest computational effort (Table 7.3).

The optimal solution (schedule) is shown in Figure 7.13. We can notice that frequent CIP operations are performed especially in the exchangers with higher fouling rates (7 to 11 in Table 7.1). The time temperature profile of the heating medium (steam) is depicted in Figure 7.14. It is clear that when many exchangers are cleaned simultaneously then utility

[1] Solution of the relaxed MINLP
[2] Termination criteria for DICOPT++: Crossover of bounds
[3] Seconds on an ULTRA workstation
[4] Solution not reached after 10,000 CPU sec

temperature reaches high levels (*e.g.* time interval 16). In addition, we can notice that at the end of the time horizon quite high steam temperatures are utilized as there is no penalty for leaving the exchangers *dirty* (fouled) at the end of the daily schedule. One way to tackle this deficiency is by augmenting the objective function including cost terms related only to the t_{iP} (last interval) variables thus reflecting the fouling state of the exchanger at the end of the day. Alternatively, a cyclic operating schedule can be applied in order to repeat the same pattern of operations (schedule) every day (cycle) by forcing the state of each exchanger to be the same at the start and end of the cycle. Consequently, if an exchanger is dirty at the end of a cycle then its performance at the start of next cycle will be decreased thus requiring a cleaning operation in short period.

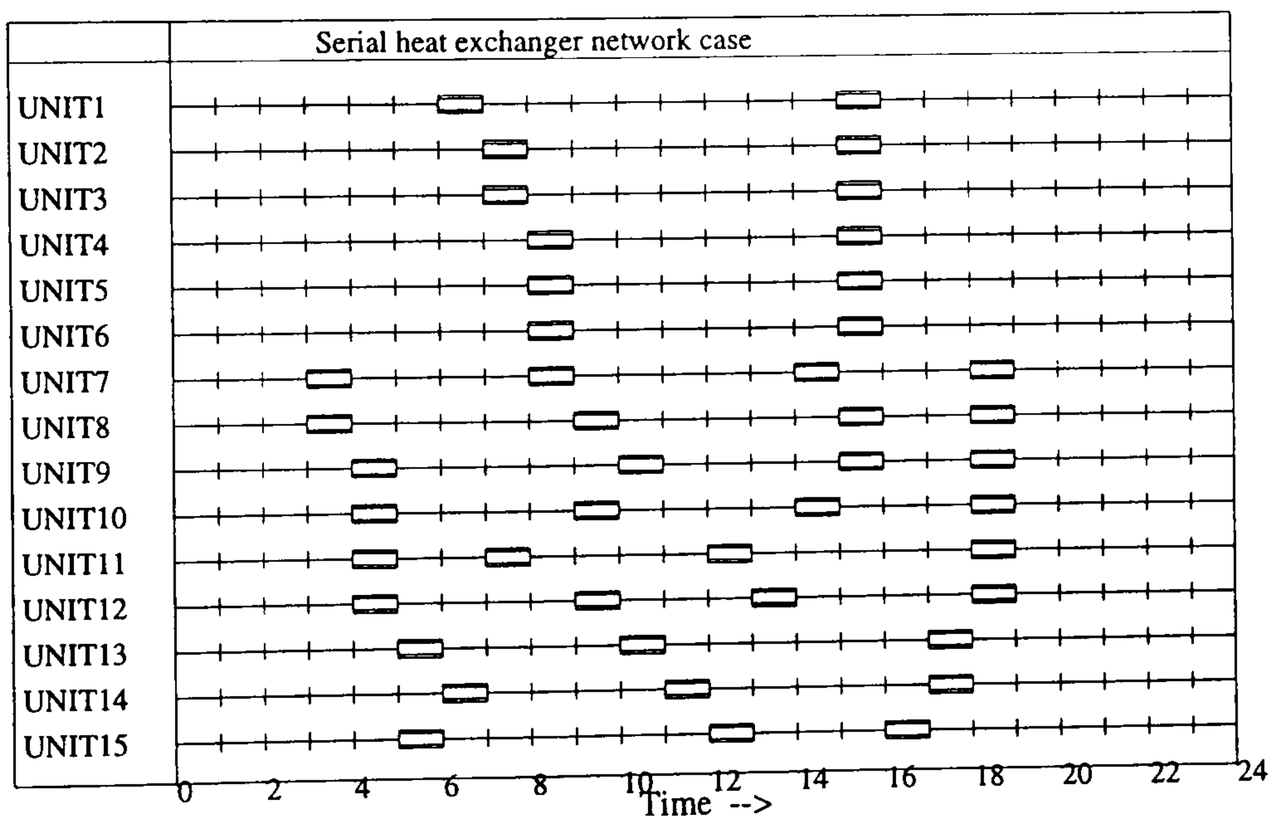


Figure 7.13: Optimal cleaning schedule for the serial heat exchanger network case

7.8.2 A Complex Arrangement of Serial Blocks

Consider the HEN shown in Figure 7.12 involving 15 heat exchangers grouped in 5 three-exchanger blocks. The heating medium is assumed to be saturated steam at a maximum

temperature of 550 K. An exponential fouling decaying behaviour is assumed for all heat exchangers as given in Table 7.4. The critical deposit mass is 15 kg/m^2. The milk inlet temperature is 333 K and the outlet temperature should be greater than 369 K. All exchangers have the same heat exchange area equal to 0.0188 m^2. The time horizon of interest is one day which is divided into 24 time intervals of equal duration.

Heat Transfer Coefficient					
Period	Units 1,2,3	Units 4,5,6	Units 7,8,9	Units 10,11,12	Units 13,14,15
1	1925	1870	1900	1925	1800
2	1800	1600	1750	1800	1730
3	1670	1380	1610	1670	1680
4	1500	1210	1450	1500	1590
5	1380	1030	1300	1380	1450
6	1200	1000	1120	1200	1360
7	1120	975	1100	1120	1260
8	1030	940	1085	1010	1180
9	990	925	1050	970	1090

Table 7.4: Fouling data for the complex HEN case

The MILP model [P2] required 220 nodes (802 CPU sec) using 1.5% margin of optimality. The solution indicates a total cost of 142,200 *rmu* while the corresponding value of the relaxed LP is 139,500 *rmu*. Again it is clear that the MILP results in a tight formulation (about 2% relative gap) even for this more complicated example.

The optimal cleaning schedule and utility temperature profiles are depicted in Figures 7.15 and 7.16 respectively. Again exchangers with high fouling rates are frequently cleaned. If an upper bound of 398 K rather than 550 K[3] is imposed on the steam temperature, then the resulting schedule is shown in Figure 7.17 while the operating cost is 145,800 *rmu* yielding a 2.5% more expensive operation compared with the previous case. For the solution of this problem, 920 nodes were examined in the branch-and-bound tree in 1140 CPU sec. An interesting aspect of the second case is that the cleaning scheduling policy has been changed considerably by increasing the required cleaning operations from 45 (original scenario) to 50. We can therefore conclude that the availability of the hot utility in the plant plays an important role in this problem. Furthermore, for even more limited hot utility availability the problem may be infeasible which is other words mean that the production must be interrupted.

Finally, this problem was also solved for the case where the heating medium is hot oil.

[3]The maximum utility temperature is about 400 K as shown in Figure 7.16

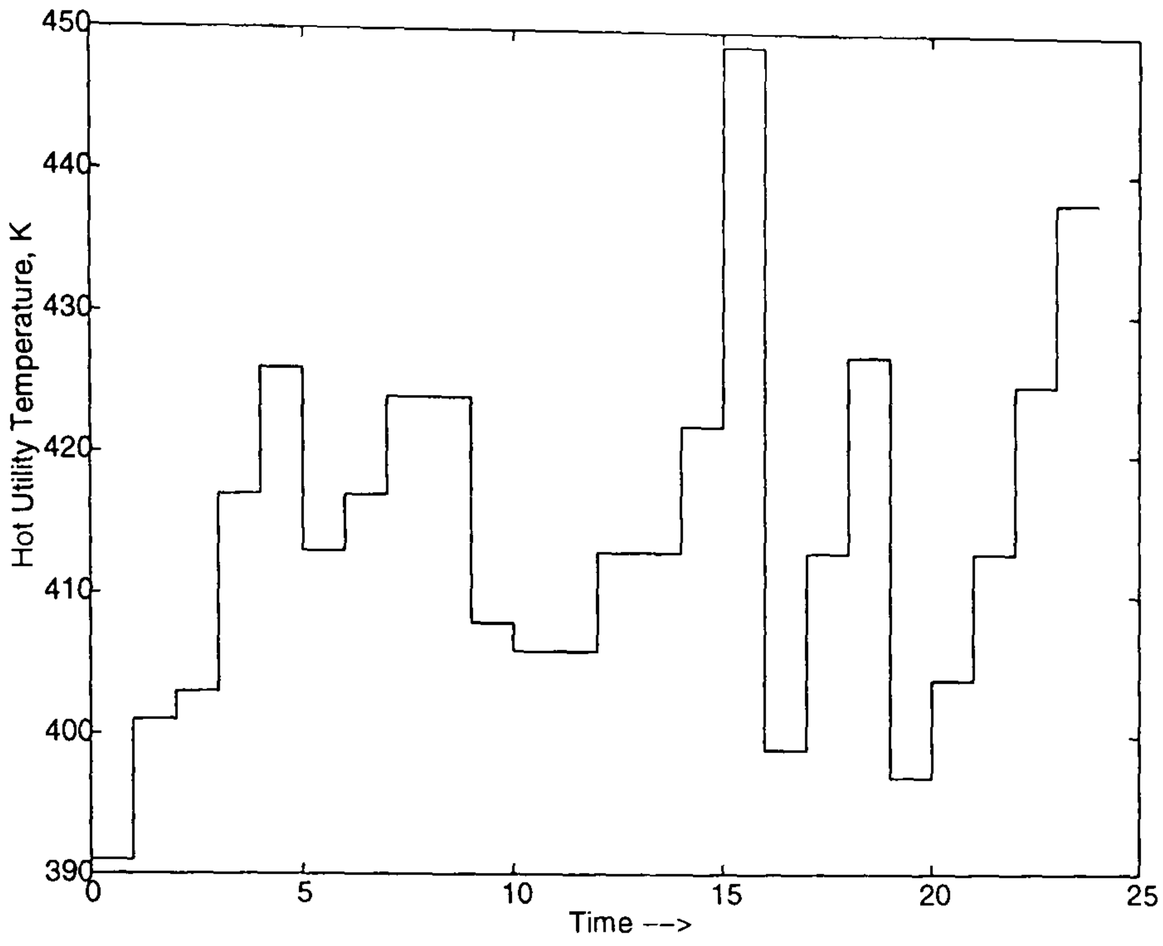


Figure 7.14: Optimal hot utility temperature profile for the serial heat exchanger network case

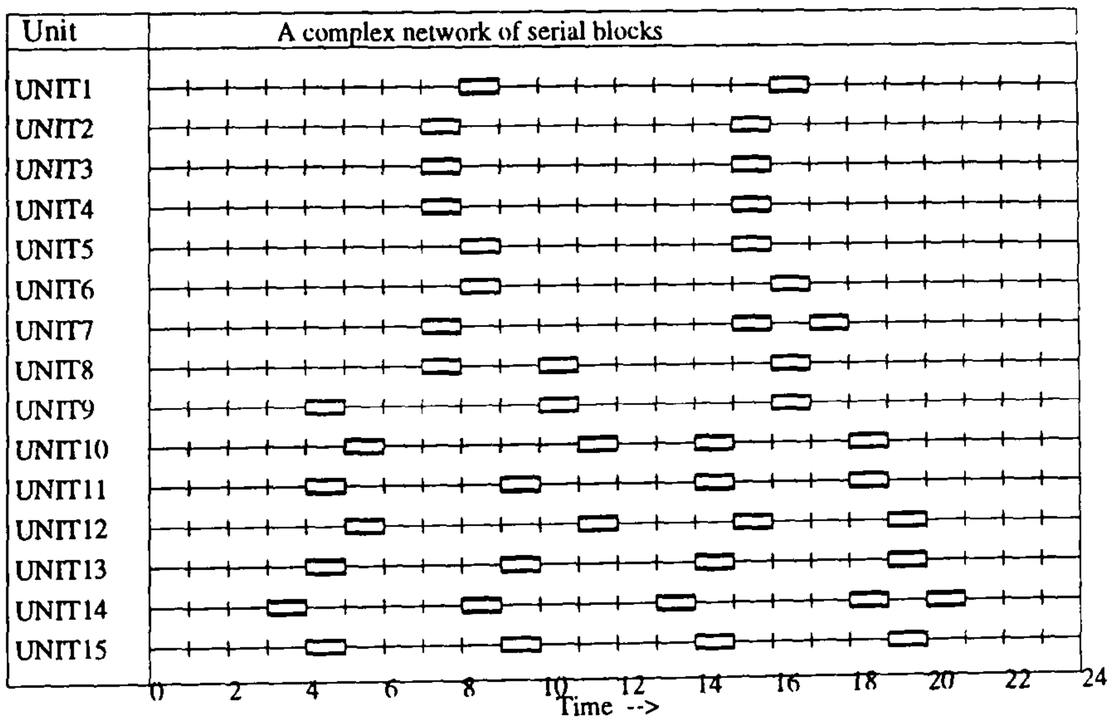


Figure 7.15: Optimal cleaning schedule for the complex heat exchanger network case

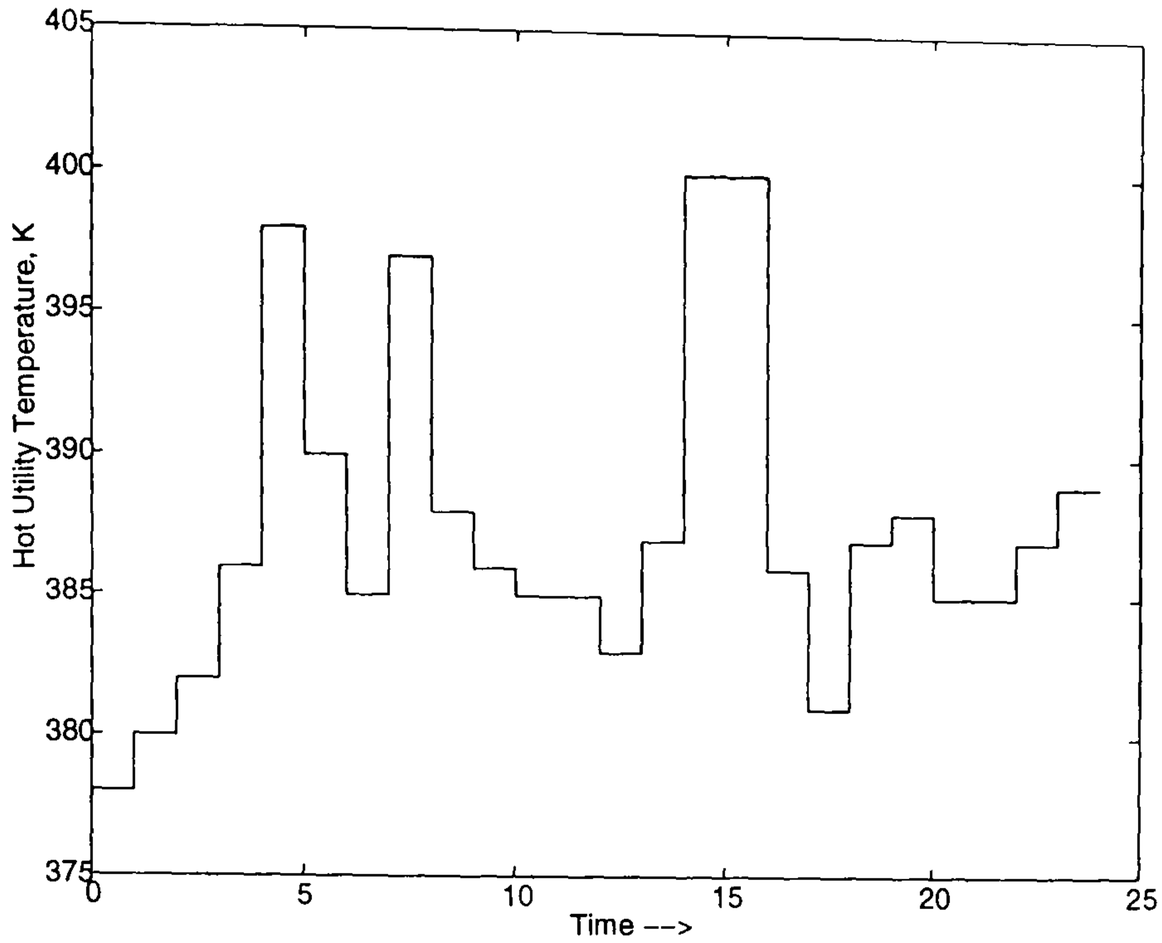


Figure 7.16: Optimal hot utility temperature profile for the complex heat exchanger network case

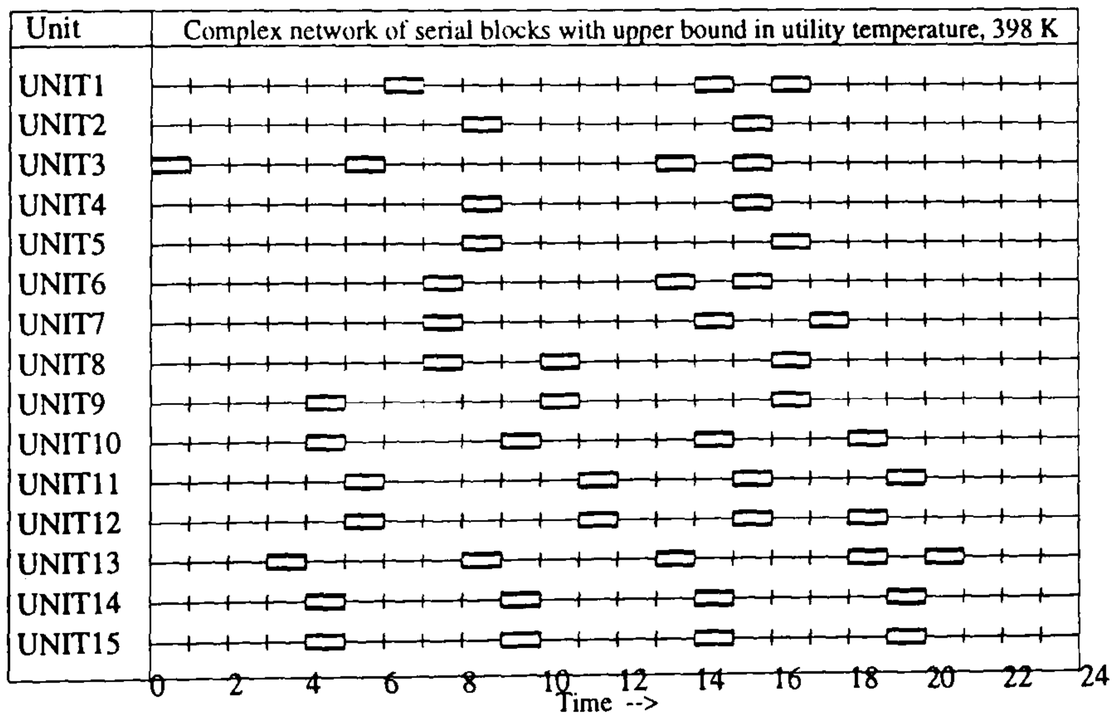


Figure 7.17: Optimal cleaning schedule for the complex heat exchanger network case with utility temperature bound

The inlet temperature of the heating medium which is subject to an upper bound of 450 K is a control variable to be manipulated by the optimization algorithm. In practice, the heating medium is circulated between the HEN and an auxiliary exchanger or furnace which controls its temperature. The profile of hot oil inlet temperature is depicted in Figure 7.18 while the cleaning schedule is the same as in the previous case. The above problem was solved within 970 CPU sec examining 210 nodes during the branch and bound procedure.

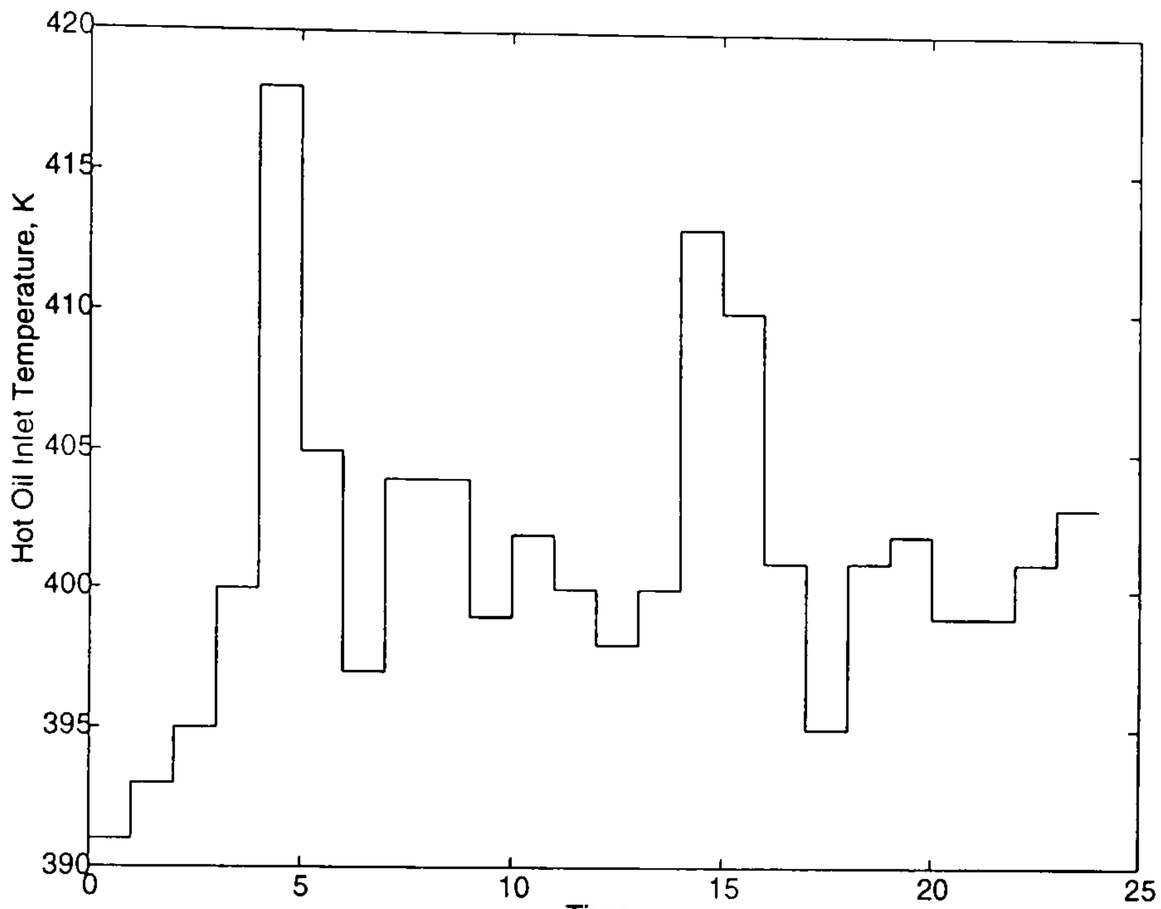


Figure 7.18: Hot oil inlet temperature profile

7.9 Concluding Remarks

Special classes of problems dealing with the short term cleaning scheduling of HENs have been considered in this chapter. Due to its practical significance a special application in HENs under milk fouling constituted the major motivation for this work. General fouling profiles have been considered to predict the behaviour of the equipment with time. It was shown that trade-offs exist between the total number and timings of cleaning operations and the cost and availability of hot utility in the plant.

First, a novel and generic MINLP model was developed which was then linearized to an MILP model. The latter model (which can be solved to global optimality) yields a very tight formulation requiring a few nodes in the branch and bound tree. On the other hand, the MINLP model cannot be used for the solution of problems with more than 10-12 exchangers over an operating horizon of 24 hours. In addition it was shown that the MINLP may lead

to suboptimal solutions. Finally, a number of examples with up to 15 exchangers have been solved to illustrate the capability and efficiency of the proposed models. It was proved that the hot utility availability in the plant can have significant effect on the network cleaning policies.

So far, this work has been concentrated on short term cleaning scheduling. However, the models presented can also be used for problems with longer time horizons. The basic idea is to develop a receding horizon policy where the time horizon of interest is first divided into a number of time slots. The optimal scheduling policy for the first slot is defined using the models presented in this chapter. Then, at the beginning of the next slot, the model data ($e.g.$ fouling profiles) are updated from the plant database and the schedule is reoptimized. This procedure is then repeated. However, this approach cannot guarantee optimal solutions. Alternatively, the models can be extended to account for cyclic operations thus providing a more rigorous approach.

Chapter 8

Conclusions & Future Directions

8.1 Conclusions

The objective of this work has been to establish advanced optimisation techniques to address some of the design and operation issues in batch plants. In this chapter, we summarise the main contributions of this thesis and also consider some possible directions for future work.

The focus of our work has been on two main aspects:

- the conceptual modelling of the plant layout problem in terms of mathematical programming formulations;
- the detailed mathematical modelling, simulation, optimal design and operation of heat treatment process under fouling with application to dairy processes.

We consider each of these separately below.

8.1.1 Plant Layout Design

In Chapter 2, a novel MILP formulation has been developed, addressing the 2-D and 3-D plant layout problem in batch plants. The approach guarantees the rigorous solution of problems with up to 25 units and of essentially unlimited size problems when rigorous optimisation is combined with simple heuristic rules. A key feature of the proposed method is the ability to explore trade-offs between capital and operating costs incorporated in a detailed economic

objective function, so that the optimal number of floors in 3-D problems may be determined. The linear form of the resulting model allows its direct application to the retrofit design case so as to explore the effect of layout limitations to retrofit and other decisions.

Extending the formulation presented in chapter 2, a novel MILP model has been described in chapter 3. The salient feature of this formulation is that it accounts for equipment of various sizes and geometries thus providing a more realistic approach to the process plant layout problem. It should be noted that, so far, the problem of resources constraints in layout decisions has been usually neglected in the literature.

This work fills a key missing step in the design of batch plants, between the conceptual and functional design stage (where size, number and type of units is selected and perhaps connectivity) and the detailed design (2D CAD and modular design).

8.1.2 Modelling, Simulation, Optimal Design and Operation of Heat Treatment Processes with application to Dairy Processes

Techniques for the overall design and operation of batch plants so far have by and large assumed simple models of individual unit operations. On the other hand, dynamics from rapid decaying performance is often key to a process. Hence, an example of such behaviour has been considered as a representative of this whole class of problems.

A detailed mathematical model for tubular heat exchangers under milk fouling has been developed in chapter 4 in terms of a set of non-linear integral partial differential and algebraic equations (IPDAEs). The model describes reactions/mass transfer operations, between the fluid bulk and the thermal layer, due to fouling. Detailed fluid dynamics sub-models were also used to account for the effect of the prevailing flow conditions on milk fouling. Typical industrial heat exchanger configurations were simulated, using appropriate discretization techniques.

To validate the model, the predictions of the model were compared with experimental data and were found to match them well within the range of experimental error. Typical industrial techniques for fouling mitigation were also verified. The effect of process parameters (*e.g.* initial protein concentration) on fouling behaviour was also investigated through a sensitivity analysis.

A new general model to predict the transient thermal behaviour of various types of plate heat exchangers has been developed in chapter 5. It accounts for the thermal interactions be-

tween channels based on simple energy conservation laws. This model was then coupled with a detailed milk fouling model to predict the equipment behaviour under fouling conditions. Suitable methods for the discretization of the model equations in the spatial domain have been identified. A parameter estimation problem was solved, based on dynamic optimisation techniques, to calculate unknown model parameters. Three different PHE complex arrangements, used for sterilization purposes in industry, were simulated. The simulation results obtained were in a good agreement with experimental data.

A systematic mathematical framework for determining optimal policies and design decisions for tubular heat exchangers has also been established in chapter 6 based on the detailed model in chapter 4. The mathematical model is formulated as an optimal control one where the objective is to minimise the total operating cost due to fouling by controlling the heating medium inlet temperature and flowrate. At the same time the optimal tube length and diameter are also determined. This is a constrained optimisation problem where path constraints are imposed on the milk outlet temperature and pressure drop. The control vector parameterisation technique was employed to reduce the above infinite dimensional optimisation problem to a finite dimensional non-linear programming problem. A sequential quadratic programming algorithm was used to solve the latter. Three different configurations were optimised. It was shown that the constant wall temperature arrangement provides the best economical results. An important conclusions is that the hot utility availability in the plant is the main operability bottleneck. The economic impact of different control schemes was also explored.

Finally, in chapter 7 the problem of optimising the short term cleaning schedules in HEN under fouling was considered. The simulation results in chapter 5 were used to simulate the performance of each heat exchanger with time. Based on a parameterisation of general fouling profiles with time an MINLP model was first developed. The objective function accounts for cleaning costs and energy requirements. The MINLP model was proved to be inefficient for the solution of large scale problem. Hence, it was then linearized to a tight MILP model which can be solved to global optimality. It was shown that the hot utility availability in the plant may have considerable effect on the overall cleaning policies.

8.2 Main Contributions of this Work

In summary, the main contributions of this work have been:

- Mathematical programming formulations have been developed for the 2-D and 3-D batch layout problem with and without equipment size constraints based on a realistic consideration of this problem than earlier approaches in the literature. The interactions between layout considerations and retrofit decisions were explored.

- A dynamic model of tubular exchangers under milk fouling has been developed. It incorporates a detailed model describing a reaction scheme and mass transfer operations occurring between the fluid bulk and layer. It provides a more rigorous mathematical way to model this phenomenon than earlier models reported in the literature.

- A general dynamic model of PHEs under milk fouling has been developed which can be used to simulate the transient behaviour of several types of PHEs.

- All the developed models were validated against experimental data. Good agreement of model predictions with experimental observations was obtained based on parameter estimation problems.

- A general framework for determining optimal control strategies and design decisions has been established. It is based on a detailed mathematical model as well as a rigorous mathematical formulation of the optimisation problem and the use of an advanced optimisation algorithm. A detailed economic objective function is defined which aims to achieve sterilization requirements at minimum cost subject to a number of operating constraints.

- New mathematical programming approaches, addressing the cleaning scheduling problem under fouling conditions, have been developed. A detailed economic objective function has been defined and a number of constraints has been imposed to account for product quality requirements and utility provision availability bounds.

8.3 Recommendations for Future Directions

A range of issues requiring further investigation have been revealed in the course of this work. In particular,

- Incorporation of layout considerations under resource constraints (*e.g.* size and geometry) in the retrofit design problem of batch plants. A small example has been presented in chapter 2 to illustrate the effect of layout limitations in the plant design. However,

the simultaneous retrofit/design and layout approach clearly results in large size problems and make their exact solution computationally expensive. It is envisaged that a decomposition-based approach can be applied to overcome this difficulty (see for example the work of Realff *et al.* (1996) on pipeless plants).

- To improve the accuracy of the dynamic model on heat exchangers under milk fouling a possible extension is to take into account the temperature profiles inside the protein particles. This will impose the definition of a new radial domain for the solid particles.

- Further incorporation of the fouling/heat exchanger model in a complete dairy plant model in order to simulate the behaviour of the overall plant operation. Based on the final model a dynamic optimisation problem for the total plant can then be posed. As mentioned by Jong and Linden (1992) substantial fouling mitigation can be achieved by the optimal design/control of other parts as holding sections, recycle flows etc.

- The models of PHEs under milk fouling can be used for the simultaneous design and operation of the equipment. Here, the objective is to find the optimal control policy (*e.g.* profiles of the heating medium inlet temperature and flowrate) and design characteristics (*e.g.* channel length, gap and width) so as to minimise a cost function and satisfy temperature requirements and pressure drop limitations.

- The work on the cleaning scheduling in HENs has been concentrated on the short term scheduling. The underlying simplicity of the models makes the extension to cyclic scheduling possible. Furthermore, the synthesis of HENs under fouling considerations constitutes an interesting path for future work.

- A long term aim of the area of research to which this thesis belongs is to implement and demonstrate the models in on-line applications on a batch pilot plant in real time. For example, the modelling of arbitrary fouling profiles in chapter 7 enables the direct use of experimental data. Furthermore, the low computational cost of the resulting optimisation problems is a significant support for on-line applications. Alternatively, the optimisation frameworks developed could be packaged as an advisory system assisting the operator in dairy plants to make the operational decisions.

- The fouling models presented here are general in the sense that they model very detailed phenomena characterizing this process. The extension of these models to other processes which are often considered as the bottleneck in batch plants, such as reactors networks where the catalyst undergoes deactivation, is straightforward.

- Finally, it is important that the assumption of perfectly known model parameters be relaxed, and a proper account of uncertainties taken. The problem of accounting for uncertainty in the design and operation of dynamic processes has been extensively recognized (Pistikopoulos, 1995). In pasteurizarion processes uncertainty arises primarily due to the variability in the milk composition and also to the kinetic parameters. One approach of dealing with uncertainty is to postulate a probability distribution of milk inlet composition and kinetic constants over finite ranges, and then derive a *robust* policy that is guaranteed to achieve the temperature requirements for *any* actual conditions within those values. In such a case, the objective function to be minimised could be the *expected value* of the total cost (see Mohideen *et al.* (1996) and Samsatli *et al.* (1988)). Alternatively, a more integrated approach is to use some combination of the *expected value* and the variance of this quantity in order to reduce the sensitivity of the optimal objective function value to variations in uncertain parameters (see the approach on steady state models by Georgiadis and Pistikopoulos (1998)).

References

Adams, W.P. and H.D. Sherali (1986). A Tight Linearization and an Algorithm for zero-one Quadratic Programming Problems. *Management Science* **32**, 1274–1290.

A Guide to Capital Cost Estimating (1988). 3rd ed.. The Institution of Chemical Engineers, U.K.

Ahmad, D.K. (1997). Condition Monitoring of a Heat Exchanger under Milk Fouling. Master's thesis. Imperial College of Science Technology and Medicine.

Amorese, L., V. Cena and C. Mustacchi (1991). A Heuristic for the Compact Location of Process Components. *Chemical Eng. Science* **32**, 119–124.

Ball, A. (1990). Process & CIP integration for quality in Food Plants. In: *Process Engineering in the Food Industry - Convenience Foods and Quality Assurance.* pp. 118–127.

Barbosa-Povoa, A. (1994). Detailed Design and Retrofit of Multipurpose Batch Plants. PhD thesis. University of London.

Barbosa-Povoa, A.P. and S. Macchietto (1994). Detailed Design of Multipurpose Batch Plants. *Comput. chem. Engng* **18**, 1013–1042.

Barton, P.I. and C.C. Pantelides (1994). The Modeling of Combined Discrete/Continuous Processes. *AIChE Journal* **40**, 966–979.

Bazaraa, M.S. and H.D. Sherali (1980). Bender's Partitioning Scheme to a new Formulation of the Quadratic Assignment Problem. *Naval Res. Logist.* **27**, 29–42.

Bazaraa, M.S. and O. Kirca (1983). A Branch and Bound Based Heuristic for solving the Quadratic Assignment Problem. *Naval Res. Logist.* **30**, 287–304.

Bazargan-Lari, M (1997). Inter-Cell Layout Design in a Cellular Manufacturing Environment-A Case Study. In: *Flexible automation and intelligent manufacturing.* Begel house, inc.. pp. 504–516.

Belmar-Beiny, M.T., S.M. Gotham, W.R. Paterson and P.J. Fryer (1993). The Effect of Reynolds Number and Fluid Temperature in Whey Protein Fouling. *Journal of the Society of Dairy Technology* **19**, 119–139.

Bird, M.R. and P.J. Fryer (1992). An Analytical Model for the Cleaning of Food Process Plant. *IChemE Symposium Series* **No 126**, 325–330.

Bird, M.R. and S.W.P. Espig (1994). Cost Optimization of Dairy Cleaning in Place (CIP) Cycles. *Trans IChemE* **72**, 17–20.

Bozer, Y., R. Meller and S. Erlebacher (1994). An Improved Type Layout Algorithm for Single and Multiple-Floor Facilities. *Management Science* **40**, 918–932.

Bradley, C.W. and P.F. Nolan (1985). Criteria for Plant Separation, Distances and Location. *I. Chem. Eng. Symp. Series* **No 93**, 247–262.

Brodkey, R.S. and H.C. Hershey (1988). *Transport Phenomena: A Unified Approach.* McGraw-Hill Inc., Singapore.

Brooke, A., D. Kendrick and A. Meeraus (1992). *GAMS: A Users Guide.* Scientific Press, Palo Alto.

Casado, E. (1990). Model Optimizes Exchanger Cleaning. *Hydrocarbon Processing* pp. 71–76.

Charalambides, M.S. (1996). Optimal Design of Integrated Batch Processes. PhD thesis. University of London.

Chen, C.L. and S. Macchietto (1988). Successive Reduced Quadratic Programming-SRQP-User's Guide. *Dept. of Chem. Eng., Imperial College, London.*

Corominas, J., A. Espuna and L. Puijaner (1993). A New Look at Energy Integration in Multipurpose Plants. *Comput. Chem. Eng.* **S17**, S15–S20.

Coulson, J.M. and J.F. Richardson (1985). *Chemical Engineering.* 3rd ed.. Pergamon Press.

CPLEX Optimization, Inc. (1994). *Using the CPLEX Barrier and Mixed Integer Solvers.* Houston, TX.

Crooks, C. (1992). Synthesis of Operating Procedures for Chemical Plants. PhD thesis. University of London.

Danckwerts, P.V. (1953). Continuous Flow Systems: Distribution of Residence Times. *Chem. Engng Sci.* **2**, 1.

Das, S.K. and W. Roetzel (1995). Dynamic Analysis of Plate Heat Exchangers with Dispersion in both Fluids. *Int. J. Heat Mass Transfer* **38**, 1127–1140.

Dedopoulos, I.T. and N. Shah (1995). Optimal Short-Term Scheduling of Maintenance and Production for Multipurpose Plants. *Ind. Eng. Chem. Res.* **34**, 192–201.

Dedopoulos, I.T. and N. Shah (1996). Long-term Maintenance Policy Optimization in Multipurpose Process Plants. *Chem. Eng. Res. Des.* **74**, 307–320.

Delplace, F. and J.C. Leuliet (1995). Modelling Fouling of a Plate Heat Exchanger with Different Flow Arrangement by Whey Protein Solutions. *Trans IChemE, Part C* **73**, 112–119.

Delplace, F., J.C. Leuliet and J.P. Tissier (1994). Fouling Experiments of a Plate Heat Exchangers by Whey Proteins Solutions. *Trans IChemE, Part C* **72**, 163–169.

Delplace, F., J.C. Leuliet and T.R. Bott (1995). Influence of Plates geometry on Fouling of Plate Heat Exchangers by Whey Proteins. *In Fouling Mitigation of industrial heat exchangers* pp. Shell Beach, California.

Douglas, J.M. (1988). *Conceptual Design of Chemical Processes.* 1st ed.. McGraw Hill.

Duran, A.M. and I.E. Grossmann (1986). An Outer-Approximation Algorithm for Class of Mixed-Integer Nonlinear Programs. *Mathematical Programming* **36**, 307–339.

Epstein, N. (1979). Optimum Evaporator Cycle with Scale Formation. *The Canadian Journal of Chemical Engineering* **57**, 659–661.

Fisher, M.L. (1981). The Lagrange Relaxation Method. *Management Science* **27**, 1–19.

Fortenberry, B.J.C. and J.F. Cox (1985). Multiple Criteria Approach to the Facilities Layout Problem. *Int. J. Prod. Res.* **23**, 773–782.

Foumeny, E.A. and P.J. Heggs (1991). *Heat Exchange Engineering. Volume 2. Compact Heat exchangers: Techniques of Size Reduction.* 1st ed.. Ellis Horwood.

Francis, R.L. and J.A. White (1974). *Facility Layout and Location.* 1st ed.. Prentice-Hall International Series.

Fryer, P.J. (1989). The Uses of Fouling Models in the Design of Food Process Plant. *Journal of the Society of Dairy Technology* **42**, 23–28.

Fryer, P.J. and N.K.H. Slater (1985). A Direct Simulation Procedure for Chemical Reaction Fouling in Heat Exchangers. *The Chemical Engineering Journal* **31**, 97–107.

Fryer, P.J. and N.K.H. Slater (1986). The Simulation of Heat Exchanger Control with tube-site Chemical Reaction Fouling. *Chemical Engineering Science* **41**, 2363–2372.

Fryer, P.J. and N.K.H. Slater (1987). A Novel Fouling Monitor. *Chemical Eng. Comm.* **57**, 139–152.

Fryer, P.J., P.J. Hobin and S.P. Mawer (1988). Optimal Design of a Heat Exchanger Undergoing Reaction Fouling. *The Canadian Journal of Chemical Engineering.* **66**, 558–562.

Fryer, P.J., P.T. Robins, C. Green, P.J.R. Schreier, A.M. Pritchard, A.P.M. Hasting, D.G. Royston and J.F. Ritchardson (1996). A Statistical Model for Fouling of a Plate Heat Exchanger by Whey protein Solution at UHT Conditions. *Trans IChemE, Part C* **74**, 189–199.

Fuchino, T., T. Itoh and M. Muraki (1997). Arrangement of Process Equipment Modules under the Consideration of Plant Safety. *Journal of Chemical Eng. of Japan, In Press.*

Garett, B.A., P. Ridges and N.J. Noyes (1985). *Fouling of Heat Exchangers: Characteristics, Cost, Prevention, Control and Removal.* 1st ed.. Prentice-Hall International Series.

Geoffrion, A.M. (1972). Generalized Benders Decomposition. *Journal of Optimization Theory and Applications* **10**, 237–260.

Georgiadis, M.C. and E.N. Pistikopoulos (1998). An Integrated Design Framework for Robust and Flexible Process Systems. *Accepted for publication in Ind. Eng. Chem. Res.*

Glover, F. (1975). Improved Linear Integer Programming Formulations of Nonlinear Integer Problems. *Management Science* **22**, 455–460.

Gonzalez, R. and M.J. Realff (1995). Robust Scheduling of Pipeless Batch Plants. In: *AIChE Annual Meeting.* San Fransisco.

gPROMS Technical Document (1998*a*). *The gEST Parameter Estimation Tool.* Process Systems Enterprise Ltd.

gPROMS Technical Document (1998*b*). *The gOPT Dynamic Optimisation Tool.* Process Systems Enterprise Ltd.

gPROMS Technical Document (1998*c*). *The gPROMS User's Guide.* Process Systems Enterprise Ltd.

Grandison, A.S. (1988). UHT Processing of Milk: Seasonal Variation in Deposit Formation in Heat Exchangers. *Journal of the Society of Dairy Technology* **41**, 43–49.

Grossmann, I.E., I. Quesada, R. Ramesh and T.V. Voudouris (1993). Bridging the Gap-Interactions of Design, Operations, Scheduling and Control. In: *NATO Advanced study institute on Batch Processing Systems.* Crested Butte, Colarado.

Gunn, D.J. (1970). The Optimised Layout of a Chemical Plant by a Digital Computer. *Computer Aided Design* **2**, 11–16.

Gunn, D.J. and H.D. Al-Asadi (1987). Computer Aided Layout of Chemical Plant: A Computational Method and Case Study. *Computer aided design* **19**, 131–140.

Hall, H.S. (1976). *Standardized Pilot Milk Plants.* 1st ed.. Food and Agriculture Organization of the United Nations.

Ishikawa, T., Y. Natori, L. Liberis and C.C. Pantelides (1997). Modelling and Optimisation of an Industrial Batch Process for the Production of Dioctyl Phthalate. *Computers & Chem. Engng* **S21**, S1239–S1244.

Jain, V. and I.E. Grossmann (1998). Cyclic Scheduling of Continuous Parallel Process Units with Decaying Performance. *AIChE Journal.*

Jarvis, R.B. and C.C. Pantelides (1992). A Differential and Algebraic Equation Solver. *Technical report, Centre for Process Systems Engineering, Imperial College.*

Jayakumar, S. and G.V. Reklaitis (1994). Chemical Plant Layout via Graph Partitioning-I. Single Level. *Comput. chem. Engng* **14**, 441–458.

Jayakumar, S. and G.V. Reklaitis (1996). Chemical Plant Layout via Graph Partitioning-II Multiple Levels. *Comput. chem. Engng* **20**, 563–578.

Jong, P. De and H.J.L.J. Van Der Linden (1992). Design and Operation of Reactors in the Dairy Industry. *Chemical Engineering Science* **47**, 3761–3768.

Jong, P. De, S. Bouman and H.J. Van Der Linden (1992). Fouling of Heat Transfer Equipment in Relation to the Denaturation of β-lactoglobulin. *Journal of the Society of Dairy Technology* **45**, 3–8.

Kern, D.Q. (1965). *Process Heat Transfer*. 1st ed.. McGraw-Hill.

Kern, R. (1977). Layout Arrangements for Distillation Columns. *Chemical Engineering* pp. 153–160.

Kondili, E., C.C. Pantelides and R.W.H. Sargent (1993). A General Algorithm for Short-Term Scheduling of Batch Operations. Part I-Mathematical Formulation. *Comput. & Chem. Engng.* **17**, 211–227.

Kusiak, A. and S.S. Heragu (1987). The Facility Layout Problem. *European Journal of Operational Research* **29**, 229–251.

Lakshmanan, C. C. (1990). Dynamic Simulation of Plate Heat Exchangers. *Int. J. Heat Mass Transfer* **33**, 995–1002.

Lalande, M., F. Rene and J.P. Tissier (1989). Fouling and its Control in Heat Exchangers in the Dairy Industry. *Biofouling* **1**, 233–250.

Lalande, M., J.P. Tissier and G. Corrieu (1985). Fouling of Heat Transfer Surfaces related to b-Lactoglobulin Denaturation during Heat Processing of Milk. *Biotechnology Progress* **1**, 131–139.

LeClercq-Perlat, M.N. and M. Lalande (1991). A Review on the Modelling of the Removal of porous Contaminant Deposited on Heat Transfer Surfaces. *International Chemical Engineering* **31**, 74–93.

Levine, L. (1997). Food Process Development and Scale up Using Modelling and Simulation. *Chemistry and Industry* **5 May**, 346–349.

Macchietto, S. (1993). Bridging the Gap-Interaction of Design, Operations, Scheduling and Control.. In: *Second International Conference on Foundations of Computer-Aided Process Operations*. Crested Butte, Colorado.

Macchietto, S. (1997). Batch Food Processing: The Proof is in the Eating. In: *Chemical Process Control, CPVC* (J. Kantor, C.E. Garcia and B. Carnahan, Eds.). CACHE Publications.

Macchietto, S. (1998). Batch Processing Engineering Revisited: Adding New Spice to Old Recipes. Presented at the 5th IFAC Symposium on Dynamics and Control of Process Systems, Corfu, Greece.

Madden, J. and K. Walters (1988). Sharpen your Knowledge of Plant Layout Skills. *Process engineering* pp. 59–62.

Marquardt, W. (1991). Dynamic Process Simulation-Recent Trends and Future Challenges. In: *Chemical Process Control, CPVC-IV* (Y. Arkun and W.H. Ray, Eds.). CACHE Publications. pp. 131–180.

Marquardt, W. (1996). Trends in Computer-Aided Process Modelling. *Computers & Chem. Engng* **20**, 591–609.

McKetta, J.J. (1984). *Chemical Engineering Design Encyclopedia.* Marcel Dekker Inc., New York.

Mecklenburgh, J.C. (1985). *Process Plant Layout.* 1st ed.. Institution of Chemical Engineers.

Mohideen, M.J., J.D. Perkins and E.N. Pistikopoulos (1996). Optimal design of Dynamic Systems under Uncertainty. *AIChE* **42**, 2251–2272.

Muller-Steinhagen, H. (1998). Mitigation of Process Heat Exchanger Fouling. *Chem. Eng. Res. Des.* **76**, 97–107.

Nolan, P.F. and C.W. Bradley (1987). A Simple Technique for the Optimization of Layout and Location for Chemical Plants Safety. *Plant/Operations Progress* **6**, 57–61.

Oh, M. and C.C. Pantelides (1996). A Modelling and Simulation Language for Combined Lumped and Distributed Parameter Systems. *Computers Chem. Engng* **20**, 611–633.

Pantelides, C.C. (1994). Unified Framework for Optimal Process Planning and Scheduling. In: *Proc. Second Conf. on Foundations of Computers Aided Operations* (D.W.T. Rippin and J.Hale, Eds.). CACHE Publications. pp. 253–274.

Pantelides, C.C. (1996). Process Modelling in the 1990s. Presented at the 5th World Congress of Chemical Engineering, San Diego, California,.

Pantelides, C.C. and H.I. Britt (1995). Multipurpose Process Modelling Environments. In: *Proc. Conf. on Foundations of Computers Aided Process Design '94* (M.F. Doherty and L.T. Biegler, Eds.). CACHE Publications. pp. 128–141.

Papageorgiou, L.G., N. Shah and C.C. Pantelides (1994). Optimal Scheduling of Heat-Integrated Multipurpose Plants. *Ind. Eng. Chem. Res.* **33**, 3168–3186.

Paterson, W.R. and P.J. Fryer (1988). A Reaction Engineering Approach to the Analysis of Fouling. *Chemical Eng. Science* **43**, 1714–1717.

Penteado and A.R. Ciric (1996). An MINLP Approach for Safe Process Plant Layout. *Ind. Eng. Chem. Res.* **35**, 1354–1361.

Perry, R.H. and D. Green (1984). *Perry's Chemical Engineering Handbook*. McGraw-Hill Inc., Singapore.

Peters, M.S. and K.D. Timmerhaus (1981). *Plant Design and Economics for Chemical Engineers*. 3rd ed.. McGraw-Hill.

Pistikopoulos, E.N. (1995). Uncertainty in Process Design and Operations. *Comp. Chem. Engng.* **19S**, S553–S563.

Realff, M.J., N. Shah and C.C. Pantelides (1996). Simultaneous Design, Layout and Scheduling of Pipeless Batch Plants. *Comput. chem. Engng* **20**, 869–883.

Reklaitis, G.V. (1992). Overview of Scheduling and Planning of Batch Process Operations. In: *NATO Advanced Study Institute On Batch Process System Engineering*. Antalya, Turkey. pp. 1623–1636.

Rippin, D.W.T. (1993). Batch Process Systems Engineering: A Retrospective and Prospective View. *Computers & Chem. Engng* **S17**, S1–S13.

Rosenblatt, M.J. (1979). The Facilities Layout Problem: A Multi-Goal Approach. *Int. J. Prod. Res.* **17**, 323–332.

Rotstein, G.E., V.T. Voudouris, E. Sorensen, N. Shah, S. Macchietto, R.A. Weiss and H. Dempster (1997). Batch Plant Optimization: A Collaborative Case study. *Comput. chem. Engng* **S21**, S319–S325.

Sahinidis, N.V. and I.E. Grossmann (1991). MINLP Model for Cyclic Multiproduct Scheduling on Continuous Parallel lines. *Comput. & Chem. Engng.* **15**, 85–103.

Samsatli, N.J., L.G. Papageorgiou and N. Shah (1988). Robustness Metrics for Dynamic Optimization Models under Parameter Uncertainty. *AIChE journal, In press.*

Sandu, C. (1989). Physicomathematical Model for milk Fouling in a Plate Heat Exchanger. PhD thesis. University of Wisconsin-Madison.

Sandu, C. and D. Lund (1982). Fouling of Heat Transfer Equipment by Food Fluids: Computational Models. *AIChE Symposium Series* **78**, 12–30.

Sandu, C. and D. Lund (1983). Fouling of Heat Exchangers: Optimum Design and Operation. In: *Fouling of heat exchanger Surfaces.* Publication Department, Engineering Foundation, New York. pp. 681–716.

Sandu, C. and D. Lund (1985). Minimizing Fouling in Heat Exchanger Design. *Biotechnology progress* **1**, 10–17.

Sandu, C. and R.K. Singh (1991). Energy Increase in Operation and Cleaning due to Heat-Exchanger Fouling in Milk Pasteurization. *Food Technology* pp. 84–91.

Shah, N. (1992). Efficient Scheduling, Planning and Design of Multipurpose Batch Plants. PhD thesis. University of London.

Shah, N. (1998). Single and Multisite Planning and Scheduling: Current Status and Future Challenges. In: *FOCAPO-98.* Snowbird, Utah, USA.

Shah, R.K., E.C. Subbarao and R.A. Mashelkar (1988). *Heat Transfer Equipment Design.* 1st ed.. Hemisphere Publishing Corporation.

Sheikh, A.K., S.M. Zubari, M.U. Haq and M.O. Budair (1996). Reliability-Based Maintenance Strategies for Heat Exchangers subject to Fouling. *Transactions of the ASME* **118**, 306–312.

Smaili, F. (1998). Optimisation of Scheduling of Cleaning in Heat Exchanger Networks subject to Fouling: Sugar Industry Case Study. In: *Fouling and Cleaning in Food Processing '98.* Department of Chemical Engineering, University of Cambridge, Cambridge.

Suzuki, A., T. Fuchino and M. Muraki (1991*a*). An Evolutionary Method of Arranging the Plot Plan for Process Plant Layout. *Journal of Chemical Eng. of Japan* **24**, 226–231.

Suzuki, A., T. Fuchino, M. Muraki and T. Hayakawa (1991*b*). Equipment Arrangement for Batch Plants in Multifloor Buildings with Integer Programming. *Journal of Chemical Eng. of Japan* **24**, 737–742.

Suzuki, A., T. Fuchino, M. Muraki and T. Hayakawa (1991*c*). Method of Determining the floor for siting of each Equipment unit of a Multipurpose Batch Plant. *Kagaku kogaku Ronbunshu (In English)* **17**, 1110.

Taborek, J., T. Aoki, R.B. Ritten, J. Palen and J.G. Knudsen (1972). Fouling: The Major Unresolved Problem in Heat Transfer. *Chem. Engng. Progr.* **68**, 59–67.

Thomaidis, T.V. and E.N. Pistikopoulos (1995). Optimal Design of Flexible and Reliable Process Systems. *IEEE Transactions on Reliability* 44, 243–250.

Toyoda, I. and P.J. Fryer (1997). A Computational Model for Reaction and Mass Transfer in Fouling from Whey Protein Solutions. In: *Fouling Mitigation of industrial heat exchange equipment.* Begell House, New York.

Vassiliadis, C.G. and E.N. Pistikopoulos (1998). On the Interaction of Chemical-Process Design under Uncertainty and Maintenance-Optimization. In: *Annual Reliability and Maintenability Symposium.* pp. 302–307.

Vassiliadis, V.S., R.W.H. Sargent and C.C. Pantelides (1994*a*). Solution of a Class of Multistage Dynamic Optimization Problems. 1. Problems without Path Constraints. *Ind. Eng. Chem. Res.* **33**, 2111–2122.

Vassiliadis, V.S., R.W.H. Sargent and C.C. Pantelides (1994*b*). Solution of a Class of Multistage Dynamic Optimization Problems. 2. Problems with Path Constraints. *Ind. Eng. Chem. Res.* **33**, 2123–2133.

Viswanathan, J. and I.E. Grossmann (1990). A Combined Penalty Function and Outer-Approximation Method for MINLP Optimization. *Comput. chem. Engng.* **14**, 769–782.

Voudouris, V.T. and I.E. Grossmann (1992). Mixed Integer Linear Programming Reformulations for Batch Process Design with Discrete Equipment. *Ind. Eng. Chem. Res* **31**, 1314–1326.

Walker, A. (1997). Foul Play. *The Chemical Engineer* **14 August**, 24–27.

Yoon, J. and D.B. Lund (1994). Comparison of two Operating Methods of a Plate Heat Exchanger under Constant Heat flux Condition and their Effect on the Temperature Profile during Milk Fouling. *Journal of Food Process Engineering* **17**, 243–262.

Zaleski, T. and K. Klepacka (1992). Approximate Method of Solving Equations for Plate Heat Exchangers. *Int. J. Heat Mass Transfer* **35**, 1125–1130.

Zhu, M.Z., M. El-Halwagi and M. Al-Ahmad (1997). Optimal Design and Scheduling of Flexible Reverse Osmosis Networks. *Journal of Membrane Science* **129**, 161–174.

Zubari, S.M., A.K. Sheikh and M.N. Shaik (1992). A Probabilistic Approach to the Maintenance of Heat-Transfer Equipment subject to Fouling. *Energy* **17**, 769–776.

Zubari, S.M., A.K. Sheikh, M.O. Budair and M.A. Badar (1997). A Maintenance Strategy for Heat Transfer Equipment Subject to Fouling: A Probabilistic Approach. *Journal of Heat Transfer* **119**, 575–580.

Referenced Papers from this Thesis

- Georgiadis, M.C. and Macchietto S., "Chemical Plant Layout: A Novel Approach", *Computers & Chem. Engng.*, **21(S)**, S337-S342, (1997).

- Georgiadis, M.C., Rotstein G.E. and Macchietto S., "Optimal Layout Design in Multipurpose Batch Plants", *Ind. Eng. Chem. Res*, **36**, 4852-4863, (1997).

- Georgiadis, M.C., Rotstein G.E. and Macchietto S., "Modelling and Simulation of Shell and Tube Heat Exchangers under Milk Fouling", *AIChE Journal*, **44**, 959-971, (1998).

- Georgiadis, M.C., Rotstein G.E. and Macchietto S.,"Optimal Design and Operation of Heat Exchangers under Milk Fouling", *AIChE Journal*, **44**, 2099-2111, (1998).

- Georgiadis, M.C., Rotstein G.E. and Macchietto S.,"Modelling and Simulation of Complex Plate Heat Exchanger Arrangements under Milk Fouling", *Computers & Chem. Engng.*, **22(S)**, S331-S338, (1998).

- Georgiadis, M.C., Shilling, G., Rotstein G.E. and Macchietto S., "A general Mathematical Programming Approach for Process Plant Layout", *Accepted for publication in Computers & Chem. Engng.*, (August, 1998).

- Georgiadis, M.C., Papageorgiou, L.G., Rotstein G.E. and Macchietto S.,"Optimal Cleaning Policies in Heat Exchanger Networks under Fouling", *Submitted for publication in AIChE Journal*, (May 1998).

- Georgiadis, M.C and Macchietto S.,"Modelling, Simulation and Parameter Estimation in Plate Heat Exchanger under Milk Fouling", *Paper in Preparation, to be Submitted for publication in Chemical Engineering Science*, (October 1998).

Appendix A

The Parameter Estimation Problem

The model described by equations 4.1 to 4.65 after the discretization over the two axial domains can be presented in a general form as follows:

$$f(x(t), \dot{x}(t), y(t), u(t), p, \theta) = 0 \tag{A.1}$$

where:

- $x(t)$ and $y(t)$ are the differential and algebraic equations in the model; $\dot{x}(t)$ are the time derivatives of $x(t)$ $(i.e.\ \dot{x} \equiv dx/dt)$
- $u(t)$ and p are the time-varying and time-invariant control parameters respectively; these describe the experiment(s) being carried out
- θ are the unknown parameters to be estimated

For the model considered here,

- concentrations, temperatures and the Biot number are the differential variables and all the others are the algebraic variables
- there are no time-varying and time invariant control parameters
- constant β and particle diameters are the unknown parameters to be estimated

The initial conditions of the systems are specified.

The parameter estimation problem makes use of experimental results gathered from a set of experiments. In general, we can have any number L of such experiments. Each experiment l ($l = 1..L$) is characterized by:

- its overall duration
- its initial conditions
- the variation of the control variables
- the values of the time invariant parameters p

Associated with each experiment, l, are also a set of data pairs collected during the experiment. These are of the form:

$$(t_{lik}, \hat{z}_{lik}) \tag{A.2}$$

where $\hat{z}_{lik}$ is the kth value measured for variable z_i during experiment l, and t_{lik} is the time at which this measurement was taken. In our problem z_i is the deposit mass for which experimental data are available at time 1 hour and for different positions along the tube. There are two set of experiments l for the two different milk inlet and outlet temperatures. All these data were taken from Belmar-Beiny *et al.* (1993). Note also that in the general case the measurement instants do not need to be equispaced; nor is it necessary for all measured variables to be recorded at the same time.

The parameter estimation problem attempts to determine values for the unknown parameters θ, that minimize the deviation between model predictions and experimental data. More specifically here a least square formulation is used that seeks to determine the value of θ that minimizes the following objective function:

$$\min_{\theta} \Phi = \sum_{l=1}^{L} W_l \sum_{i=1}^{I} w_i^2 \sum_{k=1}^{K} (z(t_{lik}) - \hat{z}_{lik})^2 \tag{A.3}$$

This is the weighted sum of the squares of the differences between the model predictions $z(t_{lik})$ and the experimentally measured values $(\hat{z}_{lik})$.

In the objective function above the deviations corresponding to different variables, i, are scaled using coefficients w_i. This can be useful for the cases where some measurements are

more reliable than others. In such cases higher values to w_i are assigned for the high priority measurements. Similarly, deviations arising from different experiments are weighted using W_i weighting factors.

For the problem considered here we assume that both experiments were performed under approximately the same conditions, and thus we do not have any reason for trusting the one set of data experiment more than the other. Therefore, we can choose:

$$W_1 = W_2 = 1.0 \tag{A.4}$$

Similarly all the variables weights w_i are also to one.

The parameter estimation problem described above with the objective function given by equation (A.3) together with the model equations (4.1) to (4.65) is a dynamic optimization problem which is formulated and solved using the *gEST* tool. The last can be used to specify and perform parameter estimation calculations using processes defined in the *gPROMS* language (*gPROMS* Technical Document, 1998a).

Appendix B

Simulation of the Cleaning Operation

The removal of milk deposit from the wall of a heat exchanger can be achieved by Cleaning-In-Place operations with detergents. The cleaning operation is simulated using the model of Bird and Fryer (1992). This model includes two simple equations. The deposit on the wall of thickness δ is described by two layers. An upper layer of thickness $x\delta$ swelled-deposit which can be remove and a lower layer of thickness $y\delta$ which is not yet removable at time t. The equations governing the rate of change of thickness of the two layers are simple expressed as:

$$\frac{d(y\delta)}{dt} = -k_y \tag{B.1}$$

$$\frac{d(x\delta)}{dt} = k_y - k_x x\delta \tag{B.2}$$

The constants k_x and k_y are given as a function of temperature by Bird and Fryer (1992). In our simulation, the cleaning solution concentration is 1 w.t.% sodium hydroxide at a velocity of 0.174 m/s and temperature 60 °C. Under these conditions (which are the optimal according to the same authors) the above rate constants are:

$$k_x = 0.00673 \quad m/s \tag{B.3}$$

$$k_y = 8.315 \cdot 10^{-7} \quad s^{-1} \tag{B.4}$$

The cleaning operation is simulated in the *gPROMS* modelling system (Oh and Pantelides, 1996) where the initial deposit thickness is taken from the simulation of the heating operation using the models in chapter 4. As expected different heating operations lead to different cleaning times. The cleaning time is defined as the time required for the deposit thickness to reach a target low value (taken here to be 10^{-9} m).

Cleaning time can be related to heating time on the basis of the simulation results. This allows the cleaning cost for the objective function used in the dynamic optimization problem to be accounted for. Assuming a cubic variation between the cleaning and heating time the following correlation can be used.

$$t_{clean} = 0.353 + 0.01237 \cdot t_{heat} - 2.55 \cdot 10^{-4} \cdot t_{heat}^2 + 1.87 \cdot 10^{-6} \cdot t_{heat}^3 \qquad hrs \qquad \text{(B.5)}$$

where t_{heat} and t_{clean} is the heating and cleaning time respectively.

In principle, one could explicitly integrate equations B.1 and B.2 within the dynamic optimization. However, this leads to a multistage optimal control problem which is very difficult to solve using current available algorithms.

BIBL
LONDON
UNIV.